SAM68, STRESS GRANULES, AND TRANSLATIONAL CONTROL OF HIV-1 n*ef* mRNA

Jorge Alejandro Henao-Mejia

Submitted to the faculty of the University Graduate School
in partial fulfillment of the requirements
for the degree
Doctor of Philosophy
in the Department of Microbiology and Immunology
Indiana University

May 2009

Accepted by the Faculty of Indiana University, in partial
fulfillment of the requirements for the degree of Doctor of Philosophy.

_____

Johnny J. He, Ph.D., Chair

_____

Janice S. Blum, Ph.D.

Doctoral Commitee

_____

Ann Roman, Ph.D.

March 24th, 2009

_____

Ronald C. Wek, Ph.D.

DEDICATION

I would like to dedicate this work to my loving wife, Juliana.

ACKNOWLEDGEMENTS

I would like to express my sincere gratitude to my advisor, Dr. Johnny He, for giving me the opportunity to develop my thesis dissertation in his laboratory, his mentorship, guidance, and support have been invaluable throughout this process. Under his tutelage I have learned a great deal about science; however, and most importantly, qualities such as hard-work, resilience, honesty, patience, and humility have been imprinted in me by his example, and they will surely accompany me through the rest of my life.

I thank Dr. Ann Roman, Dr. Janice Blum, Dr. Ronald Wek, and Dr. Jeremy Sanford, who served on my research committee; they offered much-appreciated advices in science and other related issues. I have learned a lot from their ideas, suggestions, and criticisms.

I would also like to thank all members of Dr. He's laboratory for their support and friendship. I especially would like to thank Dr. Ying Liu, Dr. Jinliang Li, and Jizhong Zhang for their contributions to and earlier work on Sam68. I stood on their shoulders for the present work.

I would like to thank to Dr. Hal Broxmeyer and Dr. Xin-Yuan Fu for allowing me to have a brief research rotation in their laboratories, but also for their many insightful and inspiring conversations.

To my fellow graduate students, I sincerely thank you for your friendship, kindness, and many joyful memories throughout these years.

I thank Maria Teresa Rugeles in the University of Antioquia, Colombia for her help and friendship. Her support has inspired me to continue a career in basic science. For that I am forever grateful.

I would like to thank my entire family for their life-long love, understanding, and encouragement. I especially owe much to Juan Sebastian, Maria Camila, Andres, Camilo, Elisa, Gladys, Joaquin, and Martha for offering me their unconditional love and support.

Finally but not least, I would like to thank my friend, companion, partner, and loving wife, Juliana for her generosity and love. Her thoughts have greatly influenced the way I approach life.

ABSTRACT

Jorge Alejandro Henao-Mejia

Sam68, Stress Granules, and Translational Control of HIV-1 *nef* mRNA

More than 20 million people have died of AIDS since the early eighties, while nearly 34 millions are currently infected with the HIV. Anti-retroviral therapy (ART) directed at key viral enzymes has changed AIDS from uniformly fatal to a manageable chronic disease. However, ART-associated drug resistance and toxicity have posed a great challenge for long-term management of the disease and have called for development of new therapeutics. In this study, we focused on the viral factor Nef and the host factor Sam68. Nef is a major pathogenic viral determinant for HIV-1, and no therapeutics have been targeted to this factor. Sam68 is indispensible for HIV-1 propagation. We revealed that Sam68 variants were very potent in preventing Nef expression. We found that these effects were associated with their ability to form a macromolecular structure called stress granules (SG). In addition, we demonstrated that these variants bound to *nef* mRNA in a sequence-specific manner. Furthermore, we showed that these variants co-localized with *nef* mRNA in SG. Importantly, we validated these findings in the context of HIV-1 infection of its natural target cells and found significant loss of Nef function in these cells. Taken together, these results demonstrate that SG induction and *nef* mRNA sequestration account for translational suppression of Nef expression and offer a new strategy for development of anti-HIV therapeutics.

Sam68 is implicated in a variety of other important cellular processes. Our findings that Sam68 variants were able to induce SG formation prompted us to investigate whether wild-type Sam68 was also recruited to SG. We found that Sam68 was increasingly recruited into SG under oxidative stress, and that its specific domains were involved. However, Sam68 knockdown had no effects on SG assembly, suggesting that Sam68 is not a constitutive component of SG assembly. Lastly, we demonstrated that Sam68 complexed with TIA-1, an essential SG component. Taken together, these results provide direct evidence for the first time that Sam68 is recruited into SG through complexing with TIA-1, and suggest that SG recruitment of Sam68 and ensuing changes in Sam68 physiological functions are part of the host response to external stressful conditions.

Johnny J. He, Ph.D., Chair

TABLE OF CONTENTS

LIST OF TABLES

LIST OF FIGURES

LIST OF ABBREVIATIONS

aa	amino acid
Act D	actinomycin D
AdOx	adenosine periodate oxidized
AIDS	acquired immunodeficiency syndrome
APOBEC3G	apolipoprotein B mRNA editing enzyme, catalytic polypeptide-like 3G
ARE	AU-rich element
ARS	sodium arsenite
ASSP1	argininosuccinate synthetase pseudogene 1
ATCC	American Tissue Culture Collection
BLAST	basic local alignment search tool
BRF-1	B-related factor 1, subunit of RNA polymerase III transcription initiation factor IIIB
BRK	breast tumor kinase
BSA	bovine serum albumin
CAT	chloramphenicol acetyltransferase
CCR5	CC Chemokine Receptor 5
CD3	cluster of differentiation 3
CD4	cluster of differentiation 4
CD44	cluster of differentiation 44
CDK9	cyclin-dependent kinase 9

Ci	Curie
CLIP	cross-linking immunoprecipitation
CPEB1	cytoplasmic polyadenylation element binding protein 1
cpm	counts per minute
CRM1	chromosome mantainance gene 1
CTE	constitutive transport element
CXCR4	CXC Chemokine Receptor 4
DAPI	4’,6’-diamidino-2-phenylindole
DDX3	DEAD box polypeptide 3
DMEM	Dulbecco's Modified Eagle Medium
DMSO	Dimethyl sulfoxide
ds	double-stranded
DTT	Dithiothreitol
EDTA	ethylene-diamine-tetra-acetic acid
eEF	eukaryotic elongation factor
EGTA	ethylene-glycol-tetra-acetic acid
eIF	eukaryotic initiation factor
Env	HIV-1 envelope
ER	endoplasmic reticulum
ERK	extracellular signal-regulated protein kinases
F Luc	firefly luciferase
FAST	Fas-activated serine/threonine phosphoprotein
FBP	formin-binding protein

FBS	fetal bovine serum
FDA	Food and Drug Administration
FISH	fluorescence *in situ* hybridization
FITC	fluorescein isothiocyanate
FMRP	fragile mental retardation protein
FRAP	fluorescence recovery after photobleaching
Fyn	Fyn proto-oncogene
G3BP	GTPase-activating protein (SH3 domain)-binding protein
GAPDH	glyceraldehyde-3-phosphate dehydrogenase
GCG	germinal cell granules
GCN2	general control non-derepressible-2
GEF	guanine nucleotide exchange factor
GFP	green fluorescent protein
GI	gastrointestinal
GLD-1	germ line development family member 1
gp120	HIV-1 glycoprotein 120
gp41	HIV-1 glycoprotein 41
GRAP	Grb2-related adaptor protein
Grb2	growth factor receptor bound protein 2
Grb7	growth factor receptor bound protein 7
GRP33	glycine-rich protein 33
GSG domain	GRP33/Sam68/GLD-1
HAART	highly active antiretroviral therapy

HBSS	Hank's-buffered salt solution
Hck	hemopoietic cell kinase
HEPES	4-(2-hydroxyethyl)-1-piperazineethanesulfonic acid
HIV-1	human immunodeficiency virus type 1
HnRNP A1	heterogeneous nuclear ribonucleoprotein A1
HRI	heme-regulated eIF2α kinase
hRIP	human Rev-interacting protein
HRP	horse radish peroxidase
HSV	herpes simplex virus
HuR	Hu antigen R
IL-2	interleukin-2
IN	HIV-1 integrase
IP	immunoprecipitation
IPTG	isopropyl-beta-D-thiogalactopyranoside
IRE	iron responsive element
IRES	internal ribosome entry site
IRP	iron regulatory protein
ITK	IL2-inducible T-cell kinase
JNK	c-Jun N-terminal kinases
kDa	Kilodaltons
Kep-1	KH domain-encompassing protein 1
KH	ribonucleoprotein particle K homology
Km	Kanamycin

KSRP	K-homology splicing regulatory protein
LB	Luria Broth
Lck	lymphocyte-specific protein tyrosine kinase
LTR	long terminal repeat
Lyn	v-yes-1 Yamaguchi sarcoma viral-related oncogene homolog
MA	HIV-1 matrix
MAPK	mitogen activated protein kinase
MEF	mouse embryonic fibroblast
MHC	major histocompatibility complex
MHV	mouse hepatitis coronavirus
MLN51	metastatic lymph node 51
NCK	non-catalytic kinase
Nef	negative regulatory factor
NES	nuclear exportation signal
NG	neuronal granules
NIH	National Institutes of Health
NLS	nuclear localization signal
NP40	Nondinet 40
NPC	nuclear pore complex
nt	nucleotide
NXF7	nuclear RNA exportation factor 7
O/N	overnight
ONPG	o-nitrophenyl β-d-galactopyranoside

ORF	open reading frame
p85PI3K	phosphatidylinositol 3-kinase, regulatory subunit, polypeptide 1
PABP	poly(A)-binding protein
PB	peripheral blood
PBMC	peripheral blood mononuclear cells
PBS	phosphate-buffered saline
PCBP2	poly(Rc)-binding protein 2
PCR	polymerase chain reaction
PE	phycoerythrin
PEG	polyethylene glycol
PERK	PKR-like ER kinase
PFA	paraformaldehyde
PHA	phytohemagglutinin
PI	propidium iodide
PKR	protein kinase R
PLCγ-1	phospholipase C gamma 1
PMR1	polysomal ribonuclease 1
PMSF	phenylmethanesulphonylfluoride
PR	HIV-1 protease
PRMT1	protein arginine methyltransferase 1
PRMT2	protein arginine methyltransferase 2
P-TEFb	positive transcription elongation factor B
QK	Quaking

R Luc	*renilla* luciferase
RACK1	receptor of activated protein kinase C 1
RanBP1	Ran binding protein 1
RasGAP	Ras GTPase activating protein
RBP	RNA binding protein
RCC1	regulator of chromosome condensation 1
Rev	regulator of virion protein expression
RFP	red fluorescent protein
RG	RNA granules
Rh	rhodamine
RHAU	DEAH (Asp-Glu-Ala-His) box polypeptide 36
RISC	RNA induced silencing complex
RNP	ribonucleoprotein
RPMI	Roswell Park Memorial Institute
RRE	Rev response element
RRM	RNA recognition motif
RSK	ribosomal protein S6 kinase
RT	reverse transcriptase
SAFB2	scaffold attachment factor B 2
Sam68	Src-associated protein in mitosis of 68 kDa
SD	synthetic defined
SDS	sodium dodecyl sulfate
SF1	splicing factor 1

SFV	Semiliki forest virus
SG	stress granules
SH2	Src homology 2
SH3	Src homology 3
Sik	Src-related intestinal kinase
siRNA	silencing RNA
SIV	simian immunodeficiency virus
SLM-1	Sam68-like mammalian protein 1
SLM-2	Sam68-like mammalian protein 2
SMN	survival of motor neuron
SRC3	steroid receptor coactivator 3
ss	single stranded
STAR	signal transduction and activation of RNA
TAP	nuclear RNA export factor 1
TAR	transactivation response element
Tat	transactivator of transcription.
TDRD3	Tudor domain containing 3
TIA-1	T cell intracellular antigen-1
TMPD	2, 6, 10, 14 tetra-methyl
TTP	tristetraprolin
U2AF	U2 small nuclear RNA auxiliary factor
UTR	untranslated region
Vif	HIV-1 viral infectivity factor

Vpr	HIV-1 viral protein R
Vpu	HIV-1 viral protein U
VSV	vesicular stomatitis virus
WB	Western blot
WNV	West Nile virus
ZAP70	zeta-chain (TCR)-associated protein kinase 70kDa
ZBP1	Z DNA binding protein 1
β-Gal	β-galactosidase

INTRODUCTION

1. HIV-1 AND THE AIDS PANDEMIC

1.1 The HIV-1 pandemic

1.1.1 Global perspective

The acquired immunodeficiency syndrome (AIDS) remains as one of the greatest public health hazards in the world today. Since the beginning of the pandemic 27 years ago, more than 20 million people have died, and approximately 34 million are currently infected with the human immunodeficiency virus type 1 (HIV-1) worldwide. The global incidence of HIV-1 infections and AIDS cases are considered to have reached a plateau. Nevertheless, approximately 2.7 million new infections occurred, and 2 million people died of AIDS in 2007 [1]. The landscape of the epidemic has changed drastically since the early 1980s, with profound implications for the social and economical development of different regions. Nowadays, 50% of people living with HIV-1 are women, the number of HIV-1-infected children younger than 15 has steadily increased since 2001, and 45% of newly infected people are between the ages of 15 and 24 years [1]. Moreover, despite the recent decrease in the overall number of yearly new infections, the total number of HIV-1-infected people continues to increase steadily due to the successful life extending HIV-1 treatments [1].

1.1.2 Regional perspective

The main concerns of the HIV-1 pandemic are focused in two regions: sub-saharan Africa and southeast Asia. Two thirds of the infected people worldwide live in sub-sahara Africa, where 1.9 million new infections and 75% of all AIDS deaths occurred in 2007 [1]. The epidemics vary considerably from country to country with HIV-1 adults prevalence ranging from 2% to above 15%, although the epidemic has stabilized in some countries in this region. Heterosexual intercourse remains the main mode of HIV-1 transmission in this region [1]. It is estimated that nearly 5 million people are currently infected in Asia, with the highest level of prevalence in southeast Asia. Countries such as Thailand show a decline in the HIV-1 prevalence, whereas in other countries such as Vietnam the epidemic is rapidly growing. Injectable drug use remains the main risk factor driving the epidemic in several Asian countries [1]. Another region of concern is central Europe and east Asia, where the annual number of new HIV-1 infections has doubled since 2001 [1].

1.1.3 The United States perspective

There were a total of 1.2 million HIV-1 infected people in the United States in 2007 [1]. The yearly number of new infections has remained stable for the past several years. Life expectancy has increased among HIV-1 infected individuals due to wide access to anti-retroviral therapy (ART), leading to an increase in the estimated number of people living with HIV-1 infection in the United States. However, the epidemiological trends in some ethnic populations are worrisome.

In 2005, blacks (including African Americans) accounted for nearly 50% of newly diagnosed AIDS and HIV-1 infections. Moreover, the rate of AIDS diagnosis for blacks was ten times that of whites and nearly three times that of hispanics. The main route of transmission for black men was sexual contact with other men, whereas for women it was heterosexual contact [2].

1.2 Clinical, virological, and immunological aspects of HIV-1 infection

The course of HIV-1 infection begins with an acute symptomatic illness, which lasts a few weeks. This is generally followed by an asymptomatic phase of chronic infection, which lasts an average of 8-10 years. Finally, AIDS develops, characterized by low CD4+ T cell counts, opportunistic infections and tumors (Fig. 1).

1.2.1 The acute phase

Clinical manifestations in acutely HIV-1-infected individuals are usually observed 2-4 weeks after exposure; they are described as a flu-like syndrome. Patients present a variety of signs and symptoms such as fever, lymphadenopathy, pharyngitis, mucocutaneous lesions, myalgia, arthralgia, headache, gastrointestinal symptoms, and weight loss [3]. The onset of clinical symptoms is associated with a peak high viremia [4], which is rapidly followed by a 100 to 1000-fold viral load drop [5]. The earliest targets of HIV are mucosal memory CD4+ CCR5+ T cells [6], which are the majority of the CD4+ T cell pool, with the

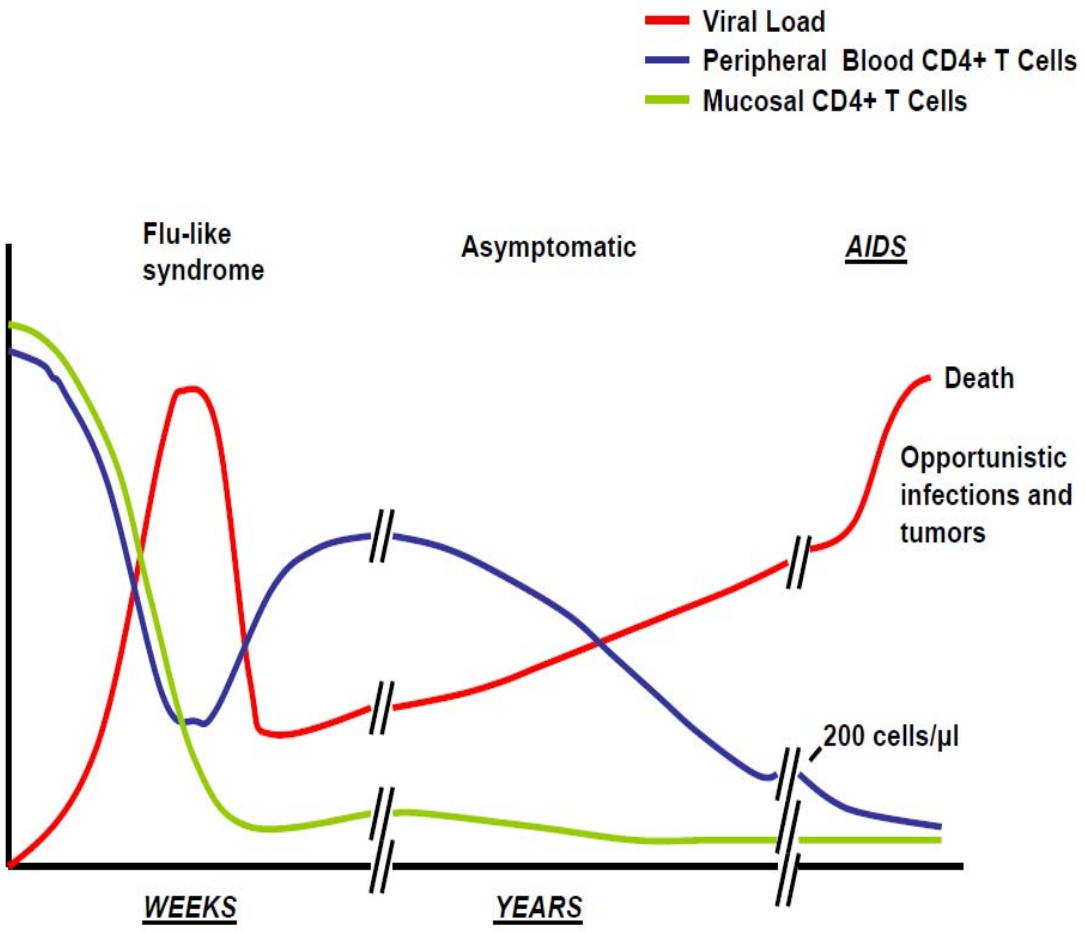

Figure 1. Natural history of HIV-1 infection. Clinical, virological and immunological evolution of a typical HIV-1-infected individual, shown as changes in HIV-1 plasma viral load (red), peripheral blood CD4+ T cell counts (blue), and gastrointestinal tract mucosa CD4+ T cell numbers (green). The X axis represents time after primary infection. The Y axis represents CD4 T cell counts on peripheral blood or gastrointestinal mucosa and viral RNA copies in plasma.

gastrointestinal (GI) tract mucosa harboring nearly 80% of the total population. Peak viremia is accompanied by a rapid and transient decrease in peripheral blood (PB) CD4+ T cell numbers, and a largely irreversible depletion of GI mucosal CD4+CCR5+ memory T cells [7-9]. A partial rise in PB CD4+ T cells is coupled with viral load drop, resolution of flu-like symptoms, and establishment of a chronic infection.

1.2.2 The chronic phase

The acute and chronic phases of the infection are markedly different. Clinically, the chronic phase is generally asymptomatic. The viremia is significantly lower than the one observed at the peak in the acute stage, but from this point it will continue a steady and slow rise [4]. PB CD4+T cells will reach a plateau after the partial recovery at the end of the acute stage, but then they fall slowly over a average period of 10 years before the onset of AIDS [5]. Recovery of mucosal CD4+ T cell levels is minimal. Moreover, this stage is characterized by a state of deleterious chronic immune hyper-activation, which is a better predictor of disease progression than viral RNA loads [10]. Continuous translocation of microbial products due to massive depletion in CD4+T cells in the gut, along with ensuing broad activation of the innate immune system seems to be the underlying mechanism behind this phenomenon [11].

1.2.3 The AIDS stage

The AIDS stage is a continuation of the immunological and virological features observed in the previous phase. PB CD4+ T cells continue to decline below 200 cells/μl, which is often associated with a sudden rise in the viral load of the patients [12]. Clinically, this stage is characterized by the onset of AIDS-related opportunistic infections or tumors such as: toxoplasmosis or Kaposi sarcoma, that eventually lead to the death of the infected individuals.

1.3 HIV-1 and its genome

HIV-1 has an approximate diameter of 120 nm and is composed of fifteen proteins and two molecules of viral genomic RNA. The HIV-1 genome is ~9 kb and encodes nine open reading frames (ORF). Three of these ORF encode the Gag, Pol and Env polyproteins which are subsequently processed into individual proteins. Gag encodes four structural proteins MA (matrix), CA (capsid), NC (nucleocapsid) and p6 that make up the core of the virion; Env generates the glycoproteins gp120 and gp41, which are the two main components of the outer virion layer; there are three Pol proteins: PR (protease), RT (reverse transcriptase), and IN (integrase), they provide essential enzymatic functions and are also encapsulated within the virion. The six additional ORFs encode the accessory viral proteins Tat, Rev, Nef, Vpr, Vpu, and Vif. Vpr induces cell cycle arrest and regulates nuclear importation of preintegration complexes in nondividing cells [13]; Vpu is involved in viral budding, enhancing virion release

from the cell [14]; Vif neutralizes a potent host antiretroviral pathway mediated by APOBEC3 [15]. Nef, Vpr, and Vif are also found within the viral particle. Tat, Rev and Nef provide essential regulatory functions that will be discussed in detail in the following sections. In addition, a number of non-coding regions required for efficient replication are located near the ends of the HIV-1 genome. These include R, a short sequence repeated at each end; U5, a unique sequence between R and PB near the 5' end; PB, which provides the primer binding site for the synthesis of the minus strand of the cDNA; PP, a stretch of purine nucleotides that provide the primer for the plus strand of cDNA; and U3, a unique sequence between PP and R near the 3' end. During reverse transcription, U3, R and U5 are duplicated at the ends of the DNA to form a structure called the long terminal repeat (LTR), allowing the virus to generate the transcriptional control elements that lie outside the transcribed region [16].

1.4 HIV-1 life cycle

Infectious HIV-1 virions initially bind to the cellular receptor CD4 and chemokine co-receptors CCR5 or CXCR4 on the surface of susceptible cells via envelope (Env) glycoprotein gp120 [17, 18] (Fig. 2). Following binding, gp41 undergoes a conformational change that promotes virus-cell membrane fusion [19], thereby allowing the viral nucleocapsid to enter the cytoplasm. The viral core is then uncoated to expose a nucleoprotein complex, which contains the viral proteins MA, RT, IN, PR, Vpr, Vif, Nef, and RNA [16]. The linear single stranded RNA genome is then reverse transcribed to a dsDNA molecule by the RT enzyme [16].

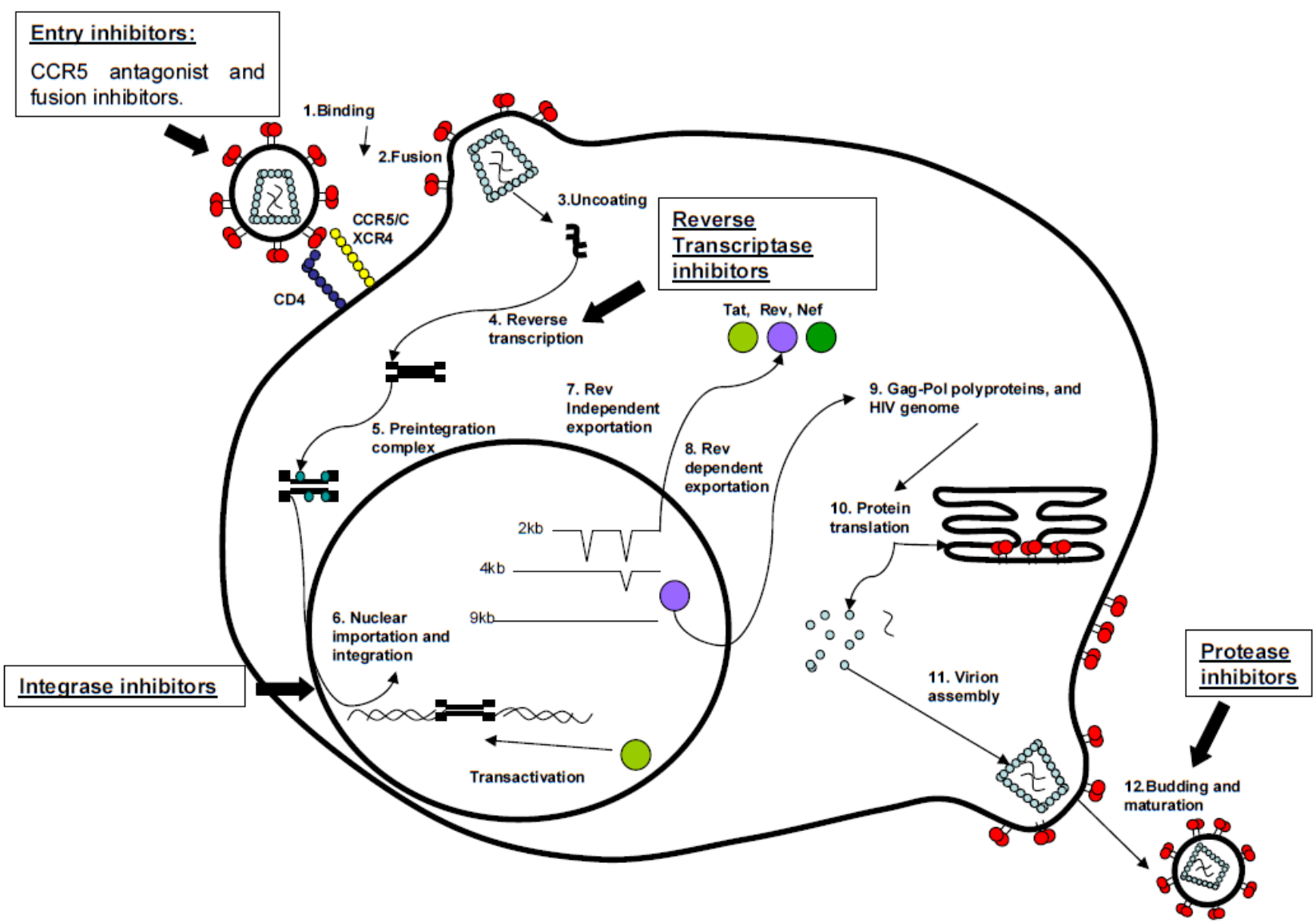
Entry inhibitors:
CCR5 antagonist and fusion inhibitors.
1.Binding
2.Fusion
3.Uncoating
CCR5/C XCR4
CD4
Reverse Transcriptase inhibitors
4. Reverse transcription
Tat, Rev, Nef
5. Preintegration complex
7. Rev Independent exportation
8. Rev dependent exportation
9. Gag-Pol polyproteins, and HIV genome
10. Protein translation
2kb
4kb
9kb
6. Nuclear importation and integration
Integrase inhibitors
Transactivation
11. Virion assembly
Protease inhibitors
12.Budding and maturation

Figure 2. HIV-1 replication cycle and targets of therapeutic intervention. 1. Binding; 2. Membrane fusion; 3. Uncoating; 4. Reverse transcription; 5. Assembly of the pre-integration complex; 6. Nuclear importation of the pre-integration complex and integration; 7. Rev-independent exportation of completely spliced mRNA and translation of Tat, Rev and Nef; 8. Rev-dependent exportation of intron containing mRNA; 9 and 10. Translation of structural proteins and viral enzymes; 11. Virion assembly; and 12. Budding and maturation. FDA-approved agents against HIV-1 and their targets are indicated (Boxes).

The dsDNA enters the nucleus as a nucleic acid-protein complex (the pre-integration complex) and is incorporated in the cell's genome by the action of the IN enzyme [16]. The integrated genome, also known as provirus, serves as a template for virus replication. Viral transcripts are expressed from the promoter located in the 5' LTR, with Tat greatly enhancing the rate of transcription [20, 21]. Completely spliced transcripts are exported to the cytoplasm by the cellular mRNA exportation machinery; translation of this RNA leads to the synthesis of the regulatory proteins Tat, Rev and Nef. Singly spliced and genome-length unspliced RNA are transported to the cytoplasm through a Rev-regulated mechanism [22, 23]. The latter RNA species upon translation give rise to the Gag and Gag-Pol polyproteins which become localized to the cell membrane, while the singly spliced RNA translates to the Env followed by its localization to the endoplasmic reticulum (ER). The polyproteins that form the viral core, namely the products of the Gag and Pol genes, initially assemble into immature nucleocapsids together with two copies of the full length viral RNA (viral genome), and immature virions begins to bud from the cell surface. As these structures bud through the plasma membrane, they become encapsulated by a layer of membrane that harbors Env glycoproteins. Coincident with budding a third viral enzyme known as protease (PR) cleaves the core proteins into their final forms, and the virion undergoes morphologic changes known as maturation [16].

1.5 HIV-1 transcription and splicing

HIV-1 mRNA is transcribed from integrated proviral DNA by RNA polymerase II, producing 5' capped and 3' polyadenylated primary RNA transcripts. The HIV-1 LTR region includes four functional domains: the transactivation region (TAR), the core promoter, the enhancer region, and the regulatory elements. The core promoter resembles that of many eukaryotic genes; it contains a TATA box and three tandem Sp1 sites [24]. General transcription factors, Sp1 and a number of host proteins interact with this region and regulate transcription initiation. The HIV-1 enhancer region consists of two tandem binding sites for the transcription factor NF-κβ and an AP2 binding site. Their recruitment significantly increases the basal transcriptional activity of the HIV-1 LTR promoter and is crucial for the initial rounds of transcription in the absence of Tat protein [25, 26]. The upstream regulatory region has positive and negative effects on the LTR transcriptional activation; it is proposed to be bound by multiple proteins including NFAT, Myb, C/EBP and AP-1, among others [27]. The presence or absence of these transcriptional regulatory factors in a specific cell is considered a limiting factor for efficient viral replication. The role of Tat and TAR on transcriptional activation will be discussed in detail in the following sections.

HIV-1 requires unspliced, singly spliced, and completely spliced mRNA to replicate efficiently. The virus depends on *cis*-signals in its genome and on the host cell RNA splicing machinery to generate a myriad of spliced viral mRNA present in the infected cell [28]. The HIV-1 genome contains five 5'-splice sites,

and nine 3'-splice sites. The sequences and locations of all but one of the 5'-splice sites and four 3'-splice sites are conserved in all strains of HIV-1 [28], highlighting the importance of splicing for the persistence of the virus. The alternative use of 5'-and 3'-splicing sites results in the generation of approximately 30 spliced mRNA species of 4 kb (singly spliced) and 2 kb (completely spliced) in size [29]. The 2 kb mRNA encodes the regulatory proteins Tat, Rev, and Nef, whereas the 4 kb mRNA encode Env, Vif, Vpu, and Vpr. In addition to the presence of splice sites, the regulation of HIV-1 alternative splicing depends on the interplay of three main factors: first, the strength of the *cis*-sequence elements adjacent to the splice sites in the pre-mRNA [30]; second, the interaction of host factors of the hnRNP A1 or hnRNP H families with negative *cis*-regulatory elements called exonic splicing silencers which results in repression of upstream weak 3'-splicing sites [28, 31]; and third, the binding of SR (seine/arginine) proteins to positive splicing enhancer elements promoting the recognition of 3'- and 5'-splicing sites [32]. This complex regulatory network leads not only to multiple mRNA species but also to large differences in the relative abundance of each of them, which seems to be decisive for viral replication.

1.6 HIV-1 translation initiation

Despite much progress in understanding of the HIV-1 replication cycle and pathogenesis over the last two decades, little is known about how HIV-1 translation initiation is regulated. As noted above, the interaction between the

primary HIV-1 transcript and the cellular splicing and processing machineries produces nearly 30 distinct capped and polyadenylated HIV-1 RNA species [33]. Although each HIV-1 RNA contains a unique 5'-untranslated region (5'UTR) that varies in length and structure, all of them share the first non-coding 289 nucleotides. Interestingly, ribosomal scanning and translation initiation are inhibited by the presence of highly conserved and structured motifs located within this region such as TAR, poly(A) signal, primer binding site, dimerization signal, and the splicing donor site [34-37]. As a result, unspliced and spliced HIV-1 RNA are thought to be poor substrates for efficient cap-dependent translation, and suggests that HIV-1 translation initiation could be controlled through the presence of internal ribosome entry sites (IRES) within the 5'UTRs [38]. Nevertheless, contradictory results have been obtained in this regard. Using bicistronic reporter constructs, two recent studies have identified IRES containing sequences within the 5'UTR and the *gag* coding sequence [39, 40]. On the other hand, at least three independent studies have concluded that an IRES was not present in the HIV-1 unspliced RNA [34-36]. An intriguing possibility comes from the fact that alternative splicing creates different 5'UTRs with distinctive RNA secondary structures [38], which in turn could be specifically recognized by cellular or viral factors that are capable of differentially modulating viral gene expression. An example of this paradigm is provided by the viral protein Gag and the host protein La autoantigen. Gag binds to the packaging signal sequence within its 5'UTR and inhibits translation at high concentrations, controlling the equilibrium between translation and packaging [41]; whereas La

autoantigen binds to TAR and promotes translation from mRNA containing the 5' HIV-1 leader sequence [42]. Lack of consistent results from the limited number of reports has called for more studies on the regulation of translation initiation of HIV-1 RNA, one of the few under-studied fields in the molecular biology of HIV.

1.7 Regulation of HIV-1 replication and pathogenesis by Tat, Rev and Nef

1.7.1 Tat

HIV-1 gene expression is temporally and spatially controlled by a cascade of sequential regulatory interactions between viral and host proteins. The first level of regulation occurs at transcription. Tat binds to the viral promoter through its direct interaction with a stem-loop target sequence of the nascent RNA transcript called TAR [21, 37]. In addition, Tat targets the cellular kinase P-TEFb (cyclin T1 and CDK9) to the TAR-Tat complex. The functional consequence of the Tat-TAR-p-TEFb complex is the phosphorylation of the C-terminal domain of RNA Polymerase II, which greatly enhances its processivity from the LTR promoter [43, 44], leading to the activation of HIV-1 gene expression. HIV-1 mainly replicates in activated T lymphocytes *in vivo and in vitro* [45]; likewise, the ability of peripheral blood lymphocytes to support HIV-1 replication correlates directly with induction of cyclin T1 and CTD kinase activity upon activation [46, 47], allowing the virus to change from a latent to a replication-active state.

1.7.2 Rev

The second level of regulation occurs at the post-transcriptional level. In higher eukaryotes, only completely spliced mRNA transcripts are exported by the constitutive mRNA export pathway into the cytoplasm for translation, while intron-containing mRNA is confined in the nucleus [48]. As mentioned before, more than 30 different viral mRNA species are present in infected cells. These RNA species include 9-kb unspliced full length transcripts that encode Gag and Gag-Pol; 4-kb singly (singly) spliced mRNA that encodes for Env, Vif, Vpr or Vpu; and 2-kb multiply (completely) spliced mRNA that encodes for Tat, Rev and Nef. In order to export the incompletely spliced and unspliced RNA to the cytoplasm for the synthesis of structural viral proteins and viral genome, HIV-1 has evolved not only to generate these species by inefficient alternative splicing [29, 49, 50], but also to have the capability to export them from the nucleus to the cytoplasm. The latter is accomplished by expression of Rev protein [22, 23]. Because of this, HIV-1 replication cycle can be divided into two phases: a Rev-independent phase and a Rev-dependent phase.

1.7.2.1 Functional domains of Rev

Rev is a 18 kDa predominantly nuclear phosphoprotein [23, 51, 52] and constantly shuttles between the nucleus and the cytoplasm [53]. Two functional domains have been delineated in Rev. The arginine-rich N-terminal domain controls three functions of Rev: a) Binding to Rev response element (RRE), a highly structured RNA sequence present in all incompletely spliced and unspliced

RNA [22, 54]; b) Nuclear and nucleolar localization [55, 56]; and c) Rev oligomerization [57, 58]. The C-terminal domain contains a stretch of leucine-rich amino acid residues and functions as a nuclear exportation signal (NES) [23, 55]. Productive HIV-1 replication requires efficient Rev nucleo-cytoplasmic shuttling activity [59-61].

1.7.2.2 Rev cytoplasmic-nuclear shuttling cycle

The Rev nucleo-cytoplasmic shuttling utilizes the cellular nuclear import and export pathways. Following Rev translation, the shuttling cycle is initiated by nuclear importation of Rev mediated by importin-β (Fig. 3) [62, 63]. Presumably, interaction of importin-β with Ran-GTP induces disassembly of the importin-β/Rev complex and releases Rev into the nucleoplasm [62, 63], where Rev binds in a cooperative manner to the stems IIB and IID of RRE through protein-protein and protein-RNA interactions. The NES of Rev interacts with chromosome maintenance gene 1 (CRM1), a member of the importin-β family receptors [64]. CRM1 interacts with Ran-GTP, establishing the appropriate Rev/RRE/CRM1/RanGTP Ribonucleoprotein (RNP) complex, which is targeted for efficient export through the nuclear pore complex (NPC) [22, 23, 65-68]. It is assumed that Rev is released in the cytoplasm upon RanGTP hydrolysis; however, the exact mechanism of this process remains unknown. Leptomycin B, a CRM-1 inhibitor prevents its interaction with Rev's NES and inhibits Rev nuclear export [69, 70]. Ran plays two roles during nucleo-cytoplasmic transportation of the target cargos. First, it provides energy via GTP hydrolysis.

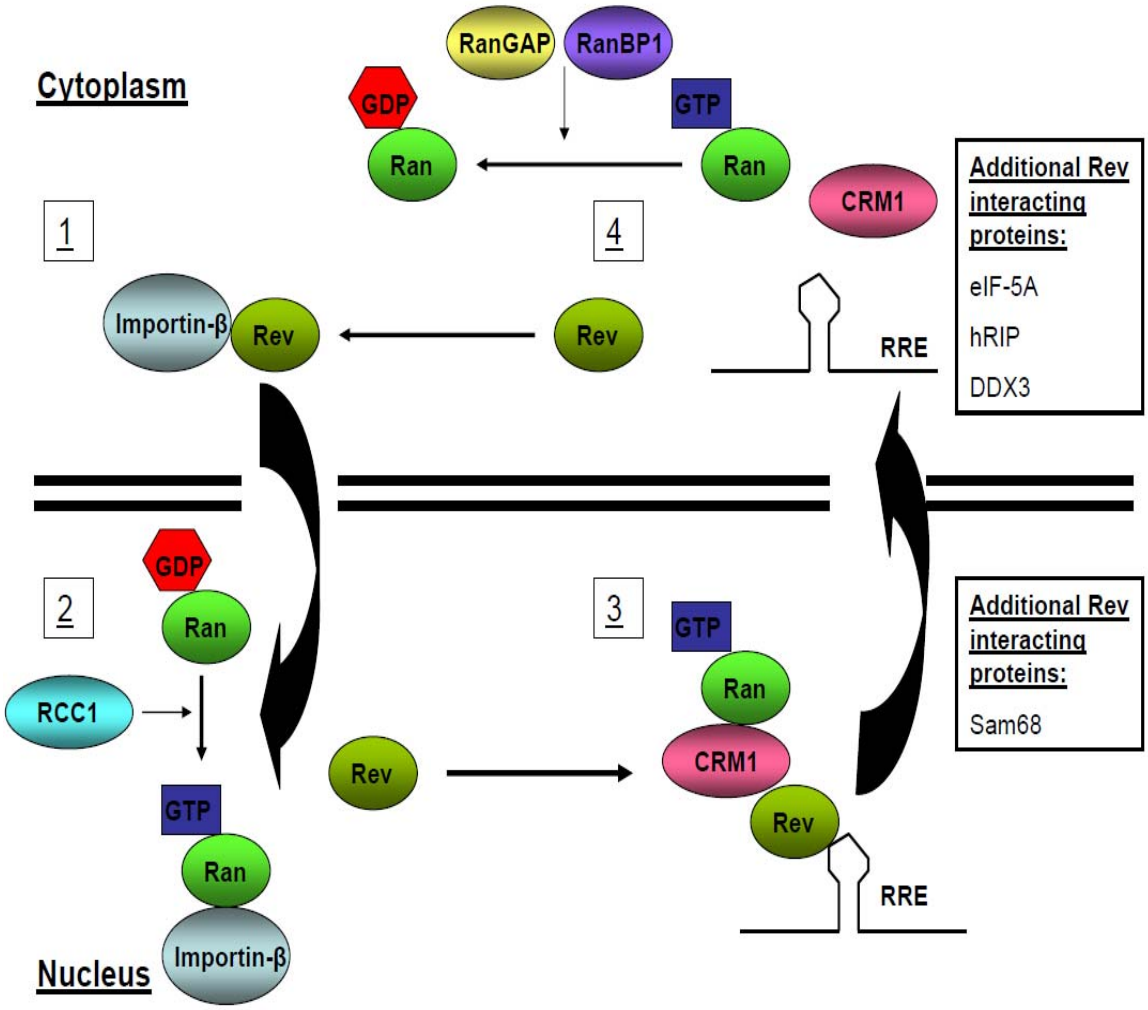

Figure 3. Rev-mediated nuclear exportation of HIV-1 RNA. After translation, Rev is imported to the nucleus by importin-β through interaction via its arginine-rich domain. Once in the nucleus, Rev oligomerizes and interacts with the RRE present in intron-containing HIV-1 RNA. Then, the Rev-RRE RNP complex binds to the nuclear exportation factor CRM1through the NES of Rev. CRM1 localizes to the nuclear pore complex and promotes exportation of the Rev/RRE/CRM1 complex. A cellular RanGDP/RanGTP gradient generated by cytoplasmic RanBP1 and nuclear RCC1 provides the energy for the transport and regulates the association and dissociation of CRM1 and Rev. Additional Rev interacting proteins are indicated.

This is necessary for translocation across the pore. Second, it also provides the directionality through the gradient of RanGTP/RanGDP that exists across the nuclear membrane [71]. The gradient is maintained by the guanine nucleotide exchange factor (GEF), regulator of chromosome condensation 1 (RCC1), the Ran GTPase-activating protein, and Ran binding protein 1(RanBP1). Because RCC1 is an exclusive nuclear protein, GDP is only exchanged to GTP in the nucleus. In contrast, RanGAP and RanBP1 are localized predominantly in the cytoplasm; therefore, GTP hydrolysis mainly occurs in this compartment [72].

1.7.2.3 Cellular proteins interacting with Rev

In addition to CRM1, other cellular proteins have been identified to be directly involved in the Rev-mediated nuclear export pathway, such as eIF-5A [73], hRIP [74-76], DDX3 [77], and Sam68 [78]. Eukaryotic initiation factor 5A (eIF5A) stimulates ribosomal peptidyltransferase activity and it was also identified as a NES binding protein. Further studies have shown that several mutants of eIF5A and antibodies directed to eIF5A specifically abrogate nucleo-cytoplasmic translocation of HIV-1 Rev (Fig. 3) [79, 80]. hRIP was cloned as a NES-interacting protein through a yeast two hybrid screening, it has been shown to be a critical cellular cofactor for Rev function and HIV-1 replication, presumably promoting release of HIV-1 RNA from the perinuclear region [75, 76]. DDX3, a nucleo-cytoplasmic shuttling ATP-dependent DEAD box RNA helicase has been shown to bind CRM1 and to localize to nuclear membrane pores. Its knockdown significantly blocks Rev-RRE function [77]. However, the *in vivo* significance of

these factors in Rev nuclear export of HIV-1 RNA is not fully understood yet. The function of Sam68 in the Rev-RRE exportation cycle will be discussed in more detail in the following sections.

1.7.3 Nef

1.7.3.1 Structural and functional aa residues in Nef

Nef is a 206 amino acid (aa) protein and has a molecular weight of ~25-33 kDa (Fig. 4). It is post-translationally modified by phosphorylation and by myristoylation of its N-terminus, which partially targets Nef to the cellular membrane [16]. Structurally, Nef contains a flexible, non-folded region of ~70aa in length, and a well conserved and folded core domain of ~120aa residues [81]. The core domain contains a consensus SH3 domain-binding sequence (PXXP), which mediates Nef binding to Src-family proteins (Src, Lyn, Hck, Lck, Fyn), regulating their kinase activities [82-85]. Nef also posseses an arginine-rich motif (RR^{105}), which mediates its interaction with PAK protein and subsequently regulates T cell activation and cytoskeletal rearrangement [86]. The flexible regions of Nef contain an acidic region ($EEEE^{62-65}$) required for its paranuclear localization and for its ability to down-regulate MHC-I cell surface expression [87]. Additionally, three pairs of amino acid residues (W^{57}/L^{58}, L^{164}/L^{165}, and D^{174}/D^{175}) have proven to be essential for CD4 down-modulation, by serving as a direct bridge between CD4 and the cellular endocytic machinery [87, 88].

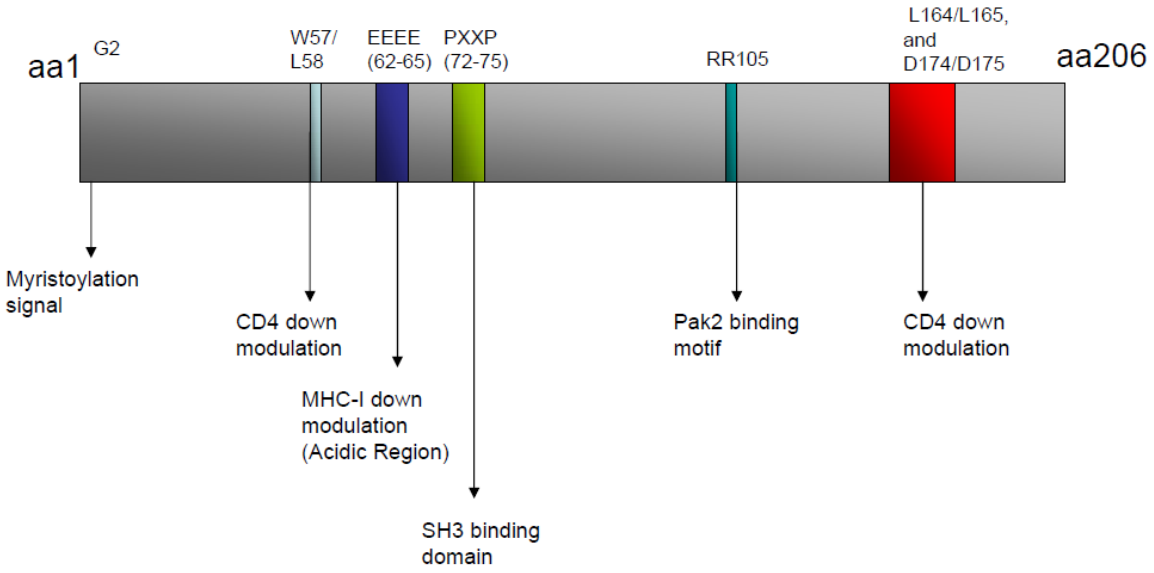

Figure 4. Functional domains of HIV-1 Nef. Each functional domain is represented by a distinct color: myristoylation signal, CD4 down modulation domains in light blue and red; MHC Class I down modulation in dark blue; SH3 binding domain in green; and Pak2 binding domain in turquoise. Relevant amino acids within those domains are also presented on the top.

1.7.3.2 Role of Nef in pathogenesis

Nef is a major pathogenic factor for HIV-1 and simian immunodeficiency virus (SIV). Deletion of the *nef* gene significantly reduces the pathology observed in SIV-infected rhesus macaques [89]. Furthermore, macaques infected with SIV encoding a *nef* gene with a point mutation codifing a premature stop codon rapidly restore the original open reading frame (ORF) [89]. In humans, infection with HIV-1 strains defective in the *nef* gene is correlated with non-progression from HIV-1 infection to AIDS [90-92]. The precise mechanisms by which Nef induces pathogenesis remain unclear. It is proposed to involve: (1) evasion of the immune system by down regulation of CD4 [93-95] and MHC-I molecules [96, 97], (2) activation of signaling pathways [98-100], and (3) enhancement of virus infectivity [101]. Finally, Nef-mediated down-regulation of CD3 surface expression seems to be critical for disease progression. SIV non-pathogenic infection of natural hosts is characterized by efficient down-regulation of CD3 in a Nef-dependent manner, preventing T cell hyper-activation. To the contrary, HIV-1 Nef protein is unable to down-regulate CD3 expression during pathogenic infection [102]; albeit the later study only explains why SIV infection of natural hosts is not pathogenic, this studys emphasizes the relevance of Nef during the *in vivo* infection and disease progression. Taken together, Nef is a required pathogenic factor during HIV-1 infection, and is a potential therapeutic target. The roles of Nef on HIV-1 pathogenesis have recently been thoroughly reviewed by Foster et al. [88].

1.8 HIV vaccines and highly active anti-retroviral therapy (HAART)

1.8.1 HIV vaccines

The complexity of the HIV-1 replication cycle and the unique structural features of the envelope proteins have made development of preventive vaccines extremely difficult, although it still remains as one of the highest public health research priorities [103]. The initial efficacy trials have attempted but failed to induce appropriate antibody responses using recombinant envelope protein gp120 [104, 105]. Probably, the broad array of HIV-1 isolates, with diverse envelope glycosylation patterns contribute to these failures [106]. The difficulty to elicit broad neutralizing antibody responses led to changes in the approaches towards development of non-protective vaccines that would elicit strong T cell responses and delay disease progression. Recently, the first proof-of-concept trial known as STEP, which used an adenoviral vector-based vaccine with peptides from Gag/Pol/Nef proteins, was prematurely terminated due to disappointing results [107]. This MRKad5 HIV-1 candidate vaccine did not prevent the infection nor had an impact on early plasma viral levels. In addition, individuals with prior immunity to adenovirus showed a higher risk to be infected when compared to the placebo group [103]. This recent failure has raised important questions regarding the T cell vaccine approach in light of new insights on the pathogenesis of HIV-1. For example, if the main target of HIV-1 infection is CD4+CCR5+ T cells, the same cells that a vaccine is designed to activate and expand, how likely is it that immunological memory would protect the host from T

cell depletion [108]? At this point, the HIV-1 vaccine field is in a confusing time. Novel approaches are required to overcome unprecedented obstacles.

1.8.2 HAART

Despite continuous disappointments in HIV-1 vaccines, development of anti-retroviral drugs has drastically changed the face of disease progression from an uniformly fatal illness to a manageable chronic disease, reducing AIDS-related mortality by 80-90% in developed countries [109, 110]. Currently, 21 of the 23 anti-retroviral drugs approved by the Food and Drug Administration (FDA) target the viral enzymes from the Pol gene: RT (11), PR (9), and IN (1). Nucleoside/nucleotide analogs and non-nucleoside inhibitors are the two classes of RT inhibitors (Fig. 2). The mechanism of action is to terminate DNA elongation during reverse transcription shortly after viral entry. PR inhibitors target the catalytic site of PR, preventing polypeptide processing and resulting in production of non-infectious viral particles. Raltegravir, the sole IN inhibitor recently introduced inhibits the strand transfer activity during the integration process. The other two anti-retroviral drugs are Enfuvirtide which targets a gp41 region of the viral envelope, hampering the membrane fusion process; and maraviroc, a CCR5 antagonist that prevents the cells from being infected [110, 111]. The initial clinical treatment regimen usually includes a nucleotide analogue RT inhibitor or a PR inhibitor, plus two nucleoside RT inhibitors [109]. Although successful therapy can reduce viral replication to undetectable levels in plasma, current treatment approaches can not eradicate the virus; furthermore, active viral

replication can continue undetected in lymphoid tissue of the gut, with progressive deleterious effects [112]. The emergence of multidrug-resistant viruses due to a high rate of mutation in the viral genome is still a major concern, which highlights the relevance to create new and safer compounds. Importantly, not a single therapeutic agent targeting the HIV-1 regulatory proteins Tat, Rev or Nef has yet been developed. Moreover, the fact that Nef plays a relevant role in disease progression and that Nef is expressed despite prolonged and clinically successful anti-retroviral treatment makes Nef an ideal target for future therapy development [113].

2. STRESS GRANULES

2.1 RNA granules

In 1993, an influential study reported that microinjected fluorescently labeled myelin basic protein mRNA localized in subcellular granule-like domains in oligodendrocytes, and that the structures were persistent, heterogenous in size and transported along microtubules [114]. This work represented the first characterization of mRNA movements in living cells and suggested that non-random localization of mRNA to granule-like structures was an important regulatory mechanism in cytoplasmic mRNA metabolism. Currently, it is well accepted that mRNAs are packaged and transported in ribonucleoprotein (RNP) particles, which are now referred as RNA granules (RG) [115]. In recent years, multiple cytoplasmic RG have been reported in eukaryotic cells. RG are RNP macromolecular structures that can contain ribosomal subunits, translation

factors, mRNA decay enzymes, poly (A) RNA and RNA binding proteins (RBP) [116]; their main function is to transport and regulate the spatial and temporal translation of specific mRNA transcripts [116, 117]. The best described RG to this date are: neuronal granules (NG) [115, 117], germ cell granules (GCG) [116], stress granules (SG) [118] and P bodies [119]; nevertheless, novel types of RG are continuously being reported [120]. Although the components and functions of each RG are different, all of them share two common features: first, they all contain translationally repressed mRNA; and second, multiple RBP can be found in more than one granule [116, 117]. Since the present work focuses on SG, SG function, composition, and assembly are discussed in detail below.

2.2 Biological functions

Cytoplasmic granules involved in the regulation of translation during heat shock were initially identified in the cytoplasm of tomato cells [121]. Since then, functionally similar structures were identified in mammalian cells, and were named stress granules (SG) [122]. Unlike other granules, SG are not present in unstressed cells, but are rapidly (30 min) induced upon exposure to a variety of stressful stimuli (oxidative stress, heat shock, osmotic stress) [122]. Under stressful conditions, mRNAs encoding housekeeping proteins are selectively targeted to SG where they are translationally arrested; allowing the cell to prioritize the synthesis of proteins involved in the stress response (e.g. molecular chaperones) [123]. Even though the sequestration of housekeeping mRNAs is still considered a key function of SG, recent studies have shown that these

complex structures play additional roles in stressed cells [124]. First, studies have shown that RNA and RBP constantly shuttle into and out of SG; Moreover, SG and P bodies are dynamically linked structures. Therefore, SG are currently considered a triage center where mRNA is redirected to reinitiation of translation, decay (P bodies) or storage [125-127]. Second, proteins involved in apoptotic signaling pathways are sequestered in SG under stressful conditions, enabling SG to modulate cell metabolism and survival [128-131]. Finally, the finding that SG also contains RNA-induced silencing complexes (RISC) has led to the proposal that RBP within SG may also regulate microRNA-induced translational silencing under stress [132, 133].

2.3 Composition

SG are composed of RNA, RBP and proteins that are not linked to RNA metabolism. Recently, a new classification for SG protein components has been proposed, in which they are divided into 4 classes based on their biological function and type of recruitent to SG [124].

Class I: This class includes stalled pre-initiation complexes targeted to SG, which include small but not large ribosomal subunits, translation initiation factors (eIF3, eIF4A, eIF4B, eIF4E, eIF4G), poly(A)-binding protein (PABP), and RNA transcripts [124, 134, 135]. These are considered universal markers for SG and the core of this cellular structure.

Class II: It is composed of RBPs involved in translational regulation and/or mRNA stability and decay. These proteins are considered reliable SG markers, although they may not be universal components. Some protein members in this class include: TIA-1 [122], HuR [136], FMRP [137], ZBP1 [138], TTP [125], pumilio [139], smaug [140], ataxin [140], staufen [141], musashi [142], DDX3 [143], PMR-1 [144], PCBP2 [145] and argonaute [132]. This list continues to rapidly grow. It is important to mention that over-expression of some of these proteins result in spontaneous SG assembly.

Class III: It consists of RBPs that regulate aspects of RNA metabolism other than translation or mRNA decay, such as alternative splicing, mRNA transportation, or editing. Members of this class include: G3BP [146], FAST [125], Caprin-1 [147], Proline-rich transcript in the brain protein [148], RHAU [149], hMex-3B [150] ,TDRD3 [151], SMN [152], LINE 1 ORF1p [153], MLN51 [154], Lin28 [155], SRC3 [156], APOBEC3G [157], IP5K [158], NXF7 [159], Grb7 [136], and hnRNP A1 [160]. As is the case for the previous class, some of these proteins induce spontaneous SG assembly when over-expressed.

Class IV: This is a newly discovered class. It includes RBP and proteins that are not related to RNA metabolism, they are recruited to SG through “piggy-back” interactions with SG core components. For example, plakophilin 3 is recruited to SG by G3BP [161]; TIA-1 binds to FAST [128], SRC3 [156], KSRP [162], and PMR1 [144] promoting their recruitment to SG. Other members of this class

include: TRAF2 [129], DIS1 [163], RACK1 [130], and RSK2 [131]. Some of these proteins are not considered reliable SG markers, since their localization is directly dependent on other proteins.

2.4 Assembly

2.4.1 Inhibition of translation initiation

Unsuccessful translation initiation leads to actively translating ribosomes to run off specific transcripts, generating mRNP complexes composed of mRNA and small ribosomal subunits (stalled preinitiation complexes), followed by polysome disassembly and the emergence of SG (Fig. 5). Inhibition of translation initiation and SG assembly can be induced by the phosphorylation of eIF2α [123, 164, 165] or by the eIF2α phosphorylation-independent inhibition of ribosome recruitment [166, 167].

2.4.1.2 eIF2α phosphorylation-dependent

During the translation initiation process, eIF2α delivers the $tRNA^{Met}$ to the AUG start codon in a GTP-dependent manner. eIF2B is a guanine nucleotide exchange factor (GEF) that recharges GDP-charged eIF2α with GTP and allows this process to occur. Phosphorylation of eIF2α Ser51 results in eIF2B inhibition leading to decreased levels of eIF2±GTP±tRNAMet, stalled cap-dependent translation initiation, and SG assembly [122, 134].

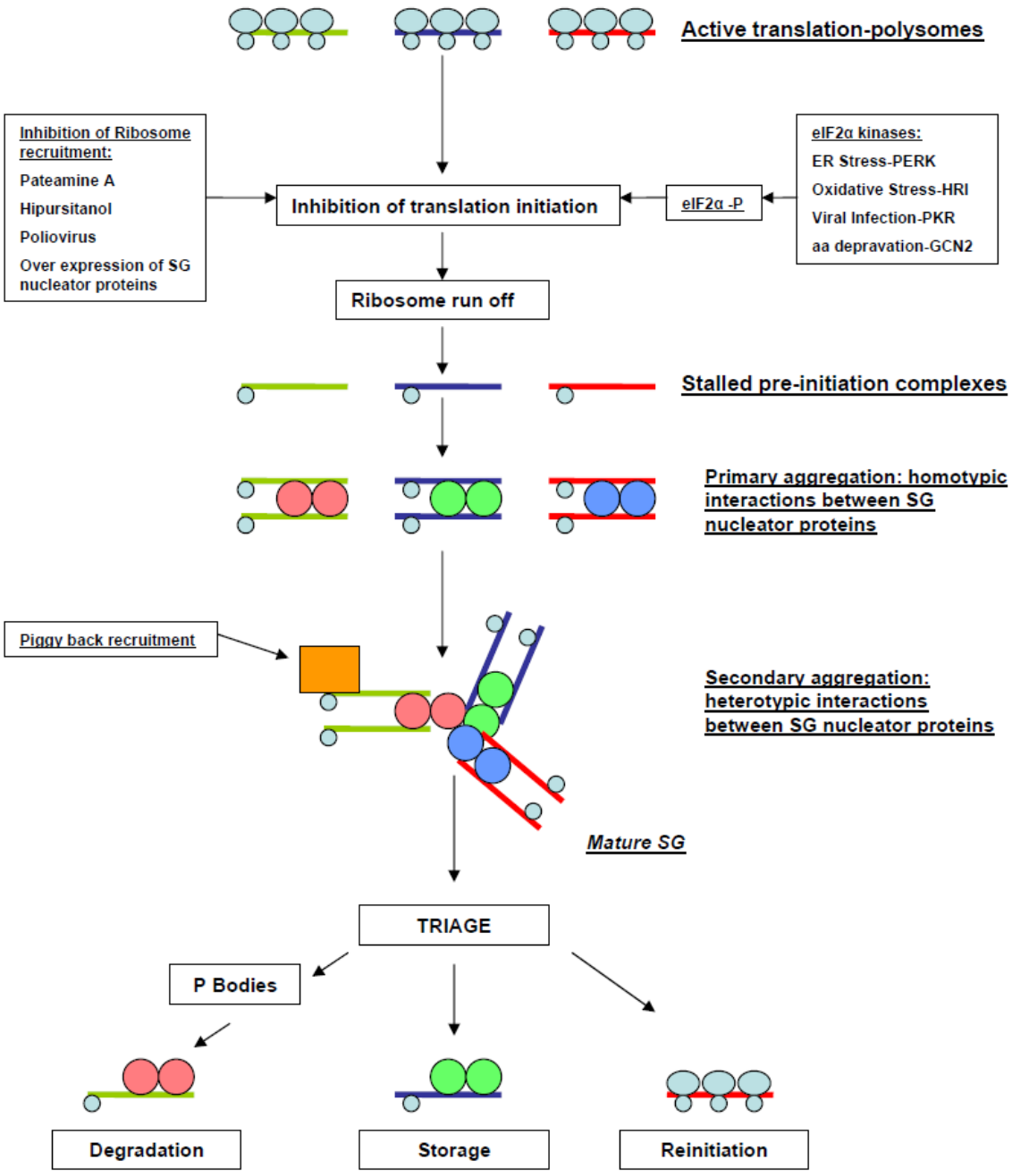
Active translation-polysomes
Inhibition of Ribosome recruitment:
Pateamine A
Hipursitanol
Poliovirus
Over expression of SG nucleator proteins
Inhibition of translation initiation
eIF2α -P
eIF2α kinases:
ER Stress-PERK
Oxidative Stress-HRI
Viral Infection-PKR
aa depravation-GCN2
Ribosome run off
Stalled pre-initiation complexes
Primary aggregation: homotypic interactions between SG nucleator proteins
Piggy back recruitment
Secondary aggregation: heterotypic interactions between SG nucleator proteins
Mature SG
TRIAGE
P Bodies
Degradation
Storage
Reinitiation

Figure 5. **A SG assembly model.** The process of SG assembly can be divided into three sequential steps. Step 1: Inhibition of translation initiation allows the elongating ribosomes to run off transcripts, generating a pool of stalled preintiation complexes, a core component of SG. Step 2: SG nucleator proteins (green, blue and red circles) bind to specific stalled preinitiation complexes and initiate primary aggregation through homotypic interactions, then primary aggregates are cross-linked by heterotypic interactions between SG nucleator proteins during secondary aggregation; in addition, non-core proteins (orange square) are recruited to SG by a "piggy-back" mechanism. Step 3: Within mature SG, transcripts are subjected to triage; they are escorted by SG proteins to P bodies for degradation, retained by RBP in SG for storage, or passively move back to polysomes for active translation.

Different stressful conditions force eukaryotic cells to halt protein synthesis through eIF2α phosphorylation. In mammalian cells, four eIF2α kinases monitor the environment for noxious elements. PERK [PKR (RNA-dependent protein kinase)-like ER kinase] is activated in response to misfolded protein in the ER; HRI (heme-regulated eIF2α kinase) is a sensor of heme depravation and oxidative stress; PKR (protein kinase R) is a double stranded RNA dependent kinase activated during viral infection; and GCN2 (general control non-derepressible-2), which senses amino acids levels through uncharged tRNA and triggers eIF2α phosphorylation during amino acid depravation [168]. Activation of each one of these kinases by thapsigargin treatment (ER stress-PERK) [135], arsenite treatment (oxidative stress-HRI) [169], viral infection (PKR) [170], or proteasome inhibition (GCN2) [164] has been shown to potently induce SG assembly (Fig. 5).

2.4.1.3 eIF2α phosphorylation-independent

Ribosome recruitment to the mRNA template during cap-dependent translation is facilitated by the 5'-cap structure, eIF4F, eIF4B and eIF4H. eIF4F is composed of three subunits: eIF4E, which binds the 5' cap structure; eIF4G, a scaffold protein that promotes the binding between the mRNA template and the preinitiation complex through interactions with eIF4E and eIF3; and eIF4A, an ATP-dependent RNA helicase, which unwinds secondary structure within the 5'UTR of mRNAs, facilitating ribosome recruitment. eIF4B and eIF4H increase the processivity of eIF4A [171]. Two recently described compounds Pateamine

A and hippuristanol inhibit translation initiation through a direct inhibitory interaction with eIF4A [172], leading to SG assembly even in phospho-deprived eIF2α (A^{51}/A^{51}) mutant cells, indicating that eIF2α phosphorylation can be dispensable for SG assembly [166, 167]. In concordance, cleavage of eIF4G by protease $2A^{pro}$ during poliovirus infection results in cap-dependent translation inhibition and induction of short-lived SG [167]. Finally, over-expression of multiple proteins induces SG formation, independently of eIF2α phosphorylation. These proteins are known as SG nucleator proteins [124] and share two important characteristics: first, all of them bind to RNA; and second, they all have the capacity to self-associate (homotypic interactions). It is hypothesized that these proteins prevent ribosome recruitment by directly competing for 48S complexes before initiation is completed, changing the equilibrium between pre-initiation complexes and polysomes and nucleating SG through their self association properties [124].

2.4.2 Primary and secondary aggregation

The mechanism by which proteins and mRNA congregate to form mature SG is not clear, and our understanding is still in the early stage. However, some models have been proposed based on previous studies. Inhibition of translation initiation generates a pool of stalled preinitiation complexes, each one with specific binding motifs given by unique RNA sequences in each transcript. At this point, multiple SG nucleator proteins such as TIA-1 or G3BP bind to specific stalled pre-initiation complexes according to the specificity through their RNA

recognition motifs (RRM), and homotypic interactions initiate primary aggregation of SG (Fig. 5) [118, 124]. Time-lapse microscopy studies have shown that SG assembly begins with formation of numerous small SG, which fuse into larger granules to form a mature structure [125]. Consequently, it is believed that after primary aggregation, heterotypic protein-protein interactions between different SG nucleator proteins cross-link smaller granules forming larger structures, which can then recruit Class IV proteins through a “piggy back” mechanism [124].

2.4.3 Triage of mRNA

Initially thought to be passive compartments for mRNA storage, SG are now considered to be a dynamic triage center that sorts mRNA for storage, decay, or reinitiation under stressful conditions [173]. The initial recognition of the dynamic nature of SG came from early experiments in which treatment with cyclohexamide, a translation elongation inhibitor and polysome stabilizing compound resulted in SG disassembly, revealing that SG and polysomes are in a dynamic equilibrium [127]. Subsequent fluorescence recovery after photobleaching (FRAP) studies have further corroborated this notion, by showing that proteins and RNA rapidly and continuously shuttle in and out of SG [125, 127, 174]. Additionally, different scaffold proteins such as FAST, TTP, BRF1 or CPEB1 have been shown to promote frequent, dynamic and stable contacts between SG and P bodies [125, 126]. The fate of each mRNA within SG (decay, storage, reinitiation) seems to be determined by SG protein components and

RNA binding motifs within each transcript. For example, ZBP1 retains and stabilizes target mRNA within SG, preventing mRNA transfer to P bodies for degradation [138], whereas TTP and BRF1 preferentially bind to transcripts with AU-rich elements (ARE) and promote mRNA decay by escorting them from SG to P bodies [125]. On the other hand, Mollet et al. [174] have reported that mRNA preferentially transits from SG to polysomes, suggesting that the mRNA flow to reinitiation is a passive event and is not mediated by RBP.

2.5 SG and viral infections

In addition to the fundamental role of SG in the translational repression of host mRNA, different lines of evidence also suggest that the SG is an important structure for viral re-programming of the host translation machinery and cellular antiviral defense [124, 175]. Mouse embryonic fibroblasts (MEF) lacking TIA-1 protein are SG deficient and produce significantly higher titers of viruses when infected with vesicular stomatitis virus (VSV), Sindibis virus and herpex simplex virus-1 (HSV-1) [176]. Moreover, infection with poliovirus [177], West Nile virus (WNV) [178], dengue virus [178], Semliki forest virus (SFV) [179] and rotavirus [180] inhibits SG formation at late stages of the infection by specifically targeting SG core components. For instance, WNV and Sendai virus encode an RNA that sequesters TIAR and inhibits SG assembly [124, 178]; Poliovirus protease 3C cleaves G3BP protein preventing SG formation at later infection, and expression of a cleavage-resistant G3BP protein results in persistence of SG and inhibition of viral replication [177]; and Rotavirus protein NS3 promotes the relocation of

PABP-1 from the cytoplasm to the nucleus inhibiting SG assembly, despite potent phosphorylation of eIF2α during infection [180]. Finally, mouse hepatitis coronavirus (MHV) induces SG assembly, which negatively impacts its replication capacity through an unknown mechanism [181]. All of the above suggest that SG function as a cellular antiviral defense mechanism, and that viruses specifically encode factors that help them evade the SG-mediated antiviral effect.

Even though some reports have linked cellular proteins involved in HIV-1 replication or anti-retroviral host factors with SG, the role of SG on HIV-1 replication is not clear. APOBEC3G, a well described cellular retroviral inhibitor incorporates into HIV-1 virions and inhibits replication by deaminating cytidines in the HIV-1 RNA minus strand, leading to lethal hyper-mutated reverse transcripts. HIV-1 Vif protein binds APOBEC3G and induces its degradation, preventing its incorporation into virions and allowing normal viral replication to continue [182]. Two recent studies have demonstrated that APOBEC3G binds to HIV-1 RNA and Vif, and moves with them between translationally active polysomes, SG and P bodies [157, 183]. The functional relevance of this finding has yet to be determined. In addition, DDX3, a highly conserved helicase, which is absolutely required for Rev-mediated nuclear exportation of unspliced HIV-1 RNA [77], also localizes to SG and P bodies during stress, and its over-expression leads to SG assembly, suggesting a possible role of SG during the metabolism of unspliced RNA in the cytoplasm [143, 149]. Finally, in a similar fashion to poliovirus

infection, it has been reported that infection of CD4+ cells with HIV-1 leads to a profound inhibition on cap-dependent translation, due to proteolytic cleavage of eIF4G by HIV-1 PR [184], suggesting that HIV-1 infection may also lead to SG assembly. Nevertheless, to date, there are no reports directly implicating SG assembly in modulation of HIV-1 gene expression or its replication cycle.

3. SAM68

3.1 Historical considerations

Sam68 was initially identified as a tyrosine phosphorylated protein associated with the p120-RasGTPase activating protein (RAS-GAP) in cells transformed with the oncogenes of the tyrosine kinase family including v-Src and called p62 [185, 186]. In 1992, human p62 was purified using affinity chromatography from NIH-3T3 cells transformed with Src using anti-phosphotyrosine antbodies, and the cDNA encoded a 443 aa polypeptide [187]. Two years later, five independent groups identified p62 as a SH3 binding protein [188-192]. Since p62 was a Src substrate during mitosis and migrated at 68 kDa, it was renamed Sam68. A number of Sam68 orthologues and homologues have been cloned from different species [193, 194], showing a high degree of amino acid sequence conservation within the putative functional domains [195]. Sam68 is a RBP which contains a single ribonucleoprotein particle K homology (KH) domain embedded in a larger evolutionary conserved domain, the GSG (GRP33, Sam68 and GLD1) domain [196]. The GSG domain-containing proteins belong to the STAR (Signal Transduction and Activators of RNA) family of proteins [195, 196].

Sam68 is the prototype member, since it has been shown to link signal transduction pathways with RNA metabolism [197]. Other members of the STAR family include: GLD-1, GRP33, QKI, SLM-1, SLM-2, How, Kep-1, and SF-1 [196].

3.2 Sam68 functional domains

As mentioned above, Sam68 contains a KH domain flanked by conserved N- and C-terminal sequences (Fig. 12) with RNA binding activity and the signaling motifs referred to as the GSG (GRP33, Sam68, GLD-1) domain. A number of RNA targets have been identified for the Sam68 GSG domain, including poly(U), poly(A), A/U-rich sequences such as UAAA and UUUA, and several mRNA [190, 198, 199]. In addition, GSG domains confer the ability to STAR family proteins to form homomultimers [200].

Sam68 has six proline-rich domains (P_0-P_5), three in the N-terminal region (P_0-P_2), and three in the C-terminal region (P_3-P_5), which are binding sites for SH3 and WW domain-containing proteins (Fig. 12). Sam68 has been shown to interact with SH3 domains of Vav [201], PRMT2 [202], grb2 [203], Grap [203, 204], p85 PI3K [205], PLCγ-1 [206], Itk [207], Nck [208], and Sik/BRK [209]. Sam68 proline-rich motifs P_3 and P_4, associate with WW domain-containing Formin Binding Proteins FBP21 and FBP30 [210].

The C-terminal region of Sam68 contains 16 tyrosine residues, which are sites of phosphorylation of multiple tyrosine kinases [188, 189, 191, 209, 211]. Tyrosine-

phosphorylated Sam68 associates with numerous SH2-containing proteins including Src family kinases [188-191, 212]. These observations are consistent with the concept that Sam68 may function as an adapter protein [189, 205]. Additionally, tyrosine phosphorylation of Sam68 regulates its subcellular localization [213] and its ability to bind RNA [209].

The predominantly nuclear localization of Sam68 is dictated by a non-conventional nuclear localization signal (NLS) embedded in the last 24 amino acids of its C-terminal domain (Fig. 12) [214]. Single point mutations at amino acids residues 429 and 439, or deletion of the entire C-terminal 24 amino acids results in cytoplasmic localization [78, 214, 215]. Moreover, phosphorylation of tyrosine 440 is required for Sam68 nuclear localization [213], suggesting that signaling pathways may regulate Sam68 subcellular localization.

Finally, STAR family proteins including Sam68 contain RGG boxes, which are important in the regulation of RNA metabolism and are potential sites for arginine methylation [216]. Sam68 interacts with protein arginine methyltransferase I (PRMT I) *in vivo*, and it is methylated in multiple arginine residues [217]. Interestingly, hypomethylated Sam68 is localized in the cytoplasm, whereas methylated Sam68 is located in the nucleus [217]; since methylation is an irreversible post-translational modification, it is suggested that methylation is part of a maturation process during nuclear importation.

3.3 Sam68 function

Although a considerable amount of information on the molecular biology of Sam68 has been accumulated during the last decade, its physiological functions are not fully understood. Like other RBP, Sam68 seems to be a multifunctional protein. To date, Sam68 has been reported to regulate almost every aspect of RNA metabolism: transcription [218], splicing [219], polyadenylation [220], nuclear exportation [221], translation [222, 223], as well as signal transduction [224]. Moreover, Sam68 is also implicated in a significant number of other important cellular processes including cell cycle regulation, apoptosis, tumorigenesis, bone metabolism, and normal brain function [225-227]. Based on the relevance to the current work, only the role of Sam68 in some aspects of mRNA metabolism will be discussed in detail in the following sections.

3.3.1 Nuclear function of Sam68

3.3.1.1 Alternative splicing

In 1999, Sam68 was identified to interact and to co-localize in nuclear dots with the nuclear splicing associated protein YT521 [228]. Since then, multiple interactions between Sam68 and splicing factors such as: U2AF [229], SAFB2 [230], hnRNP A1 [219], ASSP1 [231], and Bim [232] have been reported. As rSLM-2 protein interacts with YT521-B and regulates the splice site selection of CD44 exon v5 [233], Sam68 could be part of a signal transduction pathway that can influence splice site selection.

CD44

Sam68 was defined as the first splicing regulator protein that links signal transduction with alternative splicing [197]. Matter et al. have shown that activation of the Ras-ERK pathway in T lymphocytes triggers the phosphorylation of Sam68 by ERK-1/2, which leads to inclusion of the variable exon v5 of CD44 in a Sam68-dependent manner [197]. Further studies have shown that Sam68 is part of a multiprotein complex with Bim [232], Srm160 [234] and ASSP1 [231], which regulates splice site recognition and/or spliceosome assembly, leading to CD44 v5 exon inclusion. Expression of CD44 isoforms containing exon v5 correlates with enhanced malignancy and invasiveness of some tumors [235]. Interestingly, Sam68 haploinsufficiency delays the onset of mammary tumorigenesis and metastasis [226], but whether this is the result of dysregulation of CD44 expression remains to be determined.

Bcl-x

Sam68 has been implicated in the regulation of cell cycle progression and apoptosis [198, 218, 236, 237]. Apoptosis and alternative mRNA splicing are tightly linked processes. Splicing of mRNAs encoding apoptotic factors can yield proteins with opposite roles during apoptosis [238]. For instance, the antiapoptotic factor Bcl-x(L) and the proapoptotic factor Bcl-x(s) are produced from the Bcl-x transcript through alternative splicing [239]. Recently, it has been demonstrated that Sam68 binds to Bcl-x mRNA *in vivo;* furthermore, depletion or phosphorylation of Sam68 leads to accumulation of Bcl-x(L), whereas its up-

regulation in association with hnRNP A1 increase the leves of Bcl-x(s), which correlates with induction of apoptosis [219].

HIV-1

To date, a role of Sam68 in the regulation of HIV-1 splicing has not been identified [220], despite multiple reports linking Sam68 with HIV-1 RNA metabolism.

3.3.1.2 Exportation of retroviral unspliced RNA

Sam68 was first demonstrated to bind Rev and RRE *in vitro* and/or *in vivo*, and to be capable of substitute and synergize with HIV-1 Rev protein in 1999 [78]. Moreover, Reddy et al. [78] have shown that unlike Rev-mediated exportation, Sam68/RRE-mediated transactivation is insensitive to leptomycin B, a CRM-1 specific inhibitor. As a result, it was proposed that Sam68 activated Rev via a CRM-1-independent pathway. The relevance and specificity of Sam68 interaction with RRE remains controversial, since Sam68 in cooperation with RNA helicase A and TAP [240] can facilitate exportation of intron-containing RNA in the absence of RRE, but in the presence of different retroviral RNA exportation elements such as: CTE, RxRE, ERRE, and RRE2 [222, 240-242].

Using a substractive cloning strategy, our group has shown that HIV-1 expression down-regulates Sam68 expression in human astrocytes [243]. Additionally, human astrocytes constitutively express a lower level of Sam68. Elevation of the endogenous levels of Sam68 in astrocytes considerably restores

HIV-1 Rev function, and modestly increases HIV-1 virus production. Contrary to the previous report, we and others showed that Sam68 is unable to substitute for Rev [221, 222]; furthermore, leptomycin B disrupts the CRM-1 complex in Rev/Sam68-expressing cells, suggesting that Sam68 facilitates Rev nuclear exportation through a CRM-1-dependent pathway [221]. In support of a CRM-1-dependent process, recent independent reports have shown that Sam68 is absolutely required for Rev function and HIV-1 production, its down-modulation causes exclusive nuclear retention and co-localization of Rev and CRM-1, resulting in significant inhibition in HIV-1 replication [221, 244].

To further complicate our understanding of Sam68's role in HIV replication cycle, Sam68 has been reported to enhance p24 expression from a gag-pol reporter plasmid containing a CTE [222]. However, Sam68 over-expression increases the levels of cytoplasmic gag-pol RNA only by two fold, but protein expression by ~45 fold, suggesting that Sam68 may provide a "mark" that affects the cytoplasmic fate of specific mRNA [222]. In agreement with this finding, Mclaren et al. have reported that Sam68 promotes 3'-end processing (cleavage, polyadenylation) of HIV-1 unspliced mRNA, in the absence of a significant increase in the level of unspliced viral RNA in the cytoplasm [220]. Despite the controversy regarding the role of Sam68 in the nuclear exportation pathway of HIV RNA transcripts, two biochemical features of this process have been independently validated. First, Sam68 binding to RNA is required for transactivation of Rev function [222, 245]. As mentioned before, Sam68 binds

RNA through its single KH domain [190, 198, 199] and a RG rich region that confers non-specific RNA binding activity of Sam68 [245]. Sam68 mutants defective for RNA binding activity (ΔKH or ΔRG) fail to functionally promote nuclear exportation of intron-containing RNA [222, 245]. Moreover, tyrosine phosphorylation of Sam68 by $p59^{fyn}$ and Sik/BRK inhibits its ability to bind RNA [222, 246], and also abolishes its capacity to enhance RRE and CTE function [222, 245]. Second, Sam68 binds to Rev *in vitro* and *in vivo* [78, 243]. Reddy et al. [78] have shown that Sam68 and Sam68Δ330-433, but not Sam68Δ1-329 GST fusion proteins interact with Rev protein *in vitro*. Our group has also shown that Sam68 forms a complex with Rev *in vivo,* and that the nuclear exportation signal (NES) of Rev and the region between aa residues 321 and 410 of Sam68 are directly involved in the protein-protein interaction [243]. This suggests that sequences centered around residues 321 to 329 may play a critical role in Sam68 interaction with Rev. Additionally, other functionally relevant *in vivo* interactions between Rev and other STAR family proteins have been reported [247].

3.3.1.3 C-terminal inhibitory mutants

The early finding that Sam68 mutants lacking the C-terminal domain are located in the cytoplasm and inhibit HIV-1 replication has been independently validated [78, 248, 249]. However, the underlying mechanism of this phenomenon has not been determined. One early study has shown that C-terminal mutants impede Rev nuclear localization [78], while another showed that this mutant sequesters RRE containing RNA from the translational apparatus in perinuclear bundles [248]. Sam68 proteins with point mutations within the NLS localize in the cytoplasm and inhibit Rev/RRE transactivation [213, 215], suggesting that cytoplasmic localization, but not the structural changes as a result of amino acid deletions, is a requirement for inhibition of HIV-1 replication. Recently, our group for the first time has provided direct evidence that Sam68 mutants inhibit HIV-1 replication by blocking Rev-dependent nuclear export of HIV-1 viral RNA [249]. Moreover, the domain between aa269 and aa321 is required but not sufficient for HIV-1 Rev inhibition. Interestingly, the preliminary unpublished work from our group has also shown that Sam68 C-terminal mutants not only inhibit Rev-dependent gene expression, but also repress Rev-independent gene expression in the context of HIV-1 replication, providing an important tool for understanding how Sam68 regulates HIV-1 RNA metabolism in the cytoplasm.

3.3.2 Cytoplasmic function of Sam68

Sam68 has a predominant nuclear localization. However, during certain conditions and cellular states, Sam68 localizes to the cytoplasm, suggesting a possible role in signal transduction and RNA metabolism in this cellular compartment.

3.3.2.1 Role of Sam68 in signal transduction

Sam68 contains several protein-protein interaction domains and associates with multiple signaling molecules of the T cell receptor (TCR) [250], leptin receptor [251] and insulin receptor [252] pathways. Sam68 has been found to be tyrosine phosphorylated upon TCR activation by $p59^{fyn}$ [246, 253], ZAP70 [202], and Itk [250, 254], promoting complexes with various signaling proteins such as grb2 [203], Grap [203, 204], p85 PI3K [205], PLCγ-1 [206], and p120GAP [255, 256]. Importantly, Sam68 is tyrosine phosphorylated and recruited to signaling complexes in PBMC from HIV-1 infected individuals, probably due to the increased numbers of activated T cells in the periphery [257]. Sam68 and its role on signaling transduction will not be discussed in more detail. For a thorough review on the topic refer to Najib et al. [224].

3.3.2.2 Sam68: a translational regulator and cytoplasmic RNA granule component

As mentioned above, RNA granules (RG) are RNP macromolecular structures involved in the regulation of mRNA transport, translation and mRNA decay [116, 117]. Although the content and function of each RNA granule is different, all of them contain repressed mRNA, and multiple RBP can be found in more than one granule [116, 117].

3.3.2.2.1 Sam68 and germ cell granules

Germ cells have multiple types of RNA granules that contain translationally repressed mRNA [258]. Germ cell granules (GCG) direct the timing of maternal mRNA translation during a transcriptionally silent period in early embryogenesis [259, 260]. GCG contain polyadenylated mRNA, RNA binding proteins involved in translation and decay, and translation initiation factors [116]. A recent report has shown that Sam68 localizes to the cytoplasm of mouse oocytes and slowly accumulates in the nucleus upon fertilization. Moreover, inhibition of translation in one cell embryos leads to Sam68 accumulation in cytoplasmic granules that also contain RNA and translational initiation factors [261]. These results suggest that Sam68 is involved in translational regulation of maternal RNA. In addition, during meiotic divisions of mouse spermatocytes, Sam68 translocates to the cytoplasm and associates with polysomes, which stresses the possible role of Sam68 in translational regulation during gametogenesis [262].

3.3.2.2.2 Sam68 and neuronal granules

Neuronal granules (NG) are RNP particles that regulate the spatial and temporal translation of specific mRNA in neurons. NG contain mRNA, small and large ribosomal subunits, translational initiation factors, and RBP that regulate translation [116, 117, 263]. Sam68 has been shown to localize to stationary RNA granules in the somatodendritic domain of unstimulated hippocampal and cortex neurons, where it associates with dendritic polysomes [264-266]. In addition, neuron depolarization leads to a significant increase of Sam68 containing granules with anterograde and retrograde movement in dendrites [264], which also correlates with strong induction in the translation efficiency of the recently identified Sam68 mRNA target: eEFA1 [223]. Interestingly, in concordance with previous HIV-1 studies [248, 267], cytoplasmic mutant Sam68Δ410 localizes in NG and leads to translational repression of eEF1A [223]. Further supporting its role as a spatial and temporal translational regulator is an early report that shows Sam68 co-localization with actin mRNA in motile edges of fibroblasts [268].

3.3.2.2.3 Sam68 and stress granules

To date, little is known about the role of Sam68 in host response to external stress. However, several lines of indirect evidence suggest that Sam68 could be recruited into SG. First, GLD-1 is targeted to cytoplasmic particles that resemble P bodies and SG in *C. elegans* [269]. Second, Sam68 translocates and accumulates in cytoplasmic granules during stressful conditions such as poliovirus infection, ischemia, and puromycin treatment, which are also known to

promote SG assembly [167, 261, 270-272]. Likewise, treatment with urate crystals results in Sam68 cytoplasmic localization in neutrophils [273]. Finally, previously well-characterized SG components interact with Sam68 directly or indirectly. For instance, Sam68 interacts directly *in vivo* with FAST [274] and hnRNP A1 [160]; and forms a unique RNP complex with KSRP and intron 6 of the β-tropomyosin gene [275]. The role of Sam68-containing RNA granules in regulation of HIV-1 gene expression is not known.

Summary of the background and the hypothesis

Approximately 34 million people are currently infected with HIV worldwide. In the absence of a successful preventive vaccine, HAART is the only option for these infected individuals today. Nevertheless, despite the success of HAART in reducing viral replication and prolonging the lifespan of HIV-1-infected individuals, HAART can not eradicate the virus from the body; Moreover, multidrug-resistant viruses are still a major concern in clinical settings. Therefore, development of innovative therapeutic strategies against HIV-1 remains a priority. Importantly, not a single therapeutic agent targeting the pathogenic viral factors Tat, Rev or Nef has been developed. Previous studies from our group have shown that the cellular protein Sam68 is absolutely required for efficient HIV-1 replication, and that Sam68-NLS deleted mutants potently inhibit Rev-mediated nuclear exportation and HIV-1 gene expression through a yet to be determined cytoplasmic process [221, 243, 249]. Sam68 is a multifunctional RNA binding protein involved in every aspect of RNA metabolism

including translation. Recent reports indicate that Sam68 and its cytoplasmic mutants are active components of cellular structures involved in translational repression called RNA granules. Therefore, our underlying hypothesis is that Sam68 NLS-deleted mutants inhibit HIV-1 gene expression and replication though a cytoplasmic process involving RNA granules.

MATERIALS AND METHODS

MATERIALS

Media and supplements

Dulbecco's modified eagle's medium (DMEM), Roswell Park Memorial Institute 1640 (RPMI-1640) medium, and Hank's balanced solution (HBSS) were purchased from Lonza (Walkersville, MD). Penicillin-streptomycin-glutamine (100X), and 0.25% Trypsin-EDTA (1X) were purchased from GIBCO (Grand Island, NY). Fetal bovine serum (FBS) was purchased from Hyclone (Logan, UT). Plasmocin was purchased from Invivogen (San Diego, CA). OPTI-MEM reduced serum media was purchased from Invitrogen (Carlsbad, CA). Ampicilin sodium salt, kanamycin sulfate, imidazol and chloranphenicol were purchased from United States Biological (Swampscott, MA). All the culture media described below were prepared in house. Luria Broth (LB) liquid medium contained 0.01g/ml Bacto Tryptone, 0.005 g/ml Bacto yeast extract, 0.005 g/ml NaCl, and 1 mM NaOH. LB solid culture plates were prepared by adding 15 g Bacto agar to 1L of LB liquid medium. Working concentrations of antibiotics for liquid and solid LB were as follows: ampicilin 100 µg/ml, kanamycin 50 µg/ml, chloranphenicol 20 µg/ml. Super Optimal Broth (SOB) contained 0.02 g/ml of Bacto Tryptone, 0.005 g/ml of Bacto yeast extract, 0.5 mg/ml NaCl, 10 mM $MgCl_2$, and 10 mM $MgSO_4$. Super Optimal Broth with catabolite repression (SOC) contained 100% SOB medium and 20 mM glucose. Liquid YPD medium contained 0.02 g/ml of Difco

peptone, 10 mg/ml of yeast extract, and 2% dextrose, pH 5.8. Synthetic defined (SD) liquid media contained 0.6 mg/ml of complete amino acid supplement mixture minus histidine-leucine-tryptophan-uracil from Bio101 (Vista, CA), and 2% dextrose, pH 5.8. YPD and SD solid culture plates were prepared by adding 20 g Bacto agar to 1L of YDP or SD liquid medium, respectively.

Antibodies

Mouse anti-JR-CSF Nef (1:750, donated by Dr. K. Krohn and Dr. V. Ovod), mouse anti-Tat (1:500, donated by Dr. J. Karn) and mouse anti-Rev antibodies (1:500, donated by Dr. A. Szilvay) were obtained from the National Institutes of Health (NIH) AIDS Research and Reference Reagent Program. Sheep anti-Rev (1:2500) was from Fitzgerald (Concord, MA). Mouse anti-HA (1:1000), goat polyclonal anti-eIF3η (N20, 1:75), goat polyclonal anti-TIA-1, rabbit and mouse anti-Sam68 (1:1000), phycoerythrin (PE)-conjugated rabbit α-mouse IgG (1:175), PE-conjugated donkey anti-goat, fluorescein isothiocyanate (FITC)-conjugated donkey α-goat (1:50), FITC-conjugated goat α-mouse (1:50), rhodamine (Rh)-conjugated mouse α-rabbit (1:75), Rh-conjugated goat α-rabbit (1:50), and Rh-conjugated bovine anti-mouse (1:75) were from Santa Cruz Biotechologies (Santa Cruz, CA). Rabbit anti-GFP (1:250) was from Clontech (Mountain View, CA). Mouse anti-β-actin (1:3500), anti-sheep Horse Radish Peroxidase (HRP), normal mouse IgG, and normal rabbit IgG were from Sigma (St. Louis, MO). Anti-mouse-HRP and anti-rabbit-HRP were from GE healthcare (Buckinghamshire, UK). Anti-phospho-ERK 1/2 (1:1000), anti-ERK 1 (1:1000),

anti-phospho-JNK (1:1000), anti-JNK (1:1000), anti-phospho-p38 (1:1000), anti-phospho-eIF2α (Ser51) (1:1000), and anti-eIF2α antibodies (1:1000) were from Cell Signaling technologies (Danvers, MA). Mouse anti-G3BP (1:75) was from BD transduction laboratories (Franklin Lakes, NJ). Anti-human MHC-I hybridoma supernatant was a generous gift from Dr. Janice Blum (Indiana University).

Reagents

Poly(A)x(dT) and random hexamers were purchased from Roche (Indianapolis, IN). Actinomycin D (Act D), propidium iodide (PI), RNase A, phytohemagglutinin (PHA), o-nitrophenyl β-d-galactopyranoside (ONPG), poly-L-Lysine, polybrene, isopropyl-beta-D-thiogalactopyranoside (IPTG), phenylmethanesulphonylfluoride (PMSF), adenosine periodate oxidized (AdOx), and 4',6'-diamidino-2-phenylindole (DAPI) were from Sigma. [Methyl-^{3}H]-thymidine 5'triphosphate was from PerkinElmer (Boston, MA). [α-^{32}P] dCTP specific activity ~800 Ci/mmol, and [γ-^{32}P] ATP specific activity ~7000 Ci/mmol were from GE Healthcare (Piscataway, NJ). D-threo-[dichloroacetyl-1-^{14}C] chloranphenicol, Ficoll-Paque^{TM}, and ECL chemiluminescence reagent for Western blot detection were from Amersham Biosciences (Piscataway, NJ). Restriction endonucleases were from New England Biolabs (Beverly, MA). T4 DNA ligase and T4 polynucleotide kinase with their respective 10X reaction buffers were from USB (Cleveland, OH). TRIZOL, Superscript III reverse transcriptase, and lipofectamine 2000 were from Invitrogen. Mounting solution fluoromount-G was from SouthernBiotech (Birmingham, AL). Bactotryptone, Bacto Yeast Extract, Bacto peptone, Bacto

agar for LB bacteria culture and YDP culture media were from Becton Dickinson (Sparks, MD). Complete amino acids supplement mixture minus histidine-leucine-tryptophan-uracil for SD culture medium was from Bio101. RNasin RNase inhibitor and deoxynucleotide triphosphates (dNTPs -dATP, dCTP, dTTP, and dGTP-) were from Promega corporation (Madison, WI). Sodium arsenite was from Sigma-Aldrich (Germany). Protease inhibitor cocktail set V, EDTA-Free and G418 sulfate were from Calbiochem (LaJolla, CA). Ni-NTA agarose was from Qiagen (Valencia, CA). Coomassie Blue was from Bio-Rad laboratories (Hercules, CA). NCp7(1-71) and NCp7(12-53) purified proteins generated by peptide synthesis were kindly provided by Dr. Jean Luc Darlix (École Normale Supérieure de Lyon, France). All other chemicals were from Fisher (LaGrange, KY).

Biotechnology Systems

The Expand high fidelity PCR system and Expand long template PCR system were from Roche. The AmpliTaq Gold PCR system was from Applied Biosystems (Branchburg, NJ). The Quickchange II Site directed mutagenesis kit and Strataclone PCR cloning kit were from Stratagene (Cedar Creek, TX). The TOPO TA cloning kit was from Invitrogen. The plasmid DNA purification kits, the firefly and *renilla* luciferase assay systems, the Wizard SV Gel and PCR clean-up system for purification of DNA fragments from agarose gels, and the Wizard DNA clean-up system for purification of PCR products were from Promega Corporation. Nucleofector V kit for Jurkat cell transfection and human T cell

Nucleofector Kit for PBMC transfection were from Amaxa biosystems (Gaithersburg, MD). Bio-Rad DC Protein Assay was from Bio-Rad Laboratories. Centricon 50 spin columns for protein concentration and desalting were from Millipore (Billerica, MA). Microspin columns 6-50 for purification of radioactively labeled oligonucleotides were from Amersham Biosciences.

METHODS

Cells and cell cultures

Cell lines

Human embryonic kidney 293T cells, African green monkey kidney COS-7 cells, cervical carcinoma Hela cells, and Jurkat lymphocytic cells were purchased from the American Tissue Culture Collection (ATCC, Manassas, VA).

Stable cell lines

A killing curve for Hela cells was performed to establish Hela.cDNA3 and Hela.Δ410 stable expressing cell lines. Briefly, 1.5 x 10^4 Hela cells were plated in triplicate in a 96-well plate and incubated 24 hr to reach 30% confluency. At this point, the medium was replaced with fresh DMEM medium containing increasing concentrations of G418 (0 µg/ml, 100 µg/ml, 200 µg/ml, 300 µg/ml, 400 µg/ml, 500 µg/ml, 600 µg/ml, 700 µg/ml, 800 µg/ml, 900 µg/ml, 1000 µg/ml, 1200 µg/ml), and cell survival was determined during a period of 6 days. The

medium was replaced every 48 hr. The appropriate concentration of G418 for selection of stable expressing cells was determined to be 500 µg/ml.

Four million Hela cells were plated in a 10-cm a tissue culture plate and incubated for 24 hr until a 70-90% cell confluency was reached. Ten micrograms of cDNA3 or HA.Δ410 DNA plasmids were transfected into these cells using lipofectamine 2000 (Invitrogen) according to the manufacturer's instructions. Twenty four hours after transfection, the medium was replaced with fresh DMEM medium containing 500 µg/ml of G418, and the cells were incubated for a period of two weeks to select stable expressing cells, the medium was replaced every 48-72 hr.

Competent cells for cloning and for protein production

GC5™ chemically competent *E. coli* for cloning, and *BL21 E. coli* for protein production were purchased from GeneChoice (Frederick, MD).

Cell cultures

293T, COS-7, and Hela cells were maintained in DMEM supplemented with 10% fetal bovine serum (FBS), 100 units/ml of penicillin G sodium, 100 µg/ml of streptomycin sulfate, 0.292 mg/ml of L-glutamine, and 5 µg/ml of plasmocin, at 37°C with 10% CO_2. Hela.cDNA3 and Hela.Δ410 stable expressing cell lines were maintained in DMEM supplemented with 10% FBS, 100 units/ml of penicillin G sodium, 100 µg/ml of streptomycin sulfate, 0.292 mg/ml of L-

glutamine, and 300 µg/ml of G418, at 37^{o}C with 10% CO_2. Jurkat cells were maintained in RPMI 1640 medium supplemented with 10% FBS, 100 units/ml of penicillin G sodium, 100 µg/ml of streptomycin sulfate, 0.292 mg/ml of L-Glutamine, and 5 µg/ml of plasmocin, at 37^{o}C with 5% CO_2.

Isolation and culture of peripheral blood mononuclear cells

Peripheral blood (PB) was obtained from the Indiana Blood Center (Indianapolis, IN). Isolation of PBMC was performed by the Ficoll-Paque density gradient centrifugation. Briefly, 10 ml of PB were mixed with 20 ml of HBSS, transferred to 50 ml conical tubes, and then 15 ml of Ficoll-Paque was added to the bottom of the tube slowly. Six 50 ml conical tubes containing the mixture were centrifuged at 785*g* with no brake at room temperature (RT). The white layer with mononuclear cells was then transferred to a clean 50 ml conical tube, the volume was brought up to 50 ml with HBSS, followed by centrifugation at 440*g* for 5 min. The washing step was repeated twice. Thereafter, the cells were counted, suspended at a density of 2.5 x 10^6 cells/ml, and cultured in RPMI 1640 medium supplemented with 10% FBS, 100 units/ml of penicillin G sodium, 100 µg/ml of streptomycin sulfate, 0.292 mg/ml of L-glutamine, 3 µg/ml of phytohemagglutinin (PHA), and 50 units/ml of IL-2, at 37^{o}C with 5% CO_2. The medium was changed every two days during the length of the experiment.

Plasmids

Reporter viruses: pNL4-3.Luc(env) and pNL4-3.Luc(nef) reporter viruses were previously generated in our laboratory (unpublished). pNL4-3.Luc(env) was constructed by inserting the firefly luciferase (F Luc) gene in-frame at the nt. 6310 of NL4-3 genome (GenBank # AF 324493) with a stop codon at the 3'-end of the Luc gene. A linearized NL4-3 was obtained by PCR using the NL4-3 as the PCR template and the primers 5'-TCC CCC GGG AGC ACT ACA GAT CAT CAA TA-3' and 5'-GCT CTA GAA CAG AAA AAT TGT GG TCA C-3', while the Luc gene was obtained by PCR using the pGL3-basic (Promega Corporation) as the template and the primers: 5'-TCC CCC GGG GAA GAC GCC AAA AAC ATC AA-3 and 5'-GCT CTA GAA TTA CAC GGC GAT C-3'. Both DNAs were digested with Sma I and Xba I and ligated to obtain pNL4-3.Luc(env). Similarly, pNL4-3.Luc(nef) was constructed by inserting the Luc gene in frame at nt. 8795 of NL4-3 genome with a stop codon at the 3'-end of the Luc gene. The primers for NL4-3 were 5'-TCC CCC GGG GCC ACC CAT CTT ATA GCA AAA T-3' and 5'-GCT CTA GAA AGT GGT CAA AAA GTA GTG TGA-3', and the primers for the Luc gene were the same as above. Both DNAs were digested with Sma I and Xba I and ligated to obtain pNL4-3.Luc(nef).

Sam68 mutants: HA-tagged Sam68 and deletion mutants HA.Δ410, HA.Δ321, HA.Δ269, HA.Δ269-321, HA.269-321; as well as GFP.Sam68, RFP.Sam68, and RFP.Δ410 were previously constructed in our laboratory and described elsewhere [221, 249]. GFP.Δ410 was previously generated in our laboratory

(unpublished). Briefly, Δ410 was obtained by PCR using HA.Sam68 as the PCR template and the primers 5'-GGG GTA CCA TGC AGC GCC GGG ACG AC-3' and 5'-GGA ATT CTT AAG CTT CAT AAG AAT CTT GAA C-3'. The PCR product and the pEGFP-C1 vector (Clontech, Carlsbad, CA) were digested with Sac I and EcoR I and ligated to obtain GFP.Δ410. GFP.Δ269-321, and GFP.269-321 were previously generated in our laboratory (unpublished). Briefly, for GFP.Δ269-321, GFP.Sam68 and HA.Δ269-321 were digested with EcoR V and Hind III, the fragment obtained from HA.Δ269-321 was inserted into the digested GFP.Sam68 backbone to obtain GFP.Δ269-321. For GFP.269-321, the 269-321 fragment was PCR amplified using HA.269-321 as a template and the primers 5'-TAA TAC GAC TCA CTA TAG G-3' and 5'- CGC GGG CCC TTA TCC CCT TAC TGG TGT ACC-3'. The PCR product and pEGFP-N3 (Clontech) were digested with EcoR I and Sma I and ligated to obtain GFP.269-321. GFP.Δ321, and GFP.Δ269 were constructed as follows: Δ321 and Δ269 fragments were PCR amplified using GFP.Sam68 as the PCR template and the same forward primer 5'-TCG AGC TCA AAT GCA AGC GCC GGG ACG AC-3', with respective reserve primers 5'- CCG GAA TTC TTA TCC CCT TAC TGG TGT ACC ACG TAC C-3' or 5'- CCG GAA TTC TTA ATC ATC CAT CAT ATC CGG TAC TAG-3'. The PCR program used was: 94^{o}C for 4 min, 10 cycles of 94^{o}C for 45 sec, 58^{o}C for 45 sec and 72^{o}C for 1:30 min, followed by 35 cycles of 94^{o}C for 55 sec, 62^{o}C for 1 min and 72^{o}C for 1.5 min, and one cycle of 72^{o}C for 7 min. The PCR products and the pEGFP-C1 vector (Clontech) were digested with Sac I and EcoR I and ligated to obtain GFP.Δ269 and GFP.Δ321. HA- and GFP-tagged

ΔKH and Δ410ΔKH were constructed in the context of respective parental plasmids HA/GFP.Sam68 or HA/GFP.Δ410, using the QuickChange Site-Directed Mutagenesis kit (Stratagene), and with the primers 5'-CCT GTC AAG CAG TAT CCC AAG CTT CGC AAA GGT GGA GAC CC-3' and 5'-GGG TCT CCA CCT TTG CGA AGC TTG GGA TAC TGC TTG ACA GG-3'. The PCR program used was: 95°C for 1 min, followed by 18 cycles of 95°C for 50 sec, 55°C for 1 min and 68°C for 7 min, and one cycle of 68°C for 7 min. Finally, RFP.Δ321, RFP.Δ269, and RFP.Δ269-321 were constructed by digesting GFP.Δ321, GFP.Δ269, and GFP.Δ269-321 with EcoR I and Sac I, followed by ligation of the respective fragments to the previously digested pDsRed-C1 (Clontech) backbone.

pNL4-3 minigenes: tat, rev, nef, and *nef* deletion minigenes were constructed using pNL4-3 as a backbone and template. pNL4-3 contains unique restriction sites for BssH II (nt. 711) and Hpa I (nt. 8650). *tat* minigene sequence (nt. 711-744, 5777-6044, 8396-8650), and *nef* minigene sequence (nt. 711-744, 5976-6044, 8396-8650) were chemically synthesized and cloned into the pUC57 backbone (Genscript, Worcester, MA). Both *tat* and *nef* minigenes were generated by cloning *tat* and *nef* minigene fragments from pUC57 into the corresponding BssHII and HpaI site of pNL4-3. *rev* minigene and *nef* deletion minigenes were generated with a QuickChange site-directed mutagenesis kit (Stratagene). *rev* minigene was obtained using *tat* minigene as a template and the primers 5'-GAG GGG CGG CGA CTG GTT TGT TTC ATG ACA AAA-3' and

5'-TTT TGT CAT GAA ACA AAC CAG TCG CCG CCC CTC-3'. The PCR program used was: 95°C for 1 min, followed by 18 cycles of 95°C for 50 sec, 55°C for 50 sec and 68°C for 8 min, and one cycle of 68°C for 7 min. *nef* Δ5UTR minigene was constructed using *nef* minigene as a template and the primers 5'-TGA CCA CTT GCC ACC CAT CTT ATA CCA GTC GCC GCC CCT CGC CTC TTG-3' and 5'-CAA GAG GCG AGG GGC GGC GAC TGG TAT AAG ATG GGT GGC AAG TGG TCA-3'. The PCR program used was 95°C for 1 min, followed by 18 cycles of 95°C for 50 sec, 55°C for 50 sec and 68°C for 7.5 min, and one cycle of 68°C for 7 min. Finally, *nef* Δ3'UTR minigene was constructed using *nef* minigene as a template and the primers 5'-GAG TAC TTC AAG AAC TGC TGA AAT AAA GCT TGC CTT GAG TGC-3' and 5'-GCA CTC AAG GCA AGC TTT ATT TCA GCA GTT CTT GAA GTA CTC-3', with a PCR program of 95°C for 1 min, followed by 18 cycles of 95°C for 50 sec, 55°C for 50 sec and 68°C for 7.5 min, and one cycle of 68°C for 7 min.

Yeast three hybrid plasmids: pIIIA/MS2-2, pACTII, pAD-IRP, pBTM116, and pIIIA/IRE-MS2 were kindly provided by Dr. Marv Wickens of University of Wisconsin, Madison. Hybrid proteins Δ410, Δ269, and ΔKH with LexA DNA binding domain were previously constructed in our laboratory (unpublished), in the context of the plasmid pBTM116. pACTII/MS2 was generated by digesting pBTM116/MS2-2 with BamH I to liberate MS2 sequence, followed by ligation to the previously digested pACTII, right orientation of the insert was confirmed by Sal I digestion. pSCA-nef-3'UTR was constructed using the Strataclone PCR

cloning kit (Stratagene), and the primers 5'-TCC CCC GGG GAG GCT TAA GCA GTG GGT TC-3' and 5'-TCC CCC GGG CAT CGA GCT TGC TAC AAG GG-3'. For pMS2-Nef-3'UTR and pMS2-Nef-3'RTU, pSCA-nef-3'UTR was digested with EcoR I, and the appropriate DNA fragment was ligated into previously digested pIIIA/MS2-2, the orientation of the insert was checked with Sac I digestion.

Other plasmids: pcDNA3-βGal was constructed by digesting pCMVβ plasmid (Clontech) with Not I, and then the β-galactosidase gene was cloned at the Not I site of pcDNA3 (Invitrogen). pTopoSam68 was constructed using the TOPO TA PCR cloning kit (Invitrogen), and the primers 5'-CGG AAT TCC AGC GCC GGG ACG ACC CCG-3' and 5'-ATC CGC TCG ATT AAT AAC GTC CAT ATG GGT G-3', with a PCR program of 94^{o}C for 45 sec, 10 cycles of 94^{o}C for 45 sec, 57^{o}C for 45 sec and 72^{o}C for 1.5 min, followed by 30 cycles of 94^{o}C for 45 sec, 61^{o}C for 1 min, and 72^{o}C for 1.5 min, and one cycle of 72^{o}C for 7 min. For pETSam68 (pHis-Sam68), pTopoSam68 was digested with EcoR I, and the appropriate DNA fragment was ligated into previously digested pET30a(+) vector (Novagen, Gibbstown, NJ), the orientation of the insert was checked with EcoR V and BamH I digestion. For GFP-hdcp-1α, the hdcp1-α ORF was amplified using full-length hdcp-1α cDNA (Open Biosystems, Huntsville, AL) as the PCR template and the primers 5'- CCG GAA TTC TCA TAG GTT GTG GTT GTC TT-3' and 5'-GTC GAG CTC AAG AGG CGC TGA GTC GAG-3', with a program of 94^{o}C for 30 sec, 10 cycles of 94^{o}C for 30 sec, 51^{o}C for 45 sec, and 72^{o}C for 1.5 min, followed by 25 cycles of 94^{o}C for 30 sec, 60^{o}C for 45 sec, and 72^{o}C for 1.5 min,

and one cycle of 72^{o}C for 7 min. The PCR products and the pEGFP-C1 vector (Clontech) were digested with Sac I and EcoR I and ligated to obtain GFP hdcp-1α. Tat-myc and Nef-myc were previously generated in our laboratory (unpublished). pHCMVG was a kind gift from Dr. Joseph Sodroski of Harvard School of Medicine. The constitutively active MEK plasmid (pCA-MEK) was kindly provided by Dr. Lawrence Quilliam (Indiana University School of Medicine). The following plasmids were obtained from the NIH AIDS Research and Reference Reagent Program, Division of AIDS, NIAID, NIH: pNL4-3 by Dr. M. Martin, pYK-JR CSF by Dr. I. SY. Chen, pLAI.2 by Dr. K. Peden, pSG3.1 by Dr. S. Ghosh, pYU2, p90CF402.1.8 by B. Hahn, p89.6 by Dr. R. Collman, and pMJ4 by Dr. T. Ndung'u. GFP.TIA-1, GFP.hnRNP A1, GFP.PABP, and GFP-G3BP plasmids were kindly provided by Dr. Sonia Guil and Dr. Javier Caceres [160]. The bicistronic vector pCMV-rLuc-HIV-1IRES-fLuc was kindly provided by Dr. Ann Brasey and Nahum Sonenberg [40].

Bacterial transformation

Twenty five microliters of GC5^{TM} competent cells were mixed with 0.5-1 µl of DNA ligation reaction, and incubated in ice for 30 min. After heat-shocking the cells for 45 sec in a 42^{o}C water bath, 450 µl of RT SOC medium were added to the mixture, and then incubated at 37^{o}C for 1 hr with shacking at 240 rpm. Two hundred to four hundred microliters of culture were spread out evenly on an agar plate containing the appropriate selection antibiotic. The plate was incubated in a 37^{o}C incubator overnight (O/N).

Cell transfections

Calcium phosphate precipitation

Plasmid DNA was transfected into 293T cells with the standard calcium phosphate precipitation method. For a 10-cm tissue culture plate, 2-4 x 10^6 cells were plated and incubated for 24 hr until a 70-90% cell confluency was reached. At this point, 500 µl of a mixture of 20 µg of plasmid DNA and 0.24 M $CaCl_2$ was added dropwise into 500 µl of a 2X HEPES (50 mM Hepes, 10 mM KCl, 280 mM NaCl, 1.5 mM Na_2HPO_4, 12 mM glucose, pH 7.1) solution. The transfection mixture was incubated on ice for 20 min, and added dropwise into 293T cells. After 16 hr of incubation, medium was replaced with fresh complete DMEM. The cells were further incubated for 24-48 hr and then gene expression was examined. When using a different tissue culture plate, the number of cells and all solutions were scaled down proportionally to the surface area of the plate.

Lipofectamine

Plasmid DNA was transfected into COS-7 and Hela cells using lipofectamine 2000 (Invitrogen) according to the manufacturer's instructions. For a 12-well tissue culture plate, 24 hr before transfection, 0.5-2.5 x 10^5 cells were plated in 1ml of complete DMEM without antibiotics, so that cells reached 80-90% confluent at the moment of transfection. At this point, 4.0 µg of plasmid DNA and 2-4 µl of lipofectamine were mixed gently with 100 µl of OPTI-MEM in two separate 1.5 ml tubes, and incubated for 5 min at RT. The diluted DNA and

lipofectamine mixtures were combined and further incubated for 20 min at RT. Thereafter, the transfection mixture was added dropwise into the cells, and after 16 hr of incubation the medium was replaced with fresh complete DMEM. Twenty-four to forty-eight hours after the medium was changed, gene expression was examined. When using a different tissue culture plate, the number of cells and all solutions were scaled proportionally to the surface area of the plate.

Annealed oligonucleotide duplex control and Sam68 siRNAs were purchased from Dharmacon (Lafayette, CO), Sam68 siRNA targeting sequence was 5'-CGG AUA UGA UGG AUG AUA U-3', as described previously [234]. SiRNAs were transfected into 293T cells using lipofectamine 2000 (Invitrogen) according to the manufacturer's instructions. For a 24-well tissue culture plate, 24 hr prior to transfection, 1.5-2.5 x 10^5 cells were plated in 0.5 ml of complete DMEM without antibiotics, so that cells will be 80-90% confluent at the moment of transfection. At this point, 50-200 nM of SiRNA and 1 µl of lipofectamine were mixed gently with 50 µl of OPTI-MEM in two separate 1.5 ml tubes, and incubated for 5 min at RT. The diluted SiRNA and lipofectamine mixtures were combined and further incubated for 20 min at RT. Thereafter, the transfection mixture was added dropwise into the cells, and after 16 hr of incubation the medium was replaced with fresh complete DMEM. Twenty-four to forty-eight hours after the medium was changed, gene expression was examined. When using a different tissue culture plate, the number of cells and all solutions were scaled proportionally to the surface area of the plate.

Nucleofector

For Jurkat T cells: Plasmid DNA was transfected into Jurkat T cells using Nucleofector V kit (Amaxa biosystems) according to the manufacturer's instructions. Forty-eight hours before transfection, cells were plated at a density of 0.25 x 10^6 cells/ml in complete RPMI 1640 medium, so that cells reached a density of 0.5-1.5 x 10^6 cells/ml at the moment of transfection. An aliquot of the cell suspension was used to determine de exact cell density, and the volume of the cell suspension required to obtain 1.0 x 10^6 per sample was centrifuged at 90*g* for 10 min. The supernatant was discarded and the pellet was suspended in RT Nucleofector Solution V to a final concentration of 1.0 x 10^6 /100 µl. Thereafter, 100 µl of the cell suspension solution were mixed with 4.0 µg of plasmid DNA and transfer to an Amaxa certified cuvette. The cuvette was then inserted into the Nucleofector and the program X-05 was used to electroporate plasmid DNA into Jurkat T cells. Finally, the cell suspension solution was transferred to a 12-well plate containing 500 µl of pre-warmed complete RPMI 1640 medium and further incubated for 24 hr. At this point gene expression was determined or HIV-1 infection was performed.

For PBMC: Plasmid DNA was transfected into PBMC cells using human T cell Nucleofector Kit (Amaxa biosystems) according to the manufacturer's instructions. Freshly isolated PBMC were cultured at a density of 2.5 x 10^6 cells/ml for four days in complete RPMI 1640 suplemented with 3 µg/ml PHA, and 50 units/ml IL-2. An aliquot of the cell suspension was used to determine the

exact cell density, and the volume of the cell suspension required to obtain 6.0 x 10^6 per sample was centrifuged at 200*g* for 10 min. The supernatant was discarded and the pellet was suspended in RT human T cell Nucleofector Solution to a final concentration of 6.0 x 10^6/100 µl. Thereafter, 100 µl of the cell suspension solution were mixed with 3.0 µg of plasmid DNA and transfer to an Amaxa certified cuvette. The cuvette was then inserted into the Nucleofector and the program T-20 was used to electroporate plasmid DNA into PBMC. Finally, the cell suspension solution was transferred to a 12 well plate containing 500 µl of pre-warmed complete RPMI 1640 medium and further incubated for 48 hr. At this point HIV-1 infection was performed.

Reporter gene assays

β-Galactosidase activity assay

Cells were harvested in ice-cold phosphate-buffered saline (PBS) and pelleted at 2000*g* for 5 min. Cell pellet was suspended in cell lysis buffers for luciferase or chloramphenicol acetyltransferase (CAT) reporter assays, incubated for 30 min in ice, and then centrifuged at 12000*g* to remove cell debris, and supernatants were used as cell extracts to perform the different reporter assays. To perform β-Galactosidase assay, 10 µl of cell extracts, 3 µl of 100 X Mg^{2+} solution (0.1 M $MgCl_2$, 4.5 M β-mercaptoethanol), 66 µl of 1 X ONPG (4 mg/ml ONPG in 0.1 M Sodium phosphate, pH 7.5), and 201 µl of 0.1 M sodium phosphate (57.7 ml 1 M Na_2PO_4 and 42.3 ml of 1 M NaH_2PO_4, pH 7.5) solution were mixed. The mixture

was incubated at 37^{o}C for 30 min. Then, the optical density of the reaction containing the released o-nytropenyl was measured at 405 nm in a microplate reader (Molecular devices, Sunnyvale, CA).

Luciferase activity assay

Firefly luciferase or *Renilla* luciferase activities were measured using the luciferase assay systems form Promega corporation according to the manufacturer's instructions. Briefly, cells were harvested in ice-cold PBS and pelleted at 2000*g* for 5 min. Cell pellet was suspended in 100-500 µl of 1X firefly or *renilla* luciferase lysis buffers, incubated for 30 min in ice, and then centrifuged at 12000*g* to remove cell debris, supernatants were used as cell extracts. Eighty microliters of firefly or *renilla* luciferase substrate were mixed with 20 µl of cell extract, and then the luciferase activity was determined using an Opticomp Luminometer (MGM Instruments, Hamden, CT) in the form of count per min (cpm). To discard variations due to differences in transfection efficiency, each value was normalized to the β-galactosidase activity.

Chloramphenicol acetyltransferase activity assay

Cells were harvested in ice-cold PBS and pelleted at 2000*g* for 5 min, the cell pellet was then suspended in 100-500 µl of 0.25 M Tris-HCl, pH 8.0. The cell suspension was submitted to three cycles of freezing and thawing, and centrifuged at 12000*g* to remove cell debris, supernatants were used as cell

extracts. To perform CAT assay, 50 µl of cell extracts, 1 µl of D-threo-[dichloroacetyl-1-^{14}C] chloranphenicol, 5 µl of 5 mg/ml B-coenzyme A, 12.5 µl of 1 M Tris-HCl, pH 8.0, and 34 µl of H_2O were mixed. The mixture was incubated at 37^{o}C for 1 hr. Two hundred microliters of 2, 6, 10, 14 tetra-methyl (TMPD)/Xylene (2:1) solution were added to the mixture, and after 1 min of vigorous vortexing the solution was centrifuged at maximum speed for 2 min. The top phase was then transferred to a scintillation vial, and radioactive activity was determined using a Beckman LS6000IC Scintillation counter (Fullerton, CA). The β-galactosidase activity was used to normalize differences in transfection efficiency among transfections.

Reverse transcriptase (RT) activity assay

One milliliter of cell culture supernatants was centrifuged at 4^{o}C for 1.5 hr at 14000*g*. The virus pellet was suspended in 10 µl of dissociation buffer (0.25% Triton-X-100, 20% glycerol, 0.05 M Tris-HCl pH 7.5, 1 mM DTT, and 0.25 M KCl) followed by three cycles of freezing and thawing. A forty microliter mixture of 34 µl of RT assay buffer (0.083 M Tris-HCl pH 7.5, 0.008 M DTT, 0.0125 M $MgCl_2$ and 0.083% Triton-X-100), 1 µl of ^{3}H dTTP, and 5 µl of 5 units/ml of Poly (A)x(dt) was added to the above 10 µl virus suspension. The total 50 µl mixture was incubated at 37^{o}C for 1 hr and then spotted onto DE81 filters (Whatman, England). After three washes with 2XSSC (0.3 M NaCl, 0.03 M sodium citrate, pH 7.0), radioactivity of each filter was determined in a Beckman LS6000IS scintillation counter, and the virus titer was expressed as cpm per ml.

HIV-1 stock preparation and infection of Jurkat T cells and PBMC

The HIV-1 virus used in this study was the VSV-G pseudotyped NL4-3.Luc(env) virus. Two to four million 293 T cells were plated in a 10-cm tissue culture plate and transfected with 3 µg of pHCMVG expressing the VSV-G envelope and 18 µg of pNL4-3.Luc(env) by standard calcium phosphate transfection. Forty-eight to seventy two hours after transfection, culture supernatants were harvested, centrifuged briefly to remove cell debris, and stored at -80^{o}C. The virus titer was determined by the RT assay.

Three million Jurkat T cells and 18 x 10^6 PBMC, that were previously transfected by the nucleofector method, were centrifuged at 90*g* and 200*g*, respectively. The cell pellet was suspended in 1ml of DMEM medium containing 50 x 10^5 cpm of VSV-G pseudotyped NL4-3.Luc(env) virus, 8 µg/ml polybrene, and incubated for 6 hr at 37^{o}C, 5% CO_2, with periodic flicking to suspend the cells. The cells were centrifuged briefly as above, and washed one time with 10 ml of PBS to remove remaining free viruses. The infected cells were then suspended in 10 ml of complete RPMI 1640 medium, and allowed them to grow for 48 hr before they were harvested and assayed for Nef expression by Western blot analysis, and MHC-I cell surface expression by flow cytometry.

Immunoblotting

Cells were harvested in ice cold PBS and pelleted at 2000*g* for 5 min, and unless otherwise indicated, cell pellets were suspended in 2 vol. of RIPA buffer (10 mM $NaHPO_4$, 150 mM NaCl, 1% Triton X-100, 0.1% sodium dodecyl sulfate, 0.2% sodium azide, 0.5% sodium deoxycholate, 0.004% sodium fluoride, 1 mM sodium orthovanadate, and 1x protease inhibitor cocktail) and incubated on ice for 30 min. Whole-cell lysates were obtained by centrifugation at 12000*g* to remove cell debris, and the protein concentration was determined using a Bio-Rad DC protein assay kit (Bio-Rad). An equal amount of protein (15-100μg) in the whole cell lysates was separated by 7.5-15% sodium dodecyl sulfate-polyacrylamide gel electrophoresis (SDS-PAGE), and then electrotransfered to the HyBond-P membrane (Amersham). The membranes were blocked for one hour in 5% milk in TBST buffer solution, followed by probing with specific primary antibodies and then appropriate HRP-labeled secondary antibodies. Chemoluminescence visualization was performed using an ECL system (Amersham). Relative levels of protein were determined by densitometric scanning of the blots using the housekeeping gene β-actin as an internal standard. In case that phosphorylated proteins were to be detected, cells were lysed in phosphorylation lysis buffer (30 mM Tris-HCl pH 7.4, 150 mM NaCl, 1% Triton X-100, 0.1% SDS, 10 mM EDTA, 1 mM sodium orthovanadate, 160 mM sodium fluoride, 10 mM sodium pyrophosphate).

Soluble and insoluble cell fractions preparation

One percent Triton-X-100 soluble and insoluble cell fractions were prepared as previously described [276, 277]. Briefly, 2 x 10^6 were washed in ice-cold PBS and suspended in 250 µl of ice-cold cell lysis buffer (20 mM Tris, pH 7.5, 5 mM EDTA, 1% Triton X-100, 150 mM NaCl and 1x protease inhibitor cocktail) and incubated on ice for 30 min. The samples were then centrifuged at 20,000*g* at 4^{o}C for 20 min. The supernatant was removed and saved as the soluble fraction. The pellet was washed three times in cell lysis buffer, then suspended in 70 µl of 4 X SDS-PAGE sample buffer (8% SDS, 0.4 M DTT, 0.25 M Tris.HCl, pH 6.8, 40% glycerol and 0.1% bromophenol blue) and incubated at 60^{o}C for 30 min. An equal volume of soluble and insoluble fractions was boiled for 5 min, separated by SDS-PAGE, followed by Western blot analysis as described above.

Immunoprecipitation

Cells were washed with ice-cold PBS and suspended in 2 vol. of low stringency cell lysis buffer (50 mM Tris HCl, pH 7.5, 120 mM NaCl, 0.25% NP40, 4 mM sodium fluoride, 1 mM sodium orthovanadate, 0.2 mM EDTA, 0.2 mM EGTA, 10% glycerol, and 1x protease inhibitor cocktail) and incubated on ice for 30 min. Cell lysates were obtained by centrifugation and removal of the cell debris. Cell lysates of about 0.8-1.2 mg of total protein were incubated with 1 µg normal IgG (Sigma), polyclonal anti-Sam68 (Santa Cruz), goat anti-TIA-1 (Santa Cruz), or mouse anti-G3BP (BD transduction laboratories) at 4^{o}C for 16 hr with constant rocking. Then, 25 µl of protein A or protein A/G agarose beads (Upstate

Biotechnologies, Temecula, CA) were added to the lysates and further incubated for additional 2 hr. The agarose beads were then washed twice with 500 µl of the low stringency buffer and suspended in 60 µl of 4X SDS-PAGE sample buffer, followed by SDS-PAGE and Western blot analysis as described above.

RNA isolation, reverse transcription, and multiplex PCR

Total cellular RNA was isolated from 293T cells 48 hr post-transfection using a TRIZOL reagent (Invitrogen) according to the manufacturer's instructions. Three micrograms of RNA were reverse transcribed at 50^{o}C for 1 hr in a total volume of 20 µl containing 10 mM dNTPs (Promega), 200 U of RNasin (Promega), 500 ng of random hexamers (Roche), and 200 U of Superscript III reverse transcriptase (Invitrogen). Multiplex PCR was carried out using primers BSS 5'-GGC TTG CTG AAG CGC GCA CGG CAA GAG G-3' and SJ4.7A 5'-TTG GGA GGT GGG TTG CTT TGA TAG AG-3', as previously described [278], with modifications. Briefly, one microliter of the above reverse transcription reaction was used as the template for multiplex PCR in a total reaction volume of 50 µl containing 2.5 mM $MgCl_2$, 0.2 mM dNTPs, 1 µM of each primer, and 1 U of AmpliTaq Gold (Applied Biosystems). The PCR program was 30 cycles of 94^{o}C for 30 sec, 60^{o}C for 1 min, and 72^{o}C for 2 min. Following denaturation at 94^{o}C for 5 min, five microliters of the above PCR products were radiolabeled by 1, 2, 4, 6 or 8 additional cycles of PCR in the presence of 7.5 µCi [α-^{32}P]dCTP (specific activity ~800 Ci/mmol, GE Healthcare). The final PCR products were fractionated on an 8% polyacrylamide/6 M urea denaturing gel, followed by drying of the gel for 30

min using a vacuum gel dryer (Pharmacia biotech, San Francisco, CA), and visualized by autoradiography. In addition, the glyceraldehyde-3-phosphate deshydrogenase gene (GAPDH) was included in the RT-PCR as a loading control with GAPDH-specific primers: 5'-GAA GGT GAA GGT CGG AGT-3' and 5'-GAA GAT GGT GAT GGG ATT TC-3', and a PCR program of 25 cycles of 94^{o}C for 1 min, 50^{o}C for 1 min, and 68^{o}C for 2 min, and one cycle of 72^{o}C for 7 min.

Expression and purification of His-tagged Sam68

Previously transformed BL21 bacteria with His-Sam68 plasmid were inoculated in 3 ml of LB media containing kanamacyn (Km), and incubated O/N at 30^{o}C and 225 rpm. The O/N culture was then inoculated into 250 ml of LB Km+ media and growth at the same conditions until the OD_{600} reached 0.6. At this point, protein expression was induced by adding IPTG to a final concentration of 1 mM to the bacteria culture, and further incubated at 37^{o}C and 225 rpm for 2 hr. The cell suspension was then pelleted at 2000*g* for 20 min, suspended in 12 ml of bacteria lysis buffer (50 mM NaH_2PO_4, and 300 mM NaCl, 2 mM PMSF), and cells were lysed in a French Press (Thermo electron corporation, Waltham, MA). Bacteria cell lysates were obtained by centrifugation (4^{o}C/1200*g*/30 min) and removal of the cell debris. From this point on, all the procedures were carried out at 4^{o}C. Ten milliliters of bacteria cell lysate were mixed with 1.5 ml of previously equilibrated Ni-NTA agarose (Qiagen), and incubated for 1 hr with constant rotation. Bacteria cell lysates were let flow through, and the Ni-NTA agarose with

bound protein was washed with bacteria cell lysis buffer containing increasing concentrations of imidazol (20 mM, 40 mM, 60 mM, 80 mM and 100 mM). His-Sam68 protein was then eluted with bacteria lysis buffer containing 250 mM of imidazol. To verify proper purification, 35 µl of each fraction were separated on 7.5% SDS-PAGE, and stained with coomassie blue solution (10% acetic acid, 40% methanol, and 0.5% coomassie blue) for 2 hr, and destained in 10% acetic acid O/N. Finally, elution fractions containing purified His-Sam68 were concentrated and desalted by centrifugation at 4000*g* in a Centricon 50 column (Millipore).

Oligonucleotide annealing assay (RNA chaperone assay)

HIV-1 TAR(+) 5'-GGT CTC TCT TGT TAG ACC AGG TCG AGC CCG GGA GCT CTC TGG CTA GCA AGG AAC CC-3' and TAR(-) 5'-GGG TTC CTT GCT AGC CAG AGA GCT CCC GGG CTC GAC CTG GTC TAA CAA GAG AGA CC-3' complementary oligonucleotides were synthesized, and purified (Operon Biotechnologies, Huntsville, AL). TAR(-) oligonucleotide was radioactively labeled in a 50 µl reaction mixture containing 30 pmoles of TAR(-) oligonucleotide, 82.9 pmoles of [γ-^{32}P] ATP, 6 Units of T4 polynucleotide kinase, and 1 X T4 polynucleotide kinase buffer. The reaction mixture was incubated at 37^{o}C for 30 min, and the reaction was terminated by incubation at 65^{o}C for 10 min. Labeled 5'-end oligonucleotide was separated from precursor ATP by chromatography using the microspin 6-50 column (Amersham) according to the manufacturer's instructions. The *in vitro* annealing assay was carried out as

previously described, with modifications. Briefly, 0.03 pmoles of TAR (+) oligonucleotide, 0.03 pmoles of TAR (-) radioactively labeled oligonucleotide, 10 µl of annealing buffer (20 mM Tris-HCl pH 7.0, 30 mM NaCl, 0.1 mM $MgCl_2$, 10 µM $ZnCl_2$, and 5mM DTT), and increasing concentrations (2.5, 5, 12.5, 25, 50, or 100 pmoles) of purified His Tagged Sam68 were mixed. Increasing concentrations (0.75, 1.5, or 3.0 pmoles) of NCp7(1-71) or NCp7(12-53) were included as positive and negative controls, respectively. The reaction mixture was incubated at 37^{o}C for 2.5 min and stopped by adding 5 µl of stopping solution (20% glycerol, 30 mM NaCl, 20 mM EDTA pH 8.0, 0.2% SDS, 0.25% bromophenol blue, and 0.4 µg/µl of calf tRNA), and then single strand (ss) and double strand (ds) oligonucleotides were separated in a 12% native gel. The gel was dried for 35 min using a vacuum gel dryer (Pharmacia biotech), and visualized by autoradiography.

Immunofluorescence staining

Cells previously plated in pre-coated coverslips with poly-L-Lysine were fixed in 4% paraformaldehyde (PFA) at RT for 25 min and permeabilized in 0.3% Triton X-100 for 5 min. The cells were then blocked in 5% FBS/1% BSA at RT for 30 min, followed by incubation with: rabbit polyclonal α-Sam68 (1:50), goat polyclonal α-TIA-1 (1:50), goat polyclonal α-eIF3η (1:50), mouse monoclonal α-G3BP (1:75), or mouse monoclonal anti-HA (1:50) at RT for 16 hr. Next, the cells were incubated with PE-conjugated rabbit α-mouse IgG (1:175), FITC-conjugated goat α-mouse (1:50), FITC-conjugated donkey α-goat (1:50), Rh-conjugated mouse α-rabbit (1:75), Rh-conjugated goat α-rabbit (1:50), Rh-conjugated bovine α-rabbit (1:75) at RT for 2 hr. Between each step, the cells were extensively rinsed in PBS. To stain the nuclei, the cells were incubated in 100-500 ng/ml of 4',6'-diamidino-2-phenylindole (DAPI) at 37^{o}C for 25 min. Fluorescence images were captured using a digital video imaging microscope system consisting of an Axiovert 200 M microscope with a 100 x 1.4 UVF objective and three different excitation/emission filters (D360/40-D460/50, D470/40-D535/40, D546/10-D590), and an Axiovision video camera (Carl Zeiss, Thornwood, NY). Images were further processed to adjust contrast and brightness using the Adobe Photoshop software.

Fluorescence *in situ* hybridization (FISH)

Nef-Cy3 oligonucleotide probe 5'-TGG GAG CAG TAT CTC GAG ACC TAG A-3' (nt. 8875-8900 of NL4-3) was synthesized, fluorescently labeled and PAGE purified (Operon Biotechnologies, Huntsville, AL). FISH was performed in 293T cells 42 hr post-transfection. Briefly, transfected cells were fixed with 4% PFA at RT for 30 min and then permeabilized with 70% ethanol at 4^{o}C for 24 hr. Then, the cells were rehydrated in 2X SCC (0.3 mM NaCl, 0.03 mM sodium citrate, pH 7.0) and 50% formamide at RT for 10 min, and hybridized with 100 ng Nef-Cy3 probe at 37^{o}C O/N in a vol. of 40 µl containing 40 µg of *E. coli* tRNA, 10% dextran sulfate, 50% formamide, 2X SCC, and 20 U RNasin. The Nef-Cy3 probe was denatured at 80^{o}C for 75 sec before it was added to the cells. After sequential washes with 0.5X SCC and 0.1X SCC, each for 7 min at RT, fluorescent images were captured as above.

Flow cytometry analysis

MHC I surface expression in Jurkat T cells

One million previously transfected and infected Jurkat T cells were suspended in ice-cold PBS, plated in 96-well round bottom plates and centrifuged at 300*g* for 5 min. The cells were then suspended and incubated in 50 µl of anti-human MHC-I hybridoma supernatant (Dr. J. Blum, Indiana University School of Medicine) for 30 min at 4^{o}C. Next, the cells were incubated with PE-conjugated rabbit α-mouse IgG (1:50), and incubated for 30 min at 4^{o}C in the dark. Between each

step, the cells were extensively washed with 0.1% BSA/0.035% sodium bicorbonate/0.02% sodium azide/HBSS. Stained cells were then fixed in 2% PFA for 20 min at 4^{o}C, washed with ice-cold PBS, and suspended in 200 µl of PBS. MHC-I surface expression levels were determined using a BDFacscan Flow Cytometer from Beckton Dickinson (San Jose, CA) and analyzed using CellQuest Pro software, and presented in the form of histogram.

Cell cycle

One million cells of stable expressing cell lines Hela.cDNA3 and Hela.Δ410 were suspended in ice-cold PBS, plated in 96-well round bottom plates and centrifuged at 700*g* for 10 min. The cells were then stained in a solution containing 75 µl of propidium iodide (PI) staining solution (0.1 mg/ml PI, 0.6% NP-40) and 75 µl of RNase solution (RNase A 100 µg/ml) for 30 min in ice. Single cell DNA content for cell cycle analysis was determined using a BDFacscan Flow Cytometer (Beckton Dickinson) and analyzed using CellQuest Pro software.

Yeast three hybrid assay

The three yeast hybrid assay was performed in three stages: preparation of L40 yeast competent cells, transformation of L40 yeast competent cells and liquid culture β-Gal assay with ONPG as a substrate.

Preparation of L40 yeast competent cells: Four colonies of L40 yeast strain were inoculated in 1ml of YPD medium, transferred into a flask containing 50 ml of YPD medium, and incubated at 30^{o}C for 24 hr at 250 rpm to reach a stationary phase. An aliquot of the previous yeast culture was diluted in fresh YPD medium to produce an OD_{600}= 0.25, and further incubated at 30^{o}C for 3 hr with constant shaking at 250 rpm. Cultured cells were then centrifuged at 1000*g* for 5 min at RT, suspended in 25 ml of autoclaved water, then centrifuged again with the same parameters, and the pellet was suspended in 1.5 ml of freshly prepared, sterile 1X TE/LiAc solution (0.01 M Tris-HCl, 1mM EDTA, 0.1 M LiAc, pH 7.5). At this point L40 yeast cells are competent for transformation.

Triple transformation of L40 yeast competent cells: A 1.5 ml tube containing the following mixture was prepared for each triple transformation: 0.1 µg of each plasmid DNA (Hybrid protein 1, Hybrid protein 2, and Hybrid RNA), 0.1 mg of herris testes carrier DNA, 0.1 ml of L40 yeast competent cells, and 0.6 ml of sterile polyethylene glycol (PEG)/LiAc solution (40% PEG, 0.01 M Tris-HCl, 1mM EDTA, 0.1 M LiAc, pH 7.5). The mixture was incubated at 30^{o}C for 30 min with constant shaking at 200 rpm; afterwards, 70 µl of DMSO were added and the cells were heat shocked in a 42^{o}C water bath for 15 min, followed by a brief period of incubation in ice. The cells were then briefly centrifuged for 5 sec at 15500*g*, suspended in 100 µl of 1 X TE buffer (0.01 M Tris-HCl, 1mM EDTA), and the entire cell suspension solution was plated in SD minus histidine-leucine-tryptophan-uracil agar plates. The plates were incubated at 30^{o}C for five days.

L40 yeast competent cells were transformed with different combinations of DNA plasmids, as shown in Table 1.

Liquid culture β-Gal assay with ONPG as a substrate: The following was carried out for each SD agar plate containing triple transformed colonies. Three separate colonies were inoculated in a tube containing 1.5 ml of SD minus histidine-leucine-tryptophan-uracil liquid media, and this was performed in triplicate (3 tubes, each with 3 inoculated colonies). The cell suspensions were cultured O/N at 30^{o}C with constant shaking at 250 rpm, then the entire O/N culture was inoculated into 5 ml of YPD and further cultured at 30^{o}C (250 rpm) for 5 hr until the OD_{600} reached 0.4. At this point, 1.5 ml of cultured cells were added into each of three 1.5 ml tubes (triplicate), centrifuged at 15500*g* for 30 sec, and the cell pellet was suspended in 1 ml of Z Buffer + β-mercaptoethanol solution (60 mM Na_2HPO_4-$7H_2O$, 40 mM NaH_2PO_4-H_2O, 10 mM KCL, 1mM $MgSO_4$-$7H_2O$, 0.27% v/v β-mercaptoethanol). The cell suspension solution was centrifuged again, the pellet was suspended in 100 µl of a Z Buffer + β-Mercaptoethanol solution, concentrating the cells 15 times, followed by one cycle of freeze and thaw in liquid nitrogen and in a water bath at 37^{o}C. Seven hundred microliters of Z Buffer + β-mercaptoethanol solution were added to each tube, followed by 0.16 ml of a Z Buffer + β-mercaptoethanol solution containing 4 mg/ml ONPG, incubated at 30^{o}C for 90 min, the reaction was stopped by adding 400 µl of 1 M Na_2CO_3. Finally, 200 µl of the reaction containing the released o-nytropenyl was measured at 405 nm in a microplate reader.

Data acquisition and statistical analysis

All values expressed as mean ± SEM. Comparisons among groups were made using two-tailed Student's *t*-test. A p value of < 0.05 was considered statistically significant (*), and $p < 0.01$ highly significant (**).

Table 1. Plasmids used in yeast three hybrid assay

Hybrid protein 1	Hybrid RNA	Hybrid protein 2
MS2 (pLexA-MS2)	MS2 (pIIIA/MS2.2)	IRP(pAD-IRP)
MS2 (pLexA-MS2)	MS2-IRE (pIIIA/IRE-MS2)	IRP(pAD-IRP)
MS2 (pACTII/MS2)	MS2 (pIIIA/MS2.2)	Δ410 (pBTM116.Δ410)
MS2 (pACTII/MS2)	MS2-nef 3'UTR	Δ410 (pBTM116.Δ410)
MS2 (pACTII/MS2)	MS2-nef 3'RTU	Δ410 (pBTM116.Δ410)
MS2 (pACTII/MS2)	MS2 (pIIIA/MS2.2)	Δ269 (pBTM116.Δ269)
MS2 (pACTII/MS2)	MS2-nef 3'UTR	Δ269 (pBTM116.Δ269)
MS2 (pACTII/MS2)	MS2-nef 3'RTU	Δ269 (pBTM116.Δ269)
MS2 (pACTII/MS2)	MS2 (pIIIA/MS2.2)	ΔKH (pBTM116.ΔKH)
MS2 (pACTII/MS2)	MS2-nef 3'UTR	ΔKH (pBTM116.ΔKH)
MS2 (pACTII/MS2)	MS2-nef 3'RTU	ΔKH (pBTM116.ΔKH)

The yeast strain L40 was transformed with combinations of three DNA plasmids. Plasmids for hybrid protein 1 express a hybrid protein containing bacteriophage MS2 coat protein fused to LexA DNA binding domain. Plasmids for hybrid protein 2 express a hybrid protein containing the protein to be tested fused to the Gal4 DNA-activation domain. Plasmids for hybrid RNA express a RNA hybrid containing the RNA target for the MS2 coat protein and the *nef* 3'UTR or *nef* 3'RTU (UTR in reverse orientation). Each row represents the transformation of one combination of three different plasmids. In parenthesis is the name of the plasmid given during its generation. Iron Regulatory Protein (IRP), Iron Response Element (IRE).

RESULTS

PART 1: Suppression of HIV-1 Nef translation by Sam68 mutant-induced Stress Granules and Nef mRNA sequestration

1.1 Rev-dependent and Rev-independent reporter viruses

Multiple independent studies have shown that Sam68 cytoplasmic mutant Δ410 inhibits Rev-mediated nuclear exportation, and HIV-1 replication [78, 248, 249]. Early reports proposed a dominant-negative inhibitory mechanism, resulting in the retention of the wild-type Sam68 in the cytoplasm, preventing it from functioning in Rev-mediated nuclear export of HIV-1 RNA [78]. However, subsequent studies support an additional role of Sam68 and mutant Δ410 in cytoplasmic processes of HIV-1 RNA metabolism. For instance, Δ410 is also shown to sequester incompletely spliced HIV-1 RNA from the translation machinery in perinuclear bundles [248]. Moreover, wild-type Sam68 is found to enhance cytoplasmic utilization of intron-containing RNA [222], and to be capable of localizing into the nucleus when it is co-expressed with NLS deleted inhibitory mutants [249]. Therefore, we decided to further dissect the relationship between Δ410 presence in the cytoplasm and down-regulation of HIV-1 gene expression. As shown in figure 6, we constructed NL4-3.Luc(env) reporter virus using the same strategy as for NL4-3.CAT [279], which has the reporter gene cloned in-frame into a defective *env* gene, so that we could use the Luc in this plasmid as an indicator for the expression of singly spliced HIV-1 RNA (Rev-dependent); and

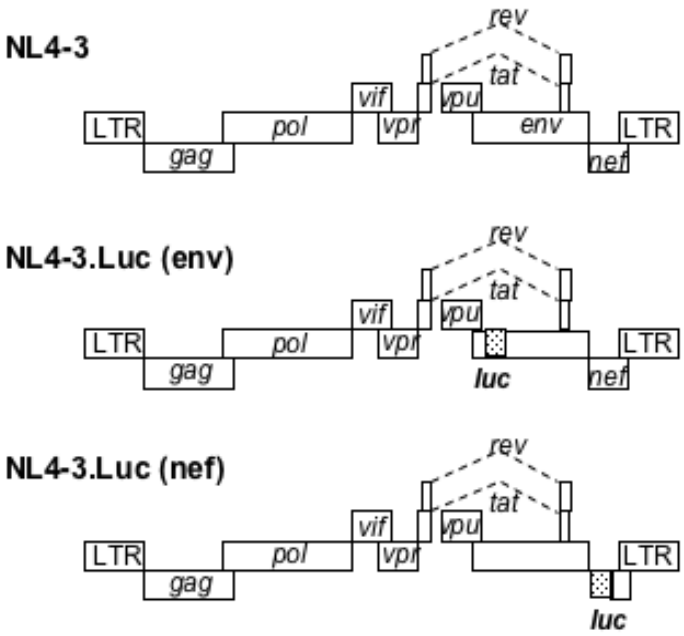

Figure 6. NL4-3, NL4-3.Luc(env) and NL4-3.Luc(nef) plasmids. In NL4-3.Luc(env), the Luc gene was cloned in frame into a non-functional *env* gene at nt position 6310 of the original NL4-3 plasmid. In NL4-3.Luc(nef), the Luc gene was cloned in frame into a non-functional *nef* gene at nt position 8795 of the original NL4-3 plasmid.

NL4-3.Luc(nef) reporter virus, which has the Luc gene cloned in the place of HIV-1 *nef* gene [13, 280, 281], so we could use it as an indicator for the expression of multiply spliced HIV-1 RNA (Rev-independent). These unique reporter viruses represent a novel model to study differential regulation of HIV-1 gene expression. Thus, we are now able to discern between Δ410 inhibitory effects due to a hindered Rev nuclear exportation pathway, or to possible Rev-independent cytoplasmic inhibitory processes.

1.2 Suppression of Rev-dependent and Rev-independent gene expression by a Sam68 mutant Δ410 lacking a nuclear localization signal

To address the possible function of Sam68 mutants in cytoplasmic processes of HIV-1 replication, we transfected 293T cells with NL4-3.Luc(env) or NL4-3.Luc(nef) in combination with Sam68 or Δ410 and determined HIV-1 production in the culture supernatants and Luc expression in the cells. In agreement with other studies, the results showed that Δ410 completely abrogated HIV-1 production in both NL4-3.Luc(env) and NL4-3.Luc(nef) transfected cells, while Sam68 had no significant effect (Fig. 7A & B). As expected, Δ410 significantly inhibited Luc expression in NL4-3.Luc(env) transfected cells (Fig. 7C), as it inhibits Rev-mediated nuclear export of HIV-1 intron-containing singly spliced *env* RNA [78, 248, 249]. But, to our great surprise, Δ410 also inhibited Luc activity in NL4-3.Luc(nef) transfected cells by about ~70% (Fig. 7D), suggesting that the inhibitory mechanism of Δ410 mutant is a post-transcriptional gene regulatory cytoplasmic process, and at least in part, independent of Rev function.

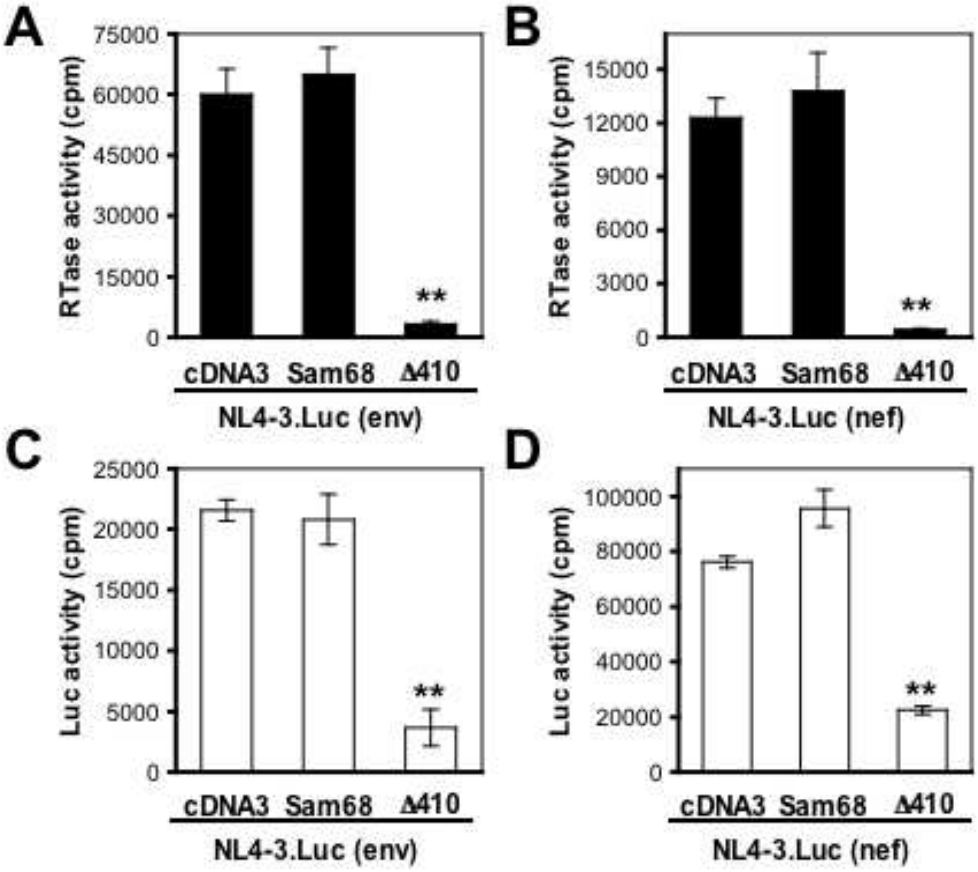
A
RTase activity (cpm)
75000
60000
45000
30000
15000
0
**
cDNA3 Sam68 Δ410
NL4-3.Luc (env)
B
RTase activity (cpm)
15000
12000
9000
6000
3000
0
**
cDNA3 Sam68 Δ410
NL4-3.Luc (nef)
C
Luc activity (cpm)
25000
20000
15000
10000
5000
0
**
cDNA3 Sam68 Δ410
NL4-3.Luc (env)
D
Luc activity (cpm)
100000
80000
60000
40000
20000
0
**
cDNA3 Sam68 Δ410
NL4-3.Luc (nef)

Figure 7. Δ410 effects on HIV-1 replication and on Rev-dependent and Rev-independent gene expression. 293T cells were plated in a 12-well plate at a density of 1.8 x 10^5 cells per well and transfected with 0.3 μg NL4-3.Luc(env) (**A** & **C**) or NL4-3.Luc(nef) (**B** & **D**), in combination with 0.9 μg of pcDNA3, Sam68 or Δ410, and 0.05 μg of pcDNA3-βGal. pcDNA3 was included as a control, and pcDNA3-βGal was used as a normalization control for reporter gene assay. Cell culture supernatants were collected for the RT activity assay 42 hr after transfection (**A** & **B**), while the cells were harvested for the luciferase activity and β-Gal activity assays (**C** & **D**). RT activity, Luciferase activity and β-Gal activity were determined as described in Materials and Methods. Luciferase activity values of each sample were normalized to the β-Gal activity of each individual sample to correct for transfection variations. RT activity and luciferease activity are determined in the form of counts per min (cpm). The data were mean ± S.E.M of triplicates. Comparisons among groups were made using two-tailed Student's *t*-test. (**) $p < 0.01$.

1.3 Suppression of HIV-1 Nef expression by Sam68 mutant Δ410

To ascertain that the previous observation was not an artifact due to intrinsic defects of these Luc reporter viruses, we transfected 293T cells with the original NL4-3 and increasing concentrations of Sam68 or Δ410 and determined Nef expression by Western blot analysis. The results showed that Δ410 expression led to a decrease of 80% in Nef expression in a dose dependent manner, while Sam68 expression slightly increased Nef expression (Fig. 8A). To determine whether this was only unique to NL4-3 Nef, we performed similar experiments with four additional HIV-1 isolates. The results showed that Δ410 expression also suppressed Nef expression from HIV-1 isolates JRCSF, YU-2 and SG-3.1 (Fig. 8B). There was no reactivity of the anti-Nef antibody to LAI.2 Nef (Fig. 8B). Similarly, there was no reactivity of the anti-Nef antibody to Nef proteins from proviruses p90CF402.1.8, p89.6, and pMJ4 (Fig. 8C). These results together showed that Δ410 suppressed Nef expression from different HIV-1 isolates.

1.4 Effects of Δ410 on the splicing and stability of completely spliced HIV-1 RNA

Sam68 has been shown to regulate CD44, and bcl-x alternative splicing [234], among others. HIV-1 gene expression involves complex and extensive splicing

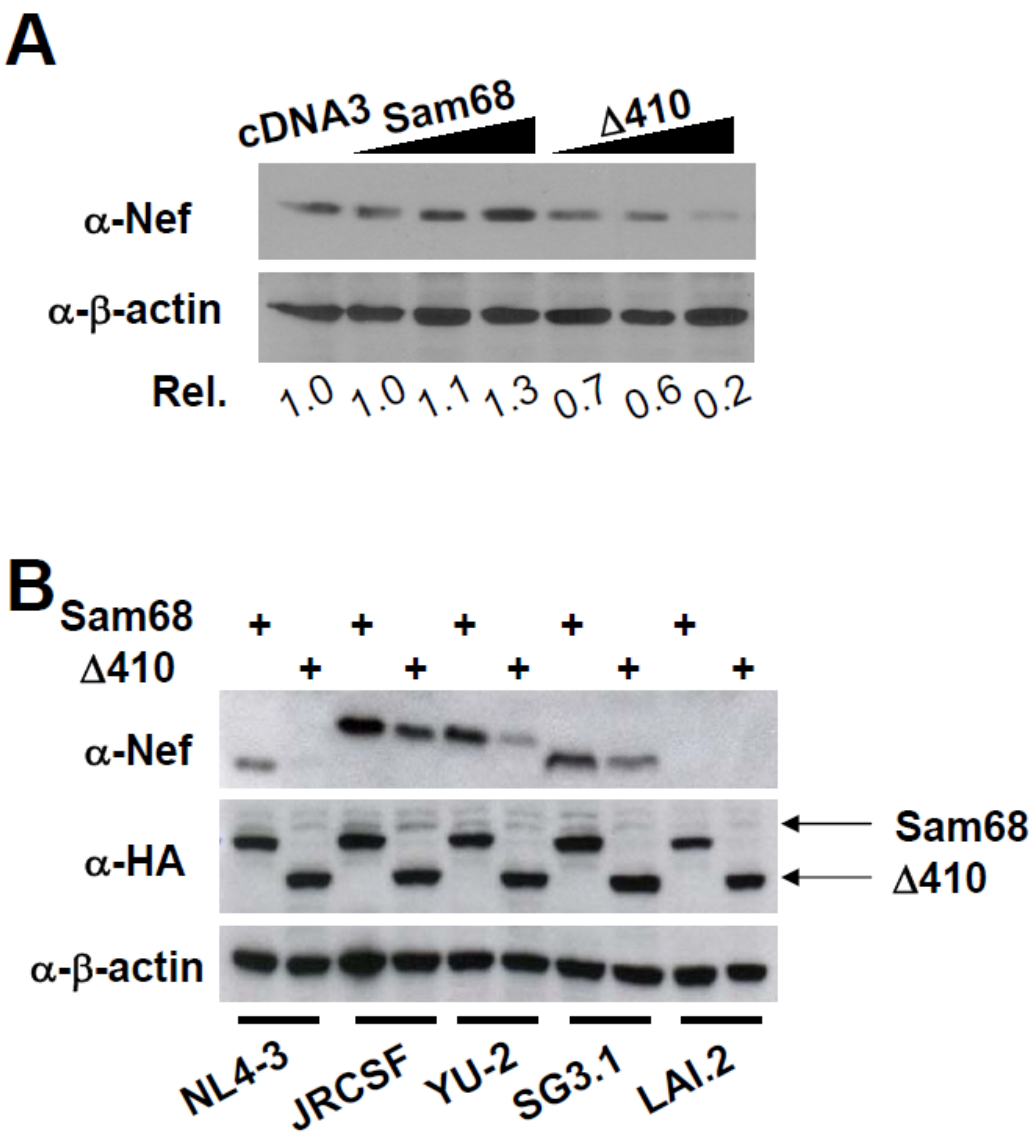
A
cDNA3 Sam68
Δ410
α-Nef
α-β-actin
Rel.
1.0 1.0 1.1 1.3 0.7 0.6 0.2
B
Sam68
Δ410
α-Nef
α-HA
α-β-actin
Sam68
Δ410
NL4-3
JRCSF
YU-2
SG3.1
LAI.2
C
HIV-1 isolates
JRCSF
p90CF
SG3.1
NL4-3
YU2
pMJ4
p89.6
α-Nef

Figure 8. Δ410 effects on HIV-1 Nef expression. A. 293T cells were plated in a 6-well plate at a density of 3.0 x 10^5 cells per well and transfected with 0.4 μg of NL4-3, and 0.4, 1.2, or 2.5 μg of HA-tagged Sam68 or Δ410. pcDNA3 was used to equalize the total amount of DNA transfected among transfections. The cells were harvested 42 hr after transfection, lysed in RIPA buffer, and 20 μg of each sample were separated by 12.5% SDS-PAGE followed by Western blot analysis using anti-Nef JRCSF, anti-HA or anti-β-actin. Relative levels of Nef protein were determined using the housekeeping gene β-actin as an internal standard, and expressed below. **B.** 293T cells were transfected with 0.4 μg of NL4-3, JRCSF, YU2, SG3.1, or LAI.2 and 2.5 μg of Sam68 or Δ410. Similar Western blot analysis was performed for Nef, Sam68 or Δ410, or β-actin. **C.** 293T cells were transfected with 0.4 μg of the following HIV-1 isolates: JRCSF, p90CF402.1, SG3.1, NL4-3, YU2, pMJ4 or p89.6. Similar Western blot analysis was performed for Nef, using anti-Nef JRCSF.

of HIV-1 RNA. Meanwhile, STAR family proteins and KH domain-containing proteins have been shown to regulate mRNA stability [282-285]. Thus, an intriguing possibility is that Δ410 may suppress Nef expression through inhibition of HIV-1 RNA splicing to generate the completely spliced RNA or through changes in the stability of these RNA. However, due to the extensive sequence overlapping between all HIV-1 transcripts, it is not possible to individually amplify HIV-1 *nef* mRNA when all the HIV-1 RNA species are present. Thus, to test this possibility, we adapted a semi-quantitative multiplex RT-PCR assay [286-288], which allows you to simultaneously amplify and radioactively label the different completely spliced HIV-1 RNA species in HIV-infected cells, and determined the effects of Δ410 on HIV-1 RNA splicing. We first optimized the input amount of RNA and cDNA, the PCR cycling, and the number of PCR labeling cycles to ensure that the amplification products were in the linear range. We determined that the optimal conditions were: three micrograms of total RNA, one microliter of reverse transcription reaction, and two PCR labeling cycles (Fig. 9A). Then, we transfected 293T cells with NL4-3 and Sam68 or Δ410, and treated the cells with or without actinomycin D (Act. D, 7.5 μg/ml), a well characterized inhibitor of RNA Pol II elongation used during mRNA stability studies, for 10 hours, followed by isolation of total RNA and reverse transcription and multiplex PCR, as previously determined. The results showed that compared to the cDNA3 transfection control, Sam68 and Δ410 both had minimal detectable effects on the RNA splicing pattern and the relative level of the completely spliced RNA (-Act. D,

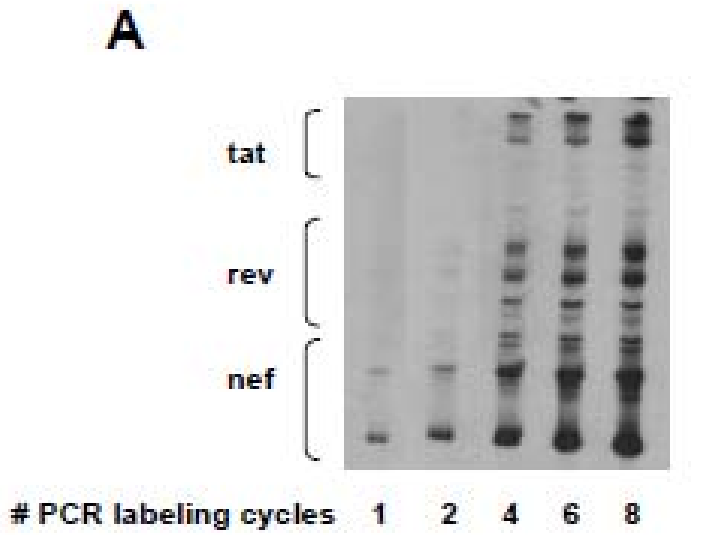
A
tat
rev
nef
PCR labeling cycles 1 2 4 6 8

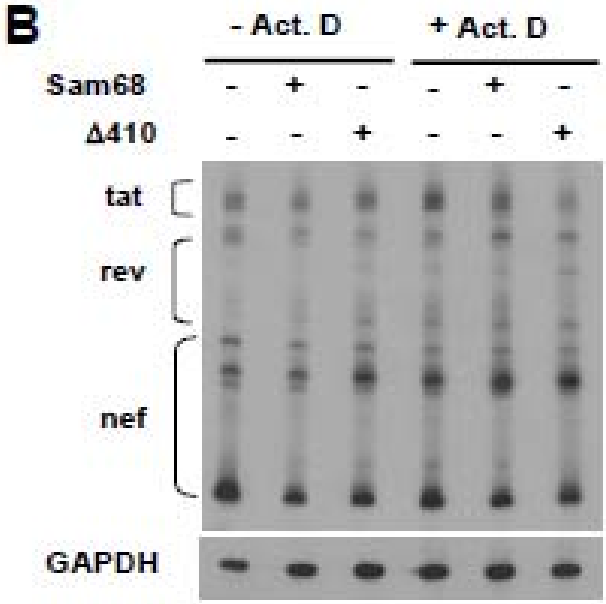
B
- Act. D
+ Act. D
Sam68 - + - - + -
Δ410 - - + - - +
tat
rev
nef
GAPDH

Figure 9. Δ410 effects on the level and stability of multiply spliced HIV-1 RNA. A. 293T cells were plated in a 6-well plate at a density of 3.2 x 10^5 cells per well and transfecetd with 0.4 µg of NL4-3. The cells were harvested 42 hr after transfection for total RNA isolation. Three micrograms of total RNA was then reverse transcribed and subjected to multiplex PCR as described in detail in the Material and Methods sections. The PCR products were labeled for 1, 2, 4, 6, and 8 PCR cycles with 7.5 µCi [α-^{32}P]dCTP, then separated on a 8% polyacrylamide/6 M urea denaturing gel, and visualized by autoradiography. **B.** 293T cells were plated in a 6-well plate at a density of 3.2 x 10^5 cells per well and transfecetd with 0.4 µg of NL4-3, and 2.5 µg of HA-tagged Sam68 or Δ410. Twenty eight hours post transfection the cells were either treated or not treated with 7.5 µg/ml of Actinomycin D for 10 hr. The cells were then harvested for total RNA isolation. Three micrograms of total RNA was then reverse transcribed, subjected to multiplex PCR, radioactively labeling, and separated as described above. The PCR products were labeled for 2 PCR cycles with 7.5 µCi [α-^{32}P]dCTP. GADPH was included as a control.

Fig. 9B). Similarly, there were no apparent differences in the RNA splicing pattern and the relative level of completely spliced RNA between cells treated with and without Act. D (Fig. 9B). These results suggest that the Nef suppression by Δ410 is mediated by a mechanism different from alterations in HIV-1 mRNA transcription or splicing.

1.5 Suppressed Nef expression as a gain of function in the cytoplasm for Δ410

As mentioned before, inhibition of HIV-1 replication by Δ410 has raised the possibility that Δ410 overrides endogenous Sam68 function through intermolecular association and subsequent sequestration in the cytoplasm, which in turn prevents endogenous Sam68 from entering into the nucleus and functioning in Rev-mediated nuclear export of HIV RNA. However, our early studies have detected a significant level of Sam68 in the nucleus of cells that over-express Δ410 [249], suggesting that Δ410 functions, at least in part, through a gain of function in the cytoplasm. Therefore, we hypothesized that if Δ410 inhibits Nef expression through a classical dominant-negative mechanism, accordingly Sam68 knock-down should have similar effects. To address this possibility, we utilized the small interference RNA (siRNA) strategy to knock down endogenous Sam68 and determined its effects on Nef expression. We first showed that Sam68 siRNA was very effective in knocking down endogenous Sam68 expression in 293T cells (Fig. 10A). We then transfected 293T cells with NL4-3 and 100 nM control or Sam68 siRNA and determined Nef expression by

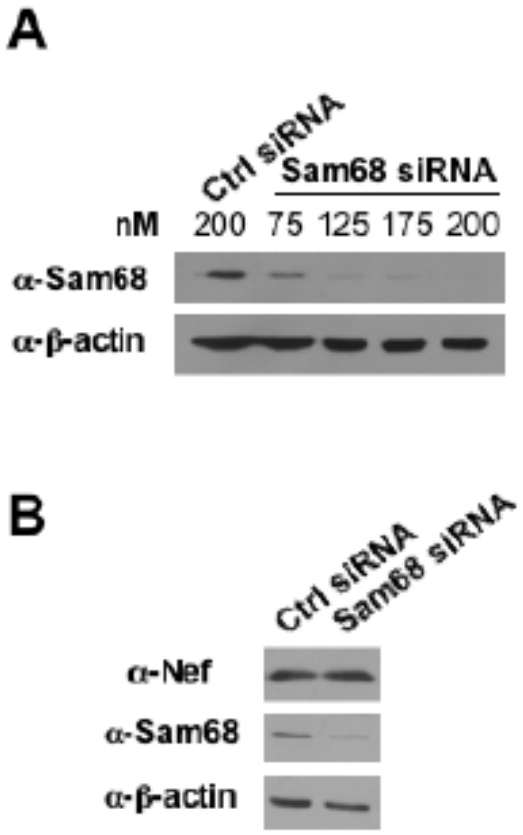

Figure 10. Effects of Sam68 knock-down on HIV-1 Nef expression. A. 293T cells were plated in a 6-well plate at a density of 3.0 x 10^5 cells per well and transfected with 200 nM control siRNA (Ctrl siRNA), or 75, 125, 175, or 200 nM Sam68 siRNA. The cells were harvested 24 hr after transfection, lysed in RIPA buffer, and 20 µg of each sample were separated by 12.5% SDS-PAGE followed by Western blot analysis using anti-Sam68, or anti-β-actin. **B.** 293T cells were plated as above and transfected with 100 nM control siRNA or Sam68 siRNA. The cells were then transfected with 0.6 µg NL4-3 24 hr after the first transfection, and continued to be cultured for additional 24 hr before harvesting the cells. Similar Western blot analysis was performed using anti-Nef JRCSF, anti-HA or anti-β-actin.

Western blot analysis. Nef expression exhibited no difference between cells expressing control or Sam68 siRNA (Fig. 10B). To further confirm these findings, we transfected 293T cells with control or Sam68 siRNA and 24 hours later with NL4-3.Luc(env) or NL4-3.Luc(nef) and determined HIV replication and Luc expression. As previously shown [221, 244], Sam68 knockdown led to inhibition of HIV-1 production of both NL4-3.Luc(env) and NL4-3.Luc(nef) by about 50% over control siRNA transfection (Fig. 11A & B). To a similar extent Sam68 knockdown inhibited Rev-dependent Luc expression in NL4-3.Luc(env) transfected cells (Fig. 11C). In contrast, Rev-independent Luc expression in NL4-3.Luc(nef) showed no significant changes between control siRNA and Sam68 siRNA transfected cells (Fig. 11D). Taken together, these results support the notion that Sam68 is an essential cellular co-factor for Rev function and suggest that Δ410 effects on Nef expression is a gain of function of this mutant in the cytoplasm.

1.6 Requirement of Sam68 domain between aa269 and aa321 for Nef suppression

Structurally, Sam68 contains the heteronuclear ribonucleoprotein particle K homology (KH) domain, an RG-rich region, proline-rich domains (P_0 to P_5), a tyrosine-rich domain, and a nuclear localization signal (NLS) (Fig. 12). Our early studies have shown that a domain located between amino acid residues 269 and 321 of Sam68 is directly involved in Δ410-induced inhibition of HIV-1 replication [249]. To determine the roles of this domain on Δ410-induced Nef suppression,

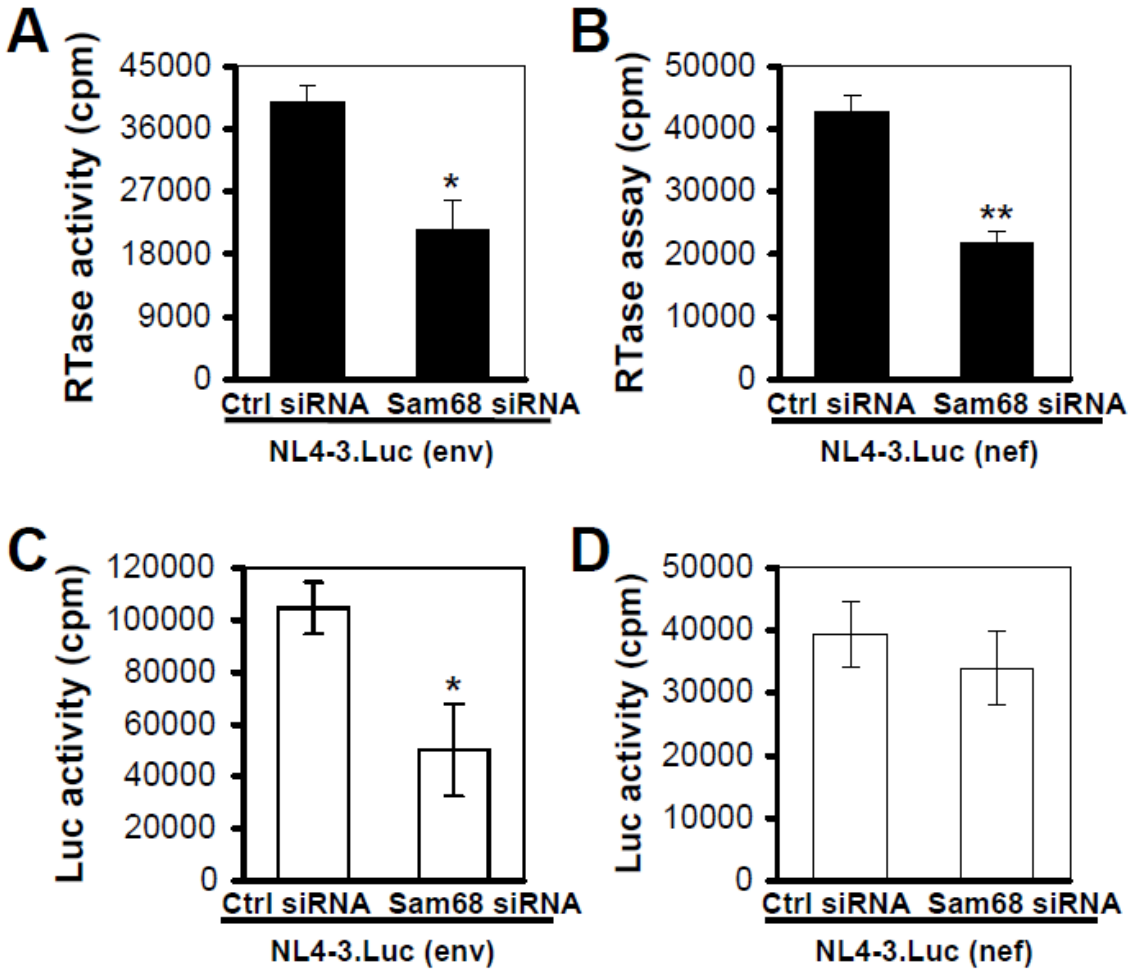
A
RTase activity (cpm)
45000
36000
27000
18000
9000
0
*
Ctrl siRNA
Sam68 siRNA
NL4-3.Luc (env)
B
RTase assay (cpm)
50000
40000
30000
20000
10000
0
**
Ctrl siRNA
Sam68 siRNA
NL4-3.Luc (nef)
C
Luc activity (cpm)
120000
100000
80000
60000
40000
20000
0
*
Ctrl siRNA
Sam68 siRNA
NL4-3.Luc (env)
D
Luc activity (cpm)
50000
40000
30000
20000
10000
0
Ctrl siRNA
Sam68 siRNA
NL4-3.Luc (nef)

Figure 11. Effects of Sam68 knock down on HIV-1 replication and on Rev-dependent and Rev-independent gene expression. 293T cells were plated in a 12-well plate at a density of 1.75 x 10^5 cells per well and transfected with 100 nM of control siRNA or Sam68 siRNA. Twenty four hours later the cells were transfected with 0.35 µg of NL4-3.Luc(env) (**A** & **C**) or NL4-3.Luc(nef) (**B** & **D**), in combination with 0.05 µg of pcDNA3-βGal. pcDNA3-βGal was used as a normalization control for reporter gene assay. Cell culture supernatants were collected for the RT activity assay 36 hr after transfection (**A** & **B**), while the cells were harvested for the luciferase activity and β-Gal activity assays (**C** & **D**). RT activity, luciferase activity and β-Gal activity were determined as described in Materials and Methods. Luciferase activity values of each sample were normalized to the β-Gal activity of each individual sample to correct for transfection variations. RT activity and Luciferease activity are determined in the form of counts per min (cpm). The data were mean ± S.E.M of triplicates. Comparisons among groups were made using two-tailed Student's *t*-test. (*) $p < 0.05$, (**) $p < 0.01$.

we constructed a panel of HA/GFP-tagged Sam68 mutants (Fig. 12), co-transfected them in combination with NL4-3 into 293T cells, and determined Nef expression by Western blot analysis. Similarly to Δ410, Δ321 with deletions of P_4, P_5 and NLS also suppressed Nef expression, whereas Δ269 containing additional deletion of P_3 and the RG rich region had no effects on Nef expression (Fig. 13A). Moreover, Δ269-321 that contains the NLS did not affect Nef expression, nor did the 269-321 domain alone. Similar results on Nef expression were obtained with a panel of HA-tagged Sam68 and its mutants (Fig. 13B). These results suggest that both exclusive cytoplasmic localization, and the aa269-321 domain that contains the P_3 and the RG rich region are required for Nef suppression.

1.7 Sam68 structure and its RNA chaperone activity

Previous results have shown that HIV-1 Nef suppression by Δ410 is not at the level of transcription [78], splicing (Fig. 9B), or due to induced mRNA degradation (Fig. 9B), suggesting that Δ410 might be exerting a deleterious effect on HIV-1 *nef* mRNA translation efficiency. The efficiency of translation of different mRNA depends on the degree of secondary structure in their 5'UTRs; highly structured 5'UTRs abrogate translation by obstructing ribosomal movement to the initiation codon [289]. Interestingly, *nef* mRNA contain a long and structured 5'UTR (Fig. 21B). RNA chaperone proteins are a class of proteins and ubiquitous in living organisms; they help RNA molecules reach their more stable conformation, and

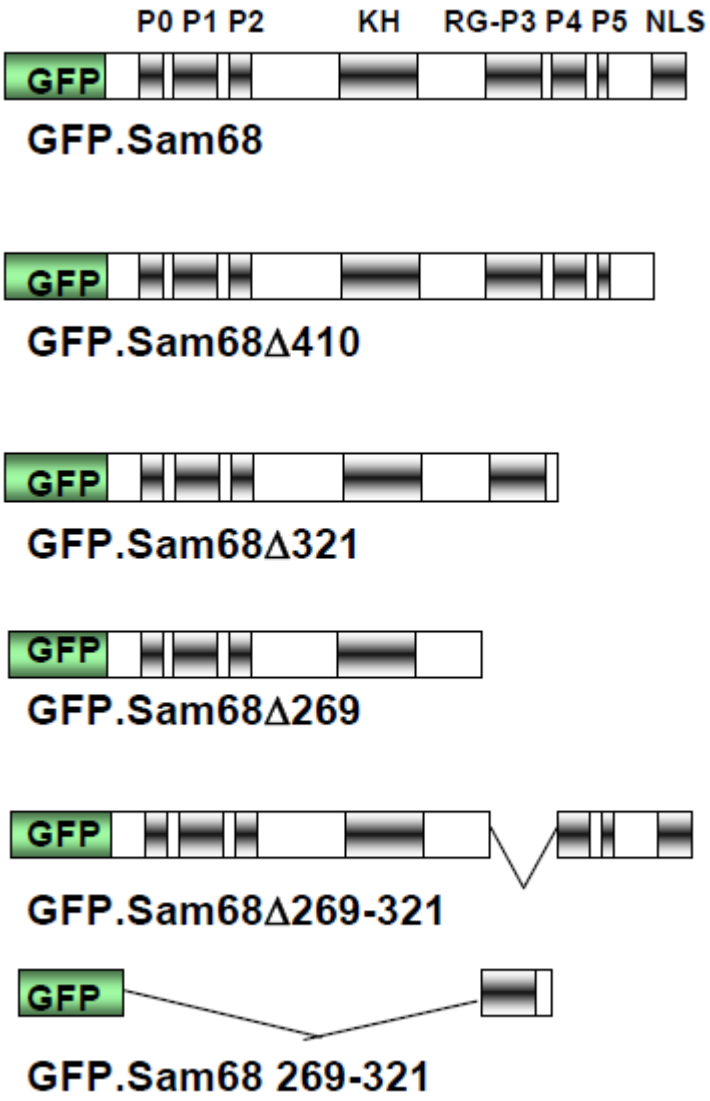

Figure 12. GFP-tagged Sam68 or its mutants. P: proline-rich domain; KH: KH domain; RG: arginine-glycine rich domain; and NLS: nuclear localization signal. The single lines in GFP.Δ269-321 and GFP.269-321 represent deleted regions.

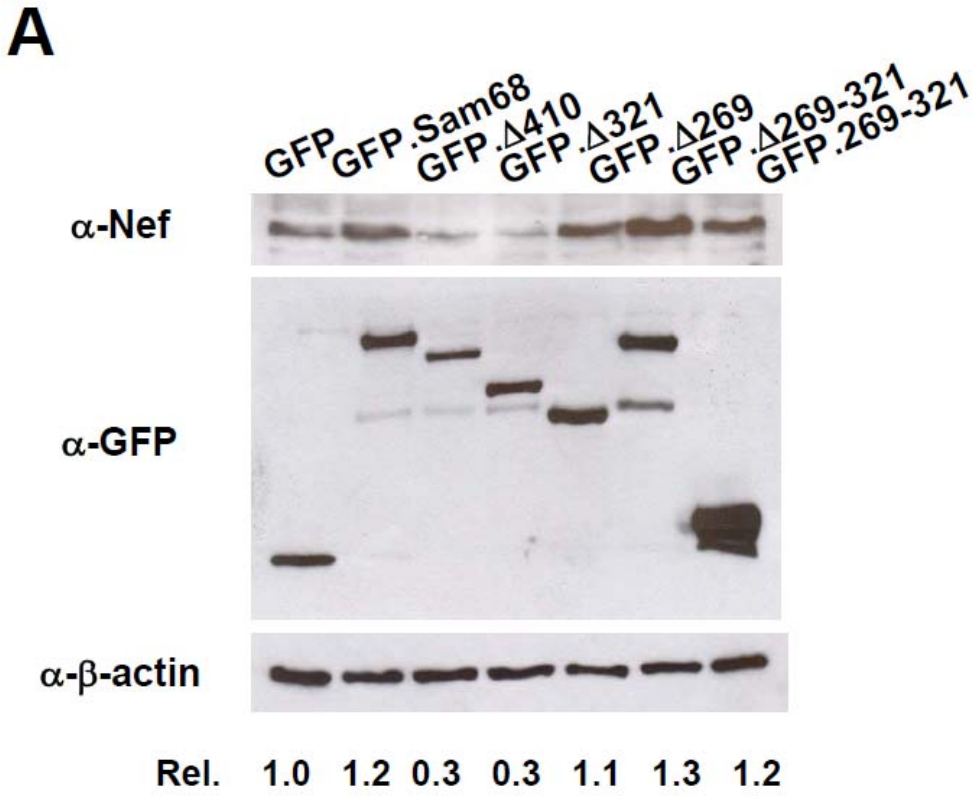
A
GFP
GFP.Sam68
GFP.Δ410
GFP.Δ321
GFP.Δ269
GFP.Δ269-321
GFP.269-321
α-Nef
α-GFP
α-β-actin
Rel. 1.0 1.2 0.3 0.3 1.1 1.3 1.2

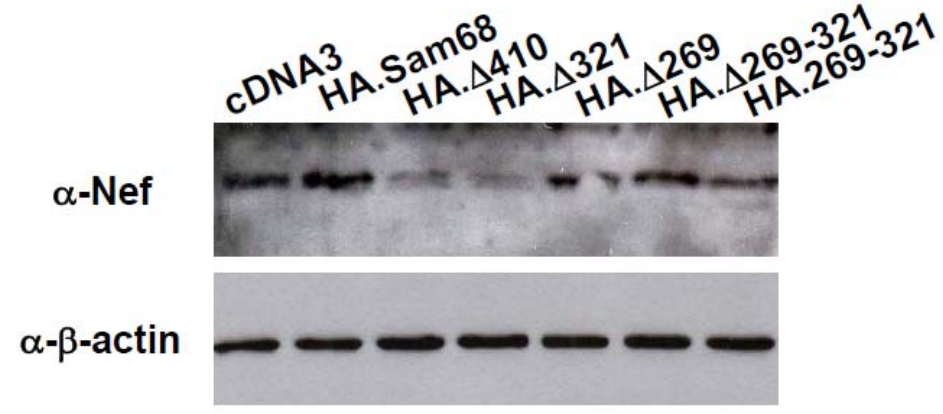
B
cDNA3
HA.Sam68
HA.Δ410
HA.Δ321
HA.Δ269
HA.Δ269-321
HA.269-321
α-Nef
α-β-actin

Figure 13. Effects of Sam68 deletion mutants on HIV-1 Nef expression. A. 293T cells were plated in a 6- well plate at a density of 3.0 x 10^5 cells per well and transfected with 0.4 μg of NL4-3, and 2.5 μg of GFP-tagged Sam68 or its mutants. The cells were harvested 42 hr after transfection, lysed in RIPA buffer, and 20 μg of each sample were separated by 12.5% SDS-PAGE followed by Western blot analysis using anti-Nef JRCSF, anti-GFP or anti-β-actin. Relative levels of Nef protein were determined using the housekeeping gene β-actin as an internal standard, and expressed below. **B.** 293T cells were transfecetd with 0.4 μg of NL4-3, and 2.5 μg of HA-tagged Sam68 or its mutants. Similar Western blot analysis was performed for Nef or β-actin.

they participate in every step of RNA metabolism: transcription, splicing, transport, and translation [290]. Well characterized chaperones include FMRP, hnRNP A1, La protein, and HIV-1 NCp7, among others [290]. Importantly, among all the functional protein classes, RNA chaperones possess the highest frequency of intrinsically disordered regions [291]. Based on all of the above, we hypothesized that Sam68 might be a RNA chaperone, and that when present in the cytoplasm (Δ410), it maintains the structure of *nef* mRNA 5'UTR, preventing ribosomal scanning, mRNA unwinding, and translation.

To test this hypothesis, we first determined the degree of intrinsic disorder in Sam68 protein. For this purpose, we used the recently described DisProt VL3-H predictor [292]. We found that Sam68 contained 51.7% of its aa residues within uninterrupted disordered regions (Fig. 14), as is the case for multiple well characterized RNA chaperones [291]; moreover, the region between aa280 to aa354 is a well limited highly disordered region (Fig. 14), suggesting that Sam68 may have chaperone functions, and that the inhibitory domain between aa269 to aa321 might be essential for this process. Multiple *in vitro* and *in vivo* assays have been developed to determine the activity of RNA chaperones [293]. One of those assays measures the capacity of these proteins to rapidly promote the annealing of complementary oligonucleotide strands (*in vitro* annealing assay) (Fig. 15B). To determine if Sam68 is in fact a RNA chaperone, we initially purified bacterial expressed His-tagged Sam68 by affinity chromatography (Fig. 15A), and then performed the *in vitro* annealing assay with His-Sam68, and

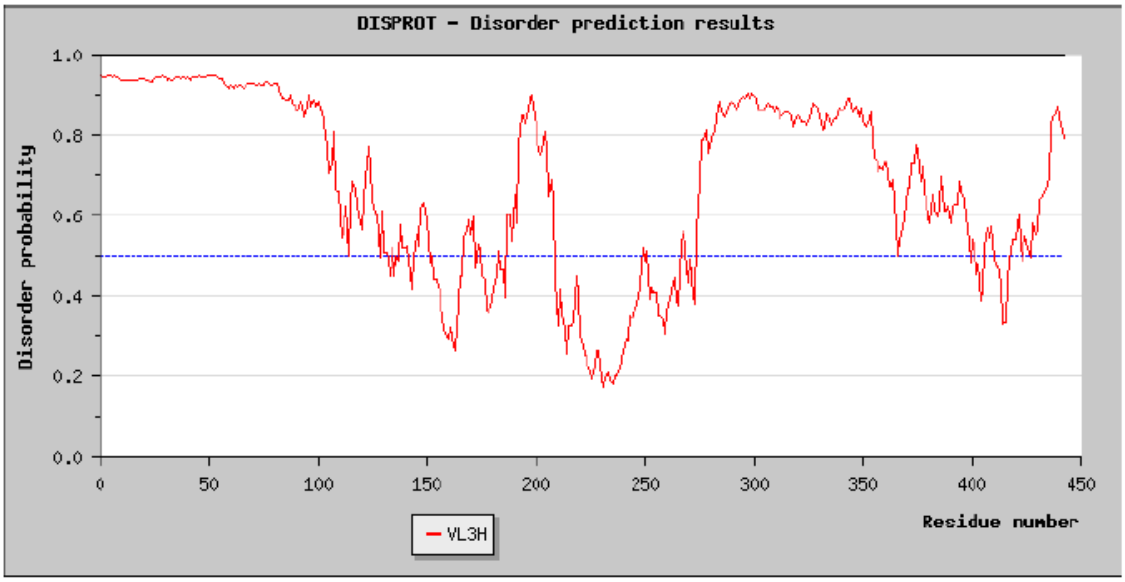

Figure 14. Prediction of intrinsically disordered regions in Sam68. Disordered regions in Sam68 protein were predicted using the Disprot VL3-H predictor. An amino acid with a disorder score above or equal to 0.5 is considered to be in a disordered environment, while below 0.5 to be ordered. The (Y) axis represents probability of disorder, while the (X) axis represents the residue number.

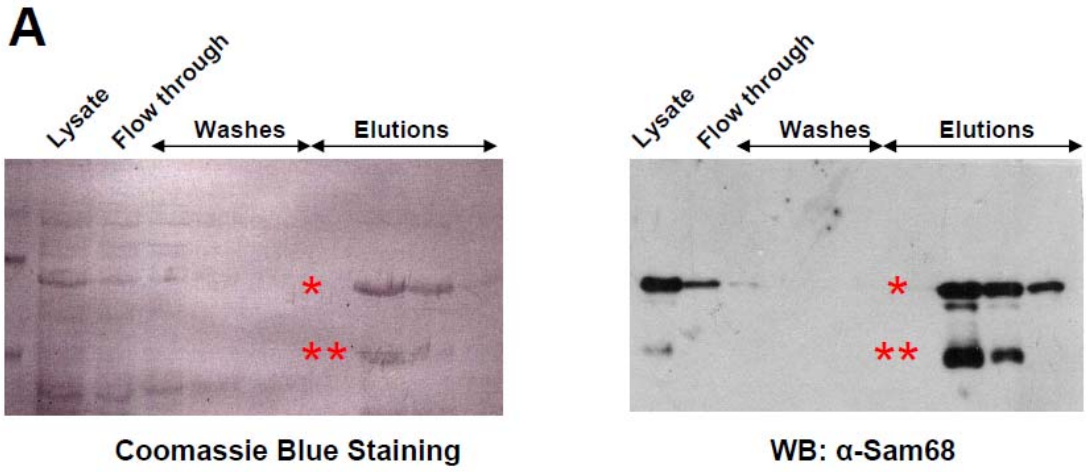
A
Lysate
Flow through
Washes
Elutions
*
**
Coomassie Blue Staining
Lysate
Flow through
Washes
Elutions
*
**
WB: α-Sam68

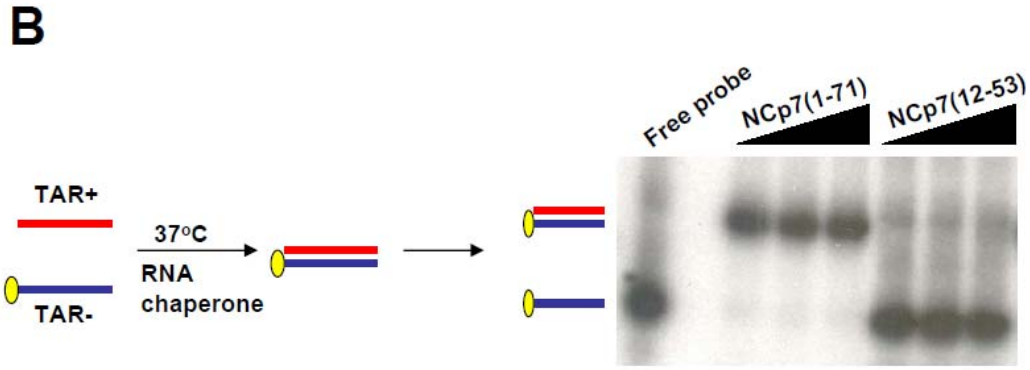
B
TAR+
TAR-
37°C
RNA
chaperone
Free probe
NCp7(1-71)
NCp7(12-53)

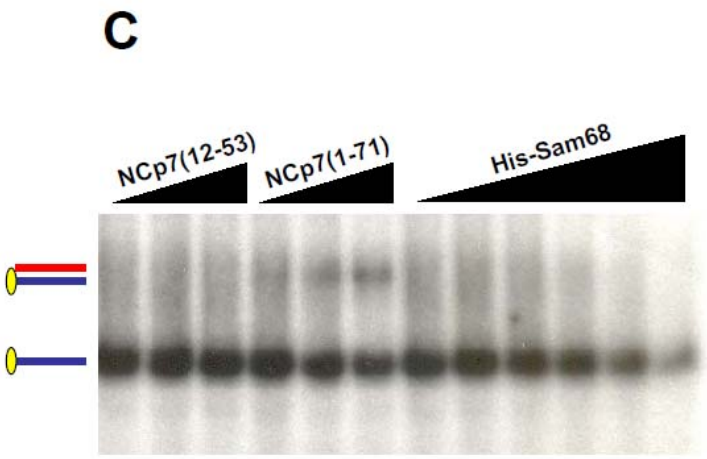
C
NCp7(12-53)
NCp7(1-71)
His-Sam68

Figure 15. ***in vitro*** **oligonucleotide annealing capability of Sam68. A.** His-tagged Sam68 was expressed on BL21 bacteria and purified as detailed in the Materials and Methods section. Then, 35 µl (right) or 5 µl (left) of each fraction were separated by 7.5% SDS-PAGE followed by coomassie blue staining (right) or Western blot analysis (left) using anti-Sam68. (*) His-Sam68, (**) degradation products of His-Sam68. **B.** *in vitro* oligonucleotide annealing by HIV-1 NC. Complementary TAR(+) (red) and radioactively labeled TAR (-) (blue) oligonucleotides were mixed in the presence of increasing concentrations (0.75, 1.5, 3.0 pmoles) of RNA chaperone NCp7(1-71) or its inactive mutant NCp7(12-53), incubated at 37^{o}C for 10 min followed by separation in a 12% native gel, and visualized by autoradiography. **C.** *in vitro* oligonucleotide annealing by Sam68. Similar assay was performed at 37^{o}C for 2.5 min in the presence of increasing concentrations of purified His-Sam68 (2.5, 5, 12.5, 25, 50, or 100 pmoles); NCp7(1-71) or NCp7(12-53) were included as positive and negative controls, respectively.

NCp7(1-71) or NCp7(12-53), as positive and negative controls, respectively. As previously reported, NCp7(1-71) promotes rapid oligonucleotide annealing and NCp7(12-53) mutant protein failed to do so (Fig. 15B & C). However, Sam68 failed to promote annealing of complementary oligonucleotides at 37^{o}C, despite using high concentrations of purified protein. These results suggest that under these conditions Sam68 does not have chaperone activity, despite its high predicted intrinsic disorder, and that its ability to suppress Nef expression does not likely involve Sam68-directed mRNA folding.

1.8 Localization of Sam68 mutants Δ410 and Δ321 in perinuclear granule-like structures.

We next examined the intracellular localization of these mutants using the panel of GFP fusion proteins (Fig. 12), to determine if there is any particular association between localization and Nef suppression. We expressed these GFP fusion proteins in COS-7 cells, as the size of these cells is relatively larger when compared to the size of 293T cells, which made these cells an ideal platform for such experiments. As expected, full-length Sam68 that contains the intact NLS was detected in the nucleus, and Δ410, Δ321, and Δ269 that all lack the NLS were localized in the cytoplasm (Fig. 16A). Moreover, Δ269-321 was expressed in the nucleus, while the 269-321 domain was detected throughout the cells (Fig. 16A). Of note was that inhibitory Δ410 and Δ321 mutants appeared in a unique granule-like structure in the cytoplasm, whereas a non-inhibitory mutant Δ269

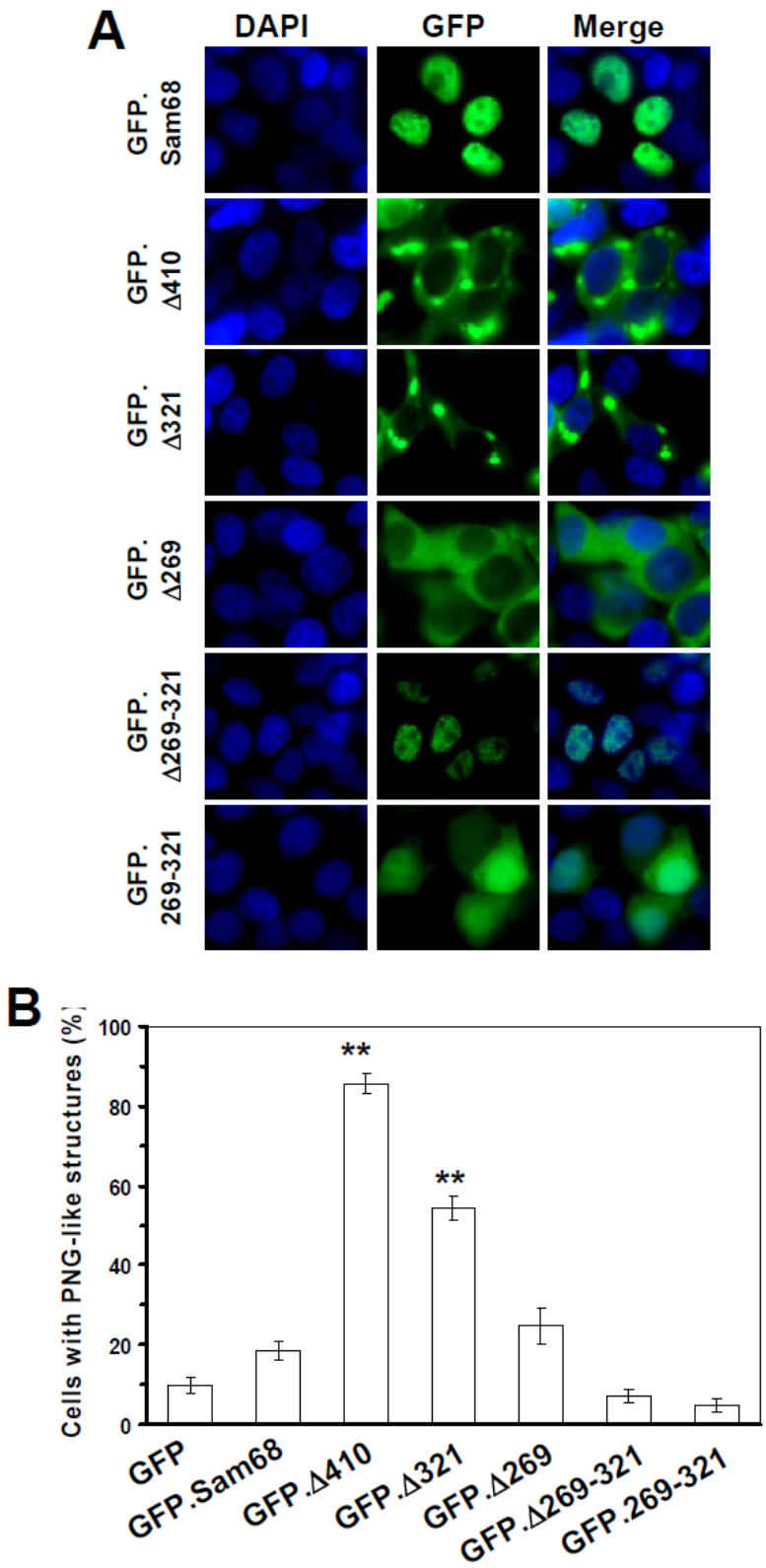
A
DAPI
GFP
Merge
GFP. Sam68
GFP. Δ410
GFP. Δ321
GFP. Δ269
GFP. Δ269-321
GFP. 269-321
B
Cells with PNG-like structures (%)
100
80
60
40
20
0
**
**
GFP
GFP.Sam68
GFP.Δ410
GFP.Δ321
GFP.Δ269
GFP.Δ269-321
GFP.269-321

Figure 16. Subcellular localization of GFP tagged Sam68 and its mutants. **A.** COS-7 were plated in a 24- well plate at a density of 0.75 x 10^5 cells per well and transfected with 0.3 µg GFP-tagged Sam68 or its mutants. The cells were fixed in 4% PFA 24 hr after transfection, and then stained in PBS containing 100 ng/ml DAPI for nuclei. Localization of GFP fusion proteins was visualized and captured using a Zeiss immunofluorescence microscope. The images were representative of each GFP fusion protein. **B.** Ten random fields were counted for a total number of 100 transfected cells in each well and for the number of cells exhibiting a granule-like structure, which were used to calculate the percentage of the granule-containing cells. The data were mean ± S.E.M. Comparisons among groups were made using two-tailed Student's *t*-test (**) $p < 0.01$.

showed an evenly cytoplasmic distribution, a typical pattern of cytoplasmic protein (Fig. 16A). The apparent association between formation of the granule-like structure and Nef suppression prompted us to quantitate the percentage of the structure-containing cells in each transfection. More than 85.67 ± 2.49% of the Δ410-transfected cells exhibited the structure, while the structure was detected in 54.33 ± 3.30% of the Δ321 transfected cells (Fig. 16B). Both were significantly higher than GFP alone (9.67 ± 2.05%), Sam68 (18.33 ± 2.36%), Δ269 (24.67 ± 4.50%), Δ269-321 (7.00 ± 1.63%) and 269-321 (4.67 ± 1.70%). There were no significant differences among cells expressing GFP alone, Sam68, Δ269, Δ269-321 and 269-321. These results suggest an association between Nef suppression and formation of the granule-like structure.

1.9 Δ410 localization into stress granules

Stress granules (SG) have been shown to regulate gene expression at the translational level in response to a variety of external stimuli [123]. Our findings that Δ410 expression resulted in Nef suppression and formation of a granule-like structure prompted us to determine whether Δ410 expression directly induced stress granules. We transfected COS-7 cells with HA-tagged Δ410, in combination with three GFP-tagged SG markers, GFP-G3BP, GFP-TIA-1, or GFP-hnRNP A1. G3BP and TIA-1 induce SG assembly when over-expressed in the absence of external stress stimuli [124], while hnRNP A1 is localized into the SG only under stress conditions [160]. We then briefly exposed the transfected

cells to sodium arsenite (ARS), a widely used oxidative stressor. We performed immunofluorescence staining for Δ410 localization using an anti-HA epitope antibody. As expected, G3BP and TIA-1 were localized in the SG irregardless of ARS treatment (Fig. 17A & B), whereas hnRNP A1 was expressed in the nucleus of cells in the absence of ARS treatment and was re-localized into the SG when the cells were exposed to ARS (Fig. 17C). In contrast, Δ410 was found to be localized in the granule-like structure in all these three co-transfections, and ARS treatment did not affect this localization. Moreover, co-localization analysis revealed that Δ410 was co-localized with G3BP and TIA-1 in both ARS-treated and untreated cells and only with hnRNP A1 in ARS-treated cells (Fig. 17A-C), confirming that the granule-like structures induced by Δ410 expression are SG. To exclude the possibility that Δ410-induced SG formation results from over-expression of these SG markers, we transfected 293T cells with GFP.Δ410 and performed immunofluorescence staining for endogenous TIA-1 using an anti-human TIA-1 antibody. Similarly, Δ410 was co-localized with endogenous TIA-1 in the SG, even though a majority of the TIA-1 protein was detected in the nucleus (Fig. 18A). Localization of Δ410 in SG was further confirmed using other endogenous SG markers such as: eIF3η and G3BP (Fig. 18B & C). Previously, It has been determined that SG are in a dynamic equilibrium with polysomes, therefore treatment with polysome stabilizing agents (cyclohexamide-CHX) dissolves SG [124]. Thus, we transfected cells with GFP.Δ410 and treated these cells with CHX and determined the status of SG. Similarly to GFP.TIA-1 and GFP.G3BP-expressing cells, CHX treatment led to SG disappearance in Δ410-

induced granules (Fig. 19A). However, it is important to mention that while GFP-TIA-1-positive SG dissolved very efficiently, GFP.G3BP positive and GFP.Δ410 positive SG disappeared only in a percentage of the cells, in concordance with previous findings that argue that SG with different protein composition behave differently. Lastly, we determined whether Δ410 was also localized in the processing bodies (P bodies), as P bodies share and exchange many structural components with SG and regulate protein translation and/or mRNA degradation in the cytoplasm [125]. We transfected COS-7 cells with a GFP-tagged P body marker hdcp-1α [294] and HA-tagged Δ410 and performed similar immunofluorescence staining for Δ410. We also treated cells with ARS as a control, as ARS is known to increase the size and number of P bodies. There was no co-localization between hdcp-1α and Δ410 in both ARS-treated and untreated cells (Fig. 19B). Taken together, these results demonstrate that Δ410 expression induces SG formation and suggest that SG formation likely contributes to Δ410-mediated Nef suppression.

1.10 Specificity of Δ410-induced Nef suppression

To ensure expression of all HIV-1 genes, HIV-1 full-length RNA transcripts undergo extensive splicing to generate various smaller RNA species. But all share the same 289-nt 5'-leader sequence that starts with TAR [37]. The fact that Δ410 completely blocks HIV-1 replication raises the possibility that Δ410 negatively regulates the translation efficiency of all HIV-1 RNAs including the *nef*

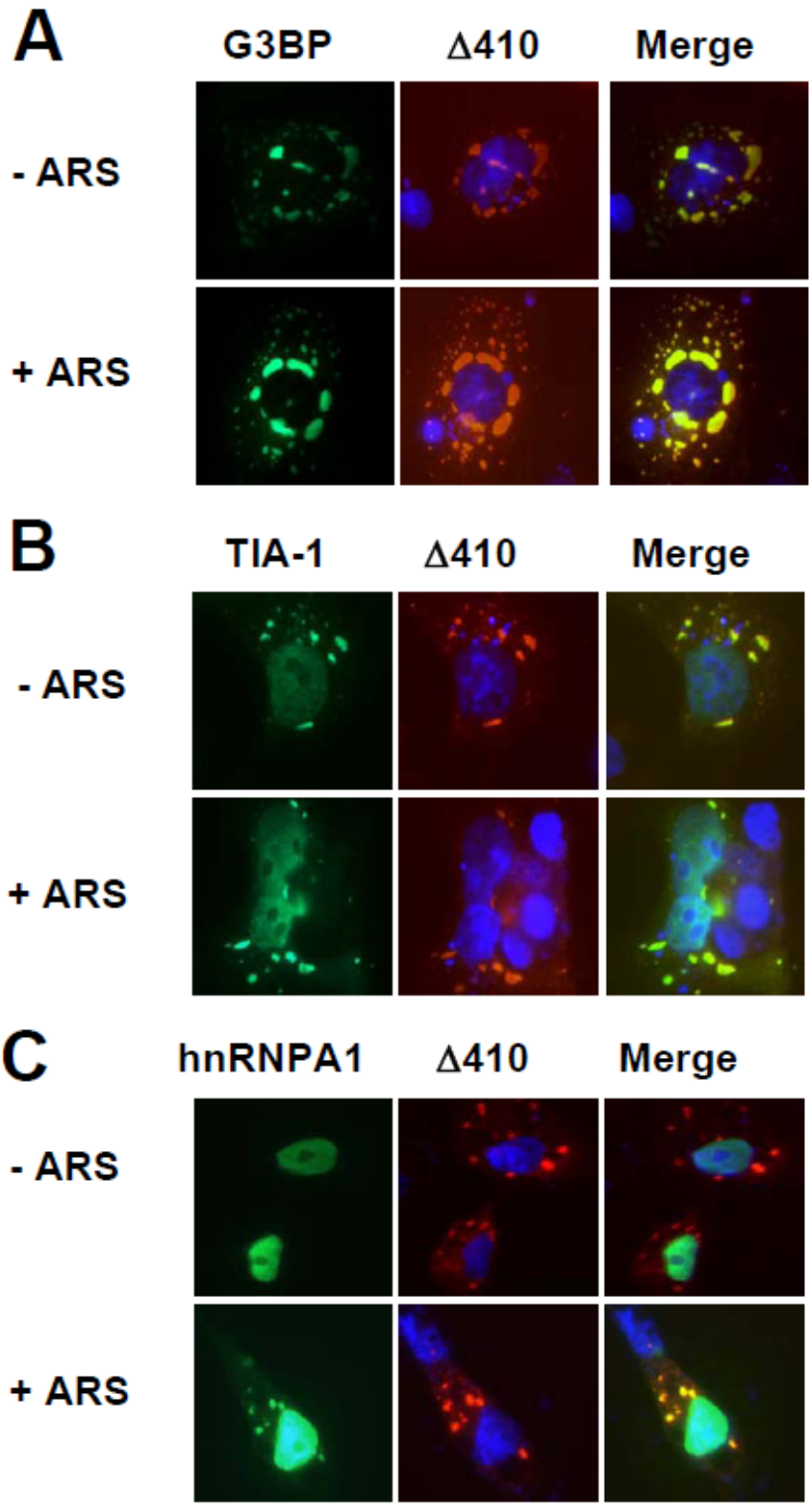
A
G3BP
Δ410
Merge
- ARS
+ ARS
B
TIA-1
Δ410
Merge
- ARS
+ ARS
C
hnRNPA1
Δ410
Merge
- ARS
+ ARS

Figure 17. Δ410 co-localization with stress granules markers G3BP, TIA-1, and hnRNP A1. COS-7 were plated in a 24-well plate at a density of 0.75 x 10^5 cells per well and transfected with 0.35 µg HA-tagged Δ410 and 0.35 µg GFP-G3BP (**A**), GFP-TIA-1 (**B**), or GFP-hnRNP A1 (**C**). Twenty four hours after transfection, the cells were treated with or without 0.5 mM sodium arsenite (ARS) for 1 hr, fixed in 4% PFA, and then stained with an anti-HA antibody followed by a PE-conjugated secondary antibody. The nuclei were counterstained with PBS containing 100 ng/ml DAPI. The images were representative of each co-transfection. Co-localization of SG markers and Δ410 was shown in the column marked as "Merge".

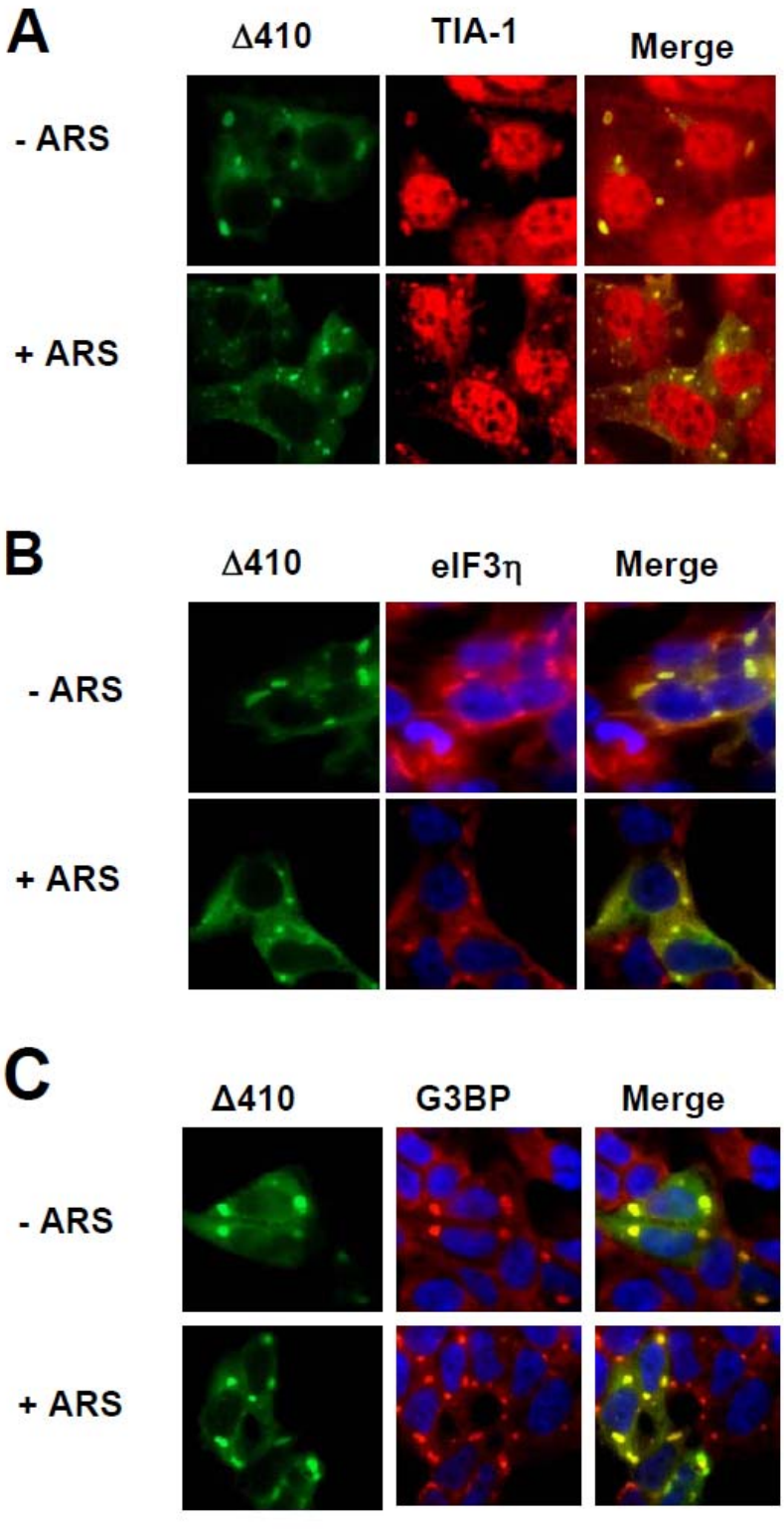
A
Δ410
TIA-1
Merge
- ARS
+ ARS
B
Δ410
eIF3η
Merge
- ARS
+ ARS
C
Δ410
G3BP
Merge
- ARS
+ ARS

Figure 18. Δ410 co-localization with endogenous stress granules markers TIA-1, eIF3η, and G3BP. 293T were plated in a 24-well plate at a density of 1.5 x 10^5 cells per well and transfecetd with 0.35 μg of GFP-tagged Δ410. Twenty four hours after transfection, the cells were treated with or without 0.5 mM sodium arsenite (ARS) for 1 hr, fixed in 4% PFA, and then stained with anti-TIA-1 (**A**), anti-eIF3η (**B**), and anti-G3BP (**C**) antibodies followed by a PE-conjugated secondary antibodies. The nuclei were counterstained with PBS containing 100 ng/ml DAPI. The images were representative of each co-transfection. Co-localization of SG markers and Δ410 was shown in the column marked as "Merge".

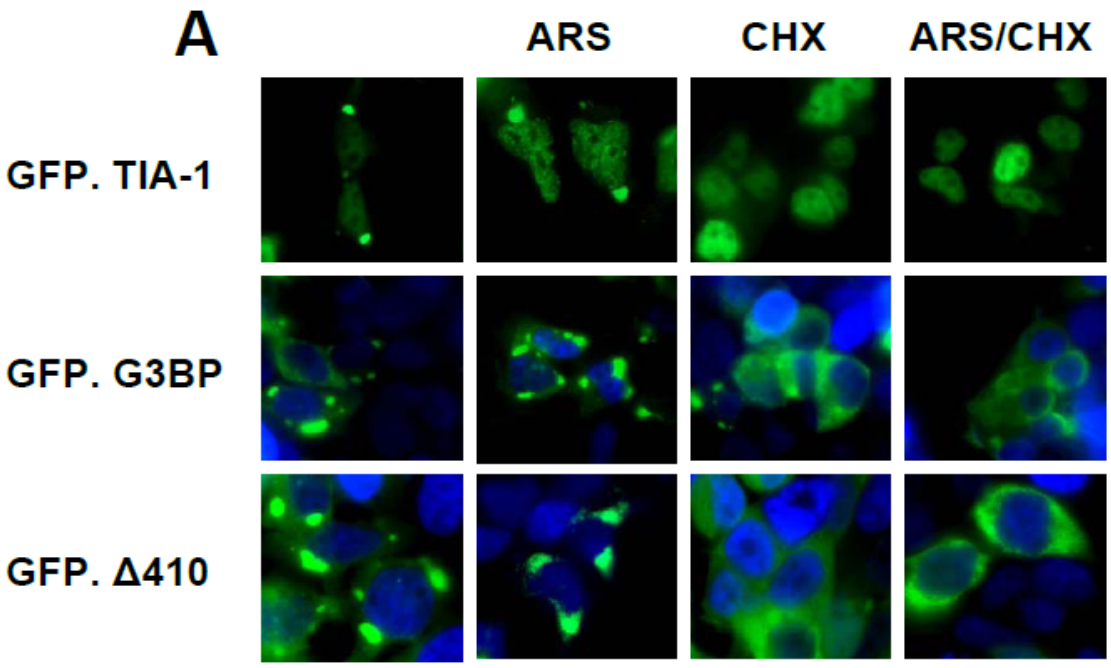
A
ARS
CHX
ARS/CHX
GFP. TIA-1
GFP. G3BP
GFP. Δ410

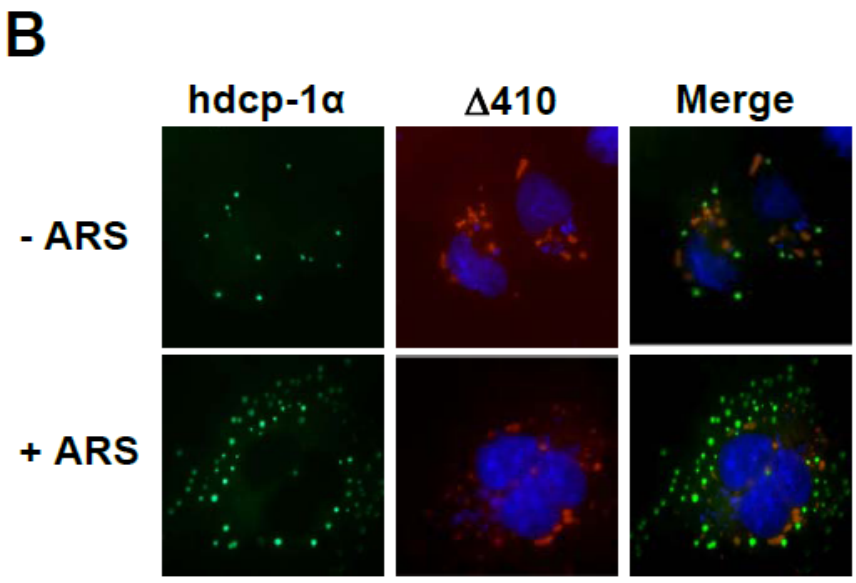
B
hdcp-1α
Δ410
Merge
- ARS
+ ARS

Figure 19. Functional behavior of Δ410-induced SG and Δ410 co-localization with P bodies marker hdcp-1α. A. 293T were plated in a 24- well plate at a density of 1.5 x 10^5 cells per well and transfected with 0.35 µg of GFP.TIA-1, GFP.G3BP or GFP.Δ410. Twenty four hours after transfection, the cells were treated with ARS as above, with 100 µg/ml cyclohexamine for 90 min, or the combination of both. The cells were then fixed in 4% PFA, and counterstained in PBS containing 100 ng/ml DAPI for nuclei. Microscopic analysis was carried out as above. **B.** COS-7 were plated in a 24- well plate at a density of 0.75 x 10^5 cells per well and transfected with 0.35 µg HA-tagged Δ410 and 0.35 µg GFP.hdcp-1α. The cells were processed, and analyzed for co-localization as previously described.

RNA. To address this possibility, we took advantage of a bicistronic reporter gene system [40]. The reporter gene system has the 5'-HIV-1 leader sequence inserted between the ORFs of *Renilla* Luc gene (R Luc) and Firefly Luc gene (F Luc) and is under the control of the CMV promoter (Fig. 20A). F Luc expression is used as a measure of the translation efficiency of the HIV-1 5' leader sequence with R Luc to normalize the transfection variations. Thus, we transfected 293T cells with this reporter gene and Sam68 or Δ410 and determined the activity of F Luc and R Luc. The results showed that there was no significant difference in the F Luc/R Luc ratio between Sam68 and Δ410 transfections, although both appeared to be slightly higher than the cDNA 3 control (Fig. 20B).

HIV-1 accessory proteins Nef, Tat and Rev are all encoded by completely spliced RNA, which contain a significant sequence overlap (Fig. 21A). Thus, it was necessary to determine whether Δ410 has similar suppressive effects on Tat and Rev expression. To address this specificity issue, we constructed *tat*, *rev* and *nef* minigenes (Fig. 21A & B) and compared Δ410 effects on their expression. We transfected each of these minigenes with Sam68 or each of its mutants and determined the minigene expression using Western blot analysis. In agreement with our earlier findings (Fig. 13A & B), both Δ410 and Δ321 suppressed Nef expression (Fig. 21C). However, Δ410 and Δ321 had little effects on Tat and Rev expression (Fig. 21C).

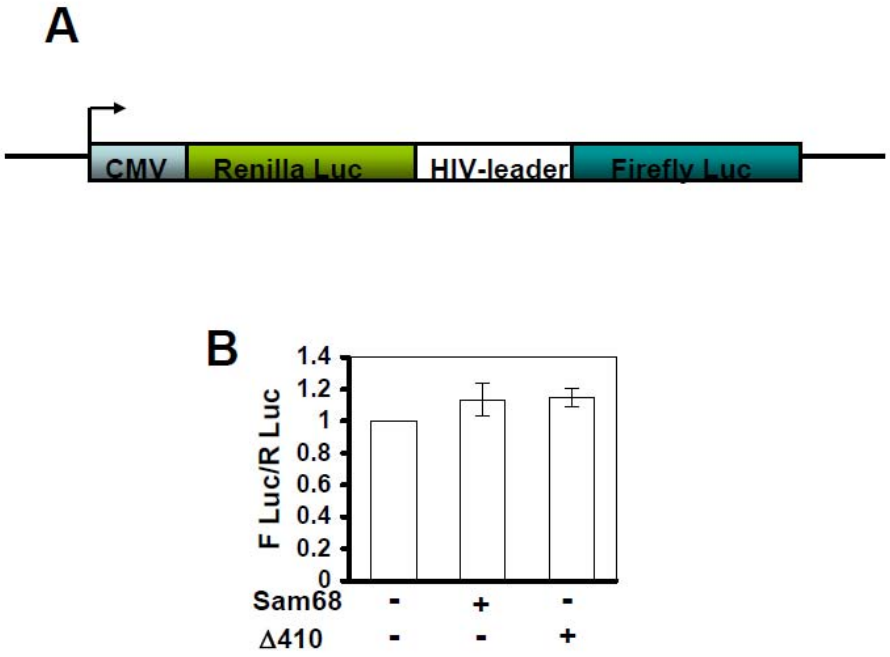

Figure 20. Effects of Δ410 on the translation efficiency of the RNA containing the 289 nt. 5' leader sequence of HIV-1. A. Scheme of the bicistronic vector cDNA3-R Luc-HIV 5'-F Luc. **B.** 293T were plated in a 12- well plate at a density of 2.2 x 10^5 cells per well and transfected with 0.1 μg of cDNA3-F Luc-HIV 5'-R Luc and 0.6 μg of Sam68, Δ410, or cDNA3. The cells were harvested 42 hr after transfection and assayed for F Luc and R Luc activity as detailed in Materials and Methods. The ratio of F Luc to R Luc was used to measure the translation activity of HIV-1 5'-R leader sequence. The data were mean ± S.E.M. of triplicates.

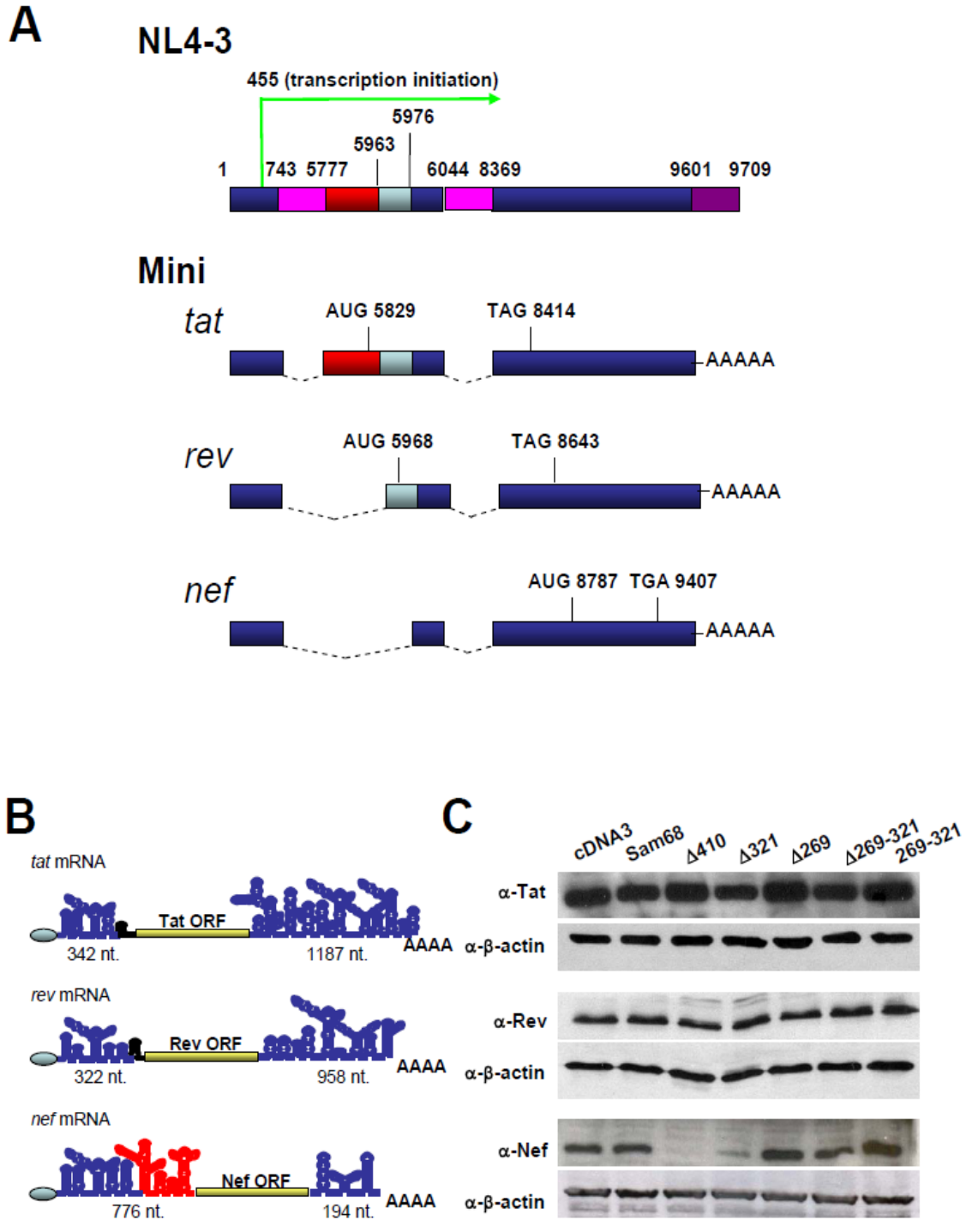
A
NL4-3
455 (transcription initiation)
5976
5963
1
743 5777
6044 8369
9601 9709
Mini
tat
AUG 5829
TAG 8414
AAAAA
rev
AUG 5968
TAG 8643
AAAAA
nef
AUG 8787 TGA 9407
AAAAA
B
tat mRNA
Tat ORF
342 nt.
1187 nt.
AAAA
rev mRNA
Rev ORF
322 nt.
958 nt.
AAAA
nef mRNA
Nef ORF
776 nt.
194 nt.
AAAA
C
cDNA3
Sam68
Δ410
Δ321
Δ269
Δ269-321
269-321
α-Tat
α-β-actin
α-Rev
α-β-actin
α-Nef
α-β-actin

Figure 21. Effects of Δ410 on *tat*, *rev* and *nef* minigene expression. A. Scheme of NL4-3 proviral DNA and *tat*, *rev*, and *nef* minigenes. Nucleotide location of the major alternative splicing sites that are used to generate the most abundant *tat*, *rev* and *nef* mRNA species, and the transcription initiation site are marked on top of the NL4-3 proviral DNA scheme. Representation of *tat, rev* and *nef* minigenes are shown below, translation start and stop codes and their locations were also marked on top of each of the minigenes. Different regions were marked with colors as follows: the region only present on *tat* mRNA was marked red, the region only present on *tat* and *rev* mRNA was marked light blue, and the region present in all *tat, rev* and *nef* mRNA was marked blue. **B.** The secondary structure of the 5'UTR and 3'UTR of all minigenes were predicted by the RNAfold program. The length in nucleotides for each 5'UTR and 3'UTR was given under each minigene. A region present in *nef* 5'UTR but not in *tat* or *rev* 5'UTRs was marked red. **C.** 293T cells were plated in a 12- well plate at a density of 1.5 x 10^5 cells per well and transfected with 0.35 μg of *tat* minigene, 0.18 μg of *rev* minigene, or 0.18 μg of *nef* minigene, in combination with 1.2 μg of HA-tagged Sam68 or its mutants. In addition, 40 ng, or 10 ng of Tat-myc were included for *rev* minigene and *nef* minigene, respectively. The cells were harvested 42 hr after transfection, lysed in RIPA buffer, and 20 μg of each sample were separated by 12.5% SDS-PAGE followed by Western blot analysis using anti-Nef JRCSF, or anti-β-actin.

To ascertain that the previous observations were not artifacts due to the use of NL4-*3 tat, rev* and *nef* minigenes, we wanted to determine the effects of Δ410 on Tat and Rev expression in the context of the original NL4-3. However, in view that Tat is known to be a poor immunogen [295], and that we failed to directly detect Rev expression by Western blot analysis (Fig. 22A) or by immunoprecipitation (Fig. 22B), using different anti-Rev antibodies from commercial sources or NIH AIDS Reagents Program, we then considered using indirect functional assays. Studies have shown that Δ410 directly inhibits Rev nuclear export function [78, 249], suggesting that this functional assay would not allow us to distinguish Δ410 effects on Rev function from Δ410 effects on Rev expression. In contrast, Δ410 has been shown to have no effect on Tat transactivation activity of the HIV-1 LTR [78]. Thus, we performed an indirect Tat functional assay. We first transfected 293T cells with LTR-CAT reporter plasmid and increasing concentrations of NL4-3, which served as a source of Tat and determined the optimal amount of NL4-3 to be 0.2 μg that gave rise to a linear response of LTR-CAT to Tat in this assay (Fig. 22C). We then transfected 293T cells with LTR-CAT, NL4-3 (0.2 μg), and Sam68 or Δ410 and determined the CAT activity in these cells. There were no differences in CAT activity among the cDNA3, Sam68 and Δ410 transfected cells (Fig. 22C). These results suggest that Δ410 did not alter Tat or Rev expression and that the suppressive effects of Δ410 were specific to Nef.

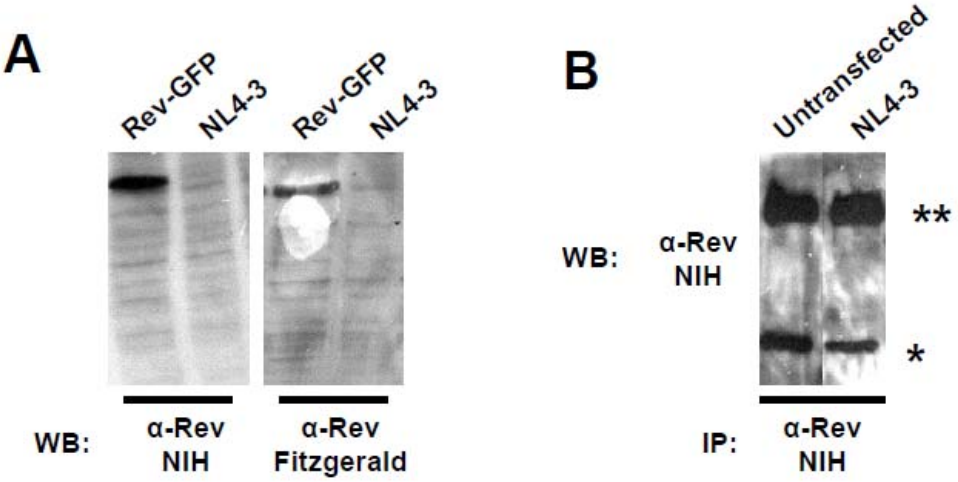
A
Rev-GFP
NL4-3
Rev-GFP
NL4-3
WB:
α-Rev NIH
α-Rev Fitzgerald
B
Untransfected
NL4-3
WB:
α-Rev NIH
**
*
IP:
α-Rev NIH

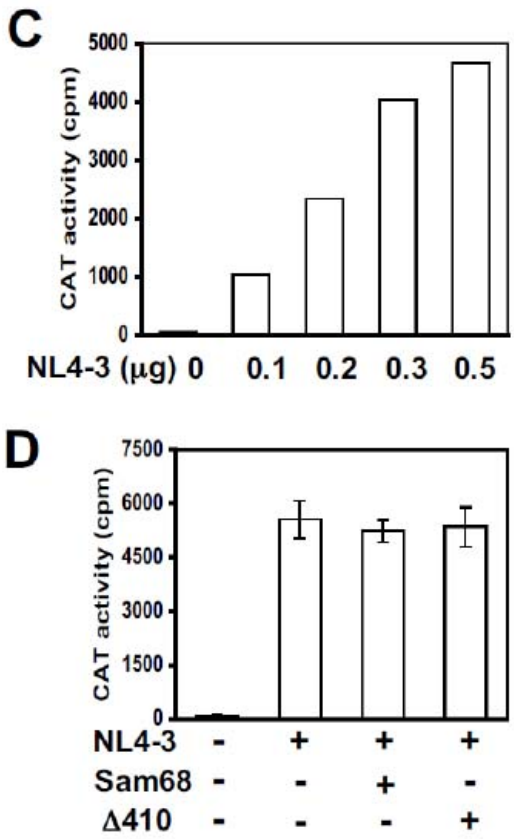
C
CAT activity (cpm)
5000
4000
3000
2000
1000
0
NL4-3 (μg) 0 0.1 0.2 0.3 0.5
D
CAT activity (cpm)
7500
6000
4500
3000
1500
0
NL4-3 - + + +
Sam68 - - + -
Δ410 - - - +

Figure 22. Effects of Δ410 on NL4-3 Tat expression. A. 293T cells were plated in a 60 mm plate at a density of 8.0 x 10^5 cells per plate and transfected with 7.0 μg of Rev-GFP (positive control), or 7.0 μg of NL4-3. The cells were harvested 42 hr after transfection, lysed in RIPA buffer, and 100 μg of each sample were separated by 12.5% SDS-PAGE followed by Western blot analysis using anti-Rev-NIH, or anti-Rev-Fitzgerald antibodies. **B.** 293T cells were transfected and lysed as above. One milligram of cell lysate was then immunoprecipitated with anti-Rev-NIH antibody, followed by Western blotting using α-Rev-NIH antibody. IgG heavy chain (**), and light chain (*). **C.** 293T cells were plated in a 24-well plate at a density of 1.25 x 10^5 cells per well and transfected with 0.1 μg of LTR-CAT, 0.05 μg of pcDNA3-βGal, and 0.05, 0.1, 0.2, 0.3 and 0.5 μg of NL4-3. pcDNA3 was used to equalize the total amount of DNA transfected among transfections and pcDNA3-βGal was used to normalize variations of the transfection efficiency among the transfections. The cells were harvested for the CAT activity assay 42 hr after transfection. **D.** Similar experiments were performed as stated in **C** except that 0.1 μg of LTR-CAT, 0.2 μg of NL4-3, and 0.6 μg of HA.Sam68, Δ410, or cDAN3 were transfected. The data were mean ± S.E.M of triplicates.

1.11 Δ410 interaction with *nef* mRNA 3'UTR

Our previous results suggest that *nef* mRNA contains a molecular determinant required for Δ410-mediated translational repression (Fig. 20-22). As the primary sequences of *tat*, *rev* and *nef* mRNA extensively overlap (Fig. 21A); we then turned our attention to the 5'- and 3'-untranslated regions (5'UTR and 3'UTR) of these mRNA. When we performed the secondary structure analysis of these mRNA using the RNAfold program [296], we found that both 5'UTR and 3'UTR regions of these mRNA significantly differed from each other in their secondary structure and length (Fig. 21B). Of particular note is part of 5'UTR of *nef* mRNA that is absent in *tat* and *rev* mRNA (marked in red, Fig. 21B). Thus, using *nef* minigene as an experimental model, we deleted this unique 5'UTR region from *nef* minigene (Fig. 23A). Meanwhile, we also constructed a *nef* minigene mutant that was deleted of the entire 3'UTR of *nef* mRNA, which is also significantly different from those of *tat* and *rev* mRNA (Fig. 21B). We then compared Nef expression from these *nef* minigene deletion mutants using the similar co-transfection and Western blot analysis approaches. The 5'UTR deletion showed little effects on Δ410- and Δ321-induced Nef suppression, while the 3'UTR deletion completely abolished Nef suppression by these two Sam68 mutants (Fig. 23B). Further corroboration of these findings was that Δ410 or Δ321 did not suppress Nef expression from an expressing cassette that only contains the *nef* ORF (Fig. 23B). These results show that 3'UTR of *nef* mRNA is the molecular determinant for the specificity of Δ410- and Δ321-induced Nef suppression.

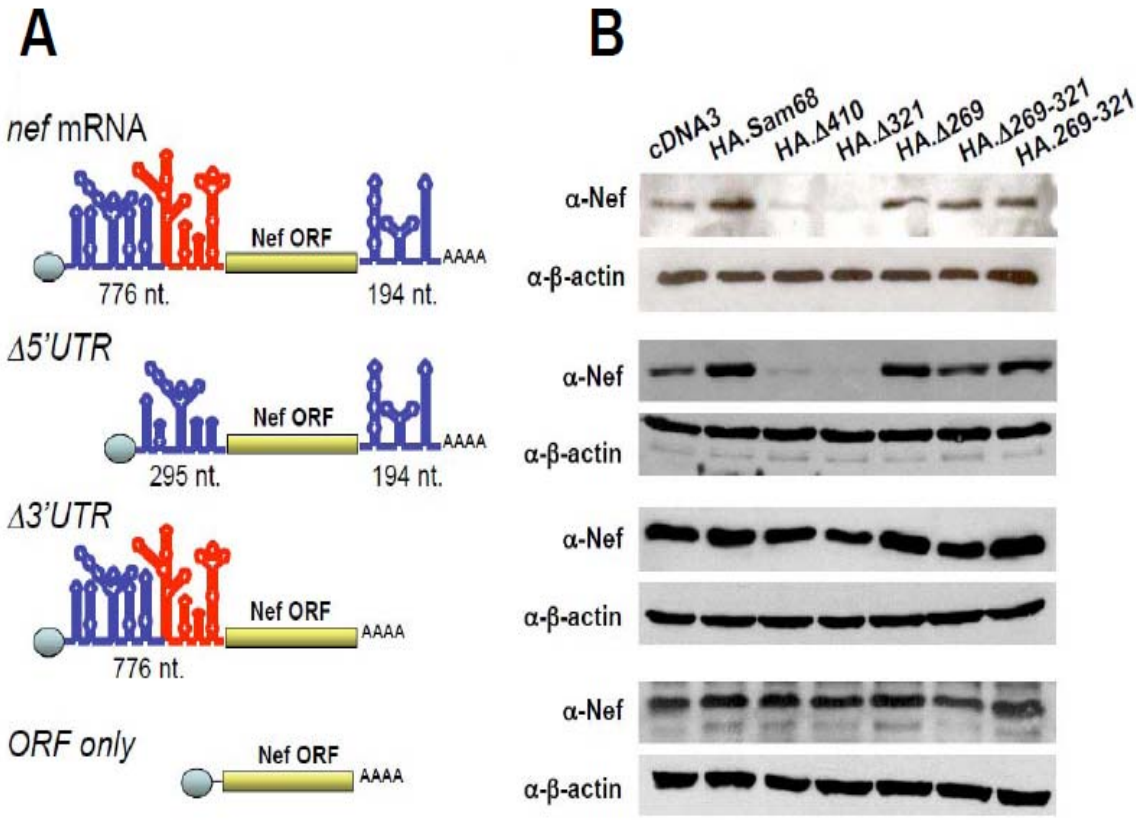

Figure 23. Effects of Δ410 on *nef* deletion minigene expression. A. The secondary structure of the 5'UTR and 3'UTR of *nef* deletion minigenes were predicted by the RNAfold program. The length in nucleotides for each 5'UTR and 3'UTR was given under each minigene. A region present in *nef* 5'UTR but not in *tat* or *rev* 5'UTRs was marked red. **B.** 293T cells were plated in a 12-well plate at a density of 1.5 x 10^5 cells per well and transfected with 0.18 μg of *nef* minigenes, 1.2 μg of HA-tagged Sam68 or its mutants, and 10 ng of Tat-myc. The cells were harvested 42 hr after transfection, lysed in RIPA buffer, and 20 μg of each sample were separated by 12.5% SDS-PAGE followed by Western blot analysis using anti-Nef JRCSF, or anti-β-actin.

The above results from the minigene experiments (Fig. 23B) prompted us to further determine whether Δ410 bound to *nef* mRNA 3'UTR, and whether the binding was correlated with its suppressive effects. We took advantage of a RNA-protein interaction-based yeast three hybrid reporter gene assay [297], which allows *in vivo* detection of RNA-protein binding. This assay system consists of three components: one hybrid protein of bacteriophage MS2 coat protein fused to LexA DNA-binding domain, the other hybrid protein containing the protein to be tested fused to the Gal4 DNA-activation domain, and one hybrid RNA that has the RNA target for the MS2 coat protein as well as the RNA to be tested. When these three components are introduced into and expressed in the appropriate yeast strain, direct binding of the test protein and the test RNA will activate the LacZ reporter gene expression in the yeast. We constructed Δ410 fusion expression plasmid and the MS2 RNA-*nef* mRNA 3'UTR hybrid RNA plasmid (MS2-*nef* 3'UTR). We also constructed MS2-*nef* 3'RTU hybrid RNA plasmid in which the *nef* mRNA 3'UTR is in a reverse orientation and used it as a cognate control. We also constructed two additional fusion expression plasmids, Δ269 which only slightly induced SG formation and did not suppress Nef expression, and ΔKH which is a RNA binding deficient Sam68 mutant. We then transfected respective plasmids into the yeast strain L40 and determined β-Gal activity of the transformants. We also included iron regulatory protein (IRP) and its iron responsive element (IRE) RNA-binding target as positive controls in these experiments. As expected, co-transfection of IRP fusion plasmid with MS2-IRE hybrid RNA activated LacZ gene expression and β-Gal activity (Table 2). Co-

transfection of Δ410 fusion plasmid and MS2-*nef* 3'UTR RNA plasmid activated LacZ gene expression and β-Gal activity, albeit to much less extent. Importantly, there was no detectable β-Gal activity in co-transfection of Δ410 fusion plasmid and MS2-*nef* 3'-RTU and in all other co-transfections expressing the Δ269 or ΔKH fusion plasmids. Taken together, these studies show that Δ410 suppresses Nef expression through its specific binding to the 3'UTR of *nef* mRNA, and suggest that Δ410-induced Nef suppression likely result from *nef* mRNA localization and sequestration into SG through binding to Δ410 and subsequent being unavailable for protein translation.

1.12 Lack of suppression of HIV-1 Nef by SG-inducing proteins TIA-1 and G3BP

Over-expression of several RNA binding proteins induce SG formation, e.g., G3BP, TIA-1, TTP, Caprin-1, FAST, FRMP, LINE-1 ORF, and smaug [124]. Thus, it is plausible to think that Nef suppression is the product of an unspecific phenomenon resulting from SG assembly; therefore, it was important to further ascertain whether expression of these SG inducing proteins also leads to Nef suppression. We tested two well-characterized SG-inducing proteins that are also often used as SG markers, TIA-1 and G3BP. We transfected 293T cells with NL4-3, in combination with GFP-TIA-1 or GFP-G3BP and determined Nef expression by Western blot analysis. As expected, over-expression of TIA-1 and G3BP induced SG formation (Fig. 24A). But, compared to the GFP control,

Table 2. Δ410 binding to 3'UTR of *nef* mRNA

Hybrid protein 1	Hybrid RNA	Hybrid protein 2	Relative β-Gal activity
MS2	MS2	IRP	0
MS2	MS2-IRE	IRP	6.763 ± 0.429
MS2	MS2	Δ410	ND
MS2	MS2-nef 3'UTR	Δ410	0.122 ± 0.025
MS2	MS2-nef 3'RTU	Δ410	ND
MS2	MS2	Δ269	ND
MS2	MS2-nef 3'UTR	Δ269	ND
MS2	MS2-nef 3'RTU	Δ269	ND
MS2	MS2	ΔKH	ND
MS2	MS2-nef 3'UTR	ΔKH	ND
MS2	MS2-nef 3'RTU	ΔKH	ND

The yeast strain L40 was transfected with hybrid protein 1, hybrid protein 2 and hybrid RNA expression plasmids as indicated. The transformants were grown in a SD (Synthetic drop) plate lacking tryptophan, leucine, uracil, and histidine for 5 days. Fifteen colonies from each transformation were inoculated into the same liquid SD medium, triplicates of each inoculation were determined for the β-Gal gene expression using the liquid culture β-Gal assay. Data are mean ± SEM. ND: No detectable β-Gal activity or no colony growth. IRP (iron regulatory protein), IRE (iron regulatory element), RTU (UTR in reverse orientation).

expression of either TIA-1 or G3BP did not alter Nef expression (Fig. 24B). These results show that not every SG formation event results in Nef suppression and provide additional evidence to support the specificity of Δ410 toward to Nef (Fig. 20-23; Table 2).

1.13 Localization of HIV-1 *nef* RNA transcripts in Δ410-induced SG

Translational suppression often occurs as a result of SG formation and selective targeting of mRNA [138, 298]. Based on the previous findings (Fig. 20-23; Table 2), we next determined whether this was indeed the case for Δ410-mediated Nef suppression. We examined the intracellular distribution of HIV-1 *nef* RNA transcripts in Δ410-expressing cells. We transfected 293T cells with HIV-1 NL4-3, GFP.Δ410, or both. NL4-3 was used as the source for *nef* mRNA transcripts. We performed fluorescence *in situ* hybridization (FISH) using a *nef*-specific Cy-5-labelled oligonucleotide probe. This probe was designed to ensure a maximal specificity and accessibility to *nef* mRNA transcripts using an algorithm-based program for mRNA secondary structure [296]. As expected, *nef*-Cy5 was exclusively detected throughout the cytoplasm of cells that were only transfected with NL4-3, and only a background level of hybridization signals was detected in GFP.Δ410-transfected cells (Fig. 25). Co-expression of NL4-3 and GFP.Δ410 led to marked changes of *nef*-Cy5 localization to a more distinct cytoplasmic pattern and its co-localization with Δ410. These results validate the

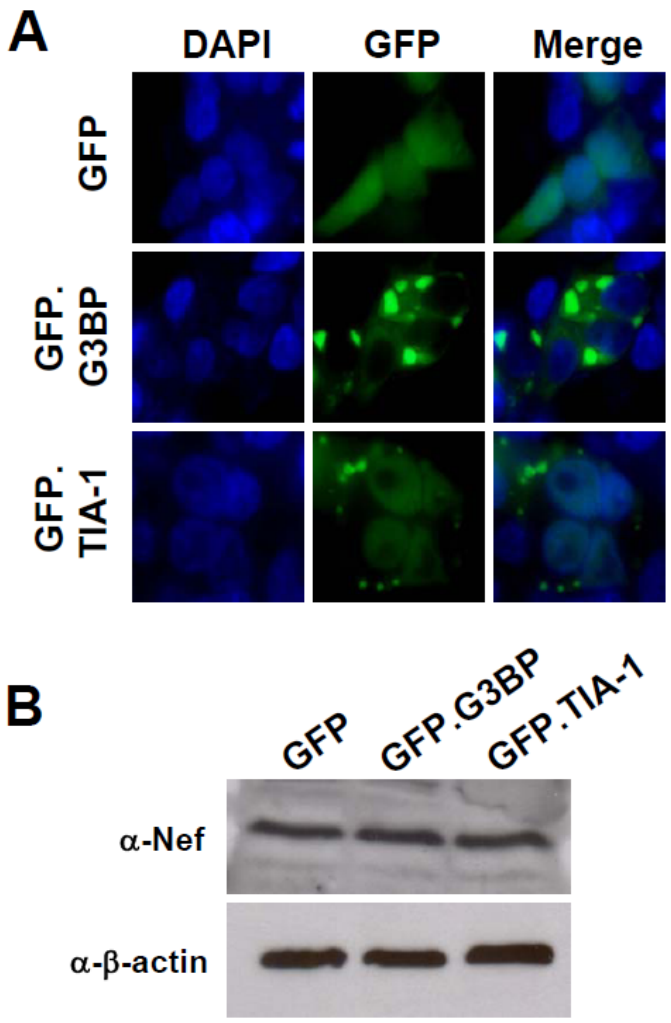

Figure 24. Effects of SG-inducing proteins on Nef expression. 293T cells were plated in a 12- well plate at a density of 3.0 x 10^5 cells per well and transfected with 0.18 µg of NL4-3, and 1.25 µg of GFP.G3BP, or GFP.TIA-1. Forty two hours after transfection, the cells were either processed for immunofluorescence microscopic imaging for SG formation (**A**), or harvested, lysed in RIPA buffer, and 20 µg of each sample were separated by 12.5% SDS-PAGE followed by Western blot analysis using anti-Nef JRCSF, or anti-β-actin (**B**).

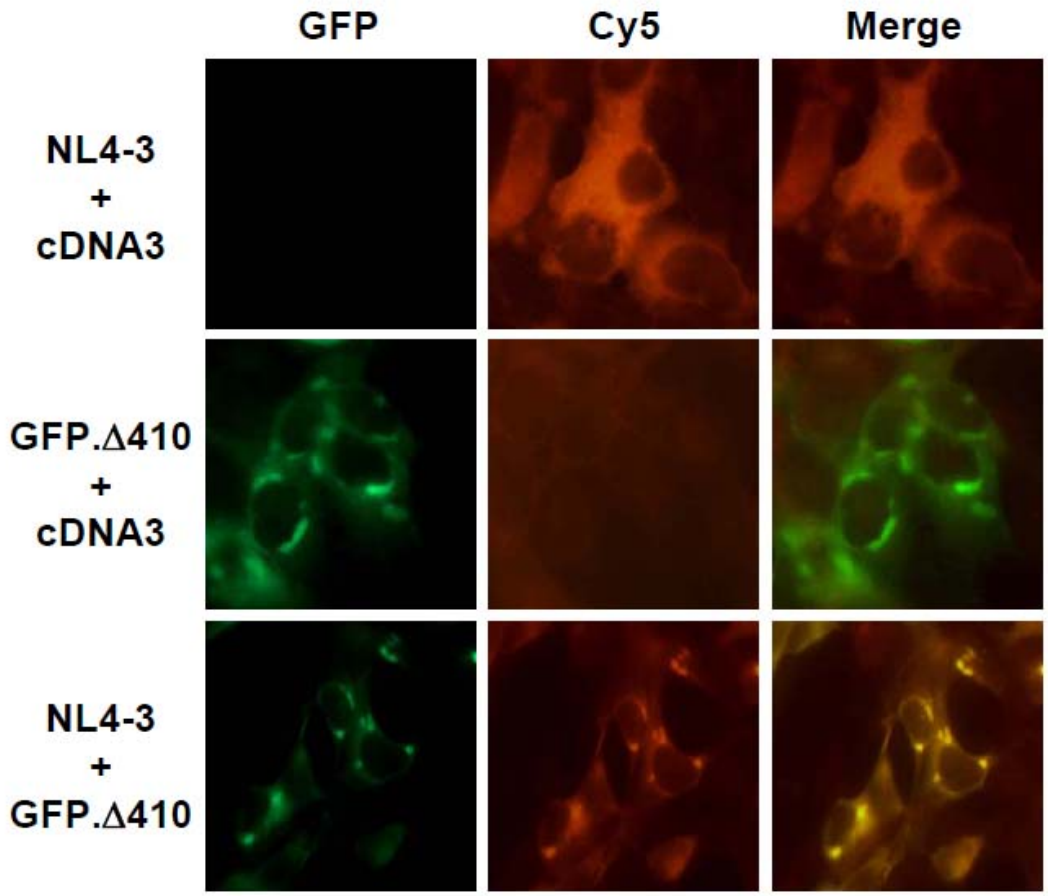

Figure 25. Effects of Δ410-induced SG formation on localization of *nef* RNA transcripts. 293T cells were plated in a 24-welll plate at a density of 1.25 x 10^5 per well and transfected with 0.4 μg of GFP.Δ410, 0.4 μg of NL4-3, or both. pcDNA3 was used to equalize the total amount of DNA among transfections. The cells were then processed for the fluorescence *in situ* hybridization as described in the Materials and Methods section, using 100 ng of a Cy5-labelled *nef* oligonucleotide. The images were representative of each co-transfection. Co-localization of Cy5-*nef* and Δ410 was shown in the column marked as "Merge".

notion that Δ410-mediated Nef suppression results from Δ410-induced SG formation and *nef* mRNA targeting and sequestration in SG.

1.14 Δ410 localization to SG and MHC-I expression in HIV-infected T lymphocytes

CD4+ T lymphocytes are the natural target cells for HIV-1 infection. Thus, we next determined whether Δ410 expression induced SG formation in Jurkat cells, commonly used CD4+ human T lymphocytes for HIV infection. We transfected Jurkat cells with RFP-tagged Δ410, in combination with GFP-tagged SG markers GFP-G3BP or GFP-TIA-1. We then performed the fluorescence microscopic imaging for RFP- and GFP-tagged proteins. In agreement with our previous findings (Fig. 17 & 18), G3BP and TIA-1 co-localized with Δ410 in cytoplasmic SG in the absence of ARS treatment (panels “merge” and “inset”, Fig. 26).

We next determined the effect of Δ410 on Nef expression in HIV-infected cells. To distinguish Δ410 effects on HIV-1 replication from those on Nef expression, we performed a single round infection assay that has previously been established to detect Nef expression in HIV-infected cells [100]. Initially, we determined the appropriate conditions to obtain optimum transfection efficiency, and Nef expression upon infection. Thus, we established that 24 hours after transfection of Jurkat cells with either GFP or GFP.Δ410, we were able to obtain transfection efficiencies of approximately 70%, cell viabilities of over 85%, and no

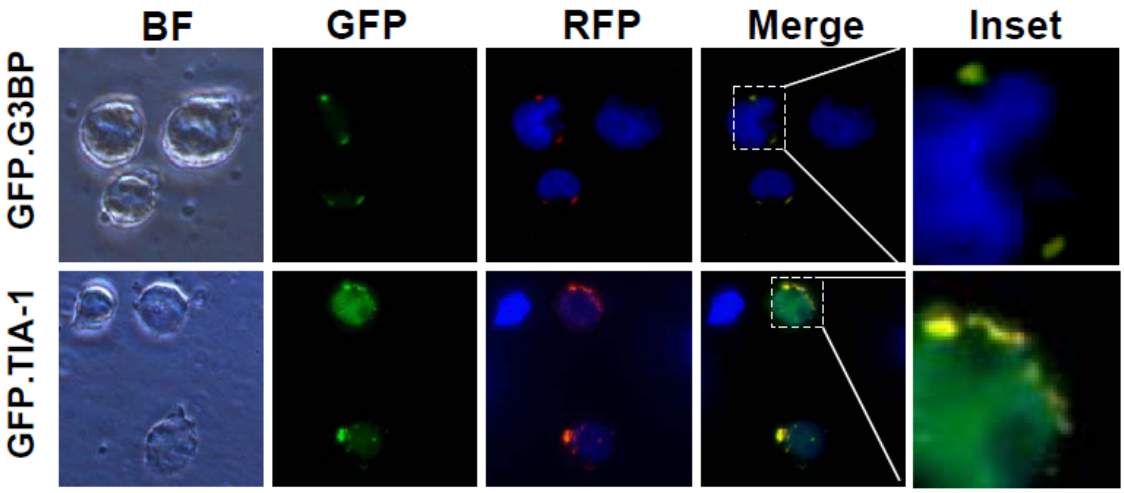

Figure 26. **Δ410-induced SG formation in Jurkat T cells. A.** 1.5 X 10^6 Jurkat T cells were transfected with 0.35 µg of GFP.G3BP or GFP.TIA-1, in combination with 0.15 µg of RFP.Δ410. Forty two hours after transfection, the cells were plated in poly-L-Lysine precoated cover-slips and processed for microscopic imaging for detection of GFP and RFP. Co-localization of GFP and RFP Δ410 was shown in the columns marked as "Merge" along with high mag "insets". BF: bright field.

differences between GFP and GFP.Δ410 transfections (Fig. 27A). In addition, infection with 50 x 10^5 VSV-G pseudotyped NL4-3.Luc(env) virus was ascertained to be an adequate viral titer for detection of Nef (Fig. 27B). We then infected the transfected cells with replication defective VSV-G pseudotyped NL4-3.Luc(env) virus and determined Nef expression by Western blot analysis 48 hours post infection. As shown in 293T cells (Fig. 8 & 13), Δ410 expression led to a decrease of Nef expression by about 40% in Jurkat cells (Fig. 27C). In parallel, we performed cell surface staining and flow cytometry analysis for MHC-I expression. Δ410 expression in HIV-infected cells showed a significant reduction in MHC I down-regulation, when compared to the cells expressing GFP only (Fig. 27D).

To extend the physiological significance from the established CD4+ Jurkat to primary CD4+ lymphocytes, we performed similar experiments in human PBMC. The transfection efficiency was estimated to be about 55%, while the cell viability was about 70%. Compared to the GFP control, GFP.Δ410 suppressed Nef suppression by about 70% in these primary cells (Fig. 27E). The difference in Δ410-induced Nef suppression between Jurkats and human PBMC is likely due to the different susceptibility of these two cells to HIV-1 infection.

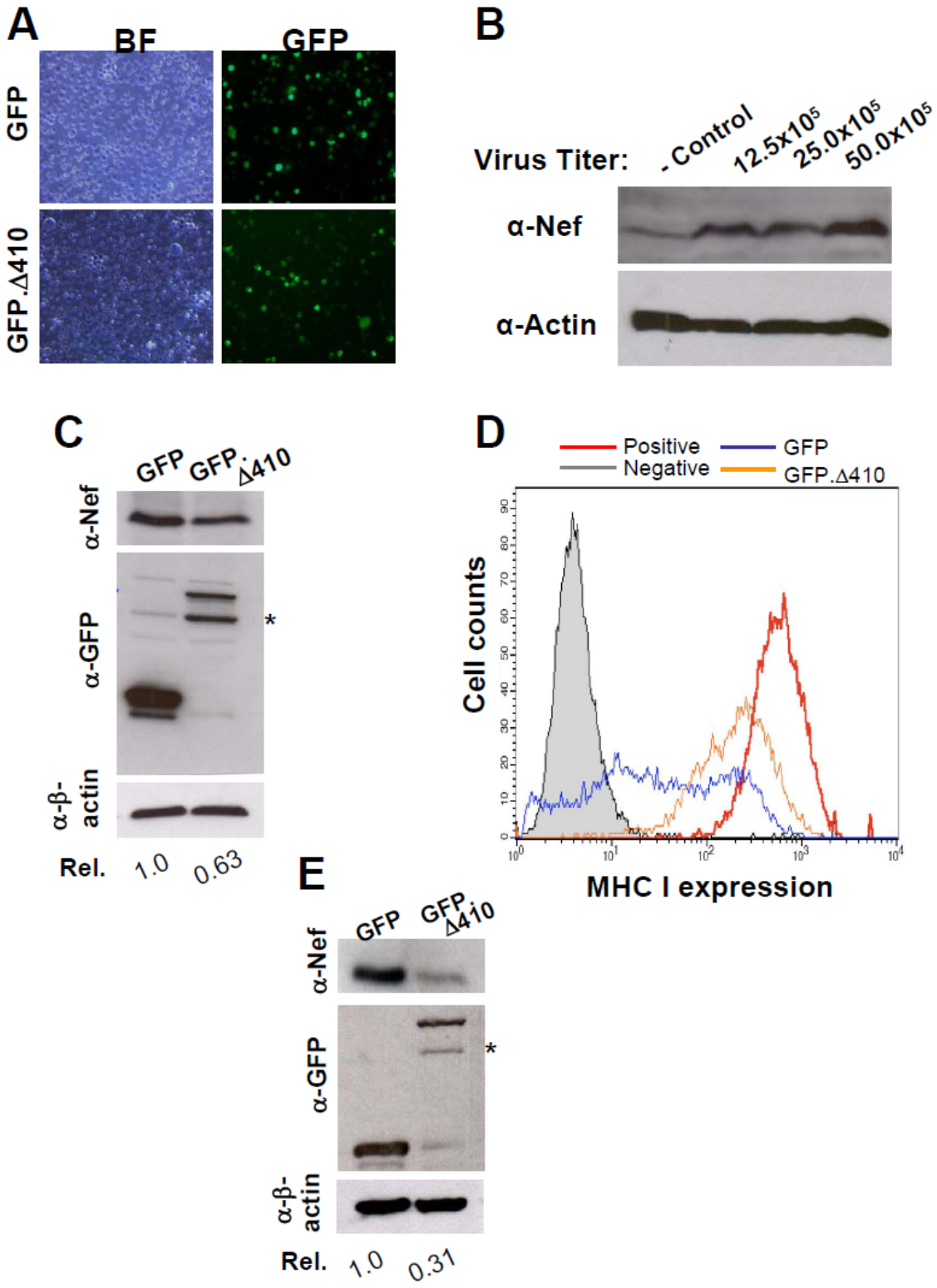
A
BF
GFP
GFP
GFP.Δ410
B
Virus Titer:
Control
12.5x10^5
25.0x10^5
50.0x10^5
α-Nef
α-Actin
C
GFP
GFP.Δ410
α-Nef
α-GFP
α-β-actin
*
Rel.
1.0
0.63
D
Positive
Negative
GFP
GFP.Δ410
Cell counts
MHC I expression
E
GFP
GFP.Δ410
α-Nef
α-GFP
α-β-actin
*
Rel.
1.0
0.31

Figure 27. Δ410 effect on Nef expression in HIV-1 infected Jurkat T cells and PBMC. A. Jurkat cells were transfected with GFP or GFP.Δ410. After 24 hr, aliquots were taken to determine the transfection efficiency by microscopic imaging and the cell viability by the trypan blue staining. BF: bright field. **B.** Four million Jurkat cells were infected with increasing concentrations (12.5, 25, or 50 x 10^5) of cpm RT count of VSV-G pseudotyped NL4-3.Luc(env) viruses. The cells were harvested 48 hr after transfection, lysed in RIPA buffer, and equal amount of protein of each sample were separated by 12.5% SDS-PAGE followed by Western blot analysis using anti-Nef JRCSF, or anti-β-actin. (**C & D**) Four million Jurkat cells were transfected with 8 μg of GFP or GFP.Δ410 and then incubated for 24 hr. Three million transfected cells were infected with 50,000 cpm RT count of VSV-G pseudotyped NL4-3.Luc(env) viruses. The cells were harvested 48 hr after infection for Western blot analysis (**C**) and for cell surface staining for MHC-I followed by flow cytometry analysis (**D**). **C.** (*) degraded GFP.Δ410; **D.** Negative and positive MHC I staining were performed in mock transfected cells. Only GFP-positive cells that were infected with VSV-G pseudotyped NL4-3.Luc(env) viruses were gated for MHC-I expression. **E.** Freshly isolated human PBMC were cultured in the presence of PHA (3 μg/ml) and IL-2 (50 units/ml) for 4 days, and 18 x 10^6 were then transfected with 9 μg of GFP or GFP.Δ410 expression plasmids, and incubated for 48 hr. Transfected cells were then infected with VSV-G pseudotyped NL4-3.Luc(env) viruses for 6 hr, and harvested for Western blot analysis as described above in **C.** (*) degraded GFP.Δ410**.**

1.15 Effects of Δ410 on cell viability and cell cycle

Future studies on Δ410 as a possible therapeutic agent for HIV-1 infection will likely depend on its toxicity to cells. Therefore, we also determined whether Δ410 had any deleterious effects on cells. We stably expressed Δ410 in Hela cells (Fig. 28A), and analyzed cell survival and cell cycle using the propidium iodide staining and flow cytometry. There was no cell death in either cell line. Despite modest accumulation of cells at the G_2 phase in Δ410 stably expressing cells, the ratio of G_0G_1 to (G_2+S) was very similar between Δ410 cells and the control cells, which were 1.71 and 1.75, respectively (Fig. 28B). These results further support possible translation of these findings into anti-HIV therapeutic development.

Based on all of the above results, we concluded that Δ410 suppressed HIV-1 Nef expression through induction of SG formation and sequestration of HIV-1 *nef* mRNA transcripts from being translated to Nef protein.

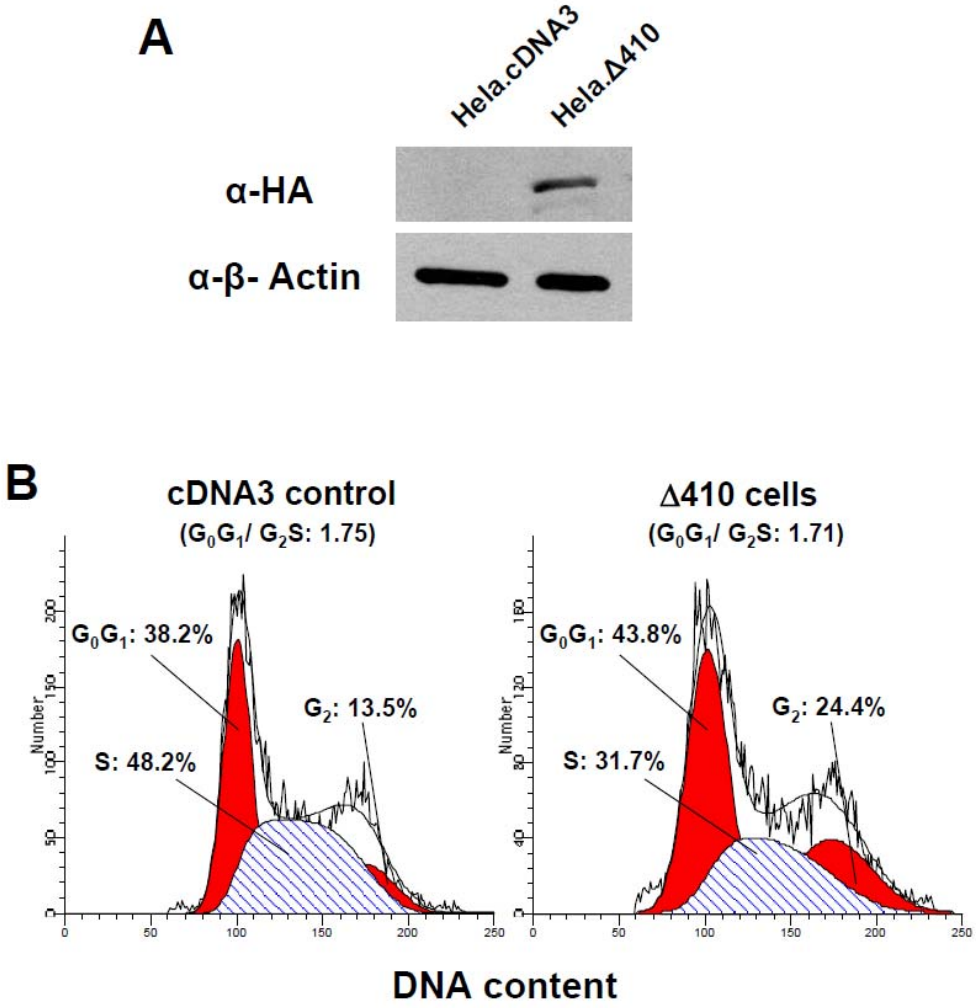

Figure 28. **Δ410 effects on the cell viability and cell cycle.** Hela cells were transfected with HA.Δ410 or its backbone expression plasmid cDNA3, and then selected for stable transfectants under the selection of 0.5 mg/ml of G418 that was pre-determined for Hela cells for about 2 weeks. Stable transfectants were then pooled and expanded as Δ410 and cDNA3 stable cell lines (**A & B**). The cells were then harvested, and either lysed in RIPA buffer, and 80 μg of cell extract from each cell line were separated by 10% SDS-PAGE followed by Western blot analysis using anti-HA, or anti-β-actin (**A**); or stained with propidium iodide, followed by flow cytometry analysis for cell cycle analysis (**B**).

PART 2: Sam68 recruitment into Stress Granules in response to oxidative stress through complexing with TIA-1

2.1 Recruitment of RFP-tagged Sam68 into SG in response to oxidative stress

Sam68 is predominantly localized in the nucleus. We previously showed that over-expression of Sam68 cytoplasmic mutants lacking the NLS results in SG formation (Fig. 17 & 18). This led us to investigate the possibility that nuclear Sam68 protein is capable of being recruited to cytoplasmic SG under stress conditions. To address this possibility, we took advantage of several well-characterized GFP-tagged SG markers GFP.TIA-1, GFP.G3BP, GFP.PABP, or GFP.hnRNP A1. As stated above, over-expression of G3BP and TIA-1 alone is sufficient to induce SG assembly [146, 299], while hnRNP A1 and PABP are recruited into SG only under stress conditions [160]. Thus, we transfected 293T cells with RFP-tagged Sam68 and each of these SG markers and exposed the cells to ARS. We then determined Sam68 localization in these cells by immunofluorescence microscopic imaging. As expected, expression of GFP.TIA-1 and GFP.G3BP induced SG formation and localized in SG irregardless of ARS treatment (Fig. 29A & B). In contrast, without ARS treatment, GFP.hnRNP A1 was detected in the nucleus (Fig. 29C), and GFP.PABP was localized in the nucleus and cytoplasm, as it tends to accumulate in the nucleus when it is over-expressed. (Fig. 29D) [300, 301], and there was no SG formation. With ARS

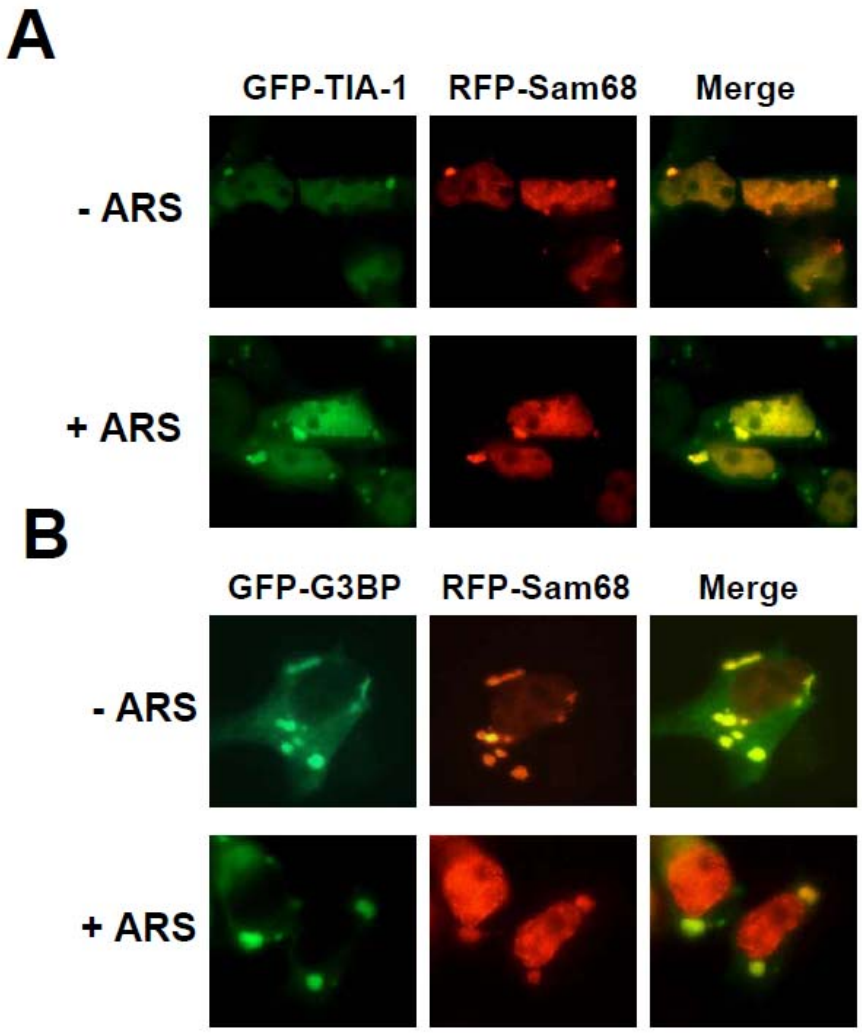
A
GFP-TIA-1
RFP-Sam68
Merge
- ARS
+ ARS
B
GFP-G3BP
RFP-Sam68
Merge
- ARS
+ ARS

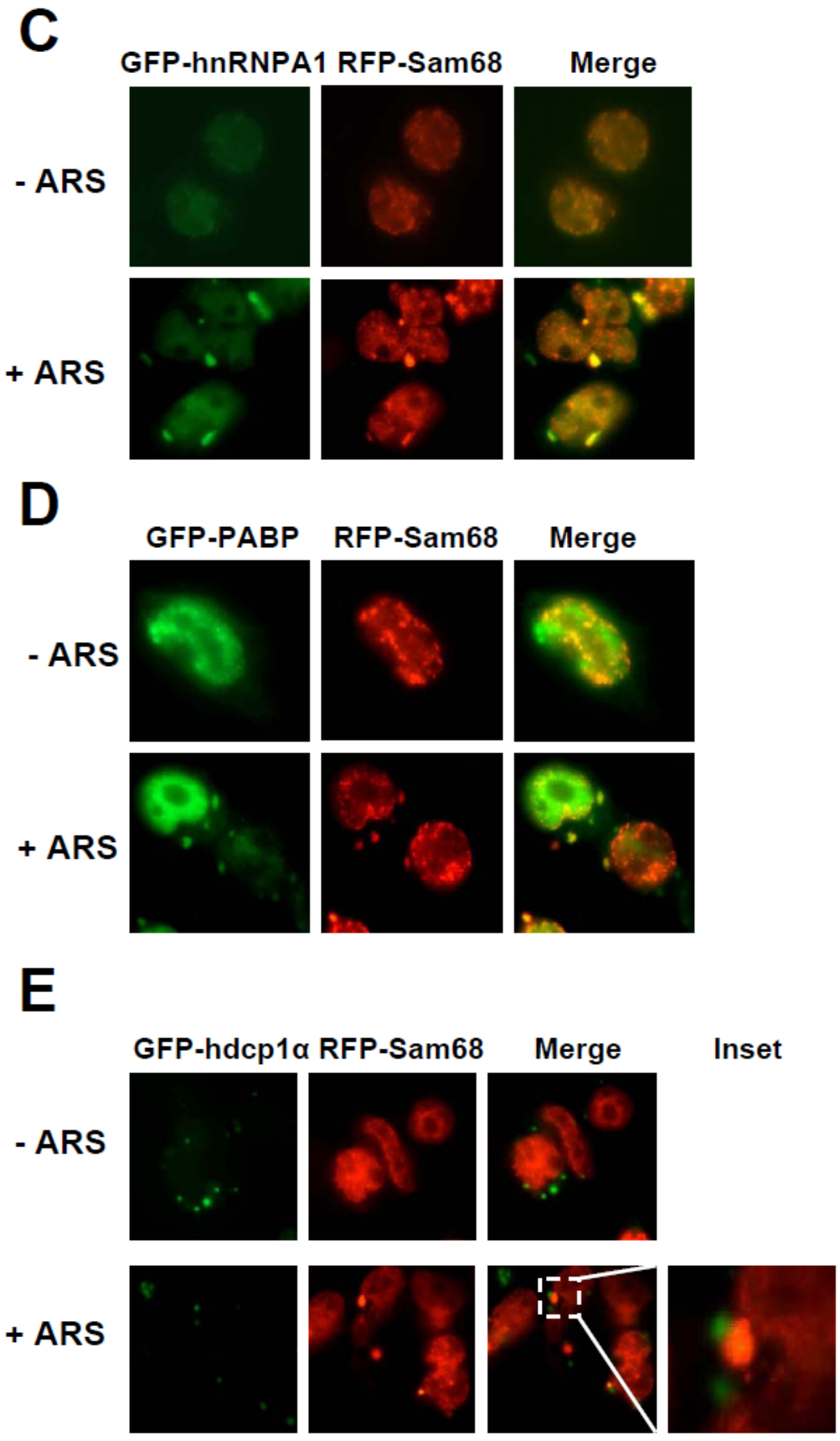
C
GFP-hnRNPA1
RFP-Sam68
Merge
- ARS
+ ARS
D
GFP-PABP
RFP-Sam68
Merge
- ARS
+ ARS
E
GFP-hdcp1α
RFP-Sam68
Merge
Inset
- ARS
+ ARS

Figure 29. Localization of RFP-Sam68 into SG upon oxidative stress. 293T were plated in a 24- well plate at a density of 1.75 x 10^5 cells per well and transfected with 0.15 µg of RFP.Sam68 and 0.3 µg of GFP.TIA-1 (**A**), GFP.G3BP (**B**), GFP.hnRNP A1 (**C**), GFP.PABP (**D**), or GFP.hdcp1α (**E**). Twenty four hours after transfection, the cells were treated with or without 0.5 mM ARS for 1 hr, fixed in 4% PFA, and then microscopic image analysis was performed for RFP and GFP. The images were representative of each co-transfection. Co-localization of SG markers and RFP.Sam68 was shown in the column marked as "Merge".

treatment, both GFP.hnRNP A1 and GFP.PABP were partially localized into the cytoplasm, importantly in SG. In GFP.TIA-1- and GFP.G3BP-expressing cells, RFP.Sam68 was expressed in the nucleus as well as in the cytoplasm, and this localization pattern did not display any significant changes between ARS-treated cells and untreated cells (Fig. 29 A & B). However, in GFP.hnRNP A1- and GFP.PABP-expressing cells, Sam68 was predominantly localized in the nucleus in the absence of ARS treatment. In the presence of ARS treatment, Sam68 was not only detected in the cytoplasm, but also co-localized with GFP.hnRNPA 1 and GFP.PABP in a percentage of the cells (Fig. 29 C & D). These results suggest that Sam68 is recruited into SG in response to oxidative stress.

We next determined whether Sam68 was also localized to other cytoplasmic RNA granules, such as P bodies, as SG and PB share many of their components [125]. Similarly, we transfected 293T cells with RFP.Sam68 and GFP-tagged hcdp1a, a well characterized P bodies marker [294], and determined their respective localization. In the absence of ARS treatment, RFP.Sam68 remained in the nucleus, while hdcp1α was localized to P bodies. In the presence of ARS treatment, RFP.Sam68 was partially re-localized to large cytoplasmic foci distinct from GFP.hdcp1α-labeled P bodies (Fig. 29E). In concordance with the notion that SG and PB are dynamically linked [125], we found that RFP.Sam68-labeled SG were in close proximity to GFP.hdcp1α-labeled P bodies (Fig. 29E, inset). These results provide additional evidence to support the early finding that Sam68 is conditionally recruited to SG.

2.2 Recruitment of endogenous Sam68 to SG in response to oxidative stress

To ascertain that Sam68 possesses the capability of being recruited into SG under oxidative stress, we first compared intracellular localization of endogenous Sam68 in cells that were treated with ARS and untreated cells using immunofluorescence staining. In untreated cells, Sam68 was predominantly localized in the nucleus. But in the ARS-treated cells, Sam68 was found to be localized in both the nucleus and the cytoplasm in the form of cytoplasmic granules in a small percentage of the cells (Fig. 30A). We next characterized these Sam68-containing cytoplasmic granules by double immunofluorescence staining for Sam68 and endogenous SG markers G3BP, eIF3η, or TIA-1. Similarly, we treated 293T cells with ARS prior to the staining. As expected, in the absence of ARS treatment, both endogenous G3BP and eIF3η were detected in the cytoplasm and endogenous TIA-1 and Sam68 in the nucleus, while ARS treatment resulted in enrichment of endogenous G3BP and eIF3η in SG and recruitment of endogenous TIA-1 into SG (Fig. 30B-D). Meanwhile, in the presence of ARS treatment, endogenous Sam68 was partially localized with endogenous G3BP, eIF3η or TIA-1-labeled SG in the cytoplasm in a small percentage of the cells (Fig. 30B-D). Taken together, these results strongly suggest that Sam68 is recruited to SG under oxidative stress.

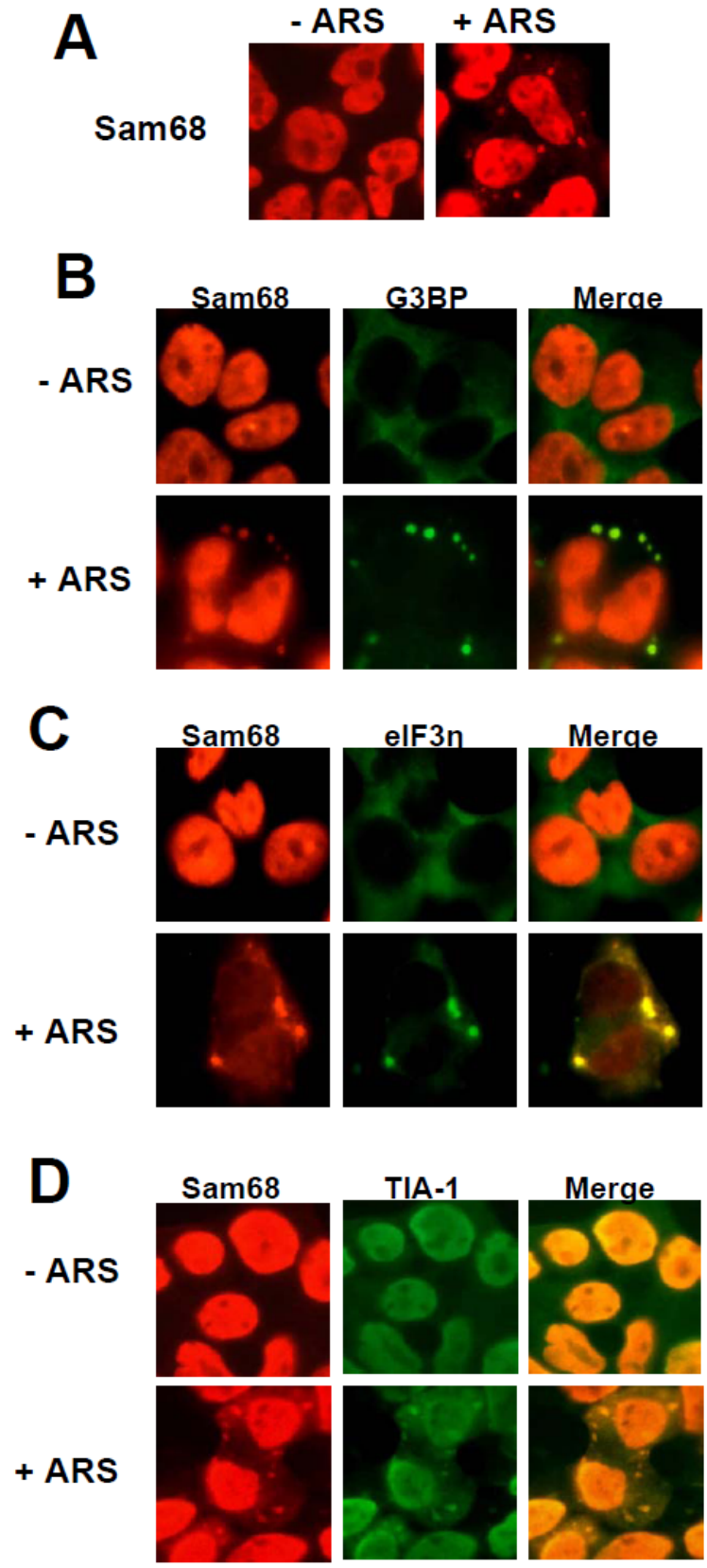
A
- ARS
+ ARS
Sam68
B
Sam68
G3BP
Merge
- ARS
+ ARS
C
Sam68
eIF3η
Merge
- ARS
+ ARS
D
Sam68
TIA-1
Merge
- ARS
+ ARS

Figure 30. Localization of endogenous Sam68 into SG upon oxidative stress. 293T cells were plated and cultured for 24 hr to reach 60-70% confluence. The cells were treated with 0.5 mM ARS (+ ARS) or without ARS (- ARS) for 1 hr prior to fixation, and then processed for double immunofluorescence staining using pairs of primary and secondary antibodies as specified below: **A.** rabbit anti-Sam68/Rh-conjugated goat anti-rabbit; **B.** rabbit anti-Sam68/Rh-conjugated goat anti-rabbit, mouse anti-G3BP/ FITC-conjugated goat anti-mouse; **C.** rabbit anti-Sam68/Rh-conjugated bovine anti-rabbit, goat anti-eIF3η/FITC-conjugated donkey anti-goat; **D.** rabbit anti-Sam68/Rh-conjugated bovine anti-rabbit, goat anti-TIA-1/FITC-conjugated donkey anti-goat. Co-localization of each SG marker with endogenous Sam68 was shown in the column marked as “Merge”.

2.3 Requirement of Sam68 proline (RG)-rich domain for its SG recruitment and eIF2α phosphorylation

As mentioned before, Sam68 can be divided into several functionally distinct domains such as KH, proline-rich (P_0-P_5), tyrosine-rich, RG-rich, and NLS (Fig. 12). To define the molecular mechanisms whereby Sam68 is recruited to SG, we took advantage of a previous described panel of GFP-tagged Sam68 mutants containing various lengths of the C-terminal deletion (Fig. 12), and attempted to determine the structural requirement of Sam68 for its SG recruitment. We transfected 293T cells with GFP.Sam68 or each of these mutants. We then treated the cells with ARS and performed immunofluorescence staining for endogenous G3BP as the SG marker. We also quantitated the GFP+ SG-containing (G3BP+) cells in each transfection. As shown previously (Fig. 17 & 18), in the absence of ARS treatment, over-expression of only GFP.Δ410 lacking the NLS and GFP.Δ321 lacking NLS and P_{4-5} were capable of inducing SG formation, while GFP.Sam68, GFP.Δ269 lacking NLS and P_{3-5}, GFP.Δ269-321 lacking P_3, and GFP.269-321 expression only P_3 showed little SG induction (Fig. 31A-F). Compared to the untreated cells, ARS treatment increased GFP.Sam68 localization in SG, i.e. GFP.Sam68/G3BP+ cells to 33.33 ± 3.06% from 16.67 ± 4.04% (p = 0.017), GFP.Δ410/G3BP+ cells to 89.33 ± 3.07% from 72.67 ± 3.06% (p = 0.006), GFP.Δ321/G3BP+ cells to 84.00 ± 4.00% from 62.67 ± 8.33% (p = 0.043). GFP.Δ269/G3BP+ cells to 42.67 ± 3.06% from 27.33 ± 3.06% (p = 0.001), GFP.Δ269-321/G3BP+ cells to 6.67 ± 3.06% from 4.00 ± 2.00% (p =

0.135) and GFP.269-321/G3BP+ cells to 18.00 ± 5.29% from 4.67 ± 1.15% (p = 0.029) (Fig. 31A-G). These results demonstrated that proline (RG)-rich domain P_3 between aa269 and aa321 was required but not sufficient for SG induction and recruitment and suggest that nuclear localization is a limiting factor for Sam68 recruitment to SG.

Over-expression of mutant proteins may override the cellular protein-folding capacity and activate the unfolded protein response [302], which results in eIF2α phosphorylation and SG assembly. Caprin-1 over-expression leads to eIF2α phosphorylation and SG formation through a mechanism involving its capacity to bind RNA via its RG-rich domain. Thus, we next determined if SG induction by Sam68 cytoplasmic mutants was mediated by eIF2α phosphorylation. We transfected 293T cells with GFP.Sam68 or each of its mutants and determined the phosphorylation status of eIF2α. We also included GFP transfection with and without ARS treatment as eIF2α phosphorylation positive and negative controls, respectively. As expected, GFP transfected cells treated with ARS resulted in the phophorylation of eIF2α (Fig. 32). However, over-expression of Sam68 or each of its mutants did not induce eIF2α phosphorylation. These results suggest that the capacity of Sam68 cytoplasmic mutants to induce SG is eIF2α phosphorylation-independent, reminiscent of other SG-inducing proteins which alter the equilibrium between mRNPs and polysomes and compete for 48S complexes before initiation is completed [124].

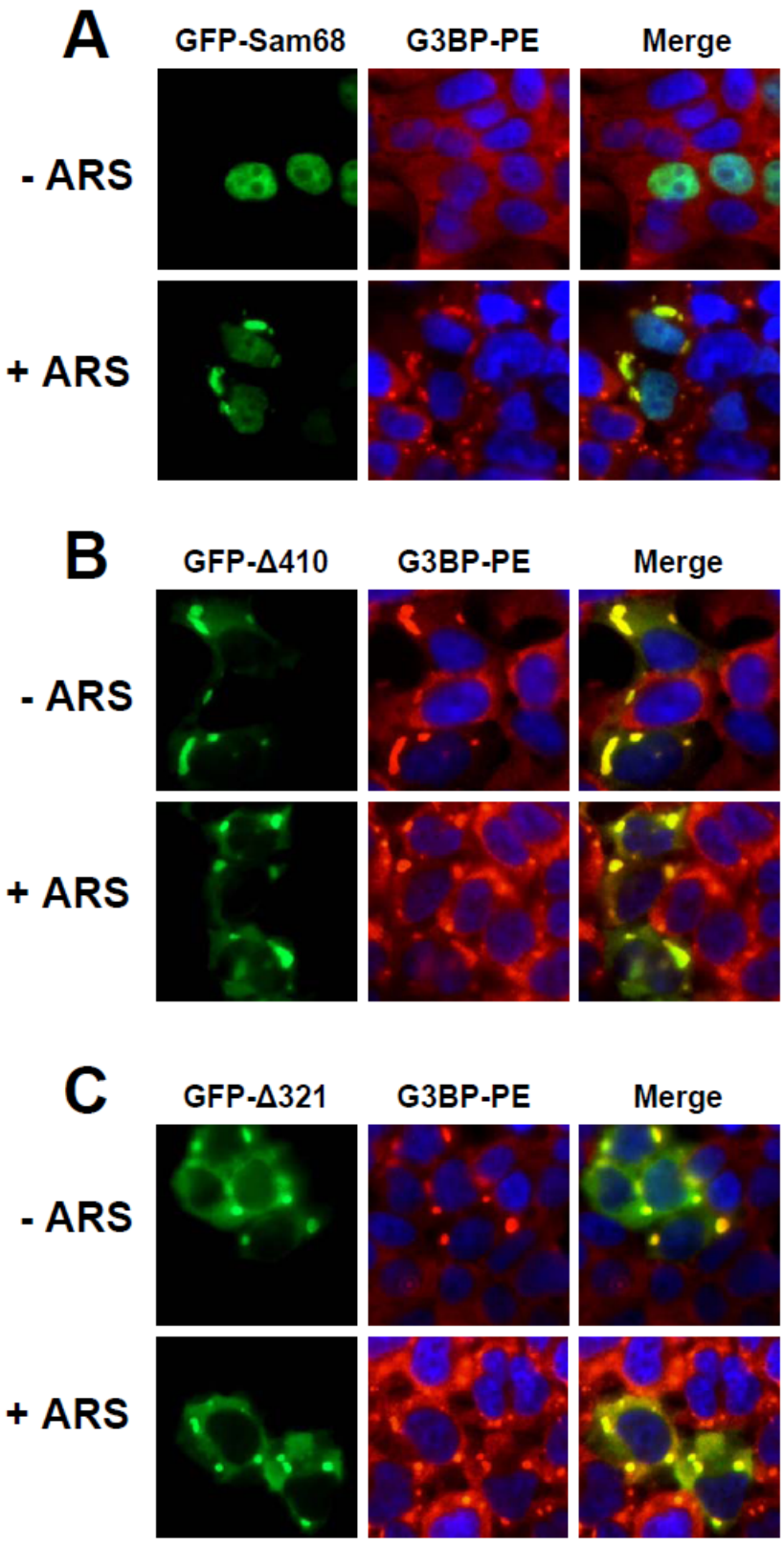
A
GFP-Sam68
G3BP-PE
Merge
- ARS
+ ARS
B
GFP-Δ410
G3BP-PE
Merge
- ARS
+ ARS
C
GFP-Δ321
G3BP-PE
Merge
- ARS
+ ARS

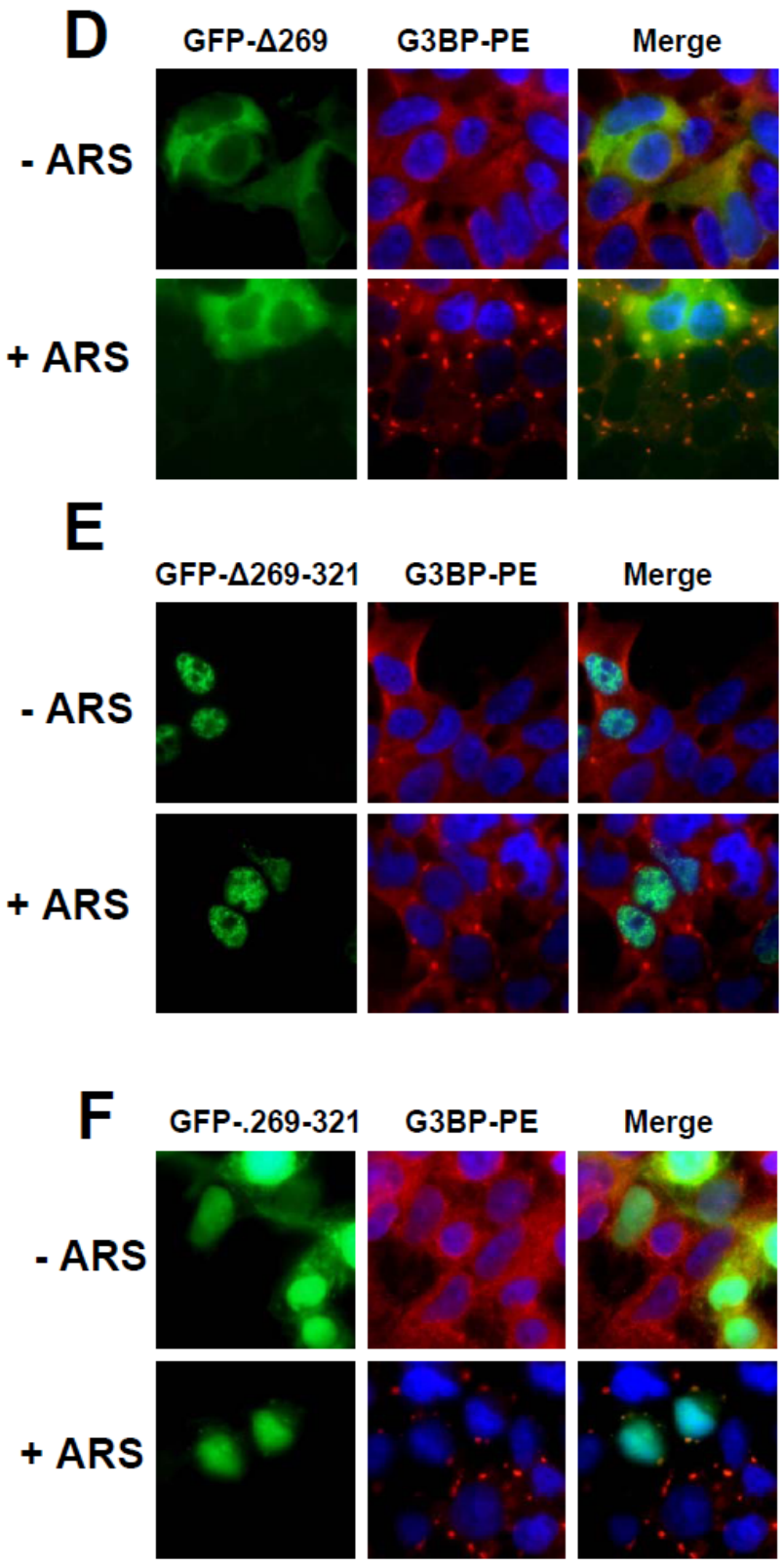
D
GFP-Δ269
G3BP-PE
Merge
- ARS
+ ARS
E
GFP-Δ269-321
G3BP-PE
Merge
- ARS
+ ARS
F
GFP-.269-321
G3BP-PE
Merge
- ARS
+ ARS

G

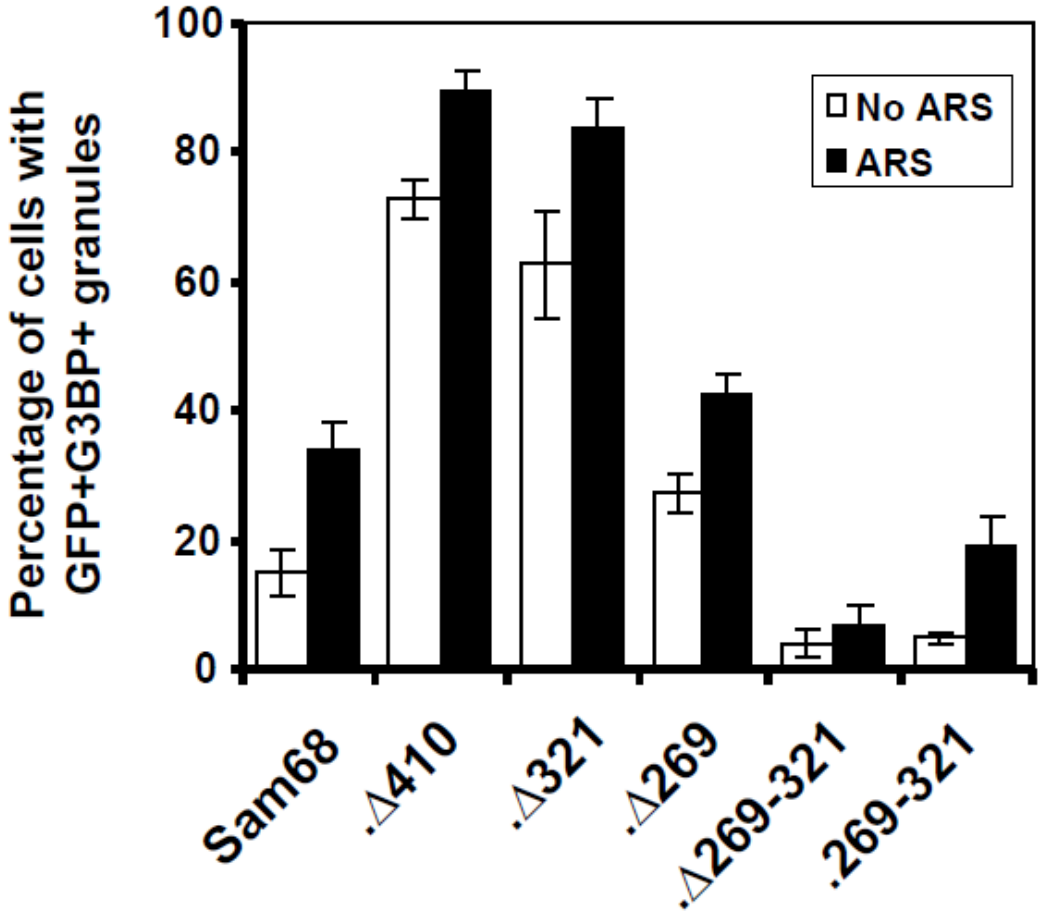
Percentage of cells with GFP+G3BP+ granules
100
80
60
40
20
0
No ARS
ARS
Sam68
.Δ410
.Δ321
.Δ269
.Δ269-321
.269-321

Figure 31. Requirement of specific Sam68 domains for its SG recruitment. (A-F). 293T were plated in a 24- well plate at a density of 1.75 x 10^5 cells per well and transfected with 0.2 µg of GFP-tagged Sam68 (**A**), or its deletion mutants containing various lengths of C-terminal deletion, i.e. ∆410 (**B**), ∆321 (**C**) or ∆269 (**D**), ∆269-321 lacking the domain of aa 269-321 (**E**), or 269-321 expressing the domain of aa 269-321 (**F**), and then treated with 0.5 mM ARS (+ ARS) or without ARS (- ARS) for 1 hr prior to fixation. The cells were then stained using a mouse anti-G3BP antibody followed by PE-conjugated goat anti-mouse secondary antibody. The cells were also counterstained in PBS containing 500 ng/ml DAPI for nuclei. The images were representative of each transfection. Co-localization of G3BP with Sam68 or each mutant was shown in the column marked as "Merge". **G.** Random 10 fields were counted for a total number of 100 transfected cells in each well, and the number of cells exhibiting GFP+G3BP+ SG was used to calculate the percentage of the GFP+ SG-containing cells. The data were mean ± S.E.M. Comparisons among groups were made using two-tailed Student's *t*-test.

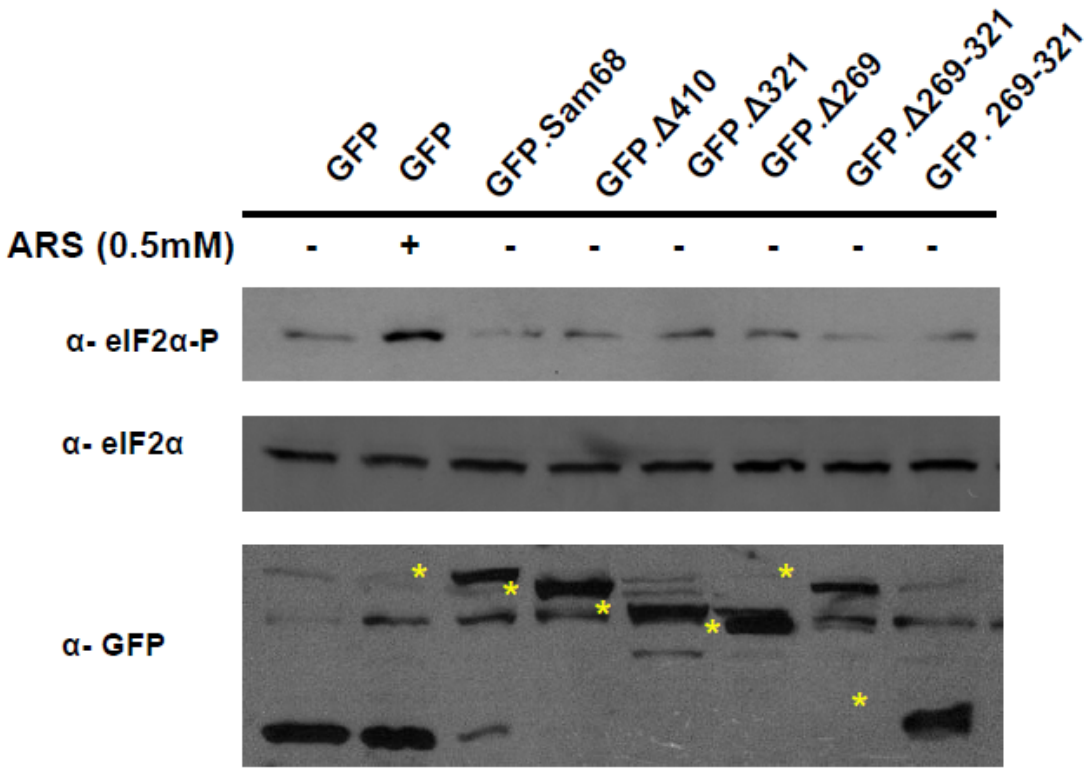

Figure 32. Effects of GFP-tagged Sam68 or its mutants on eIF2α phosphorylation. 293T cells were plated in a 12- well plate at a density of 4.0 x 10^5 cells per well and transfected with 0.4 μg of GFP-tagged Sam68 or each of its mutants as indicated. The cells were harvested 42 hr after transfection, lysed in phosphorylation lysis buffer, and 45 μg of each sample were separated by 15% SDS-PAGE followed by Western blot analysis using anti-eIF2α, anti-phosphorylated eIF2α (α-eIF2α-P), or anti-GFP antibodies. Cells that were transfected with GFP and treated with 0.5 mM ARS or without ARS were included as positive and negative controls for eIF2α phosphorylation, respectively, in the Western blot analysis. *: GFP-tagged proteins.

2.4 Role of Sam68 KH domain in its SG recruitment and aggregation

Sam68 KH domain is involved in its RNA binding [198], self association [200], and translocation to the cytoplasm [303]. The RNA binding property is critical for SG localization of several RBP [124]. Moreover, a recent study has shown that removal of the RNA recognition motifs (RRM) from TIA-1 leads to large insoluble aggregates and as a result, abrogates the ability of TIA-1 to induce SG assembly [299]. Thus, we further determined the role of RNA binding, i.e. KH domain, on Sam68 SG recruitment. To this end, we constructed two KH domain deletion mutants GFP.ΔKH and GFP.Δ410ΔKH using GFP.Sam68 and GFP.Δ410 as respective backbones (Fig. 33A). We transfected 293T cells with GFP.ΔKH or GFP.Δ410ΔKH, treated the cells with ARS, and performed immunofluorescence staining for G3BP as a SG marker. We also included GFP.Sam68 and GFP.Δ410 as controls in these experiments. As shown above, GFP.Δ410 co-localized with G3BP in SG in the absence and presence of ARS treatment, whereas Sam68 localized to SG only in the cells treated with ARS (Fig. 33B & D). In contrast, both GFP.ΔKH and GFP.Δ410ΔKH failed to co-localize with G3BP in SG in the presence or absence of oxidative stress (Fig. 33C & E). As previously reported [303], GFP.ΔKH expression led to its localization in nuclear microaggregates (Fig. 33C), while GFP.Δ410.ΔKH was enriched in a single large perinuclear aggregate per cell (Fig. 33E). These findings are reminiscent of the insoluble aggregates induced by over-expression of TIA-1 ΔRRM mutants [299],

with the exception that Δ410ΔKH-expressing cells displayed normal assembled SG under the ARS treatment.

To further characterize the aggregation nature of these mutants, we transfected 293T cells with GFP.Sam68 or each of its mutants including these two KH mutants, separated the cellular proteins into 1% Triton X-soluble or -insoluble fractions as previously described [276, 277], and performed Western blot analysis to compared the extent of their aggregation. GFP.Sam68, GFP.Δ410, and GFP.Δ321 that were all localized to SG were detected in soluble and insoluble fractions (Fig. 34A). In contrast, GFP.Δ269 and GFP.269-321 which were rarely co-localized into SG were found mainly in the soluble fraction. In agreement with immunofluorescence microscopic imaging (Fig. 33C & E), both GFP.ΔKH and GFP.Δ410ΔKH were exclusively detected in the insoluble fractions (Fig. 34A).

Since we found that KH mutants failed to bind to *nef* 3'UTR (Table 2), and to localize to SG (Fig. 33C & E), we hypothesized that neither of these mutants should have a deleterious effect on HIV-1 Nef expression. Therefore, we transfected 293T cells with HIV-1 provirus NL4-3 and these KH deletion mutants as well as their respective backbones and performed Western blot analysis for Nef expression. As previously shown [304], GFP.Δ410 significantly suppressed and GFP.Sam68 slightly increased Nef expression (Fig. 34B). In concordance, GFP.ΔKH and GFP.Δ410ΔKH not only failed to suppress Nef

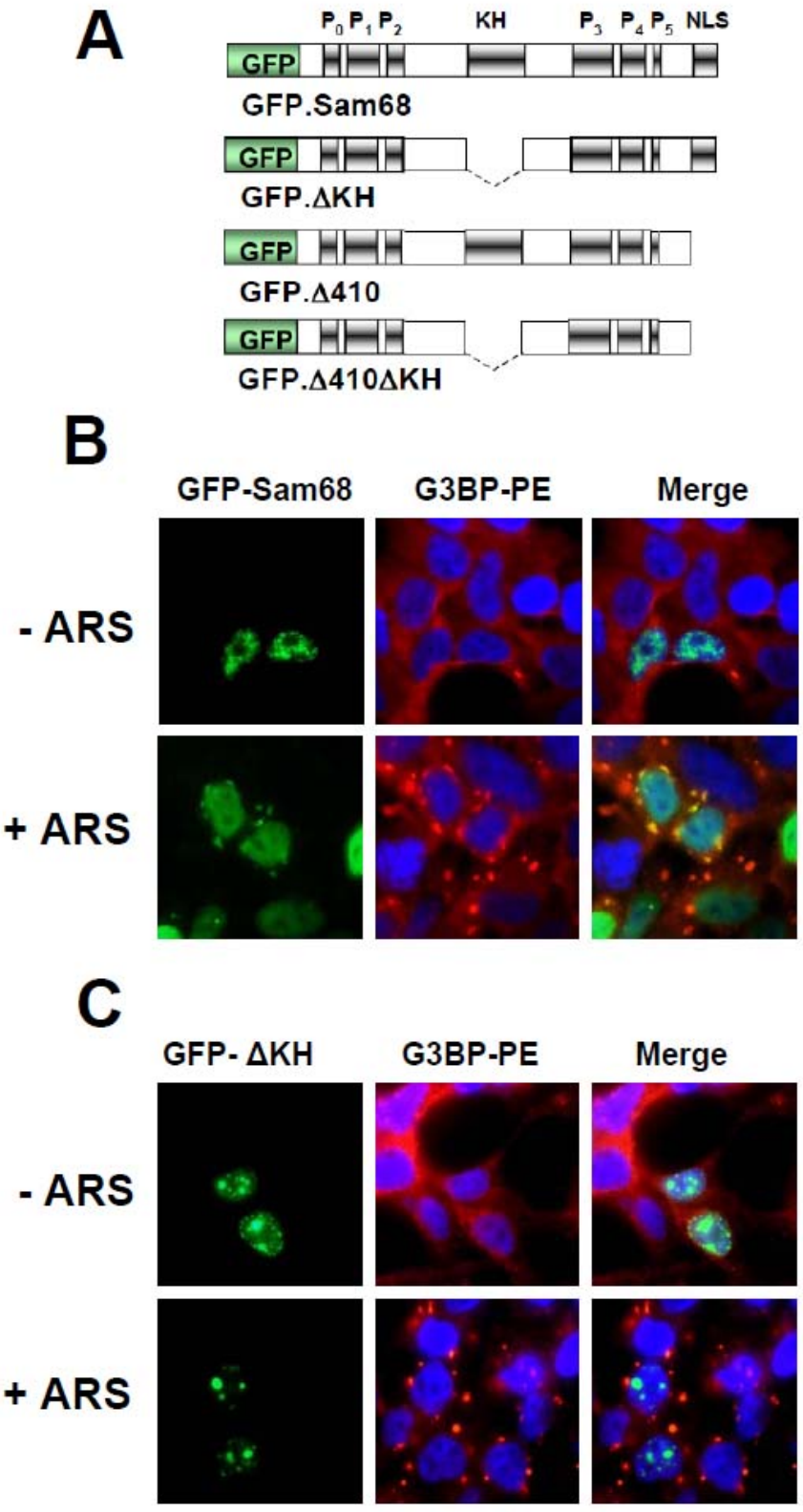
A
P0 P1 P2
KH
P3 P4 P5
NLS
GFP
GFP.Sam68
GFP
GFP.ΔKH
GFP
GFP.Δ410
GFP
GFP.Δ410ΔKH
B
GFP-Sam68
G3BP-PE
Merge
- ARS
+ ARS
C
GFP- ΔKH
G3BP-PE
Merge
- ARS
+ ARS

D

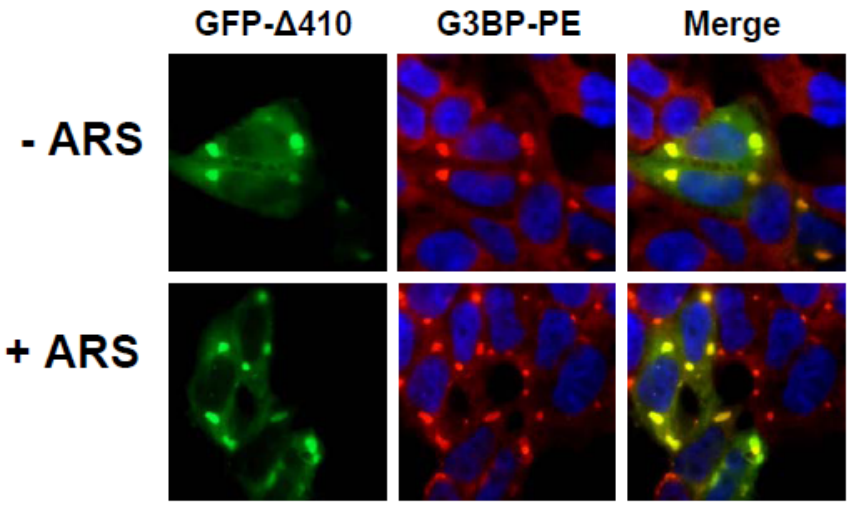
GFP-Δ410
G3BP-PE
Merge
- ARS
+ ARS

E

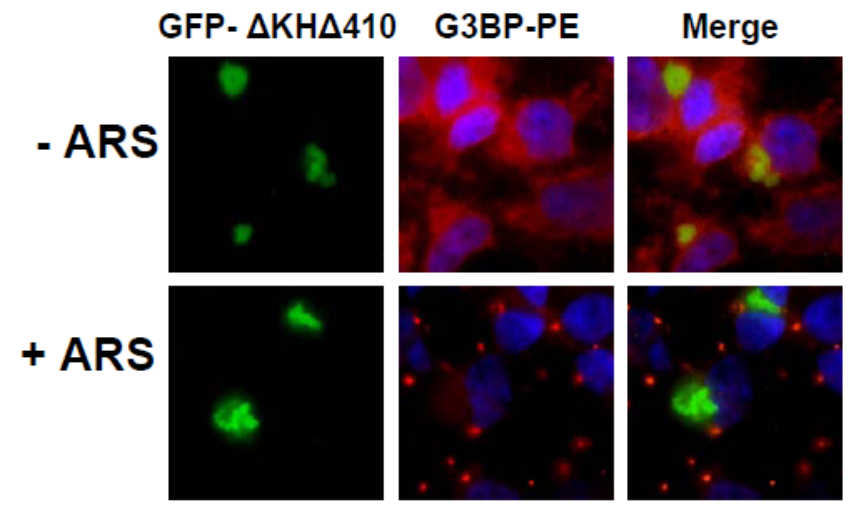
GFP- ΔKHΔ410
G3BP-PE
Merge
- ARS
+ ARS

Figure 33. Role of Sam68 KH domain in SG recruitment. A. A scheme of KH domain deletion mutants: P: proline-rich domain; KH: KH domain; and NLS: nuclear localization signal. The dotted lines represent deleted regions. (**B-E**). 293T were plated in a 24- well plate at a density of 1.75 x 10^5 cells per well and transfected with 0.2 µg of GFP-tagged Sam68 (**B**), or its deletion mutants ΔKH (**B**), Δ410 (**C**) or ΔKHΔ410 (**E**), and then treated with 0.5 mM ARS (+ ARS) or without ARS (- ARS) for 1 hr prior to fixation. The cells were then stained using a mouse anti-G3BP antibody followed by PE-conjugated goat anti-mouse secondary antibody. The cells were also counterstained in PBS containing 500 ng/ml DAPI for nuclei. The images were representative of each transfection. Co-localization of G3BP with Sam68 or each mutant was shown in the column marked as "Merge". Panel (**C**) was also used in Fig. 18C.

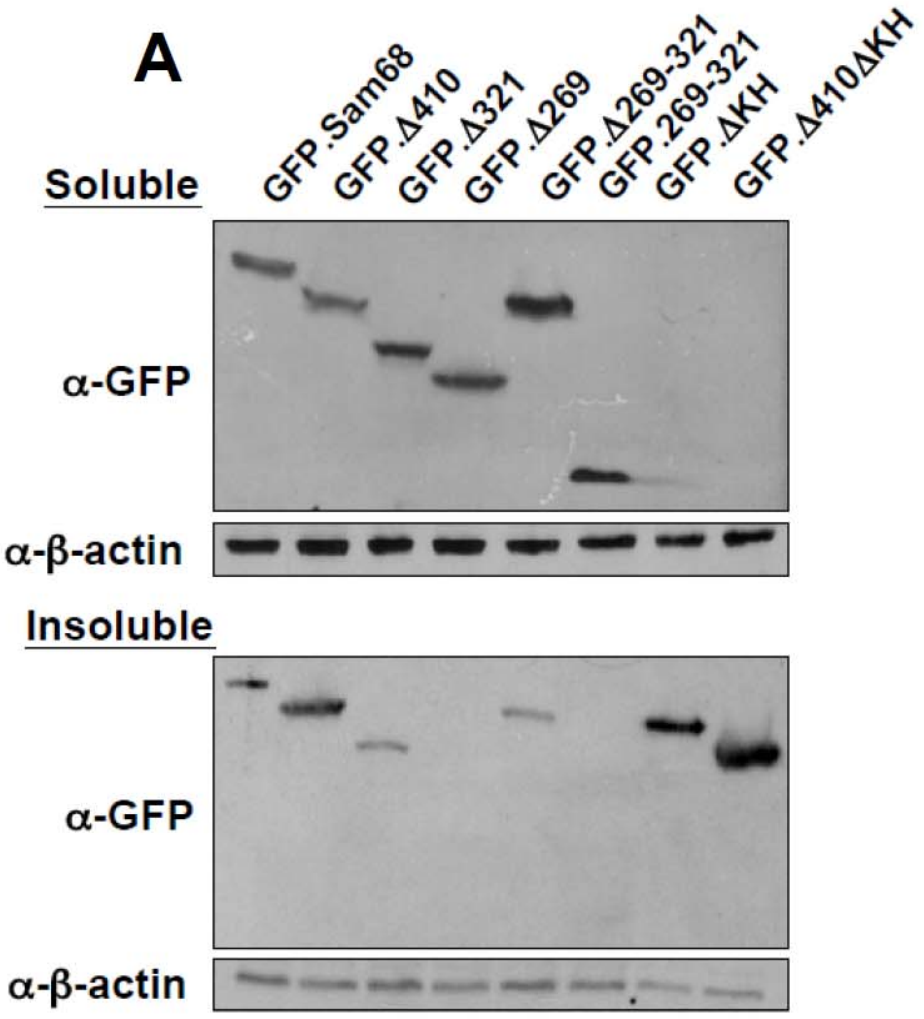
A
GFP.Sam68
GFP.Δ410
GFP.Δ321
GFP.Δ269
GFP.Δ269-321
GFP.269-321
GFP.ΔKH
GFP.Δ410ΔKH
Soluble
α-GFP
α-β-actin
Insoluble
α-GFP
α-β-actin

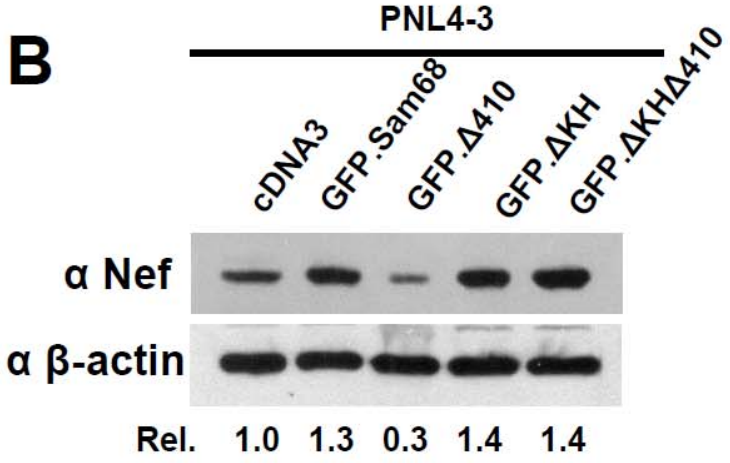
B
PNL4-3
cDNA3
GFP.Sam68
GFP.Δ410
GFP.ΔKH
GFP.ΔKHΔ410
α Nef
α β-actin
Rel. 1.0 1.3 0.3 1.4 1.4

Figure 34. Role of Sam68 KH domain in Sam68 solubility and HIV-1 *nef* mRNA translation. A. 293T cells were transfected with GFP-tagged Sam68 or each of its mutants as indicated, then cell lysates were separated into soluble and insoluble fractions as described in Materials and Methods, followed by separation by 15% SDS-PAGE and Western blot analysis using anti-GFP or anti-β-actin antibody. **B.** 293T cells were plated in a 12- well plate at a density of 1.5 x 10^5 cells per well and transfected with 0.2 μg of NL4-3, and 1.2 μg of GFP-tagged Sam68 or its ΔKH mutants. The cells were harvested 42 hr after transfection, lysed in RIPA buffer, and 20 μg of each sample were separated by 12.5% SDS-PAGE followed by Western blot analysis using anti-Nef JRCSF, or anti-β-actin.

translation, but to the contrary increased Nef expression (Fig. 34B). The mechanisms underlying increased Nef expression by Sam68 and these two KH deletion mutants deserves further investigation. Taken together, these results suggest that Sam68 KH domain is not directly involved in SG induction by Sam68 cytoplasmic mutants or SG recruitment of Sam68, but is absolutely required for maintaining native and functional structure of Sam68 protein in the cells.

2.5 Effects of Sam68 knockdown on SG assembly

Expression of some cellular proteins is absolutely required for SG assembly, and knock-out of these proteins is associated with a muted SG response to multiple stress stimuli [146, 148, 169, 299]. The finding that Sam68 was recruited to SG while some of its mutants induced SG assembly raised the possibility that Sam68 was an essential component of SG assembly. To address this possibility, we utilized the small interference RNA (siRNA) strategy to knock-down endogenous Sam68 and determined its effects on SG formation under oxidative stress. As shown before (Fig. 10A), compared to control siRNA, Sam68 siRNA was very effective in knocking down endogenous Sam68 expression (Fig. 35A). We then transfected 293T cells with control siRNA or Sam68 siRNA, treated the cells with ARS, and performed immunofluorescence staining for G3BP as the SG marker. There were no apparent changes in the size or morphology of SG (Fig. 35B) and in the percentage of SG-containing cells between control siRNA and Sam68

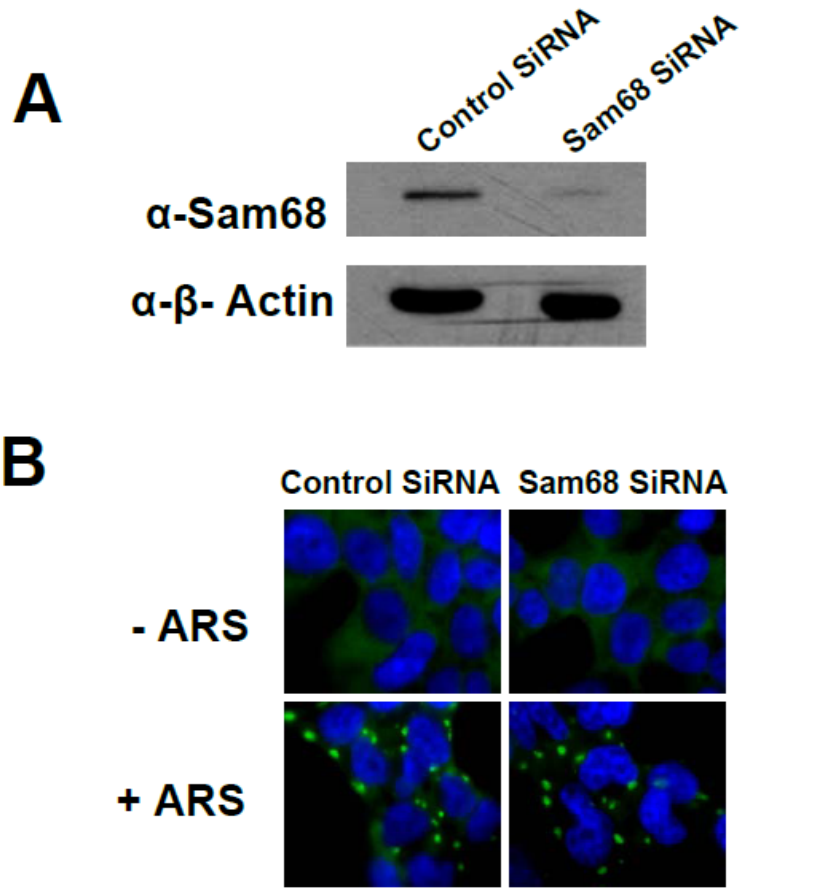
A
Control SiRNA
Sam68 SiRNA
α-Sam68
α-β- Actin
B
Control SiRNA
Sam68 SiRNA
- ARS
+ ARS
C
Percentage of cells with G3BP+SG
120
100
80
60
40
20
0
No ARS
ARS
Control SiRNA
Sam68SiRNA

Figure 35. Effects of Sam68 knockdown on SG assembly. A. 293T cells were plated at a density of 1.75 x 10^5 per well and transfected with 75 nM of control siRNA or Sam68 siRNA. The transfection efficiency was estimated to be over 95%, determined by inclusion of a fluorescence-labeled control siRNA in the transfection. The cells were harvested 24 hr after transfection for Western blot analysis using anti-Sam68 or anti-β-actin antibodies. **B.** 293T cells were plated and transfected with control siRNA or Sam68 siRNA as above. The cells were treated with 0.5 mM ARS (+ ARS) or without ARS (- ARS) for 1 hr prior to fixation. The cells were then stained using a mouse anti-G3BP antibody followed by FITC-conjugated anti-mouse antibody. Transfected cells were also stained with 500 ng/ml of DAPI for nuclei. The images were representative of each transfection. **C.** Quantitation of G3BP+ granules-containing cells in **B**. Random 10 fields were counted for a total number of 100 transfected cells in each well, and the number of cells exhibiting G3BP+ SG was used to calculate the percentage of SG-containing cells. The data were mean ± S.E.M of triplicate samples, which was expressed as percentage of the total number cells.

siRNA (Fig. 35C). These results suggest that Sam68 is not an essential cellular cofactor for SG assembly, at least under the oxidative stress.

2.6 Interaction of Sam68 with TIA-1 and its SG recruitment

There are several possible ways by which a protein can be recruited into SG, and one of the common pathways is through interaction with constitutive core components of SG or so-called the “piggy-back” mechanism [124]. To investigate whether this was the case for Sam68 SG recruitment, we initially performed a BLAST search in a database, which predicts human protein-protein interactions [305], for possible interacting proteins for Sam68. We obtained a list of 108 proteins as potential Sam68-interacting targets, among which was TIA-1. TIA-1 has been shown to recruit multiple proteins to SG through direct binding including FAST, a protein that has recently been shown to directly bind Sam68 [274]; and KSRP, which forms a unique RNP complex with Sam68 and intron 6 of the β-tropomyosin gene [275]. Thus, we focused on Sam68/TIA-1 interaction. We first transfected 293T cells with HA-tagged Sam68 (HA.Sam68), GFP.TIA-1, or both and performed immunoprecipitation (IP) followed by Western blotting analysis (WB). We performed direct Western blot analysis for the input lysates to ensure comparable levels of protein expression among transfections (WB-input; Fig. 36A-C), as well as IP with control IgG antibody followed by WB with α-HA or α-GFP to ensure no non-specific background binding (WB-input; Fig. 36A). IP with α-HA antibody followed by WB with α-GFP antibody showed complex formation between Sam68 and TIA-1 in cells co-expressing Sam68 and TIA-1

(WB-IP, 2nd panel; Fig. 36B), and α-HA antibody showed similar IP efficiency between cells expressing Sam68 alone and cells expressing both Sam68 and TIA-1 (WB-IP, 1st panel; Fig. 36B). Conversely, IP with α-TIA-1 antibody followed by WB with α-HA antibody also showed that Sam68 complexed with TIA-1 in cells expressing both Sam68 and TIA-1 (WB-IP, 1st panel; Fig. 36C). Next, we determined whether there was complex formation between endogenous Sam68 and endogenous TIA-1 using the similar IP/WB approach, we obtained similar results (Fig. 36D & E).

To determine whether this complex formation between Sam68 and TIA-1 was responsible for Sam68 SG recruitment under oxidative stress conditions, we then characterized Sam68 interaction with TIA-1 using a similar panel of HA-tagged Sam68 and mutants. We transfected 293T cells with HA.Sam68 or each of its mutants, in combination with GFP-TIA-1, and analyzed their binding to TIA-1 using the similar IP/WB strategy. We first performed WB with α-GFP or α-HA antibody to ensure a comparable level of Sam68 and each of its mutants and a comparable level of TIA-1 expression among transfections (WB-Input, Fig. 37A). We then performed IP with α-HA antibody followed by WB with α-GFP antibody as well as WB with α-HA antibody. Similar to Sam68, Δ410 showed complexed formation with TIA-1, so did Δ321 but to a lesser extent (WB-IP, 1st panel; Fig. 37A). On the other hand, Δ269 or Δ269-321 did not show any complex formation with TIA-1, even though that Sam68 and all mutants showed no difference in the

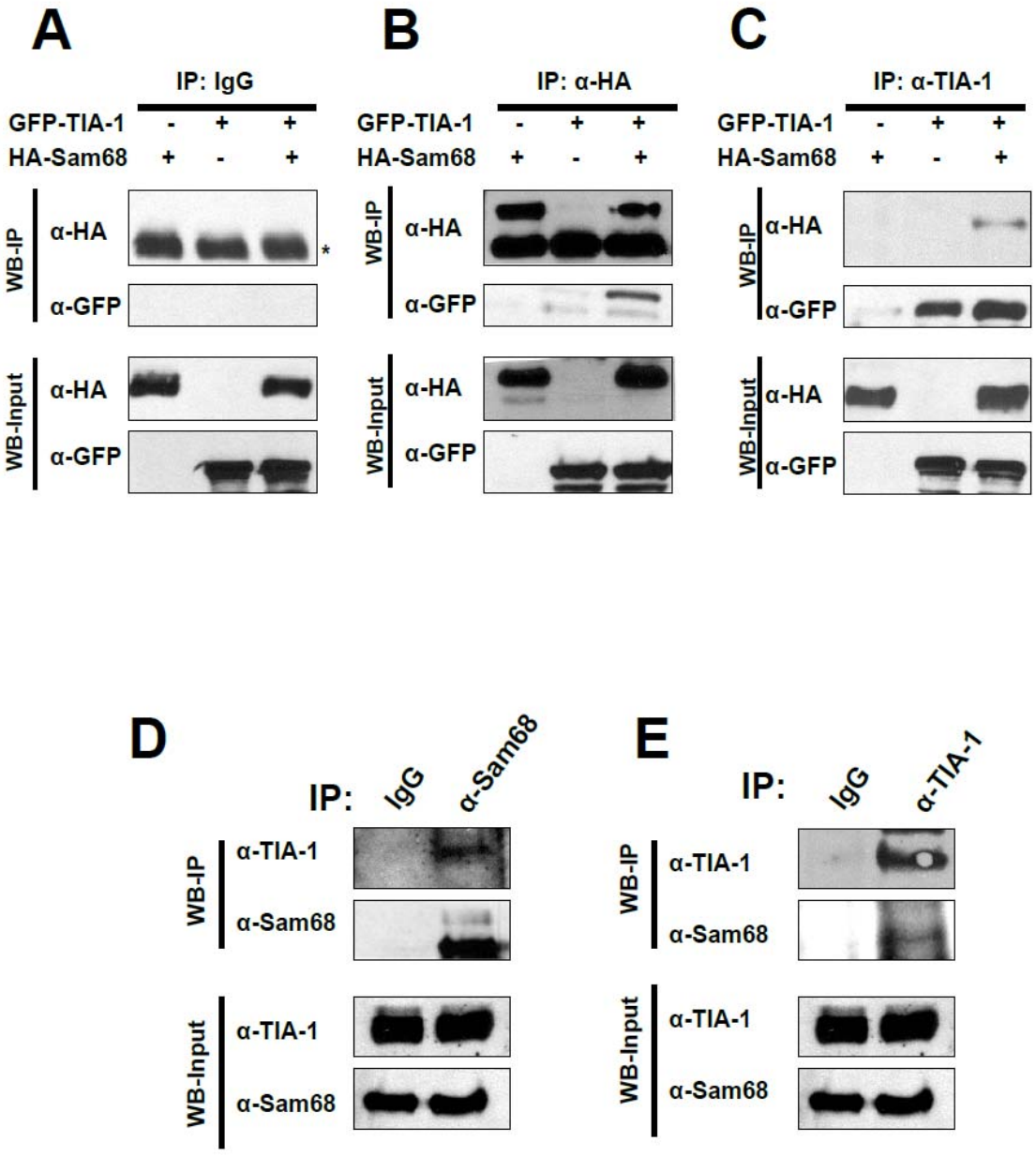
A
IP: IgG
GFP-TIA-1 - + +
HA-Sam68 + - +
WB-IP
α-HA
α-GFP
WB-Input
α-HA
α-GFP
*
B
IP: α-HA
GFP-TIA-1 - + +
HA-Sam68 + - +
WB-IP
α-HA
α-GFP
WB-Input
α-HA
α-GFP
C
IP: α-TIA-1
GFP-TIA-1 - + +
HA-Sam68 + - +
WB-IP
α-HA
α-GFP
WB-Input
α-HA
α-GFP
D
IP: IgG α-Sam68
WB-IP
α-TIA-1
α-Sam68
WB-Input
α-TIA-1
α-Sam68
E
IP: IgG α-TIA-1
WB-IP
α-TIA-1
α-Sam68
WB-Input
α-TIA-1
α-Sam68

Figure 36. Complex formation between Sam68 and TIA-1. (**A-C**). 293T cells were plated at a density of 2.0 x 10^6 per 35mm plate and transfected with 3.0 µg of HA.Sam68, 3.0 µg of GFP.TIA-1, or both and harvested 48 hr after transfection for cell lysates. One milligram of cell lysates was then immunoprecipitated with 1.0 µg of normal IgG (**A**), anti-HA (**B**), or anti-TIA-1 (**C**) antibodies, followed by Western blotting using anti-HA or anti-GFP antibody (WB-IP). Equal amount of input lysates were directly blotted to ensure comparable Sam68 and TIA-1 expression among transfections (WB-Input). *: reactive IgG bands. (**D & E**). Cell lysates were prepared from 293T cells and blotted for endogenous Sam68 and TIA-1 expression (WB-Input), and 1.5 milligrams were immunoprecipitated with 1.0 µg of normal IgG, α-Sam68 (**D**), or α-TIA-1 (**E**), followed by Western blot analysis using anti-TIA-1 or anti-Sam68 antibodies (WB-IP).

IP efficiency with α-HA antibody (WB-IP, 2nd panel; Fig. 37A). These results showed that Sam68 domain 269-321 was involved in interaction with TIA-1.

To further corroborate the role of the domain between aa269 and aa321 in TIA-1 binding and its relationship to Sam68 SG recruitment, we transfected 293T cells with GFP-TIA-1 in combination with HA.Δ410 or HA.Δ269-321, followed by immunofluorescence staining using α-HA antibody. As shown above, Δ410 was co-localized with TIA-1 in SG (Fig. 37B). However, Δ269-321 remained in nucleus, even though that TIA-1 was detected in SG in the cytoplasm (Fig. 37B). Taken together, these results show that Sam68 domain aa269-321 (P_3/RG-rich) is directly involved in Sam68 binding to TIA-1 and strongly suggest that Sam68 interaction either in a direct or indirect manner is responsible for Sam68 recruitment into SG.

2.7 Interaction of Sam68 with G3BP

Our previous results showed that Sam68 deletion mutant Δ321 is strongly recruited to SG (Fig. 31); however, it binds weakly to TIA-1 (Fig. 37A), suggesting that additional factors could be involved in Sam68 recruitment to SG. G3BP, which is absolutely required for SG assembly [146], was initially identified by its affinity to RAS-GAP SH3 domain [306], and was subsequently shown to associate with full length RAS-GAP only in growing cells and in an activated Ras dependent manner [307]. Interestingly, Sam68 also interacts with Ras-

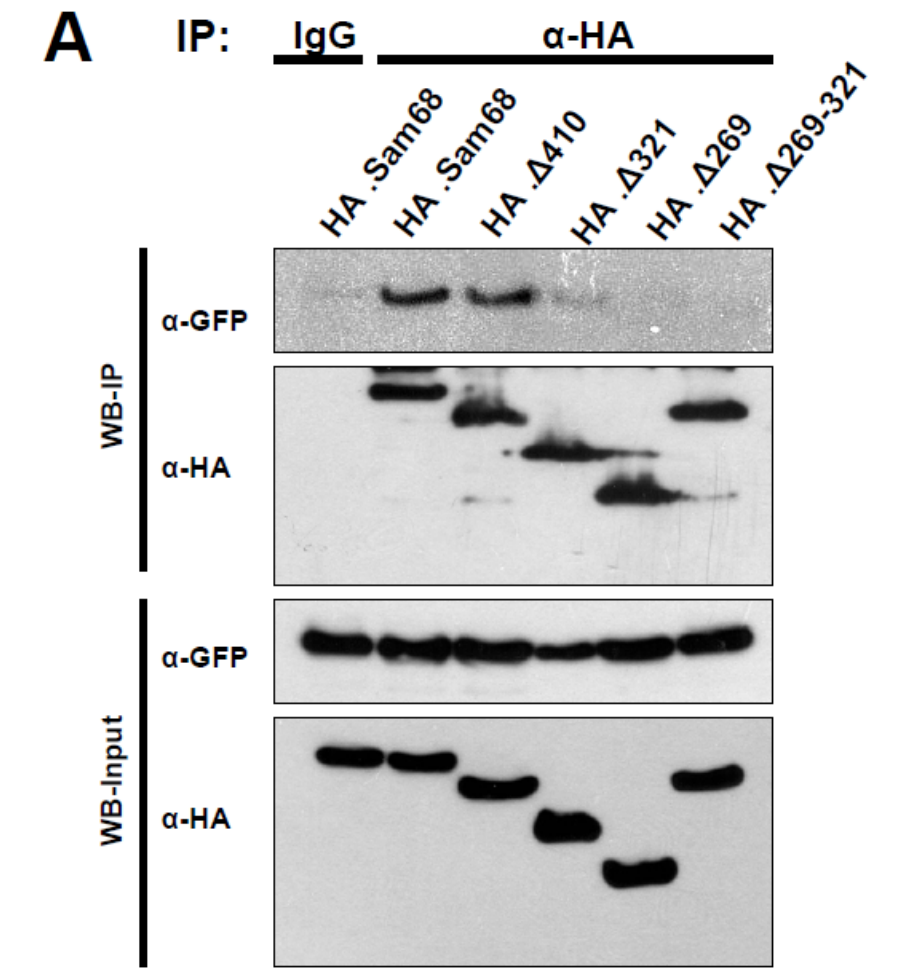
A
IP:
IgG
α-HA
HA .Sam68
HA .Sam68
HA .Δ410
HA .Δ321
HA .Δ269
HA .Δ269-321
WB-IP
α-GFP
α-HA
WB-Input
α-GFP
α-HA

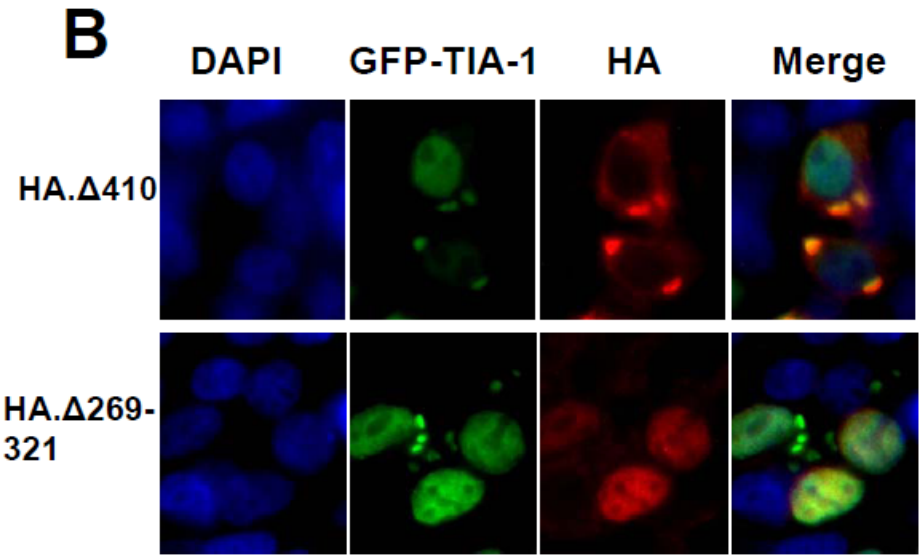
B
DAPI
GFP-TIA-1
HA
Merge
HA.Δ410
HA.Δ269-321

Figure 37. Complex formation between Sam68 deletion mutants and TIA-1. **A.** 293T cells were plated at a density of 2.0 x 10^6 per 35mm plate and transfected with 3.0 µg of HA.Sam68 or its mutants, and 3.0 µg of GFP.TIA-1, and harvested 48 hr after transfection for cell lysates. One milligram of cell lysates were then immunoprecipitated with 1.0 µg of normal IgG, or anti-HA, followed by Western blotting using anti-HA or anti-GFP antibody (WB-IP). Equal amount of input lysates were directly blotted to ensure comparable Sam68 or its mutants, and TIA-1 expression among transfections (WB-Input). **B.** 293T were plated in a 24-well plate at a density of 2.5 x 10^5 cells per well and transfected with 0.3 µg of HA.Δ410 or HA.Δ269-321, and 0.3 µg of GFP.TIA-1. The cells were then stained using an anti-HA antibody followed by PE-conjugated goat anti-mouse antibody. Transfected cells were also stained with 500 ng/ml of DAPI for nuclei. The images were representative of each transfection.

GAP only in mitotic cells, possibly through a third protein, yet to be identified [308]. Hence, it has been suggested that Sam68 and G3BP might cooperate in a pathway that links RAS-GAP and RNA [309]. Thus, we decided to determine if Sam68 and G3BP interacted *in vivo.* We transfected 293T cells with HA.Sam68, GFP.G3BP, or both and performed IP followed by WB analysis. IP with α-HA antibody followed by WB with α-G3BP antibody showed complex formation between Sam68 and G3BP in cells co-expressing Sam68 and G3BP (WB-IP, 2nd panel; Fig. 38B), and α-HA antibody showed similar IP efficiency between cells expressing Sam68 alone and cells expressing both Sam68 and G3BP (WB-IP, 1st panel; Fig. 38B). Conversely, IP with α-G3BP antibody followed by WB with α-HA antibody also showed similar results (WB-IP, 1st panel; Fig. 38C). Importantly, direct Western blot analysis for the input lysates showed comparable levels of protein expression among transfections (WB-input; Fig. 38A-C), and IP with control IgG antibody followed by WB with α-HA or α-G3BP did not show any non-specific background binding (Fig. 38A). Next, we tried to determine whether the complex formation between HA.Sam68 and GFP.G3BP was RNA dependent, using a similar IP/WB approach in the presence of RNase, and we obtained similar results (Fig. 38D). Finally, we failed to detect any complex formation between endogenous Sam68 and endogenous G3BP (Fig. 38E). These results suggest that exogenous Sam68 and G3BP interact directly or indirectly *in vivo* in a RNA independent manner; however, since we were not able to detect an interaction between endogenous proteins, at this point we can not rule out the

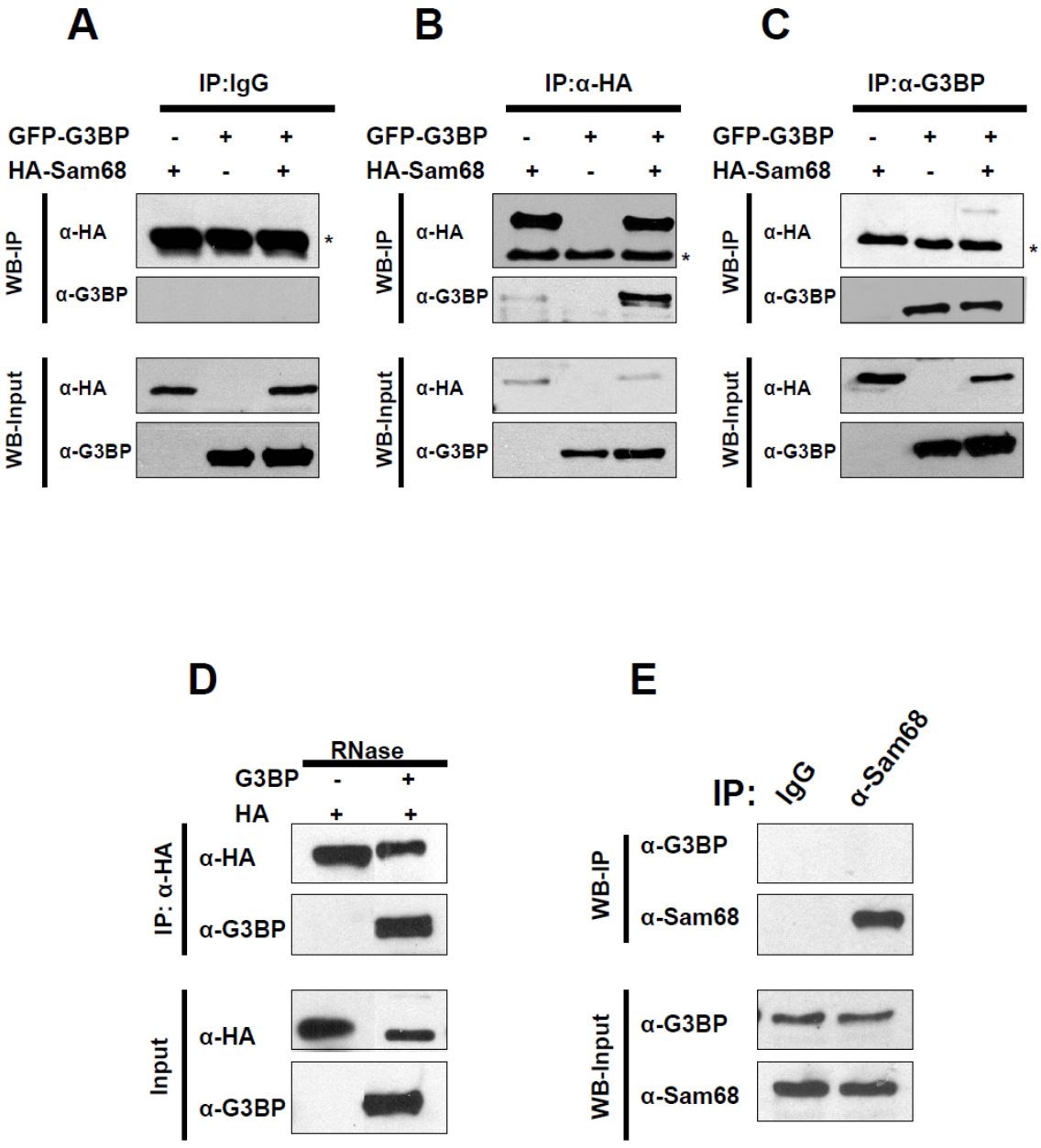
A
IP:IgG
GFP-G3BP - + +
HA-Sam68 + - +
WB-IP
α-HA
α-G3BP
WB-Input
α-HA
α-G3BP
B
IP:α-HA
GFP-G3BP - + +
HA-Sam68 + - +
WB-IP
α-HA
α-G3BP
WB-Input
α-HA
α-G3BP
C
IP:α-G3BP
GFP-G3BP - + +
HA-Sam68 + - +
WB-IP
α-HA
α-G3BP
WB-Input
α-HA
α-G3BP
D
RNase
G3BP - +
HA + +
IP: α-HA
α-HA
α-G3BP
Input
α-HA
α-G3BP
E
IP: IgG α-Sam68
WB-IP
α-G3BP
α-Sam68
WB-Input
α-G3BP
α-Sam68

Figure 38. Complex formation between Sam68 and G3BP. (**A-C**). 293T cells were plated at a density of 2.0 x 10^6 per 35mm plate and transfected with 3.0 µg of HA.Sam68, 3.0 µg of GFP.G3BP, or both and harvested 48 hr after transfection for cell lysates. One milligram of cell lysates was then immunoprecipitated with 1.0 µg of normal IgG (**A**), anti-HA (**B**), or anti-G3BP (**C**) antibodies, followed by Western blotting using anti-HA or anti-G3BP antibody (WB-IP). Equal amount of input lysates were directly blotted to ensure comparable Sam68 and G3BP expression among transfections (WB-Input). *: reactive IgG heavy chain. **D.** 293T cells were plated at a density of 2.0 x 10^6 per 35mm plate and transfected with 3.0 µg of HA.Sam68 and 3.0 µg of GFP.G3BP, and harvested 48 hr after transfection for cell lysates. One milligram of cell lysates were then immunoprecipitated with 1.0 µg of normal IgG, or anti-HA antibodies, in the presence of 0.1 µg/ml of RNase A, followed by Western blotting using anti-HA or anti-G3BP antibody (IP). **E.** Cell lysates were prepared from 293T cells and blotted for endogenous Sam68 and G3BP expression (WB-Input), and 1.5 milligrams were immunoprecipitated with 1.0 µg of normal IgG, or anti-Sam68 antibodies, followed by Western blot analysis using anti-G3BP or anti-Sam68 antibodies (WB-IP).

possibility that this is an artifact phenomenon due to overexpression of exogenous proteins.

2.8 Effect of a protein methyltransferase inhibitor on Sam68 localization during oxidative stress

Recent studies suggest that arginine methylation is important for SG assembly dynamics [151, 310]. Conversely, Sam68 subcellular localization has been shown to be tightly regulated by arginine methylation on its domain between aa269 to aa321. Therefore, we decided to determine the effects of adenosine periodate (AdOx), a global inhibitor of protein methyltransferase activity, on Sam68 localization during oxidative stress. We transfected cells with GFP.Sam68 and treated these cells with ARS, or ARS in combination with AdOX, and determined Sam68 localization to SG. Our results showed that treatment with AdOX did not prevent Sam68 localization to cytoplasmic granules during oxidative stress (Fig. 39). In the present work, we did not determine Sam68 methylation levels; and so, since methylation is an irreversible postranslational modification, it is reasonable to argue that during AdOX treatment a fraction of Sam68 proteins remained methylated, and that this fraction could be actively recruited to SG. Future studies should address this issue.

Taken together all of the above results, we concluded that Sam68 was recruited to SG under oxidative stress in a small percentage of the cells, likely through a

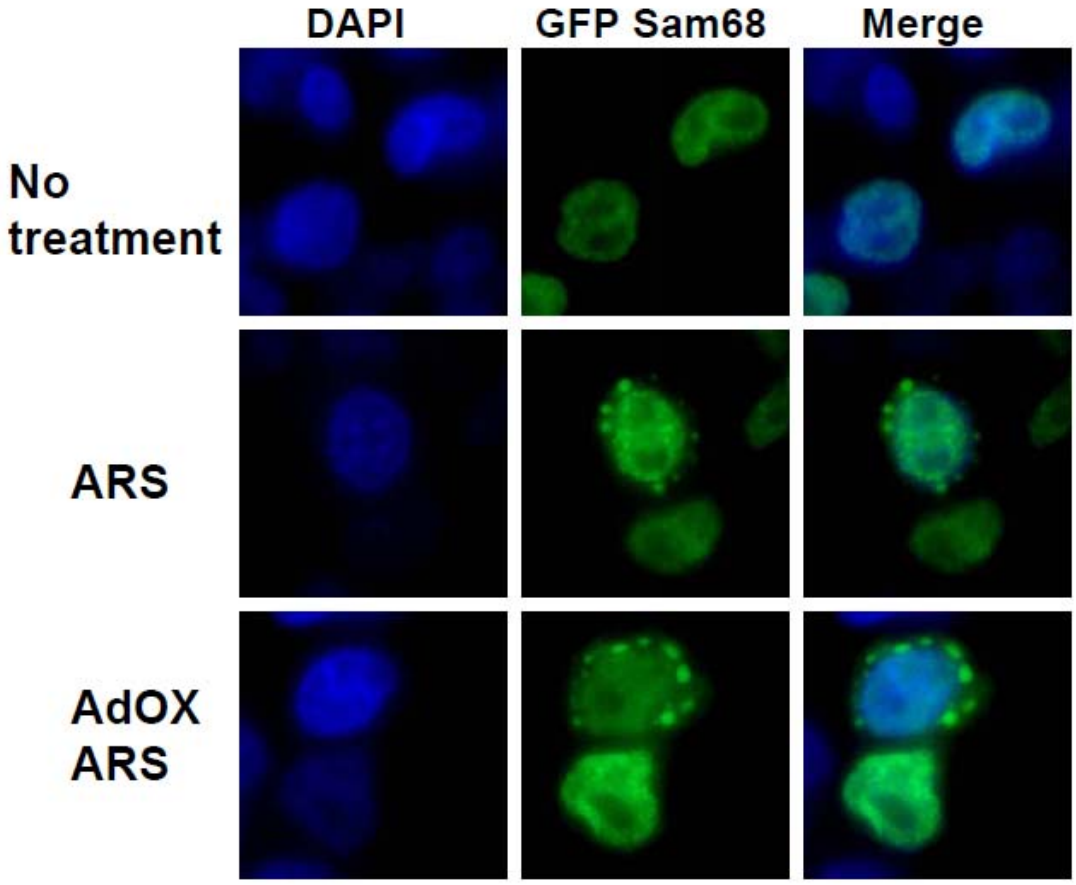

Figure 39. Effects of a protein methyltransferase inhibitor on Sam68 localization under oxidative stress. 293T were plated in a 24-well plate at a density of 2.5 x 10^5 cells per well and transfected with 0.35 µg of GFP.Sam68. Twenty four hours after transfection, the cells were treated with 0.7 mM of AdOX for an additional 24 hr, and then treated with 0.5 mM ARS (ARS) or without ARS for 1 hr prior to fixation. The cells were also counterstained in PBS containing 500 ng/ml DAPI for nuclei. Microspcopy analysis was carried out as above.

“piggy back” mechanism involving its interaction with TIA-1, the core SG component.

PART 3: Role of the ERK pathway on eIF2α phophorylation and SG assembly under oxidative stress.

Cellular growth, differentiation and programmed death are tightly regulated processes, and require sensing mechanisms and coordinated responses from biosynthetic pathways such as protein translation. The negative effect of different forms of stress on cell growth and differentiation are well documented [311, 312]. Furthermore, treatment of cells with growth factors or mitogens increases protein translation, while multiple forms of environmental stresses have the opposite effect [313]. Therefore, it has been proposed that the protein biosynthetic pathway is in direct communication with growth/stress activated signaling cascades [314]. However, during physiological (epithelial surfaces) or pathological conditions (cancer-hypoxia), multi-cellular organisms are exposed simultaneously to stressful and growth stimuli, and the process by which cells make critical decisions regarding cell growth and death in this dual environment is not well understood yet.

The mitogen-activated protein kinase (MAPK) superfamily consists of three main protein kinase families: the extracellular signal-regulated protein kinases (ERKs), the c-Jun N-terminal kinases (JNKs), and the p38 family of kinases. The ERK module responds primarly to growth factors and mitogens, while JNKs and p38

families respond to environmental stresses and cytokines [315]. Consequently, it has been shown that ARS (oxidative stress) treatment leads to opposite effects on the MAPK cascades; it activates JNK and p38, while it blocks the ERK pathway through a activated p38 mediated process [316, 317]. Therefore, using the MAPK pathways and oxidative stress as a model, we set out to determine the effects of simultaneous growth (ERK activation) and stress (ARS) signals on a key regulator of the protein biosynthetic pathway (eIF2α) and on SG assembly.

3.1 Effects of arsenite treatment on MAPK

Previous studies have reported that ARS treatment of fibroblasts or cardiomyocytes prevents mitogen-induced phosphorylation of ERK-1/2, and that this effect is dependent on p38 activation [316, 317]. Therefore, we initially tried to establish if this phenomenon is also present in human embryonic kidney 293T cells. Thus, we treated 293T cells with ARS for different periods of time up to one hour, and determined the activation of ERK-1/2, JNK, and p38 kinases by Western blot analysis using antibodies against the phosphorylated forms of the kinases. Coordinately, JNK and p38 were potently activated between 10 and 20 minutes after ARS treatment (5^{th} & 7^{th} panels; Fig. 40A; Fig. 43A); in contrast, ERK-1/2 phosphorylation declined rapidly (1^{st} panel; Fig.40A; Fig. 43A). Since our aim was to determine the role of the ERK pathway on eIF2α phosphorylation, we also determined eIF2α phophorylation status under these conditions using the same approach. As previously shown (Fig. 32B), eIF2α was rapidly

A

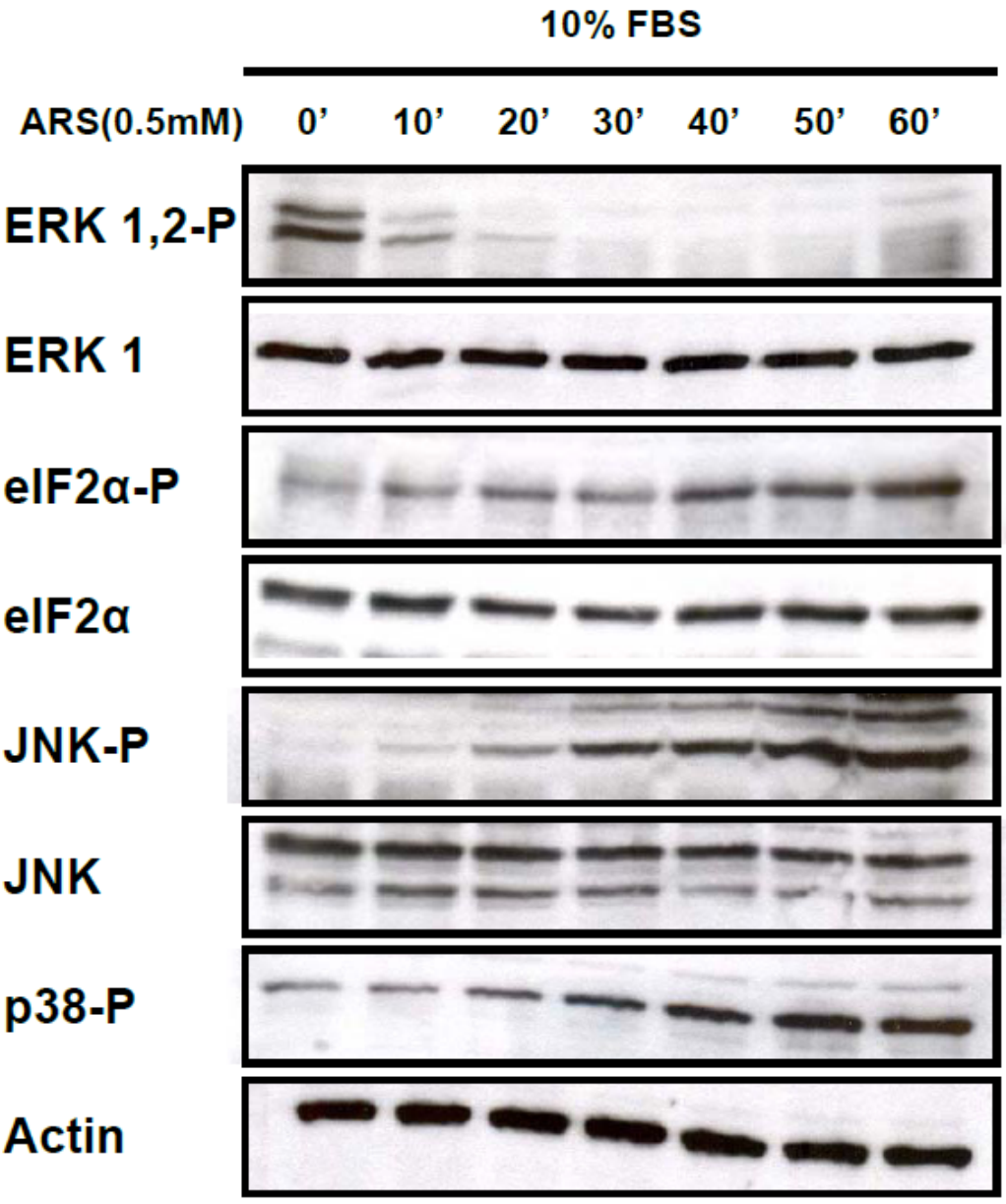
10% FBS
ARS(0.5mM)
0’
10’
20’
30’
40’
50’
60’
ERK 1,2-P
ERK 1
eIF2α-P
eIF2α
JNK-P
JNK
p38-P
Actin

B

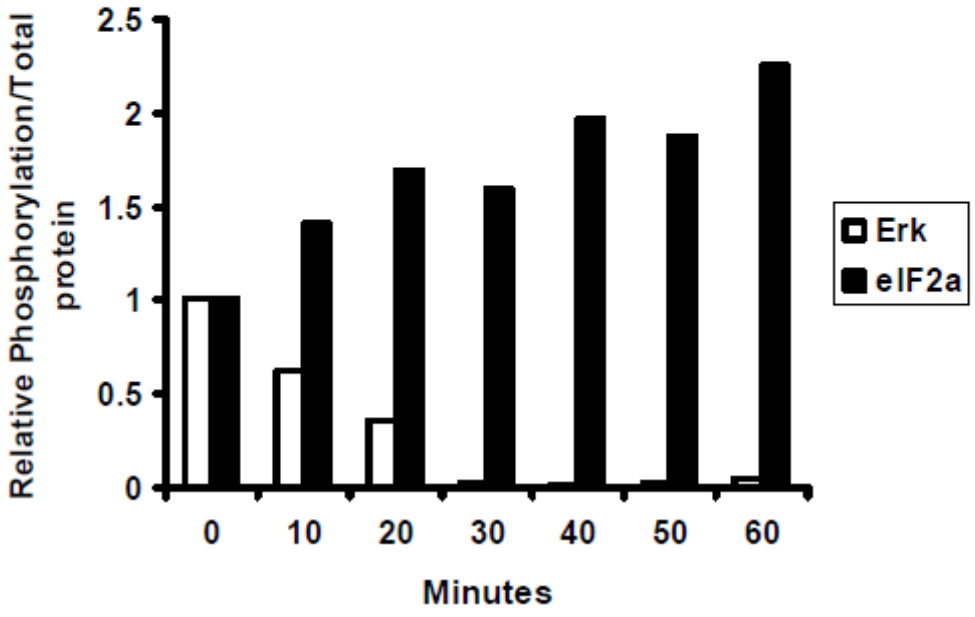
Relative Phosphorylation/Total protein
2.5
2
1.5
1
0.5
0
0
10
20
30
40
50
60
Minutes
Erk
eIF2a

Figure 40. Effects of arsenite treatment on MAPK activation and eIF2α phosphorylation. A. 293T cells were plated in a 12-well plate at a density of 3.5 x 10^5 cells per well, twenty four hours later the cells were treated with 0.5 mM ARS for 0, 10, 20, 30, 40, 50, and 60 min, then harvested, lysed in phosphorylation lysis buffer, and 45 µg of each sample were separated by 10% SDS-PAGE followed by Western blot analysis using anti-ERK-1, anti-phosphorylated ERK-1/2 (ERK 1,2-P), anti-eIF2α, anti-phosphorylated eIF2α (eIF2α-P), anti-JNK, anti-phosphorylated JNK (JNK-P), anti-phosphorylated p38 (p38-P), or anti-β-actin. **B.** Relative levels of phosphorylated ERK-1/2 and eIF2α proteins were determined using total ERK-1 and eIF2α as internal standards, and expressed on the *y* axis. The data were average of two independent experiments.

phosphorylated 10 minutes after ARS treatment was initiated (3rd panel; Fig. 40A; Fig. 43A). Interestingly, we observed a gradual increase in JNK, p38, and eIF2α phosphorylation during the time frame of the experiment, whereas ERK-1/2 dephosphorylation was abrupt and sustained (Fig. 40A & B; Fig. 43A). These results further support the notion that the effects of ARS on MAPK and eIF2α are not cell type specific, and the similar but opposite kinetics of ERK dephosphorylation and eIF2α phosphorylation suggest a possible regulatory connection between the ERK pathway and eIF2α mediated translational control.

3.2 Delayed eIF2α phosphorylation in cells expressing a constitutively active ERK

Only two previous studies have reported a relationship between the ERK pathway and eIF2α phosphorylation. Monick et al. have showed that alveolar macrophages exhibit a constitutively high ERK activity, which promotes hypophosphorylation of eIF2α and subsequently, general protein synthesis and cell survival [318]; meanwhile, Thiaville et al. have shown that in amino acid deprived hepatoma cells, MEK-ERK signaling is required for GCN2-dependent eIF2α phosphorylation [319]. To ascertain the role of the ERK pathway on eIF2α phophorylation in 293T cells under oxidative stress, we initially took advantage of the well documented phenomenon of ERK activation during serum starvation. We reasoned that by increasing the basal levels of ERK activation through serum deprivation, the kinetics of ERK dephosphorylation would be modified upon ARS treatment, allowing us to detect the impact of an active ERK pathway on eIF2α

phosphorylation status during oxidative stress (ARS). Thus, we serum starved 293T cells and then treated the cells with ARS for different periods of time as stated above, and determined the phosphorylation levels of ERK-1/2, JNK, p38, and eIF2α by Western blot analysis. Our results showed that JNK, p38, and eIF2α phophorylation kinetics were similar to those of 293T cells grown in media complete with serum (3rd, 5th, and 7th panels; Fig. 41A); in addition, rapid and potent dephosphorylation of ERK-1/2 was still observed (1st panel; Fig. 41A). These results suggest that inhibition of the ERK pathway by ARS treatment overrides the initial increase in the basal levels of activated ERK pathway.

To overcome the potent downregulatory effect of ARS on ERK activation, we decided to hyper-activate the MEK-ERK portion of this signaling pathway by using a constitutively active MEK (CA-MEK) mutant [320] and to determine its effects on eIF2α phosphorylation under oxidative stress. Thus, we transfected 293T cells with CA-MEK, and then treated the cells with ARS in the same fashion as in our previous experiments (Fig. 40-41) followed by similar Western blot analysis. As it was the case for untransfected cells, ARS treatment resulted in a gradual activation of JNK and p38 (5th & 7th panels, Fig. 42A; Fig. 43B); on the other hand, CA-MEK led to constant and stable high levels of phosphorylated ERK-1/2 (1st panel; Fig. 42A; Fig. 42B; Fig. 43B), overcoming the inhibitory effects of ARS treatment. Interestingly, the kinetics of eIF2α phosphorylation greatly differed from our previous results. In contrast to the rapid phosphorylation

A

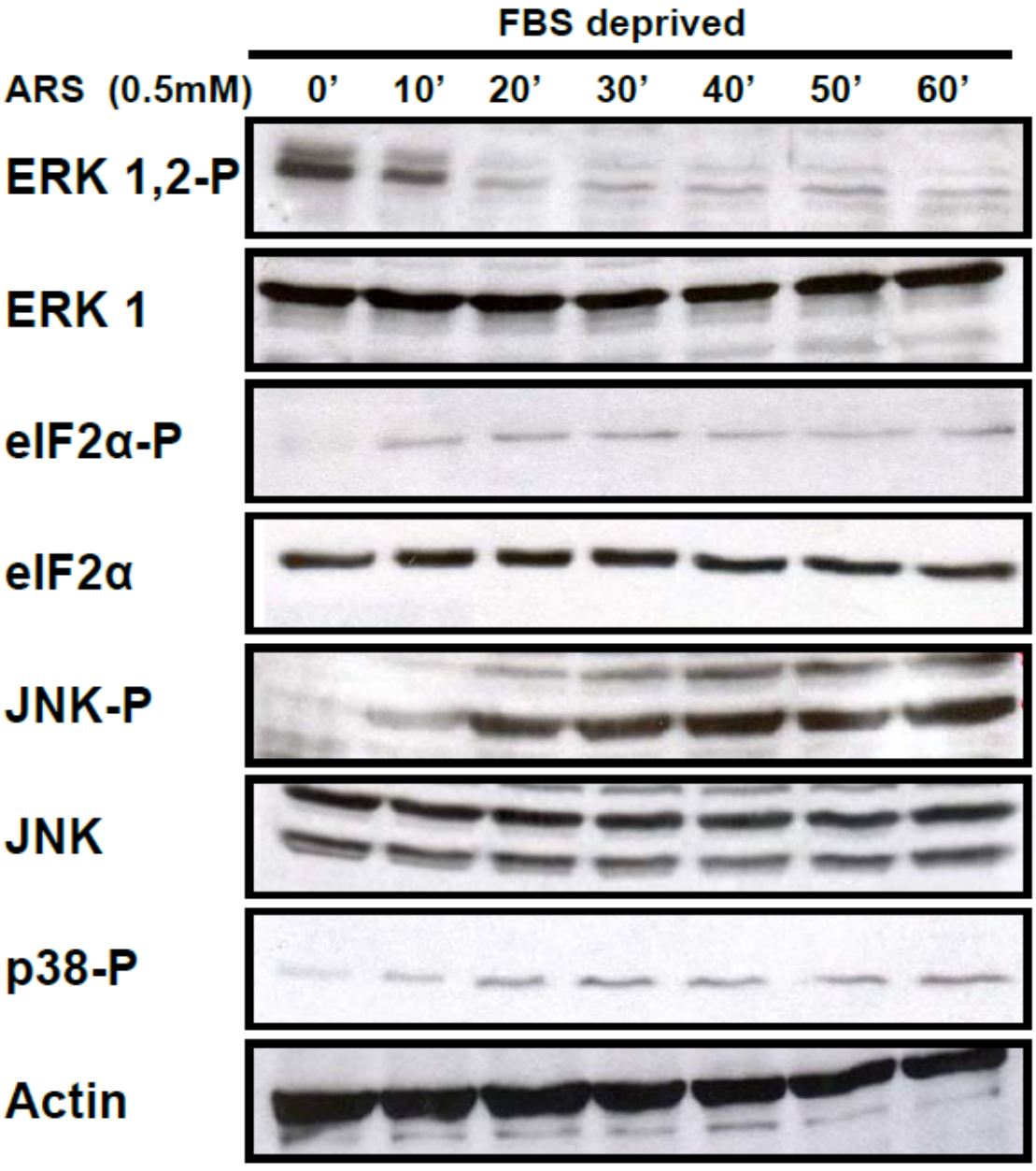
FBS deprived
ARS (0.5mM)
0'
10'
20'
30'
40'
50'
60'
ERK 1,2-P
ERK 1
eIF2α-P
eIF2α
JNK-P
JNK
p38-P
Actin

B

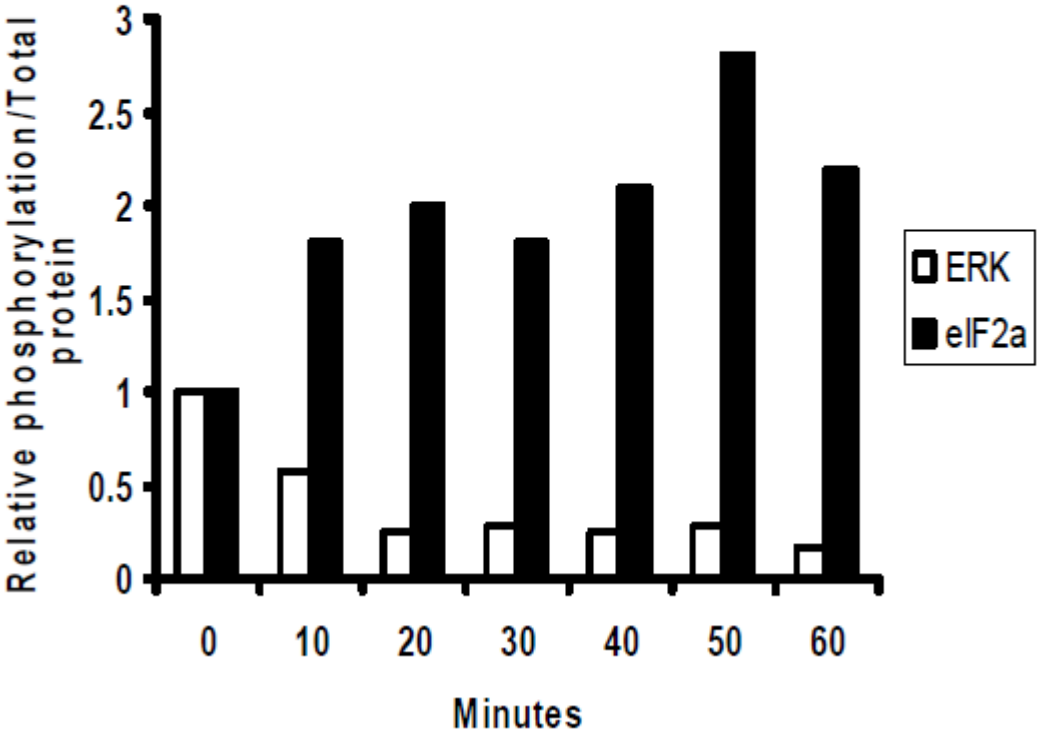
Relative phosphorylation/Total protein
3
2.5
2
1.5
1
0.5
0
0
10
20
30
40
50
60
Minutes
ERK
eIF2a

Figure 41. Effects of arsenite treatment on MAPK activation and eIF2α phosphorylation in serum starved cells. A. 293T cells were plated in a 12-well plate at a density of 3.5 x 10^5 cells per well, twenty four hours later the cells were serum starved for additional 16 hr, and then treated with 0.5 mM ARS for 0, 10, 20, 30, 40, 50, and 60 min. Subsequently, the cells were harvested, lysed in phosphorylation lysis buffer, and 45 µg of each sample were separated by 10% SDS-PAGE followed by Western blot analysis using anti-ERK-1, anti-phosphorylated ERK-1/2 (ERK 1,2-P), anti-eIF2α, anti-phosphorylated eIF2α (eIF2α-P), anti-JNK, anti-phosphorylated JNK (JNK-P), anti-phosphorylated p38 (p38-P), or anti-β-actin. **B.** Relative levels of phosphorylated ERK-1/2 and eIF2α proteins were determined using total ERK-1 and eIF2α as internal standards, and expressed on the *y* axis. The data were average of two independent experiments.

A

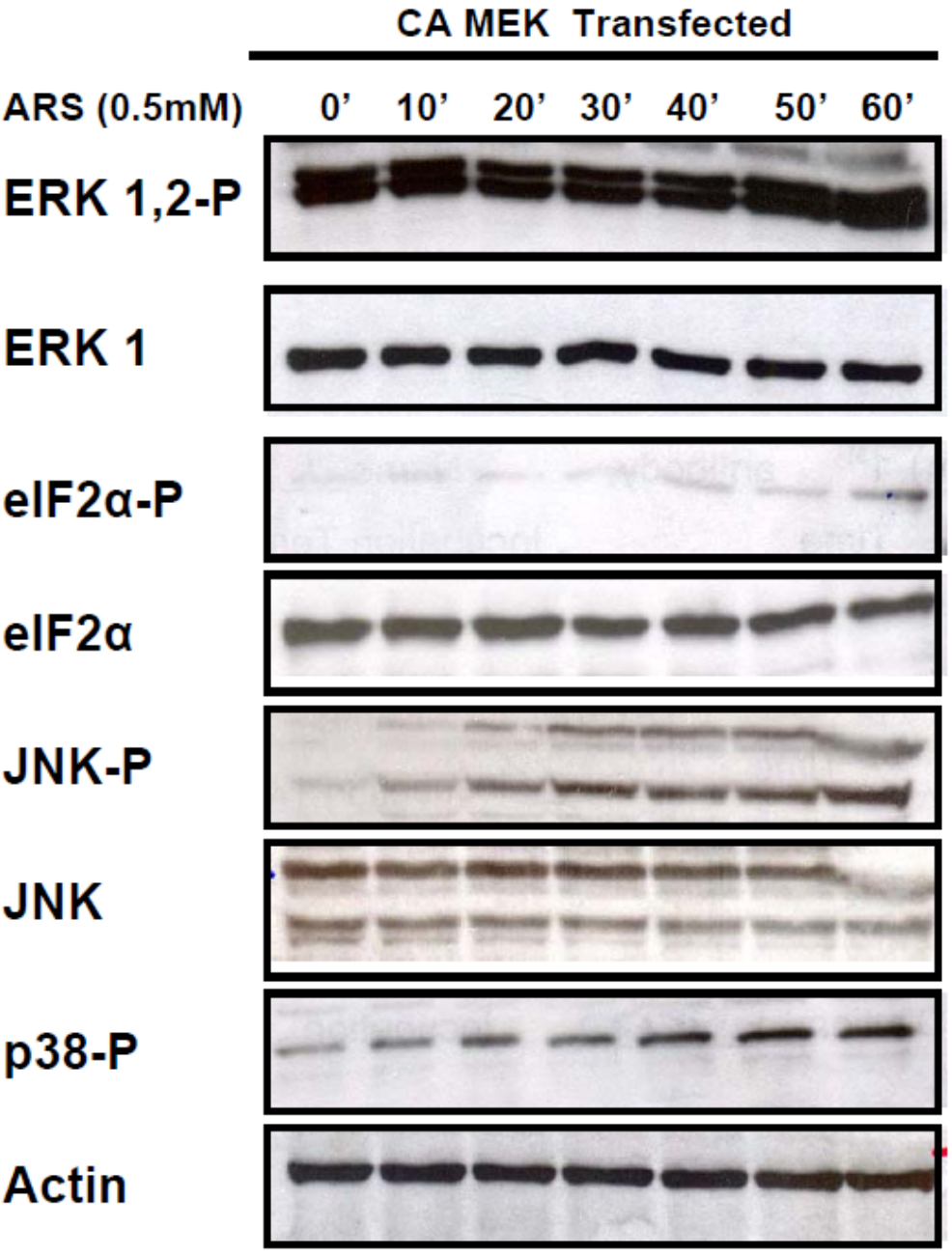
CA MEK Transfected
ARS (0.5mM)
0’ 10’ 20’ 30’ 40’ 50’ 60’
ERK 1,2-P
ERK 1
eIF2α-P
eIF2α
JNK-P
JNK
p38-P
Actin

B

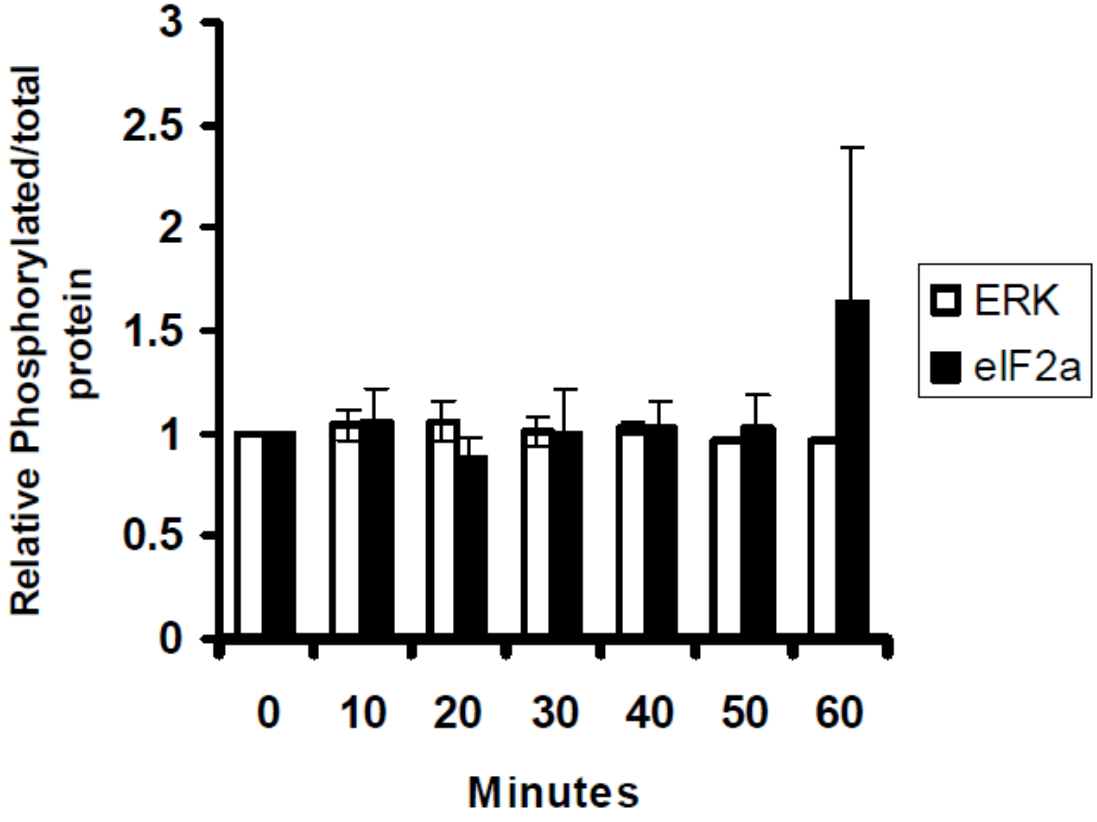
Relative Phosphorylated/total protein
3
2.5
2
1.5
1
0.5
0
0
10
20
30
40
50
60
Minutes
ERK
eIF2a

Figure 42. Effects of constitutively activated ERK expression on eIF2α phosphorylation under oxidative stress. A. 293T cells were plated in a 12-well plate at a density of 3.5 x 10^5 cells per well and transfected with 0.7 µg of CA MEK. Thirty six hours later the cells were treated with 0.5 mM ARS for 0, 10, 20, 30, 40, 50, and 60 min. Subsequently, the cells were harvested, lysed in phosphorylation lysis buffer, and 45 µg of each sample were separated by 10% SDS-PAGE followed by Western blot analysis using anti-ERK-1, anti-phosphorylated ERK-1/2 (ERK 1,2-P), anti-eIF2α, anti-phosphorylated eIF2α (eIF2α-P), anti-JNK, anti-phosphorylated JNK (JNK-P), anti-phosphorylated p38 (p38-P), or anti-β-actin. **B.** Relative levels of phosphorylated ERK-1/2 and eIF2α proteins were determined using total ERK-1 and eIF2α as internal standards, and expressed on the *y* axis. The data were mean ± S.E.M.

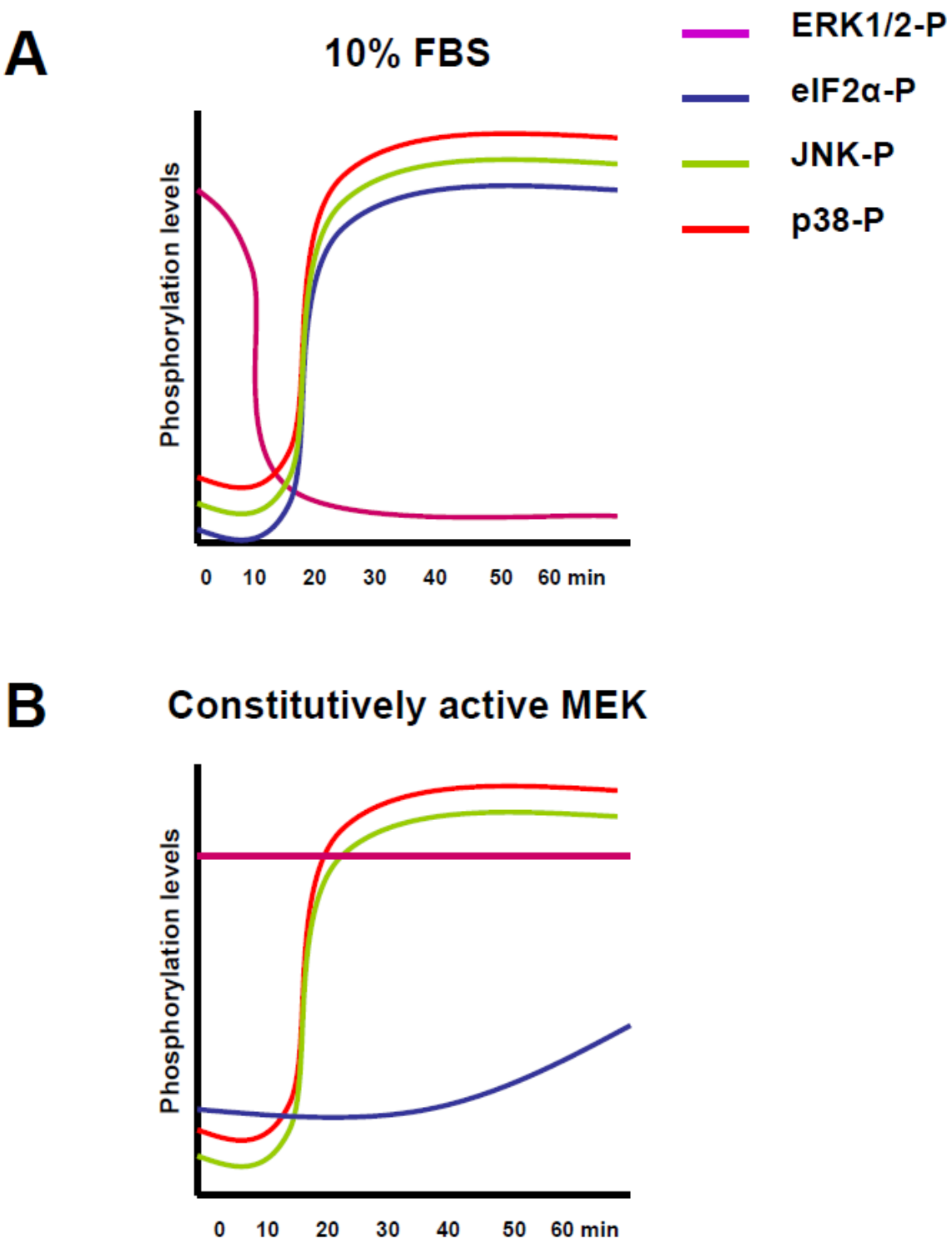
A
10% FBS
ERK1/2-P
eIF2α-P
JNK-P
p38-P
Phosphorylation levels
0 10 20 30 40 50 60 min
B
Constitutively active MEK
Phosphorylation levels
0 10 20 30 40 50 60 min

Figure 43. Kinetics of MAPK and eIF2α phosphorylation during oxidative stress. Representation of the phosphorylation kinetics of ERK-1/2 (purple), JNK (green), p38(red), and eIF2α (blue) in ARS treated 293T cells without (**A**), or with (**B**) a constitutively active ERK pathway.

observed in untransfected cells (Fig. 40 & 41; Fig. 43A), eIF2α remained hypo-phosphorylated for the most part of the treatment, and an increase in its phosphorylation levels was only detected in the last time point evaluated (3rd panel; Fig. 42A & 42B; Fig. 43B). Taken together, these results suggest that the ERK pathway regulates eIF2α-mediated translational control under oxidative stress through a yet undetermined mechanism.

3.3 Normal stress granules assembly in cells expressing a constitutively active ERK

Based in our previous results, we hypothesized that ERK constitutive activation might lead to impaired SG assembly due to reduced levels of eIF2α phosphorylation. Hence, we transfected 293T cells with CA-MEK mutant, and then treated the cells with ARS for one hour followed by immunofluorescence staining for endogenous G3BP as the SG marker. As previously shown (Fig. 30B), in the absence of ARS treatment, G3BP was detected widespread throughout the cytoplasm, but in SG upon ARS treatment. Importantly, we did not observe a significant difference between the number of untransfected and CA-MEK transfected cells containing SG (Fig. 44). These results suggest that ERK activation does not influence SG assembly; however, a definitive answer should come from future studies that will address the role of activation of the ERK pathway on the kinetics of SG assembly, during oxidative stress.

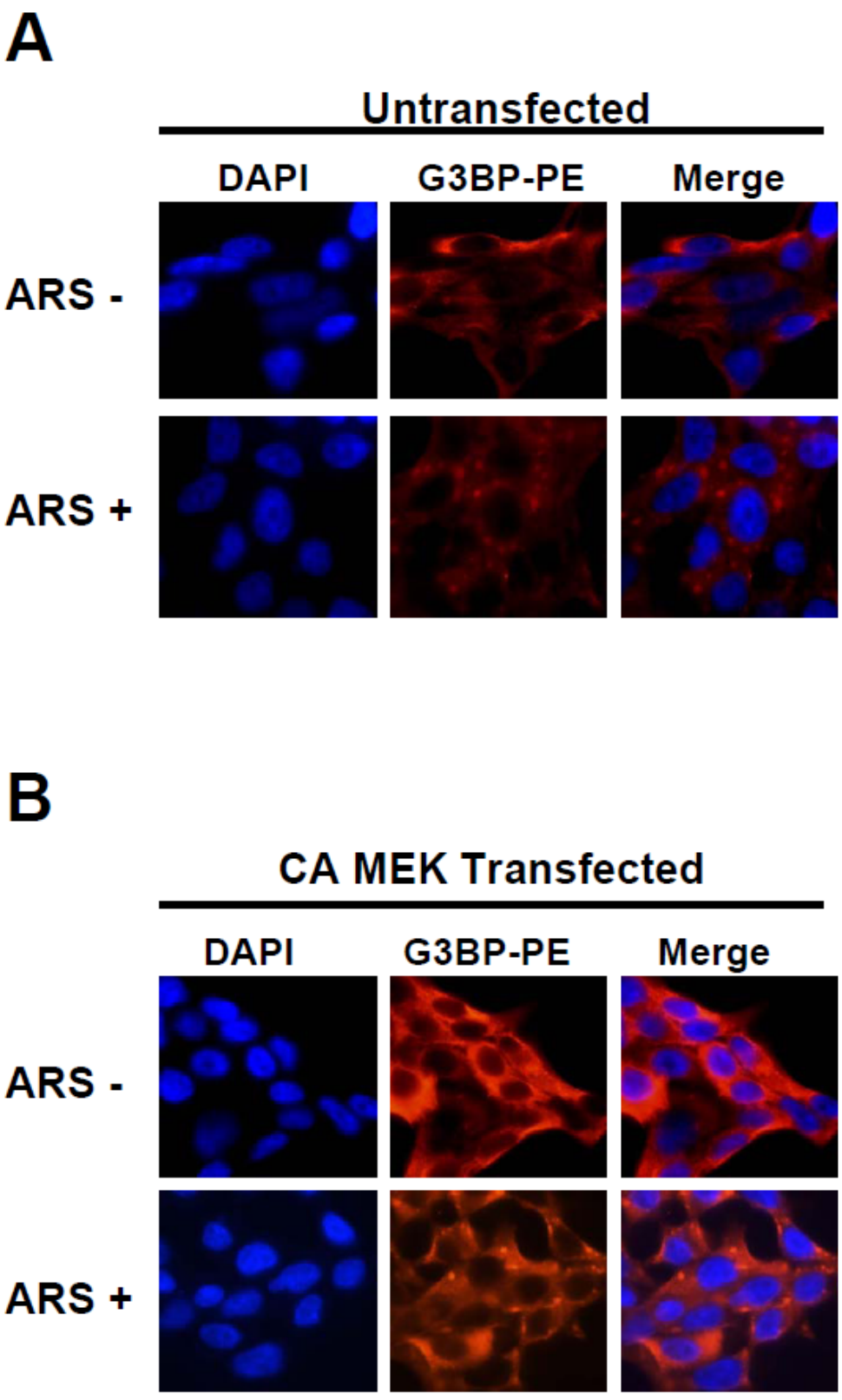
A
Untransfected
DAPI
G3BP-PE
Merge
ARS -
ARS +
B
CA MEK Transfected
DAPI
G3BP-PE
Merge
ARS -
ARS +

Figure 44. Effects of constitutively activated ERK expression on SG assembly under oxidative stress. 293T were plated in a 24-well plate at a density of 1.75 x 10^5 cells per well and transfected with 0.35 µg of CA MEK (**B**), or left untransfected (**A**); and then treated with 0.5 mM ARS (+ ARS) or without ARS (- ARS) for 1 hr prior to fixation. The cells were then stained using a mouse anti-G3BP antibody followed by PE-conjugated goat anti-mouse secondary antibody. The images were representative of each condition. Co-localization of G3BP with nuclei was shown in the column marked as "Merge".

Based in all of the above, we concluded that ERK activation changes the kinetics of eIF2α phosphorylation under oxidative stress, through a yet undetermined mechanism.

DISCUSSION

Summary of the results

In the first part of the current study, using a pair of newly constructed NL4-3-based luciferase reporter viruses, we revealed that expression of a Sam68 NLS-deleted Δ410 mutant led to a significant decrease in Luc gene expression which was substituted for the HIV-1 *nef* gene (Fig. 7D) and HIV-1 Nef expression (Fig. 8). This mutant did not alter HIV-1 transcription, pre-mRNA splicing, RNA stability (Fig. 9B), or the translation of a reporter gene containing only the 5' leader sequence of HIV-1 RNA (Fig. 20B). Moreover, further removal of the domain between aa269 and 321 abrogated the suppressive effect (Fig. 13) and formation of a granule-like structure in the cytoplasm (Fig. 16). The granule-like structure induced by this mutant was identified as a stress granule (SG) (Fig. 17 & 18). A novel minigene assay demonstrated that Δ410-induced suppression was specific to HIV-1 Nef through the uniquely structured 3'UTR of *nef* mRNA (Fig. 23). This was further corroborated by the findings that Δ410 bound to the *nef* mRNA 3'UTR in a direct manner (Table 2). Moreover, HIV-1 *nef* mRNA transcripts were co-localized with Δ410-induced SG (Fig. 25). Importantly, SG induction and Nef suppression by Δ410 also occurred in the context of HIV-1 infection of CD4+ T lymphocytes (Fig. 26 & 27). Thus, we concluded that Δ410 suppressed HIV-1 Nef expression through induction of SG formation and sequestration of HIV-1 *nef* mRNA transcripts from being translated to Nef protein.

Based on our previous results, in the second part of the present study, we demonstrated that both exogenous and endogenous Sam68 were recruited into SG in a percentage of the cells upon oxidative stress (Fig. 29 & 30). Removal of the P_3 (RG-rich) domain aa269-321, or the KH domain aa171-211, abrogated the ability of Sam68 to be recruited into SG and translationally repress Nef expression (Fig. 31; Fig. 33 & 34). Moreover, Sam68 RNA binding deficient mutants (ΔKH, ΔKHΔ410) formed insoluble protein aggregates different from SG (Fig. 33 & 34). Knock down of Sam68 expression had no effects on SG assembly (Fig. 35). Importantly, Sam68 formed a complex with TIA-1 through the P_3 (RG-rich) domain aa269-321, deletion of which prevented Sam68 recruitment into SG (Fig. 36 & 37). Thus, we concluded that Sam68 was recruited to SG under oxidative stress, likely through a "piggy back" mechanism involving its interaction with TIA-1, a core SG component.

Finally, in an attempt to determine the effect of a growth signal (ERK activation) on eIF2α-mediated translational control during oxidative stress, we showed that ARS treatment had opposite effects on MAPK in 293T cells; while ARS gradually activated the p38 and JNK pathways in a time dependent manner; the ERK pathway was rapidly and potently inhibited (Fig. 40 & 41; Fig. 43A). Moreover, hyper-activation of the ERK pathway by a constitutively active MEK mutant led to delayed eIF2α phosphorylation (Fig. 42 & 43B); however, this did not resulted in impaired SG assembly (Fig. 44). Therefore, we concluded that ERK activation

changes the kinetics of eIF2α phosphorylation under oxidative stress through a yet undetermined mechanism.

Distinct functions of Sam68 NLS-deleted mutants on HIV-1 gene expression

Sam68 has been shown to be absolutely required for HIV-1 replication and Rev-dependent gene expression [221, 243, 244] (Fig. 11A-C). Sam68 possesses a non-conventional NLS at its C terminus, and deletion of this NLS results in Sam68 cytoplasmic localization [214], and impaired HIV-1 replication [78, 243]. Therefore, it is not surprising that inhibition of HIV-1 replication by Sam68 NLS-deleted mutant Δ410 has been shown to behave in a dominant negative fashion, i.e., formation of dimer or oligomers between Δ410 and wild-type Sam68 and subsequent retention of the wild-type Sam68 in the cytoplasm, which in turn prevents wild-type Sam68 from functioning in Rev-mediated nuclear export of HIV RNA [78, 249]. However, different lines of evidence suggest additional roles for Sam68 cytoplasmic mutants; for instance, Δ410 was also shown to be co-localized with unspliced and partially spliced HIV-1 RNA in perinuclear bundles and to sequester these RNA from the cellular translational machinery [248]. Moreover, wild-type Sam68 promotes translation of intron containing RNA [222], and is also found in the nucleus when it is co-expressed with the NLS-deleted mutants [249]. The current study demonstrated that Δ410 suppressed HIV-1 Nef translation (Fig. 8). Taken together, these studies have shown that Δ410 negatively regulates HIV-1 replication at two distinct steps of the virus life cycle:

Rev-mediated nuclear export of incompletely spliced HIV-1 RNA and translation of HIV-1 *nef* mRNA in the cytoplasm.

Inhibition of Nef expression by Sam68 NLS-deleted mutants in the cytoplasm

Sam68 has been shown to regulate transcription, pre-mRNA alternative splicing, and translation [218, 219, 223, 234]. Thus, different nuclear or cytoplasmic mechanisms could explain Δ410-mediated Nef suppression. Previous reports have determined that Sam68 or its mutants do not have inhibitory effects on the HIV-1 LTR promoter [78]; in concordance, our results showed little changes in the transcription levels of multiply spliced HIV-1 RNA (Fig. 9B). Furthermore, Δ410 did not change the splicing pattern, nor did it decrease the stability of these mRNA species (Fig. 9B). These results suggest that Nef suppression is not due to a loss of function of wild-type Sam68 within the nucleus, but instead it is a gain of function for Δ410 in the cytoplasm. This notion was further supported by the data obtained using a Sam68 siRNA, showing that Sam68 knockdown did not suppress Nef expression (Fig. 10B) or Luc expression when placed in the *nef* gene (Fig. 11D). Subsequent studies on the structure-function relationship of Sam68 in terms of Nef suppression allowed three definitive conclusions: first, deletion of the Sam68 NLS, resulting in cytoplasmic localization, is required for this inhibition to occur (Fig. 13; Fig. 16A; Fig. 45A); second, RNA binding is mandatory since deletion of the KH domain abrogates the suppressive effect of NLS-deleted mutants (Fig. 34B & 45A); and third, Sam68 domain aa269-321 was

A. Nef expression

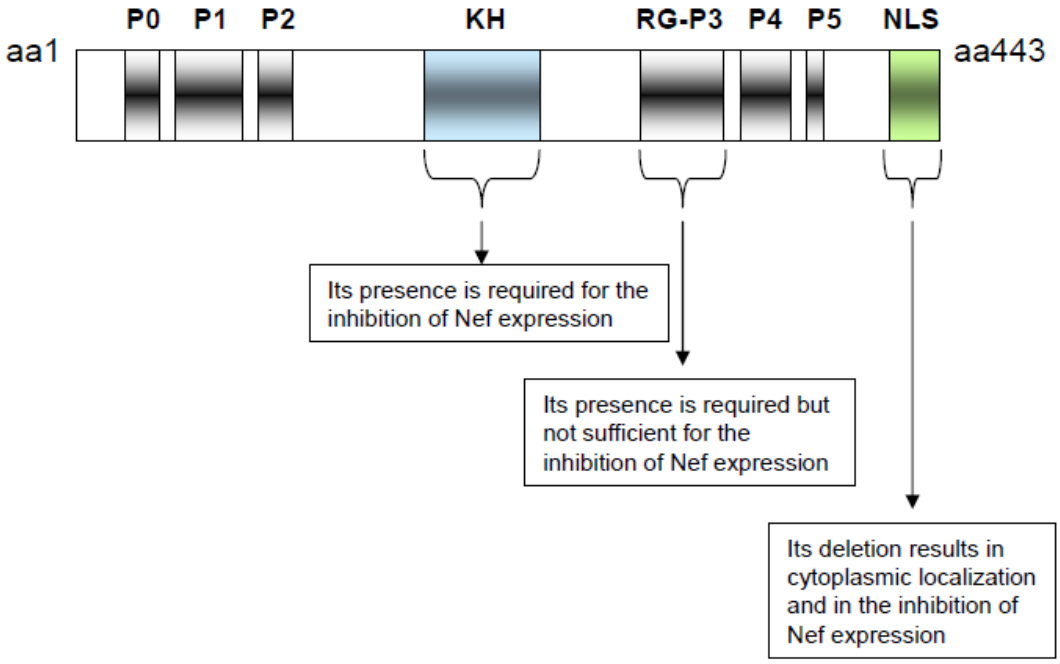

B. SG assembly/recruitment

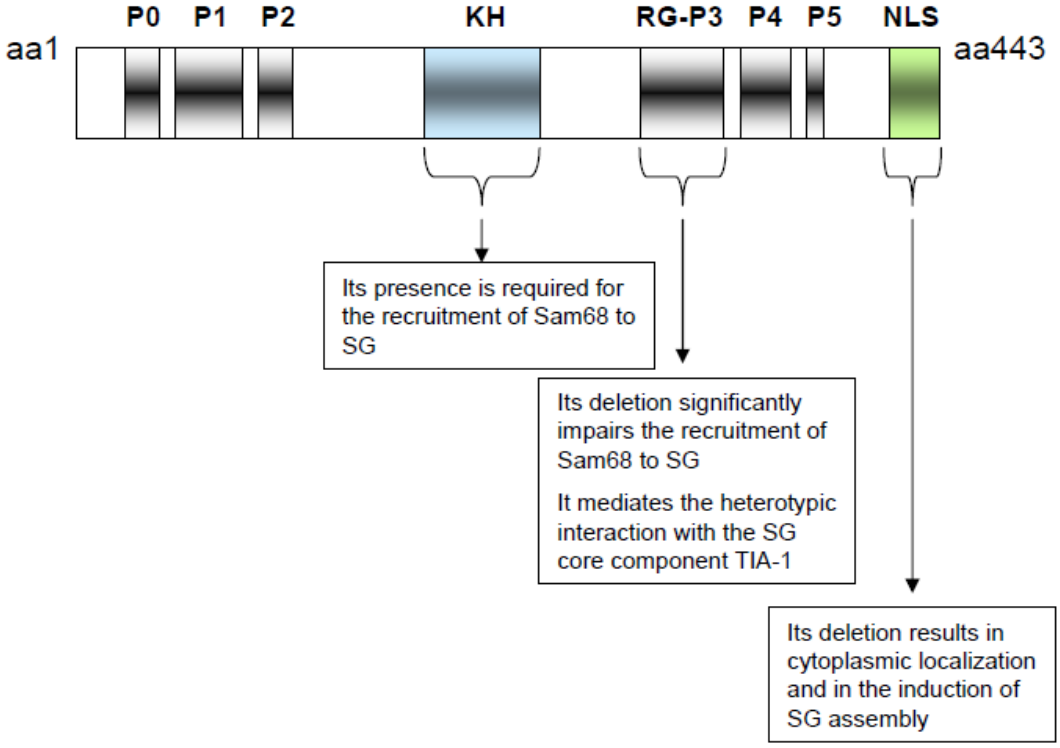

Figure 45. Role of Sam68 domains on Nef suppression and stress granule recruitment/assembly. P: proline-rich domain (gray); KH: KH domain (light blue); RG: arginine-glycine-rich domain (gray); and NLS: nuclear localization signal (light green). The roles of each domain on Nef suppression (**A**) or stress granule (SG) recruitment/assembly (**B**) are indicated (boxes)

indispensable but not sufficient for Nef suppression by Δ410 and Δ321 mutants (Fig. 13 & 45A). The roles of the NLS and the KH domain on Sam68 function and localization had been extensively studied in the past; however, the function of the domain aa269-321 is less clear at this moment. This domain is located in the proline-rich region (P_3), which also overlaps the arginine-glycine (RG)-rich region [195]. Some of the functions that have been attributed to these proline- and RG-rich regions include protein-protein interaction, intracellular localization and non-specific RNA binding [210, 217, 245]. The RG-rich region is also a potential site for protein methylation [217]. Nevertheless, whether any of these properties contribute to Nef suppression remains to be determined.

Role of SG nucleation on Nef suppression by Sam68 NLS-deleted mutants

Heterogeneous nuclear RNAs (hnRNAs or pre-mRNAs) are synthesized, post-transcriptionally processed and transported in the form of heterogeneous nuclear ribonucleoprotein (hnRNP) particles [321]. mRNAs are generally assumed to be translationally repressed to prevent ectopic expression while en route to the specific site of translation in the cytoplasm [322]. Viral mRNA including HIV-1 should be no exception. The movement of the viral mRNA in the cytoplasm requires their interaction with multiple host proteins, which give rise to RNA granules [323]. Multiple copies of HIV-1 mRNA have indeed been detected in these granules [324]. Thus, it is likely that changes in the components of this cellular machinery lead to aberrant targeting of HIV-1 mRNA to the translation machinery or to the sites of virion assembly [325, 326]. Our results showed that

Δ410 and Δ321 mutants were capable of inducing SG formation and this phenomenon was associated with their ability to suppress Nef expression (Fig. 13; Fig. 16; Fig. 31).

SG are one type of RNA granules that form in response to a variety of external stimuli including over expression of proteins such as TIA-1 [299], G3BP [146], caprin-1 [147], staufen [141], FMRP [327], and pumilio [139]. SG formation has been recently recognized as a very effective way to spatially and temporally regulate gene expression by storing translationally arrested mRNA [298, 328]. Consistent with these findings, HIV-1 *nef* RNA transcripts were detected in these SG induced by the Δ410 mutant (Fig. 25). Although, less is known about the mechanism by which specific mRNAs are included or excluded from SG, different reports suggest that this process relies on the mRNA binding specificity of RBP recruited to SG [138, 298], which in turn seems to be highly dependent on mRNA secondary structure [124]. Our results showed that SG induction and inhibition of Nef expression by Sam68 NLS-deleted mutants required the RG/P_3-rich region (aa269-aa321) (Fig. 13 & 45A). Interestingly, RG-rich regions have been shown to be essential for SG assembly/recruitment of different RBP [146]. In the case of Sam68, the RG-rich region is involved in non-specific RNA binding [245], probably mediated by positively charged side chains, while the KH domain mandates its sequence-specific RNA binding [329]. Therefore, our results suggest that SG nucleation by Sam68 cytoplasmic mutants is mediated by heterotypic/homotypic protein-protein interactions with the P_3, while the

sequence specific interactions between the *nef* mRNA and Sam68 mutants is likely due to the ability of the RG-rich region to confer the neighboring KH domain with the capacity to bind specific RNA [245], as is the case for the STAR family member BBP/SF1 [330]. In concordance, Sam68 RNA binding defective mutants (ΔKH) are incapable of suppressing Nef expression, inducing SG, or binding to the *nef* 3'UTR (Fig. 33 & 34; Table 2). Notably, TIA-1 and G3BP expression did not suppress Nef expression, although their expression induced SG formation (Fig. 24), further supporting that Δ410 dictates the targeting specificity of *nef* mRNA to SG. Finally, in agreement with our previous findings that no changes were observed on the stability of multiply spliced HIV-1 RNA (Fig. 9B), we determined that Δ410 was not localized to the P bodies (Fig. 19B), in which mRNA decay often occurs [294].

Differential regulation of *tat, rev* and *nef* mRNA

In different cell types or stages of infection, the expression of *tat, rev,* and *nef* transcripts is reported to vary independently [331], indicating that cellular host factors finely tune their level of expression at the post-transcriptional stage. Indeed, multiple studies link the expression of host factors with specific exon utilization during HIV-1 splicing [332]; but little is known about differential translational regulation of HIV-1 gene expression. Interestingly, *tat, rev* and *nef* mRNA show a significant sequence homology; however, their 5'UTRs and 3'UTRs differ considerably in length and structure (Fig. 21B), which predispose them to differential regulation by host factors. For example, *nef* possesses a

longer and more structured 5'UTR, thus a different mRNA scanning mechanism may be employed when compared to *tat* and *rev*. Conversely, their 3'UTRs are also significantly dissimilar; hence, translational silencer proteins or miRNAs can have differential specificity for individual transcripts. Using a novel minigene strategy, we unequivocally showed that Δ410 only suppressed Nef not Tat or Rev expression (Fig. 21), and that the 3'UTR of *nef* mRNA was directly involved in this process (Fig. 23). The Yeast three-hybrid assay confirmed that Δ410 bound to the 3'UTR of *nef* mRNA while Δ269 or ΔKH did not (Table 2). Since Δ410 fails to bind the *nef* 3'UTR in reverse orientation (Table 2), and to suppress Tat and Rev (Fig. 21& 22), we concluded that the *nef* 3' UTR structure is critical for Δ410-mediated targeting of *nef* mRNA to SG, and its subsequent translational repression.

Physiological relevance of Nef suppression by Sam68-NLS deleted mutants

Nef is a major pathogenic factor during HIV and SIV infection of primates, its deletion or mutation significantly reduces the pathology observed in rhesus macaques and humans infected with SIV or HIV-1, respectively [89]. Nef expression in lymphoid and monocytic cells regulates two key aspects of HIV-1 infection and AIDS pathogenesis: evasion of the humoral and cellular immune response, and sustained hyperactivation of the immune system [102]. Importantly, although clinically successful antiretroviral therapy can reduce viral replication to undetectable levels in plasma, Nef is continuously being expressed in latently infected PBMC [113], making Nef an ideal candidate for future

antiretroviral therapies. In agreement with our previous results, we showed that Δ410 was able to induce SG formation in a CD4+ T cell line (Fig. 26), and to suppress Nef expression in these cells (Fig. 27C) and in human PBMC (Fig. 27E). In addition, Δ410 expression partially restored surface expression of MHC-I molecules (Fig. 27D). These results show that down-regulation of Nef expression by Δ410 is observed in the natural target cells for HIV-1. Therefore, it is conceivable that targeting Δ410 to infected cells could inhibit HIV replication through inhibition of Rev-mediated exportation, and sequestration of *nef* mRNA through SG induction, eliminating Nef expression and function and as a result, halting the disease progression to AIDS.

Sam68, a new constituent of SG

Sam68 has recently been shown to be in cytoplasmic RNA granules in hippocampal neurons and during early embryogenesis [223, 261]. To date, little is known about the role of Sam68 in host response to external stress; however, different lines of indirect evidence suggest that Sam68 could be recruited into SG in response to various stresses. Sam68 translocates and accumulates in cytoplasmic granules under stressful conditions such as: poliovirus infection, ischemia, and puromycin treatment, which are also known to promote SG assembly [167, 261, 270-272]. Likewise, treatment with urate crystals results in Sam68 cytoplasmic localization in neutrophils [273]. Moreover, multiple previously characterized SG components are complexed with Sam68 in a direct or indirect manner [219, 274, 275]. During the first part of the current study, we

found that Sam68 cytoplasmic mutants are capable of inducing SG formation and inhibiting HIV-1 Nef translation through sequestration of Nef mRNA. We report here that exogenous and endogenous Sam68 re-localizes with well characterized SG markers (TIA-1, G3BP, PABP and eIF3η) upon ARS treatment (Fig. 29 & 30). Sam68 also co-localized in SG with its previously characterized interacting protein hnRNP A1 during oxidative stress (Fig. 29). In contrast, Sam68 was not found present within P bodies under any conditions tested here (Fig. 29E). However, similar to other proteins that serve as scaffold proteins between SG and P bodies [125, 128], or proteins that promote the movement of RNA from one structure to the other [125], some Sam68 containing granules were consistently in close contact with P bodies. The relevance of this finding and its relation with translational regulation will warrant future experiments.

The nuclear envelope as a limiting factor for Sam68 re-localization to SG during oxidative stress

Despite the fact that Sam68 possesses a NLS, it is found in the cytoplasm under various conditions, including poliovirus infection [270], ischemia [271], urate crystals treatment [273], HIV infection [333], sperm cell meiosis [262], mitosis [308], neuronal depolarization [264], signaling transduction [224], and in occasional cells in mouse tissue [227]. The finding that Sam68 can be rapidly accumulated in the cytoplasm during acute conditions such as depolarization and ischemia suggests a shuttling mechanism; however, classical heterokaryon assays have failed to detect any apparent nuclear-cytoplasmic shuttling of

Sam68 [248]. On the other hand, it is possible that Sam68 localization in the cytoplasm results from alteration in the nuclear importation machinery (poliovirus infection) [334], disruption of the nuclear membrane and nuclear protein leakage (meiosis, mitosis) [335], or a high concentration of sam68 binding proteins that prevents nuclear importation just after translation (T cells, adipocytes) [336, 337]. Furthermore, there are multiple nuclear RBP proteins that have been described to localize to SG upon oxidative stress. Some of them (TIA-1, HuR, FMRP) constantly shuttle between the nucleus and the cytoplasm with mRNA and are retained in the cytoplasm during SG assembly [127, 137, 338]; others (hnRNP A1) undergo post-translational modifications during stress, which regulate their export/import rates and SG localization [160]. The current study shows that oxidative stress significantly enhanced Sam68 recruitment into SG although only in a small percentage of the cells (Fig. 30 & 31), and deletion of its NLS directly induces SG in a majority of the cells (Fig. 31 & 45B). Therefore, it is conceivable that the nuclear envelope is a limiting factor for Sam68 recruitment to SG, while oxidative stress does not lead to Sam68 shuttling from the nucleus to cytoplasmic SG. Instead, it seems plausible that Sam68 recruitment to SG only occurs in cells that have Sam68 in the cytoplasm. One of the likely scenarios is possible variations on Sam68 localization in somatic cells during cell cycle progression, and this scenario deserves further investigation.

Role of the KH and RG rich domains in the process of Sam68 re-localization to SG

Several proteins are recruited to SG via RNA-binding KH or RG rich domains. Deletion of RG-rich sequences from proteins such as FMRP [327], Caprin 1 [147], G3BP [146], or RHAU [149] prevents their accumulation on SG; similarly, KH domains target PCBP2 [145], ZBP1 [138], or hMex 3B [150] proteins to SG. As mention before, Sam68 binds RNA through a single KH domain (aa171-211), and it also contains a heavily methylated P_3/RG-rich domain (aa269-321) that is involved in non-specific RNA binding [245], homotypic interactions [249], HIV replication inhibition [249, 267], and cellular localization [217]. Here, we demonstrated that deletion of each of these two domains abrogated Sam68 recruitment to SG (Fig. 31; Fig. 33; Fig. 45B); however, their deletion differentially altered the localization of Sam68 mutant proteins. Deletion of the P_3/RG-rich domain resulted in a diffuse cytoplasmic (Δ269) or nuclear (Δ269-321) localization, whereas deletion of the KH domain led to formation of insoluble protein aggregates that are different from SG (Fig. 31; Fig. 33 & 34). Therefore, our results and the fact that Δ410 selectively targets mRNA to free mRNP/monosomes fractions [267], further support our previous inference that cytoplasmic Sam68 binds to pre-initiation complexes through its KH domain, and that the P_3/RG-rich region promotes nucleation of SG through homo-heterotypic interactions (Fig. 46).

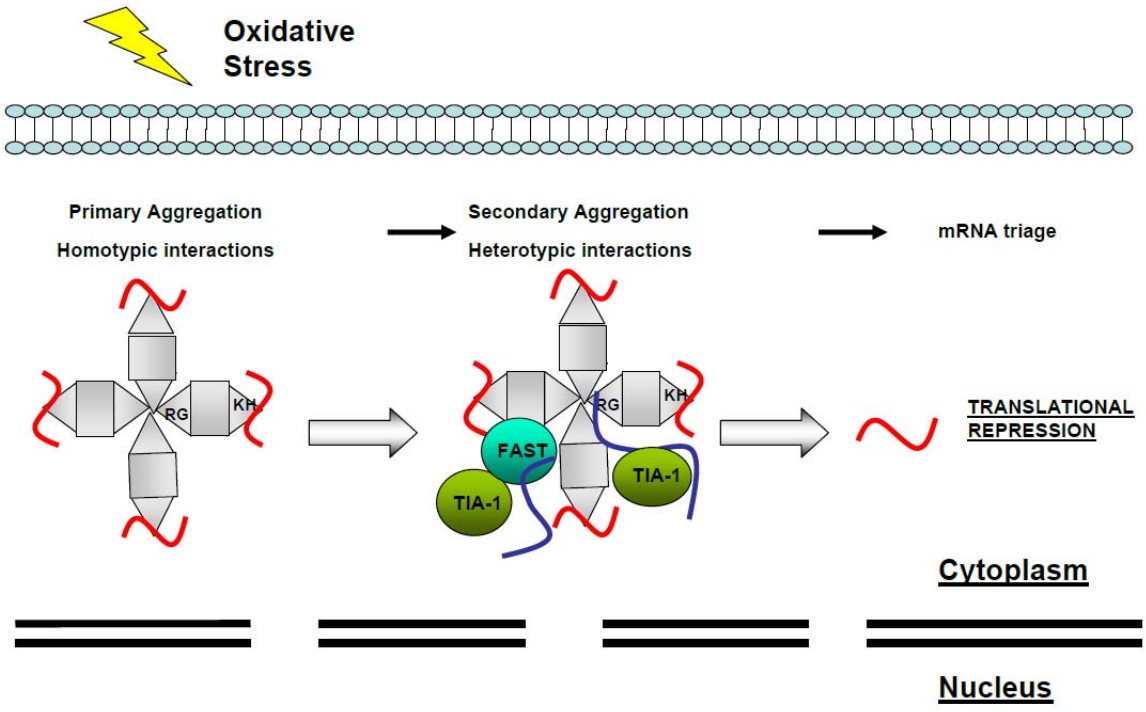

Figure 46. A working model for Sam68 recruitment to stress granules. 1. Large quantities of cytoplasmic Sam68-NLS mutants or endogenous Sam68 (gray) in the presence of oxidative stress initiate stress granule (SG) nucleation through homotypic interactions, mediated by the RG-rich domain located between aa269 and aa321. 2. The small Sam68 primary aggregates are then cross-linked and recruited to mature SG in a secondary aggregation process, mediated by direct or indirect heterotypic interactions between Sam68 and SG core components such as TIA-1 or FAST. 3. Sam68 binds to specific mRNAs (red- i.e. *nef* mRNA) through its KH domain in a sequence specific manner, which are then targeted to mature SG for translational repression.

Role of heterotypic protein interactions in Sam68 recruitment to SG

Recently, SG protein components have been classified into four categories: stalled initiation complexes (universal markers), RBP linked to translational regulation (reliable markers), RBP that regulate aspects of mRNA metabolism other than translation or decay, and proteins recruited to SG by core components through “piggy-back” interactions [124]. SRC3, KSRP, PMR1, and FAST are proteins recruited to SG through interactions with the SG core component TIA-1 [128, 144, 156, 162]. Interestingly, Sam68 directly interacts with FAST [274], and forms a unique RNP complex with KSRP and intron 6 of the β-tropomyosin gene [275]. Here, we showed that Sam68 was not a core component of SG, since its knockdown does not affect SG assembly (Fig. 35). In addition, using the bioinformatics and immunoprecipitation/Western blot analysis, we demonstrated that Sam68 bound to TIA-1 through its domain between aa269 and aa321 (Fig. 36 & 37; Fig. 45B), and that its deletion resulted in impaired co-localization with TIA-1 in SG (Fig. 37B). Therefore, it is plausible to speculate that when present in the cytoplasm, Sam68 is targeted to SG through its interaction with TIA (Fig. 46). However, whether this is a direct interaction, or mediated by RNA or FAST, remains to be determined. Importantly, TIA-1 may not be the only core component recruiting Sam68 to SG, as results showed a possible interaction with G3BP (Fig. 38), and as mentioned above, Simarro et al. reported a direct interaction with FAST [274]. Dissecting the relevance of each of these interactions should be the focus of future studies.

The STAR family: an emerging class of proteins targeted to cytoplasmic RNA granules

The extended family of STAR proteins is involved in multiple aspects of mRNA metabolism. Two best characterized members, GLD-1 and Quakin 6, are *bona fide* translational repressors and involved in sexual identity [282], tumor suppression [283], and cell differentiation [284]. GLD-1 is targeted to cytoplasmic particles that resemble P bodies and SG in *C. elegans* [269]. The mouse *qk* gene produces three major isoforms with different cellular localization. QK-5 is predominantly nuclear, while QK-6 and QK-7 are localized in the cytoplasm. Interestingly, over-expression of QKI-6 and QKI-7 but not QKI-5 leads to their localization in cytoplasmic foci similar to SG [339]. All of the above, in addition to the results reported here that Sam68 is a novel component of SG (Fig. 29 & 30), indicate that STAR family proteins, when present in the cytoplasm, can regulate mRNA translation through targeting mRNA to cytoplasmic granules. A number of RNA targets have been identified for Sam68, including poly (U), poly (A), A/U-rich sequences such as UAAA and UUUA, and several other cellular mRNA [190, 199, 200, 223, 340, 341]. Further characterization of Sam68 interaction with these RNAs, identification of additional cellular RNA targets, and elucidation of translational control of these RNA under oxidative stress will certainly add to our understanding of Sam68 biological functions, and their relation to RG localization.

Role of the ERK signaling pathway on eIF2α phosphorylation during oxidative stress

The biological targets of ARS are still unknown. However, it is thought that ARS interacts with cysteine-rich-redox-proteins such as glutathione and thioredoxin, to generate oxidative stress. One of the initial characteristic cellular responses to ARS exposure is the inhibition of protein synthesis by eIF2α phosphorylation, in an HRI kinase-mediated process [169]. Increased phosphorylation of eIF2α during stress is the result of a balance between the activity of the stress-induced eIF2α kinases [168], and the rate of eIF2α dephosphorylation by PP1-GADD34 phosphatase [342]. Importantly, the equilibrium of this reaction can be shifted by signaling pathways in a cell specific manner. For example, activation of the MEK/ERK pathway enhances eIF2α phosphorylation by GCN2 in liver cells [319]; whereas it inhibits JNK activity in alveolar macrophages, which leads to PP1 activation, eIF2α dephosphorylation, and protein synthesis [318]. During the present work, we showed that ARS treatment inactivates the MEK/ERK pathway in 293T cells (Fig. 40 & 41; Fig. 43A), and that its constitutive activation led to delayed phosphorylation kinetics of eIF2α (Fig. 42; Fig. 43B). Whether the decreased rates of eIF2α phosphorylation are the result of increased HRI activity, or PP1 activity is still to be determined. Moreover, the impact of these finding on cell survival or SG assembly should be further investigated in the future.

PERSPECTIVES

Since the introduction of HAART therapy in the 1990s, the face of the pandemic and the course of the HIV/AIDS disease have changed drastically. In contrast to the uniform fatality observed in the early eighties, HIV infection is now considered a chronic and manageable disease [109, 110]. Nevertheless, even though successful therapy can reduce viral replication to undetectable levels in plasma, it can not eradicate the virus from the body. Furthermore, active viral replication can continue undetected in lymphoid tissue of the gut, with progressive deleterious effects [112]. As our understanding of the HIV/AIDS pathogenesis increases, HIV-1 regulatory proteins Tat, Rev and Nef have come into the light as key determinants for disease progression. Tat is a critical viral factor for HIV-associated dementia [343], whereas Nef increases immune activation and promotes evasion of the immune system [88]. Importantly, there are no current therapies directed to either of these viral proteins. Therefore, host factors that regulate Tat, Rev or Nef expression or their biological functions are potential therapeutic targets for treatment of HIV-1 infection.

The consensus binding site for Sam68

In the current study, we have demonstrated that Sam68 NLS-deleted mutants are potent inhibitors of HIV-1 replication, and that Sam68 is absolutely required for efficient Rev-mediated nuclear exportation. Both findings have been independently validated [78, 244]. Therefore, Sam68 is an ideal antiretroviral

therapeutic target. However, its therapeutic potential will likely depend on a clear understanding of its biological functions. Consequently, defining Sam68 mRNA targets should be the initial step in this course of action. Previous reports have identified a number of mRNA targets for Sam68 [190, 199, 200, 223, 340, 341], however, no consensus RNA binding motif has been identified yet. The recently described cross-linking immunoprecipitation (CLIP) method may allow an elucidation of the target specificity of Sam68 *in vivo* [344]. In this procedure, Sam68 could be immunoprecipitated from previously UV cross-linked and RNase treated cell lysates, generating 40-60 nt cross-linked tags, which are then cloned and sequenced revealing a possible consensus RNA motif. Then, the presence of the consensus binding motif could be determined within the human and HIV-1 genomes using BLAST analysis. Subsequent experiments will address the role of Sam68 in the metabolism of the identified mRNA targets.

Sam68 function on Rev-mediated nuclear export

Rev exportation of intron-containing HIV-1 RNA is required for viral replication. Previous results in our laboratory have demonstrated that specific binding of Sam68 to Rev facilitates its nuclear exportation in a CRM-1-dependent manner [221, 243], and that its presence is absolutely required for this process to occur efficiently. However, the exact role of Sam68 in the Rev nuclear export pathway remains undetermined. The reasonable next step will be to determine if Sam68 is present in the nuclear exportation megacomplex Rev/RRE/CRM1/RanGTP/RCC1, using sub-cellular fractionation and sucrose

gradient centrifugation. In addition, our previous results suggest that Sam68 may promote the formation of this megacomplex; thus, similar experiments could be performed in cells depleted of Sam68, and the integrity of the complex can be evaluated in this context. Future work regarding other aspects of this process such as: Sam68-mediated RanGTP hydrolysis or targeting to the nuclear pore complex will likely follow the initial experiments.

Roles of Sam68 in HIV-1 replication in activated T cells.

HIV-1 requires activation of T cells for efficient viral replication [5]. Therefore, regulatory molecules of the TCR signaling pathway can have a great impact on disease progression. As previously mentioned, Sam68 interacts with and becomes phosphorylated by two major Src kinases that are activated upon T cell activation [224]. Furthermore, Sam68 has been shown to be tyrosine phosphorylated and recruited to signaling complexes in PBMC of HIV-1 infected individuals [333]. Therefore, It is reasonable to speculate that Sam68 might be required for proper T cell activation and consequently for HIV-1 replication. To determine the role of Sam68 on HIV-1 gene expression in activated T cells, future experiments should take advantage of our previously tested Sam68 siRNA to effectively knock down Sam68 in T cells, and of NL4-3.Luc(nef) reporter virus, in which Luc expression is insensitive to the absence of Sam68 in 293T cells. Hence, HIV-1 gene expression can be examined in activated T cells with normal and reduced Sam68 levels. In addition, HIV-1 LTR is potently transactivated in

activated T cells; thus, subsequent work can also address the relationship between Sam68, T cell activation and HIV-1 LTR activity.

Sam68-NLS mutants as a potential anti-HIV therapy

Nef is considered a major HIV-1 pathogenic factor; therefore, it is conceivable to speculate that suppression of Nef expression by Sam68-NLS mutants may be able to complement the current anti-HIV therapies that are mainly targeted at HIV-1 protease and reverse transcriptase, providing a better treatment outcome. To test this possibility, we could initially determine the efficacy of Sam68-NLS mutants to inhibit HIV-1 replication and Nef expression on an infected organism. Thus we could take advantage of the recently developed humanized mouse model, which recapitulates most of the immunological features observed in humans infected with HIV-1 [345]. Using a liposome based strategy; humanized mice infected with HIV-1 could be treated with DNA vectors expressing Sam68-NLS mutant Δ410, thus we would be able to evaluate the effective expression of Δ410 in lymphoid tissues and its effect on HIV-1 replication and immunodeficiency progression. Similar experiments could be performed on rhesus macaques infected with SIV. However, any Δ410-based anti-HIV therapy should be pursued only with the certainty that Δ410 expression results in minimal interference with endogenous Sam68 function.

Identification of host factors that differentially regulate the expression of Tat, Rev and Nef

Ribosomal movement to the initiation codon is abrogated in transcripts with long and structured 5'UTRs [289]; therefore, RNA helicases such as DHX29 or DDX3, are required to cooperatively unwind the cap-proximal region of those mRNAs, facilitating translation initiation [346, 347]. Interestingly, some of those cellular proteins are absolutely required for HIV-1 replication [77]. Furthermore, the *nef* mRNA 5'UTR is significantly longer and more structured than the rest of HIV-1 RNAs (Fig. 21), suggesting that efficient translation of *nef* mRNA might require additional host factors. Since Nef is a critical pathogenic determinant during HIV-1 infection, cellular proteins involved in *nef* mRNA translational could be potential therapeutic targets. Using our unique minigene system as an experimental model, subsequent experiments should address the role of RNA helicases involvement in efficient ribosomal scanning on Nef expression and HIV-1 replication.

miRNAs are small endogenous non-coding RNAs that post-transcriptionally repress gene expression by base-pairing with the 3'UTR of the target mRNA [348]. miRNAs dampen HIV-1 replication in activated T cells and contribute to viral latency in resting T lymphocytes [349, 350]. The extensive splicing during HIV-1 replication generates a myriad of mRNAs with significant sequence homology but with unique ORFs, 5'UTRs and 3'UTRs. Therefore, a specific RNA sequence that is present in the 3'UTR of *tat* mRNA might also be located in the

5'UTR of *nef* mRNA, suggesting that the host miRNA machinery might finely tune HIV-1 gene expression, adding an additional layer of complexity to the regulation of HIV-1 gene expression. This novel possibility should be addressed in future experiments, using the minigene system as an experimental model.

Characterization of different types of SG

The protein composition of SG varies during different stressful conditions, and this dictates the shape, biochemical properties, and the function of each type of SG. For instance, SG which contain G3BP are significantly larger than TIA-1 + SG; or SG induced by overexpression of some proteins (G3BP or Δ410) are significantly more resistant to CHX treatment than endogenous SG; and SG induced by overexpression of particular proteins specifically results in translational repression of target mRNAs. Consequently, understanding how proteins regulate SG function could shed some light into the biochemical mechanisms of SG-post-transcriptional gene expression regulation. To address this issue, we could initially characterize the response of SG composed of endogenous or overexpressed proteins to chemical compounds which are known to affect SG stability such as translational inhibitors, microtubule destabilizng agents, or transcritptional inhibitors. Importantly, using a similar approach, we could determine the role of specific proteins (i.e. TIA-1 or G3BP) on the assembly and stability of SG. These series of characterization experiments will be very informative for the SG field.

Roles of SG in HIV-1 replication

SG are now recognized as important cellular structures for viral reprogramming of the host translation machinery and cellular antiviral defense [124, 175]. Importantly, in a similar fashion as poliovirus, HIV-1 infection leads to a profound inhibition of cap dependent translation, due to proteolytic cleavage of eIF4G by HIV-1 PR [184], suggesting that at some stage during HIV-1 infection SG should be assembled. Hence, using a previously constructed expression vector for HIV-1 PR, an important next step will be to address in detail the effects of HIV-1 PR on the integrity of translational initiation factors, and its impact in SG assembly. Follow-up studies can then focus on SG assembly in the context of HIV-1 replication, and on the possibility that HIV-1 viral proteins inhibit SG formation by specifically targeting SG core components.

REFERENCES

1. *Report on the globals AIDS epidemic*. 2008 [cited; Available from: http://www.unaids.org/en/KnowledgeCentre/HIVData/GlobalReport/2008/2008_Global_report.asp.
2. *HIV/AIDS among african americans*. 2008 [cited; Available from: http://www.cdc.gov/hiv/topics/aa/resources/factsheets/pdf/aa.pdf
3. Hicks, C.B., C. Gay, and G. Ferrari, *Acute HIV infection: the impact of anti-retroviral treatment on cellular immune responses.* Clin Exp Immunol, 2007. **149**(2): p. 211-6.
4. Lyles, R.H., et al., *Natural history of human immunodeficiency virus type 1 viremia after seroconversion and proximal to AIDS in a large cohort of homosexual men. Multicenter AIDS Cohort Study.* J Infect Dis, 2000. **181**(3): p. 872-80.
5. Douek, D.C., L.J. Picker, and R.A. Koup, *T cell dynamics in HIV-1 infection.* Annu Rev Immunol, 2003. **21**: p. 265-304.
6. Douek, D.C., et al., *HIV preferentially infects HIV-specific CD4+ T cells.* Nature, 2002. **417**(6884): p. 95-8.
7. Guadalupe, M., et al., *Severe CD4+ T-cell depletion in gut lymphoid tissue during primary human immunodeficiency virus type 1 infection and substantial delay in restoration following highly active antiretroviral therapy.* J Virol, 2003. **77**(21): p. 11708-17.
8. Brenchley, J.M., et al., *CD4+ T cell depletion during all stages of HIV disease occurs predominantly in the gastrointestinal tract.* J Exp Med, 2004. **200**(6): p. 749-59.
9. Mehandru, S., et al., *Primary HIV-1 infection is associated with preferential depletion of CD4+ T lymphocytes from effector sites in the gastrointestinal tract.* J Exp Med, 2004. **200**(6): p. 761-70.
10. Leng, Q., et al., *Immune activation correlates better than HIV plasma viral load with CD4 T-cell decline during HIV infection.* J Acquir Immune Defic Syndr, 2001. **27**(4): p. 389-97.
11. Brenchley, J.M., et al., *Microbial translocation is a cause of systemic immune activation in chronic HIV infection.* Nat Med, 2006. **12**(12): p. 1365-71.
12. Pantaleo, G., C. Graziosi, and A.S. Fauci, *New concepts in the immunopathogenesis of human immunodeficiency virus infection.* N Engl J Med, 1993. **328**(5): p. 327-35.
13. He, J., et al., *Human immunodeficiency virus type 1 viral protein R (Vpr) arrests cells in the G2 phase of the cell cycle by inhibiting p34cdc2 activity.* J Virol, 1995. **69**(11): p. 6705-11.
14. Neil, S.J., T. Zang, and P.D. Bieniasz, *Tetherin inhibits retrovirus release and is antagonized by HIV-1 Vpu.* Nature, 2008. **451**(7177): p. 425-30.

15. Mariani, R., et al., *Species-specific exclusion of APOBEC3G from HIV-1 virions by Vif.* Cell, 2003. **114**(1): p. 21-31.
16. Frankel, A.D. and J.A. Young, *HIV-1: fifteen proteins and an RNA.* Annu Rev Biochem, 1998. **67**: p. 1-25.
17. Alkhatib, G., et al., *CC CKR5: a RANTES, MIP-1alpha, MIP-1beta receptor as a fusion cofactor for macrophage-tropic HIV-1.* Science, 1996. **272**(5270): p. 1955-8.
18. Feng, Y., et al., *HIV-1 entry cofactor: functional cDNA cloning of a seven-transmembrane, G protein-coupled receptor.* Science, 1996. **272**(5263): p. 872-7.
19. Gallo, S.A., et al., *The HIV Env-mediated fusion reaction.* Biochim Biophys Acta, 2003. **1614**(1): p. 36-50.
20. Laspia, M.F., A.P. Rice, and M.B. Mathews, *HIV-1 Tat protein increases transcriptional initiation and stabilizes elongation.* Cell, 1989. **59**(2): p. 283-92.
21. Berkhout, B., R.H. Silverman, and K.T. Jeang, *Tat trans-activates the human immunodeficiency virus through a nascent RNA target.* Cell, 1989. **59**(2): p. 273-82.
22. Malim, M.H., et al., *Functional dissection of the HIV-1 Rev trans-activator--derivation of a trans-dominant repressor of Rev function.* Cell, 1989. **58**(1): p. 205-14.
23. Malim, M.H., et al., *The HIV-1 rev trans-activator acts through a structured target sequence to activate nuclear export of unspliced viral mRNA.* Nature, 1989. **338**(6212): p. 254-7.
24. Harrich, D., et al., *Role of SP1-binding domains in in vivo transcriptional regulation of the human immunodeficiency virus type 1 long terminal repeat.* J Virol, 1989. **63**(6): p. 2585-91.
25. Perkins, N.D., et al., *Transcription factor AP-2 regulates human immunodeficiency virus type 1 gene expression.* J Virol, 1994. **68**(10): p. 6820-3.
26. Mallardo, M., et al., *An NF-kappaB site in the 5'-untranslated leader region of the human immunodeficiency virus type 1 enhances the viral expression in response to NF-kappaB-activating stimuli.* J Biol Chem, 1996. **271**(34): p. 20820-7.
27. Stevens, M., E. De Clercq, and J. Balzarini, *The regulation of HIV-1 transcription: molecular targets for chemotherapeutic intervention.* Med Res Rev, 2006. **26**(5): p. 595-625.
28. Stoltzfus, C.M. and J.M. Madsen, *Role of viral splicing elements and cellular RNA binding proteins in regulation of HIV-1 alternative RNA splicing.* Curr HIV Res, 2006. **4**(1): p. 43-55.
29. Neumann, M., et al., *Splicing variability in HIV type 1 revealed by quantitative RNA polymerase chain reaction.* AIDS Res Hum Retroviruses, 1994. **10**(11): p. 1531-42.

30. O'Reilly, M.M., M.T. McNally, and K.L. Beemon, *Two strong 5' splice sites and competing, suboptimal 3' splice sites involved in alternative splicing of human immunodeficiency virus type 1 RNA.* Virology, 1995. **213**(2): p. 373-85.
31. Del Gatto-Konczak, F., et al., *hnRNP A1 recruited to an exon in vivo can function as an exon splicing silencer.* Mol Cell Biol, 1999. **19**(1): p. 251-60.
32. Caputi, M., et al., *A bidirectional SF2/ASF- and SRp40-dependent splicing enhancer regulates human immunodeficiency virus type 1 rev, env, vpu, and nef gene expression.* J Virol, 2004. **78**(12): p. 6517-26.
33. Jacquenet, S., et al., *Dual effect of the SR proteins ASF/SF2, SC35 and 9G8 on HIV-1 RNA splicing and virion production.* Retrovirology, 2005. **2**: p. 33.
34. Geballe, A.P. and M.K. Gray, *Variable inhibition of cell-free translation by HIV-1 transcript leader sequences.* Nucleic Acids Res, 1992. **20**(16): p. 4291-7.
35. Miele, G., et al., *The human immunodeficiency virus type 1 5' packaging signal structure affects translation but does not function as an internal ribosome entry site structure.* J Virol, 1996. **70**(2): p. 944-51.
36. Parkin, N.T., et al., *Mutational analysis of the 5' non-coding region of human immunodeficiency virus type 1: effects of secondary structure on translation.* EMBO J, 1988. **7**(9): p. 2831-7.
37. Berkhout, B., *Structure and function of the human immunodeficiency virus leader RNA.* Prog Nucleic Acid Res Mol Biol, 1996. **54**: p. 1-34.
38. Yilmaz, A., C. Bolinger, and K. Boris-Lawrie, *Retrovirus translation initiation: Issues and hypotheses derived from study of HIV-1.* Curr HIV Res, 2006. **4**(2): p. 131-9.
39. Buck, C.B., et al., *The human immunodeficiency virus type 1 gag gene encodes an internal ribosome entry site.* J Virol, 2001. **75**(1): p. 181-91.
40. Brasey, A., et al., *The leader of human immunodeficiency virus type 1 genomic RNA harbors an internal ribosome entry segment that is active during the G2/M phase of the cell cycle.* J Virol, 2003. **77**(7): p. 3939-49.
41. Anderson, E.C. and A.M. Lever, *Human immunodeficiency virus type 1 Gag polyprotein modulates its own translation.* J Virol, 2006. **80**(21): p. 10478-86.
42. Svitkin, Y.V., A. Pause, and N. Sonenberg, *La autoantigen alleviates translational repression by the 5' leader sequence of the human immunodeficiency virus type 1 mRNA.* J Virol, 1994. **68**(11): p. 7001-7.
43. Mancebo, H.S., et al., *P-TEFb kinase is required for HIV Tat transcriptional activation in vivo and in vitro.* Genes Dev, 1997. **11**(20): p. 2633-44.
44. Zhu, Y., et al., *Transcription elongation factor P-TEFb is required for HIV-1 tat transactivation in vitro.* Genes Dev, 1997. **11**(20): p. 2622-32.
45. Spina, C.A., H.E. Prince, and D.D. Richman, *Preferential replication of HIV-1 in the CD45RO memory cell subset of primary CD4 lymphocytes in vitro.* J Clin Invest, 1997. **99**(7): p. 1774-85.

46. Garriga, J., et al., *Upregulation of cyclin T1/CDK9 complexes during T cell activation.* Oncogene, 1998. **17**(24): p. 3093-102.
47. Flores, O., et al., *Host-cell positive transcription elongation factor b kinase activity is essential and limiting for HIV type 1 replication.* Proc Natl Acad Sci U S A, 1999. **96**(13): p. 7208-13.
48. Zenklusen, D. and F. Stutz, *Nuclear export of mRNA.* FEBS Lett, 2001. **498**(2-3): p. 150-6.
49. Purcell, D.F. and M.A. Martin, *Alternative splicing of human immunodeficiency virus type 1 mRNA modulates viral protein expression, replication, and infectivity.* J Virol, 1993. **67**(11): p. 6365-78.
50. Schwartz, S., et al., *Cloning and functional analysis of multiply spliced mRNA species of human immunodeficiency virus type 1.* J Virol, 1990. **64**(6): p. 2519-29.
51. Cochrane, A.W., et al., *Purification of biologically active human immunodeficiency virus rev protein from Escherichia coli.* Virology, 1989. **173**(1): p. 335-7.
52. Cochrane, A.W., C.H. Chen, and C.A. Rosen, *Specific interaction of the human immunodeficiency virus Rev protein with a structured region in the env mRNA.* Proc Natl Acad Sci U S A, 1990. **87**(3): p. 1198-202.
53. Meyer, B.E. and M.H. Malim, *The HIV-1 Rev trans-activator shuttles between the nucleus and the cytoplasm.* Genes Dev, 1994. **8**(13): p. 1538-47.
54. Hope, T.J., et al., *Steroid-receptor fusion of the human immunodeficiency virus type 1 Rev transactivator: mapping cryptic functions of the arginine-rich motif.* Proc Natl Acad Sci U S A, 1990. **87**(19): p. 7787-91.
55. Fischer, U., et al., *The HIV-1 Rev activation domain is a nuclear export signal that accesses an export pathway used by specific cellular RNAs.* Cell, 1995. **82**(3): p. 475-83.
56. Hope, T.J., et al., *Mutational analysis of the human immunodeficiency virus type 1 Rev transactivator: essential residues near the amino terminus.* J Virol, 1990. **64**(11): p. 5360-6.
57. Hope, T.J., et al., *trans-dominant inhibition of human immunodeficiency virus type 1 Rev occurs through formation of inactive protein complexes.* J Virol, 1992. **66**(4): p. 1849-55.
58. Zapp, M.L., et al., *Oligomerization and RNA binding domains of the type 1 human immunodeficiency virus Rev protein: a dual function for an arginine-rich binding motif.* Proc Natl Acad Sci U S A, 1991. **88**(17): p. 7734-8.
59. Ernst, R.K., et al., *A structured retroviral RNA element that mediates nucleocytoplasmic export of intron-containing RNA.* Mol Cell Biol, 1997. **17**(1): p. 135-44.
60. Nasioulas, G., et al., *Production of avian leukosis virus particles in mammalian cells can be mediated by the interaction of the human immunodeficiency virus protein Rev and the Rev-responsive element.* Proc Natl Acad Sci U S A, 1995. **92**(25): p. 11940-4.

61. Watanabe, S., et al., *Human GM-CSF induces HIV-1 LTR by multiple signalling pathways.* Biochimie, 2002. **84**(7): p. 633-42.
62. Henderson, B.R. and P. Percipalle, *Interactions between HIV Rev and nuclear import and export factors: the Rev nuclear localisation signal mediates specific binding to human importin-beta.* J Mol Biol, 1997. **274**(5): p. 693-707.
63. Palmeri, D. and M.H. Malim, *Importin beta can mediate the nuclear import of an arginine-rich nuclear localization signal in the absence of importin alpha.* Mol Cell Biol, 1999. **19**(2): p. 1218-25.
64. Adachi, Y. and M. Yanagida, *Higher order chromosome structure is affected by cold-sensitive mutations in a Schizosaccharomyces pombe gene crm1+ which encodes a 115-kD protein preferentially localized in the nucleus and its periphery.* J Cell Biol, 1989. **108**(4): p. 1195-207.
65. Fornerod, M., et al., *The human homologue of yeast CRM1 is in a dynamic subcomplex with CAN/Nup214 and a novel nuclear pore component Nup88.* EMBO J, 1997. **16**(4): p. 807-16.
66. Fukuda, M., et al., *CRM1 is responsible for intracellular transport mediated by the nuclear export signal.* Nature, 1997. **390**(6657): p. 308-11.
67. Ossareh-Nazari, B., F. Bachelerie, and C. Dargemont, *Evidence for a role of CRM1 in signal-mediated nuclear protein export.* Science, 1997. **278**(5335): p. 141-4.
68. Stade, K., et al., *Exportin 1 (Crm1p) is an essential nuclear export factor.* Cell, 1997. **90**(6): p. 1041-50.
69. Askjaer, P., et al., *The specificity of the CRM1-Rev nuclear export signal interaction is mediated by RanGTP.* J Biol Chem, 1998. **273**(50): p. 33414-22.
70. Wolff, B., J.J. Sanglier, and Y. Wang, *Leptomycin B is an inhibitor of nuclear export: inhibition of nucleo-cytoplasmic translocation of the human immunodeficiency virus type 1 (HIV-1) Rev protein and Rev-dependent mRNA.* Chem Biol, 1997. **4**(2): p. 139-47.
71. Gorlich, D., *Nuclear protein import.* Curr Opin Cell Biol, 1997. **9**(3): p. 412-9.
72. Izaurralde, E., et al., *The asymmetric distribution of the constituents of the Ran system is essential for transport into and out of the nucleus.* EMBO J, 1997. **16**(21): p. 6535-47.
73. Ruhl, M., et al., *Eukaryotic initiation factor 5A is a cellular target of the human immunodeficiency virus type 1 Rev activation domain mediating trans-activation.* J Cell Biol, 1993. **123**(6 Pt 1): p. 1309-20.
74. Fritz, C.C., M.L. Zapp, and M.R. Green, *A human nucleoporin-like protein that specifically interacts with HIV Rev.* Nature, 1995. **376**(6540): p. 530-3.
75. Sanchez-Velar, N., et al., *hRIP, a cellular cofactor for Rev function, promotes release of HIV RNAs from the perinuclear region.* Genes Dev, 2004. **18**(1): p. 23-34.
76. Yu, Z., et al., *The cellular HIV-1 Rev cofactor hRIP is required for viral replication.* Proc Natl Acad Sci U S A, 2005. **102**(11): p. 4027-32.

77. Yedavalli, V.S., et al., *Requirement of DDX3 DEAD box RNA helicase for HIV-1 Rev-RRE export function.* Cell, 2004. **119**(3): p. 381-92.
78. Reddy, T.R., et al., *Inhibition of HIV replication by dominant negative mutants of Sam68, a functional homolog of HIV-1 Rev.* Nat Med, 1999. **5**(6): p. 635-42.
79. Bevec, D., et al., *Inhibition of HIV-1 replication in lymphocytes by mutants of the Rev cofactor eIF-5A.* Science, 1996. **271**(5257): p. 1858-60.
80. Schatz, O., et al., *Interaction of the HIV-1 rev cofactor eukaryotic initiation factor 5A with ribosomal protein L5.* Proc Natl Acad Sci U S A, 1998. **95**(4): p. 1607-12.
81. Arold, S.T. and A.S. Baur, *Dynamic Nef and Nef dynamics: how structure could explain the complex activities of this small HIV protein.* Trends Biochem Sci, 2001. **26**(6): p. 356-63.
82. Arold, S., et al., *RT loop flexibility enhances the specificity of Src family SH3 domains for HIV-1 Nef.* Biochemistry, 1998. **37**(42): p. 14683-91.
83. Dutartre, H., et al., *The human immunodeficiency virus type 1 Nef protein binds the Src-related tyrosine kinase Lck SH2 domain through a novel phosphotyrosine independent mechanism.* Virology, 1998. **247**(2): p. 200-11.
84. Lee, C.H., et al., *A single amino acid in the SH3 domain of Hck determines its high affinity and specificity in binding to HIV-1 Nef protein.* EMBO J, 1995. **14**(20): p. 5006-15.
85. Saksela, K., G. Cheng, and D. Baltimore, *Proline-rich (PxxP) motifs in HIV-1 Nef bind to SH3 domains of a subset of Src kinases and are required for the enhanced growth of Nef+ viruses but not for down-regulation of CD4.* EMBO J, 1995. **14**(3): p. 484-91.
86. Sawai, E.T., et al., *A conserved domain and membrane targeting of Nef from HIV and SIV are required for association with a cellular serine kinase activity.* J Biol Chem, 1995. **270**(25): p. 15307-14.
87. Baugh, L.L., J.V. Garcia, and J.L. Foster, *Functional characterization of the human immunodeficiency virus type 1 Nef acidic domain.* J Virol, 2008. **82**(19): p. 9657-67.
88. Foster, J.L. and J.V. Garcia, *Role of Nef in HIV-1 replication and pathogenesis.* Adv Pharmacol, 2007. **55**: p. 389-409.
89. Kestler, H.W., 3rd, et al., *Importance of the nef gene for maintenance of high virus loads and for development of AIDS.* Cell, 1991. **65**(4): p. 651-62.
90. Deacon, N.J., et al., *Genomic structure of an attenuated quasi species of HIV-1 from a blood transfusion donor and recipients.* Science, 1995. **270**(5238): p. 988-91.
91. Kirchhoff, F., et al., *Brief report: absence of intact nef sequences in a long-term survivor with nonprogressive HIV-1 infection.* N Engl J Med, 1995. **332**(4): p. 228-32.
92. Salvi, R., et al., *Grossly defective nef gene sequences in a human immunodeficiency virus type 1-seropositive long-term nonprogressor.* J Virol, 1998. **72**(5): p. 3646-57.

93. Aiken, C., et al., *Mutational analysis of HIV-1 Nef: identification of two mutants that are temperature-sensitive for CD4 downregulation.* Virology, 1996. **217**(1): p. 293-300.
94. Garcia, J.V. and A.D. Miller, *Serine phosphorylation-independent downregulation of cell-surface CD4 by nef.* Nature, 1991. **350**(6318): p. 508-11.
95. Anderson, S.J., et al., *The cytoplasmic domain of CD4 is sufficient for its down-regulation from the cell surface by human immunodeficiency virus type 1 Nef.* J Virol, 1994. **68**(5): p. 3092-101.
96. Schwartz, O., et al., *Endocytosis of major histocompatibility complex class I molecules is induced by the HIV-1 Nef protein.* Nat Med, 1996. **2**(3): p. 338-42.
97. Williams, M., et al., *Human immunodeficiency virus type 1 Nef domains required for disruption of major histocompatibility complex class I trafficking are also necessary for coprecipitation of Nef with HLA-A2.* J Virol, 2005. **79**(1): p. 632-6.
98. Arora, V.K., et al., *Lentivirus Nef specifically activates Pak2.* J Virol, 2000. **74**(23): p. 11081-7.
99. Renkema, G.H. and K. Saksela, *Interactions of HIV-1 NEF with cellular signal transducing proteins.* Front Biosci, 2000. **5**: p. D268-83.
100. Wei, B.L., et al., *Activation of p21-activated kinase 2 by human immunodeficiency virus type 1 Nef induces merlin phosphorylation.* J Virol, 2005. **79**(23): p. 14976-80.
101. Chowers, M.Y., et al., *Optimal infectivity in vitro of human immunodeficiency virus type 1 requires an intact nef gene.* J Virol, 1994. **68**(5): p. 2906-14.
102. Schindler, M., et al., *Nef-mediated suppression of T cell activation was lost in a lentiviral lineage that gave rise to HIV-1.* Cell, 2006. **125**(6): p. 1055-67.
103. Fauci, A.S., et al., *HIV vaccine research: the way forward.* Science, 2008. **321**(5888): p. 530-2.
104. Pitisuttithum, P., et al., *Randomized, double-blind, placebo-controlled efficacy trial of a bivalent recombinant glycoprotein 120 HIV-1 vaccine among injection drug users in Bangkok, Thailand.* J Infect Dis, 2006. **194**(12): p. 1661-71.
105. Flynn, N.M., et al., *Placebo-controlled phase 3 trial of a recombinant glycoprotein 120 vaccine to prevent HIV-1 infection.* J Infect Dis, 2005. **191**(5): p. 654-65.
106. Derdeyn, C.A., et al., *Envelope-constrained neutralization-sensitive HIV-1 after heterosexual transmission.* Science, 2004. **303**(5666): p. 2019-22.
107. Steinbrook, R., *One step forward, two steps back--will there ever be an AIDS vaccine?* N Engl J Med, 2007. **357**(26): p. 2653-5.
108. Boasso, A., G.M. Shearer, and M. Clerici, *The hunt for an HIV vaccine: time to rethink recent failures.* Lancet, 2008. **371**(9628): p. 1897-8.

109. Hammer, S.M., et al., *Antiretroviral treatment of adult HIV infection: 2008 recommendations of the International AIDS Society-USA panel.* JAMA, 2008. **300**(5): p. 555-70.
110. Ho, D.D. and P.D. Bieniasz, *HIV-1 at 25.* Cell, 2008. **133**(4): p. 561-5.
111. Simon, V., D.D. Ho, and Q. Abdool Karim, *HIV/AIDS epidemiology, pathogenesis, prevention, and treatment.* Lancet, 2006. **368**(9534): p. 489-504.
112. Chun, T.W., et al., *Persistence of HIV in gut-associated lymphoid tissue despite long-term antiretroviral therapy.* J Infect Dis, 2008. **197**(5): p. 714-20.
113. Fischer, M., et al., *Cellular viral rebound after cessation of potent antiretroviral therapy predicted by levels of multiply spliced HIV-1 RNA encoding nef.* J Infect Dis, 2004. **190**(11): p. 1979-88.
114. Ainger, K., et al., *Transport and localization of exogenous myelin basic protein mRNA microinjected into oligodendrocytes.* J Cell Biol, 1993. **123**(2): p. 431-41.
115. Kiebler, M.A. and G.J. Bassell, *Neuronal RNA granules: movers and makers.* Neuron, 2006. **51**(6): p. 685-90.
116. Anderson, P. and N. Kedersha, *RNA granules.* J Cell Biol, 2006. **172**(6): p. 803-8.
117. Sossin, W.S. and L. DesGroseillers, *Intracellular trafficking of RNA in neurons.* Traffic, 2006. **7**(12): p. 1581-9.
118. Kedersha, N. and P. Anderson, *Mammalian stress granules and processing bodies.* Methods Enzymol, 2007. **431**: p. 61-81.
119. Parker, R. and U. Sheth, *P bodies and the control of mRNA translation and degradation.* Mol Cell, 2007. **25**(5): p. 635-46.
120. Gaillard, H. and A. Aguilera, *A Novel Class of mRNA Containing Cytoplasmic Granules Are Produced in Response to UV-Irradiation.* Mol Biol Cell, 2008.
121. Nover, L., *125 years of experimental heat shock research: historical roots of a discipline.* Genome, 1989. **31**(2): p. 668-70.
122. Kedersha, N.L., et al., *RNA-binding proteins TIA-1 and TIAR link the phosphorylation of eIF-2 alpha to the assembly of mammalian stress granules.* J Cell Biol, 1999. **147**(7): p. 1431-42.
123. Anderson, P. and N. Kedersha, *Stressful initiations.* J Cell Sci, 2002. **115**(Pt 16): p. 3227-34.
124. Anderson, P. and N. Kedersha, *Stress granules: the Tao of RNA triage.* Trends Biochem Sci, 2008. **33**(3): p. 141-50.
125. Kedersha, N., et al., *Stress granules and processing bodies are dynamically linked sites of mRNP remodeling.* J Cell Biol, 2005. **169**(6): p. 871-84.
126. Wilczynska, A., et al., *The translational regulator CPEB1 provides a link between dcp1 bodies and stress granules.* J Cell Sci, 2005. **118**(Pt 5): p. 981-92.

127. Kedersha, N., et al., *Dynamic shuttling of TIA-1 accompanies the recruitment of mRNA to mammalian stress granules.* J Cell Biol, 2000. **151**(6): p. 1257-68.
128. Li, W., et al., *FAST is a survival protein that senses mitochondrial stress and modulates TIA-1-regulated changes in protein expression.* Mol Cell Biol, 2004. **24**(24): p. 10718-32.
129. Kim, W.J., et al., *Sequestration of TRAF2 into stress granules interrupts tumor necrosis factor signaling under stress conditions.* Mol Cell Biol, 2005. **25**(6): p. 2450-62.
130. Arimoto, K., et al., *Formation of stress granules inhibits apoptosis by suppressing stress-responsive MAPK pathways.* Nat Cell Biol, 2008. **10**(11): p. 1324-32.
131. Eisinger-Mathason, T.S., et al., *Codependent functions of RSK2 and the apoptosis-promoting factor TIA-1 in stress granule assembly and cell survival.* Mol Cell, 2008. **31**(5): p. 722-36.
132. Leung, A.K., J.M. Calabrese, and P.A. Sharp, *Quantitative analysis of Argonaute protein reveals microRNA-dependent localization to stress granules.* Proc Natl Acad Sci U S A, 2006. **103**(48): p. 18125-30.
133. Leung, A.K. and P.A. Sharp, *microRNAs: a safeguard against turmoil?* Cell, 2007. **130**(4): p. 581-5.
134. Kedersha, N., et al., *Evidence that ternary complex (eIF2-GTP-tRNA(i)(Met))-deficient preinitiation complexes are core constituents of mammalian stress granules.* Mol Biol Cell, 2002. **13**(1): p. 195-210.
135. Kimball, S.R., et al., *Mammalian stress granules represent sites of accumulation of stalled translation initiation complexes.* Am J Physiol Cell Physiol, 2003. **284**(2): p. C273-84.
136. Tsai, N.P., P.C. Ho, and L.N. Wei, *Regulation of stress granule dynamics by Grb7 and FAK signalling pathway.* EMBO J, 2008. **27**(5): p. 715-26.
137. Kim, S.H., et al., *Fragile X mental retardation protein shifts between polyribosomes and stress granules after neuronal injury by arsenite stress or in vivo hippocampal electrode insertion.* J Neurosci, 2006. **26**(9): p. 2413-8.
138. Stohr, N., et al., *ZBP1 regulates mRNA stability during cellular stress.* J Cell Biol, 2006. **175**(4): p. 527-34.
139. Vessey, J.P., et al., *Dendritic localization of the translational repressor Pumilio 2 and its contribution to dendritic stress granules.* J Neurosci, 2006. **26**(24): p. 6496-508.
140. Baez, M.V. and G.L. Boccaccio, *Mammalian Smaug is a translational repressor that forms cytoplasmic foci similar to stress granules.* J Biol Chem, 2005. **280**(52): p. 43131-40.
141. Thomas, M.G., et al., *Staufen recruitment into stress granules does not affect early mRNA transport in oligodendrocytes.* Mol Biol Cell, 2005. **16**(1): p. 405-20.
142. Kawahara, H., et al., *Neural RNA-binding protein Musashi1 inhibits translation initiation by competing with eIF4G for PABP.* J Cell Biol, 2008. **181**(4): p. 639-53.

143. Lai, M.C., Y.H. Lee, and W.Y. Tarn, *The DEAD-box RNA helicase DDX3 associates with export messenger ribonucleoproteins as well as tip-associated protein and participates in translational control.* Mol Biol Cell, 2008. **19**(9): p. 3847-58.
144. Yang, F., et al., *Polysome-bound endonuclease PMR1 is targeted to stress granules via stress-specific binding to TIA-1.* Mol Cell Biol, 2006. **26**(23): p. 8803-13.
145. Fujimura, K., F. Kano, and M. Murata, *Identification of PCBP2, a facilitator of IRES-mediated translation, as a novel constituent of stress granules and processing bodies.* RNA, 2008. **14**(3): p. 425-31.
146. Tourriere, H., et al., *The RasGAP-associated endoribonuclease G3BP assembles stress granules.* J Cell Biol, 2003. **160**(6): p. 823-31.
147. Solomon, S., et al., *Distinct structural features of caprin-1 mediate its interaction with G3BP-1 and its induction of phosphorylation of eukaryotic translation initiation factor 2alpha, entry to cytoplasmic stress granules, and selective interaction with a subset of mRNAs.* Mol Cell Biol, 2007. **27**(6): p. 2324-42.
148. Kim, J.E., et al., *Proline-rich transcript in brain protein induces stress granule formation.* Mol Cell Biol, 2008. **28**(2): p. 803-13.
149. Chalupnikova, K., et al., *Recruitment of the RNA Helicase RHAU to Stress Granules via a Unique RNA-binding Domain.* J Biol Chem, 2008. **283**(50): p. 35186-98.
150. Courchet, J., et al., *Interaction with 14-3-3 adaptors regulates the sorting of hMex-3B RNA-binding protein to distinct classes of RNA granules.* J Biol Chem, 2008. **283**(46): p. 32131-42.
151. Goulet, I., et al., *TDRD3, a novel Tudor domain-containing protein, localizes to cytoplasmic stress granules.* Hum Mol Genet, 2008. **17**(19): p. 3055-74.
152. Hua, Y. and J. Zhou, *Survival motor neuron protein facilitates assembly of stress granules.* FEBS Lett, 2004. **572**(1-3): p. 69-74.
153. Goodier, J.L., et al., *LINE-1 ORF1 protein localizes in stress granules with other RNA-binding proteins, including components of RNA interference RNA-induced silencing complex.* Mol Cell Biol, 2007. **27**(18): p. 6469-83.
154. Baguet, A., et al., *The exon-junction-complex-component metastatic lymph node 51 functions in stress-granule assembly.* J Cell Sci, 2007. **120**(Pt 16): p. 2774-84.
155. Balzer, E. and E.G. Moss, *Localization of the developmental timing regulator Lin28 to mRNP complexes, P-bodies and stress granules.* RNA Biol, 2007. **4**(1): p. 16-25.
156. Yu, C., et al., *An essential function of the SRC-3 coactivator in suppression of cytokine mRNA translation and inflammatory response.* Mol Cell, 2007. **25**(5): p. 765-78.
157. Kozak, S.L., et al., *The anti-HIV-1 editing enzyme APOBEC3G binds HIV-1 RNA and messenger RNAs that shuttle between polysomes and stress granules.* J Biol Chem, 2006. **281**(39): p. 29105-19.

158. Brehm, M.A., et al., *Intracellular localization of human Ins(1,3,4,5,6)P5 2-kinase.* Biochem J, 2007. **408**(3): p. 335-45.
159. Katahira, J., et al., *Nuclear RNA export factor 7 is localized in processing bodies and neuronal RNA granules through interactions with shuttling hnRNPs.* Nucleic Acids Res, 2008. **36**(2): p. 616-28.
160. Guil, S., J.C. Long, and J.F. Caceres, *hnRNP A1 relocalization to the stress granules reflects a role in the stress response.* Mol Cell Biol, 2006. **26**(15): p. 5744-58.
161. Hofmann, I., et al., *Identification of the junctional plaque protein plakophilin 3 in cytoplasmic particles containing RNA-binding proteins and the recruitment of plakophilins 1 and 3 to stress granules.* Mol Biol Cell, 2006. **17**(3): p. 1388-98.
162. Rothe, F., et al., *Identification of FUSE-binding proteins as interacting partners of TIA proteins.* Biochem Biophys Res Commun, 2006. **343**(1): p. 57-68.
163. Ogawa, F., M. Kasai, and T. Akiyama, *A functional link between Disrupted-In-Schizophrenia 1 and the eukaryotic translation initiation factor 3.* Biochem Biophys Res Commun, 2005. **338**(2): p. 771-6.
164. Mazroui, R., et al., *Inhibition of the ubiquitin-proteasome system induces stress granule formation.* Mol Biol Cell, 2007. **18**(7): p. 2603-18.
165. DeGracia, D.J. and B.R. Hu, *Irreversible translation arrest in the reperfused brain.* J Cereb Blood Flow Metab, 2007. **27**(5): p. 875-93.
166. Dang, Y., et al., *Eukaryotic initiation factor 2alpha-independent pathway of stress granule induction by the natural product pateamine A.* J Biol Chem, 2006. **281**(43): p. 32870-8.
167. Mazroui, R., et al., *Inhibition of ribosome recruitment induces stress granule formation independently of eukaryotic initiation factor 2alpha phosphorylation.* Mol Biol Cell, 2006. **17**(10): p. 4212-9.
168. Wek, R.C., H.Y. Jiang, and T.G. Anthony, *Coping with stress: eIF2 kinases and translational control.* Biochem Soc Trans, 2006. **34**(Pt 1): p. 7-11.
169. McEwen, E., et al., *Heme-regulated inhibitor kinase-mediated phosphorylation of eukaryotic translation initiation factor 2 inhibits translation, induces stress granule formation, and mediates survival upon arsenite exposure.* J Biol Chem, 2005. **280**(17): p. 16925-33.
170. Smith, J.A., et al., *Reovirus induces and benefits from an integrated cellular stress response.* J Virol, 2006. **80**(4): p. 2019-33.
171. Gingras, A.C., B. Raught, and N. Sonenberg, *eIF4 initiation factors: effectors of mRNA recruitment to ribosomes and regulators of translation.* Annu Rev Biochem, 1999. **68**: p. 913-63.
172. Bordeleau, M.E., et al., *Stimulation of mammalian translation initiation factor eIF4A activity by a small molecule inhibitor of eukaryotic translation.* Proc Natl Acad Sci U S A, 2005. **102**(30): p. 10460-5.
173. Kedersha, N. and P. Anderson, *Stress granules: sites of mRNA triage that regulate mRNA stability and translatability.* Biochem Soc Trans, 2002. **30**(Pt 6): p. 963-9.

174. Mollet, S., et al., *Translationally repressed mRNA transiently cycles through stress granules during stress.* Mol Biol Cell, 2008. **19**(10): p. 4469-79.
175. Beckham, C.J. and R. Parker, *P bodies, stress granules, and viral life cycles.* Cell Host Microbe, 2008. **3**(4): p. 206-12.
176. Li, W., et al., *Cell proteins TIA-1 and TIAR interact with the 3' stem-loop of the West Nile virus complementary minus-strand RNA and facilitate virus replication.* J Virol, 2002. **76**(23): p. 11989-2000.
177. White, J.P., et al., *Inhibition of cytoplasmic mRNA stress granule formation by a viral proteinase.* Cell Host Microbe, 2007. **2**(5): p. 295-305.
178. Emara, M.M. and M.A. Brinton, *Interaction of TIA-1/TIAR with West Nile and dengue virus products in infected cells interferes with stress granule formation and processing body assembly.* Proc Natl Acad Sci U S A, 2007. **104**(21): p. 9041-6.
179. McInerney, G.M., et al., *Importance of eIF2alpha phosphorylation and stress granule assembly in alphavirus translation regulation.* Mol Biol Cell, 2005. **16**(8): p. 3753-63.
180. Montero, H., et al., *Rotavirus infection induces the phosphorylation of eIF2alpha but prevents the formation of stress granules.* J Virol, 2008. **82**(3): p. 1496-504.
181. Raaben, M., et al., *Mouse hepatitis coronavirus replication induces host translational shutoff and mRNA decay, with concomitant formation of stress granules and processing bodies.* Cell Microbiol, 2007. **9**(9): p. 2218-29.
182. Chiu, Y.L. and W.C. Greene, *The APOBEC3 cytidine deaminases: an innate defensive network opposing exogenous retroviruses and endogenous retroelements.* Annu Rev Immunol, 2008. **26**: p. 317-53.
183. Marin, M., et al., *Human immunodeficiency virus type 1 Vif functionally interacts with diverse APOBEC3 cytidine deaminases and moves with them between cytoplasmic sites of mRNA metabolism.* J Virol, 2008. **82**(2): p. 987-98.
184. Ventoso, I., et al., *HIV-1 protease cleaves eukaryotic initiation factor 4G and inhibits cap-dependent translation.* Proc Natl Acad Sci U S A, 2001. **98**(23): p. 12966-71.
185. Ellis, C., et al., *Phosphorylation of GAP and GAP-associated proteins by transforming and mitogenic tyrosine kinases.* Nature, 1990. **343**(6256): p. 377-81.
186. Moran, M.F., et al., *Src homology region 2 domains direct protein-protein interactions in signal transduction.* Proc Natl Acad Sci U S A, 1990. **87**(21): p. 8622-6.
187. Wong, G., et al., *Molecular cloning and nucleic acid binding properties of the GAP-associated tyrosine phosphoprotein p62.* Cell, 1992. **69**(3): p. 551-8.
188. Fumagalli, S., et al., *A target for Src in mitosis.* Nature, 1994. **368**(6474): p. 871-4.

189. Richard, S., et al., *Association of p62, a multifunctional SH2- and SH3-domain-binding protein, with src family tyrosine kinases, Grb2, and phospholipase C gamma-1.* Mol Cell Biol, 1995. **15**(1): p. 186-97.
190. Taylor, S.J. and D. Shalloway, *An RNA-binding protein associated with Src through its SH2 and SH3 domains in mitosis.* Nature, 1994. **368**(6474): p. 867-71.
191. Vogel, L.B. and D.J. Fujita, *p70 phosphorylation and binding to p56lck is an early event in interleukin-2-induced onset of cell cycle progression in T-lymphocytes.* J Biol Chem, 1995. **270**(6): p. 2506-11.
192. Weng, Z., et al., *Identification of Src, Fyn, and Lyn SH3-binding proteins: implications for a function of SH3 domains.* Mol Cell Biol, 1994. **14**(7): p. 4509-21.
193. Di Fruscio, M., et al., *The identification of two Drosophila K homology domain proteins. Kep1 and SAM are members of the Sam68 family of GSG domain proteins.* J Biol Chem, 1998. **273**(46): p. 30122-30.
194. Fung, E.T., et al., *Identification of a Torpedo homolog of Sam68 that interacts with the synapse organizing protein rapsyn.* FEBS Lett, 1998. **437**(1-2): p. 29-33.
195. Lukong, K.E. and S. Richard, *Sam68, the KH domain-containing superSTAR.* Biochim Biophys Acta, 2003. **1653**(2): p. 73-86.
196. Vernet, C. and K. Artzt, *STAR, a gene family involved in signal transduction and activation of RNA.* Trends Genet, 1997. **13**(12): p. 479-84.
197. Matter, N., P. Herrlich, and H. Konig, *Signal-dependent regulation of splicing via phosphorylation of Sam68.* Nature, 2002. **420**(6916): p. 691-5.
198. Lin, Q., S.J. Taylor, and D. Shalloway, *Specificity and determinants of Sam68 RNA binding. Implications for the biological function of K homology domains.* J Biol Chem, 1997. **272**(43): p. 27274-80.
199. Itoh, M., et al., *Identification of cellular mRNA targets for RNA-binding protein Sam68.* Nucleic Acids Res, 2002. **30**(24): p. 5452-64.
200. Chen, T., et al., *Self-association of the single-KH-domain family members Sam68, GRP33, GLD-1, and Qk1: role of the KH domain.* Mol Cell Biol, 1997. **17**(10): p. 5707-18.
201. Lazer, G., et al., *The association of Sam68 with Vav1 contributes to tumorigenesis.* Cell Signal, 2007.
202. Espejo, A., et al., *A protein-domain microarray identifies novel protein-protein interactions.* Biochem J, 2002. **367**(Pt 3): p. 697-702.
203. Trub, T., et al., *The role of a lymphoid-restricted, Grb2-like SH3-SH2-SH3 protein in T cell receptor signaling.* J Biol Chem, 1997. **272**(2): p. 894-902.
204. Najib, S. and V. Sanchez-Margalet, *Sam68 associates with the SH3 domains of Grb2 recruiting GAP to the Grb2-SOS complex in insulin receptor signaling.* J Cell Biochem, 2002. **86**(1): p. 99-106.
205. Taylor, S.J., et al., *Functional interaction between c-Src and its mitotic target, Sam 68.* J Biol Chem, 1995. **270**(17): p. 10120-4.

206. Maa, M.C., et al., *A protein that is highly related to GTPase-activating protein-associated p62 complexes with phospholipase C gamma.* Mol Cell Biol, 1994. **14**(8): p. 5466-73.
207. Bunnell, S.C., et al., *Identification of Itk/Tsk Src homology 3 domain ligands.* J Biol Chem, 1996. **271**(41): p. 25646-56.
208. Lawe, D.C., C. Hahn, and A.J. Wong, *The Nck SH2/SH3 adaptor protein is present in the nucleus and associates with the nuclear protein SAM68.* Oncogene, 1997. **14**(2): p. 223-31.
209. Derry, J.J., et al., *Sik (BRK) phosphorylates Sam68 in the nucleus and negatively regulates its RNA binding ability.* Mol Cell Biol, 2000. **20**(16): p. 6114-26.
210. Bedford, M.T., et al., *Arginine methylation inhibits the binding of proline-rich ligands to Src homology 3, but not WW, domains.* J Biol Chem, 2000. **275**(21): p. 16030-6.
211. Lang, V., et al., *A dual participation of ZAP-70 and scr protein tyrosine kinases is required for TCR-induced tyrosine phosphorylation of Sam68 in Jurkat T cells.* Eur J Immunol, 1997. **27**(12): p. 3360-7.
212. Weng, Z., et al., *Structure-function analysis of SH3 domains: SH3 binding specificity altered by single amino acid substitutions.* Mol Cell Biol, 1995. **15**(10): p. 5627-34.
213. Lukong, K.E., et al., *Tyrosine phosphorylation of sam68 by breast tumor kinase regulates intranuclear localization and cell cycle progression.* J Biol Chem, 2005. **280**(46): p. 38639-47.
214. Ishidate, T., et al., *Identification of a novel nuclear localization signal in Sam68.* FEBS Lett, 1997. **409**(2): p. 237-41.
215. Reddy, T.R., *A single point mutation in the nuclear localization domain of Sam68 blocks the Rev/RRE-mediated transactivation.* Oncogene, 2000. **19**(27): p. 3110-4.
216. Burd, C.G. and G. Dreyfuss, *Conserved structures and diversity of functions of RNA-binding proteins.* Science, 1994. **265**(5172): p. 615-21.
217. Cote, J., et al., *Sam68 RNA binding protein is an in vivo substrate for protein arginine N-methyltransferase 1.* Mol Biol Cell, 2003. **14**(1): p. 274-87.
218. Babic, I., E. Cherry, and D.J. Fujita, *SUMO modification of Sam68 enhances its ability to repress cyclin D1 expression and inhibits its ability to induce apoptosis.* Oncogene, 2006. **25**(36): p. 4955-64.
219. Paronetto, M.P., et al., *The RNA-binding protein Sam68 modulates the alternative splicing of Bcl-x.* J Cell Biol, 2007. **176**(7): p. 929-39.
220. McLaren, M., K. Asai, and A. Cochrane, *A novel function for Sam68: enhancement of HIV-1 RNA 3' end processing.* RNA, 2004. **10**(7): p. 1119-29.
221. Li, J., et al., *Direct participation of Sam68, the 68-kilodalton Src-associated protein in mitosis, in the CRM1-mediated Rev nuclear export pathway.* J Virol, 2002. **76**(16): p. 8374-82.

222. Coyle, J.H., et al., *Sam68 enhances the cytoplasmic utilization of intron-containing RNA and is functionally regulated by the nuclear kinase Sik/BRK.* Mol Cell Biol, 2003. **23**(1): p. 92-103.
223. Grange, J., et al., *Specific interaction between Sam68 and neuronal mRNAs: Implication for the activity-dependent biosynthesis of elongation factor eEF1A.* J Neurosci Res, 2008.
224. Najib, S., et al., *Role of Sam68 as an adaptor protein in signal transduction.* Cell Mol Life Sci, 2005. **62**(1): p. 36-43.
225. Lukong, K.E. and S. Richard, *Motor coordination defects in mice deficient for the Sam68 RNA-binding protein.* Behav Brain Res, 2008. **189**(2): p. 357-63.
226. Richard, S., et al., *Sam68 haploinsufficiency delays onset of mammary tumorigenesis and metastasis.* Oncogene, 2008. **27**(4): p. 548-56.
227. Richard, S., et al., *Ablation of the Sam68 RNA binding protein protects mice from age-related bone loss.* PLoS Genet, 2005. **1**(6): p. e74.
228. Hartmann, A.M., et al., *The interaction and colocalization of Sam68 with the splicing-associated factor YT521-B in nuclear dots is regulated by the Src family kinase p59(fyn).* Mol Biol Cell, 1999. **10**(11): p. 3909-26.
229. Tisserant, A. and H. Konig, *Signal-regulated Pre-mRNA occupancy by the general splicing factor U2AF.* PLoS ONE, 2008. **3**(1): p. e1418.
230. Sergeant, K.A., et al., *Alternative RNA splicing complexes containing the scaffold attachment factor SAFB2.* J Cell Sci, 2007. **120**(Pt 2): p. 309-19.
231. Thornton, J.K., et al., *The tumour-suppressor protein ASPP1 is nuclear in human germ cells and can modulate ratios of CD44 exon V5 spliced isoforms in vivo.* Oncogene, 2006. **25**(22): p. 3104-12.
232. Batsche, E., M. Yaniv, and C. Muchardt, *The human SWI/SNF subunit Brm is a regulator of alternative splicing.* Nat Struct Mol Biol, 2006. **13**(1): p. 22-9.
233. Stoss, O., et al., *The STAR/GSG family protein rSLM-2 regulates the selection of alternative splice sites.* J Biol Chem, 2001. **276**(12): p. 8665-73.
234. Cheng, C. and P.A. Sharp, *Regulation of CD44 alternative splicing by SRm160 and its potential role in tumor cell invasion.* Mol Cell Biol, 2006. **26**(1): p. 362-70.
235. Herrlich, P., S. Pals, and H. Ponta, *CD44 in colon cancer.* Eur J Cancer, 1995. **31A**(7-8): p. 1110-2.
236. Busa, R., et al., *The RNA-binding protein Sam68 contributes to proliferation and survival of human prostate cancer cells.* Oncogene, 2007. **26**(30): p. 4372-82.
237. Taylor, S.J., R.J. Resnick, and D. Shalloway, *Sam68 exerts separable effects on cell cycle progression and apoptosis.* BMC Cell Biol, 2004. **5**: p. 5.
238. Schwerk, C. and K. Schulze-Osthoff, *Regulation of apoptosis by alternative pre-mRNA splicing.* Mol Cell, 2005. **19**(1): p. 1-13.
239. Boise, L.H., et al., *bcl-x, a bcl-2-related gene that functions as a dominant regulator of apoptotic cell death.* Cell, 1993. **74**(4): p. 597-608.

240. Reddy, T.R., et al., *Sam68, RNA helicase A and Tap cooperate in the post-transcriptional regulation of human immunodeficiency virus and type D retroviral mRNA.* Oncogene, 2000. **19**(32): p. 3570-5.
241. Yang, J.P., et al., *Functional interaction of Sam68 and heterogeneous nuclear ribonucleoprotein K.* Oncogene, 2002. **21**(47): p. 7187-94.
242. Reddy, T.R., W.D. Xu, and F. Wong-Staal, *General effect of Sam68 on Rev/Rex regulated expression of complex retroviruses.* Oncogene, 2000. **19**(35): p. 4071-4.
243. Li, J., et al., *Expression of exogenous Sam68, the 68-kilodalton SRC-associated protein in mitosis, is able to alleviate impaired Rev function in astrocytes.* J Virol, 2002. **76**(9): p. 4526-35.
244. Modem, S., et al., *Sam68 is absolutely required for Rev function and HIV-1 production.* Nucleic Acids Res, 2005. **33**(3): p. 873-9.
245. Chen, T., et al., *Identification of Sam68 arginine glycine-rich sequences capable of conferring nonspecific RNA binding to the GSG domain.* J Biol Chem, 2001. **276**(33): p. 30803-11.
246. Wang, L.L., S. Richard, and A.S. Shaw, *P62 association with RNA is regulated by tyrosine phosphorylation.* J Biol Chem, 1995. **270**(5): p. 2010-3.
247. Reddy, T.R., et al., *A role for KH domain proteins (Sam68-like mammalian proteins and quaking proteins) in the post-transcriptional regulation of HIV replication.* J Biol Chem, 2002. **277**(8): p. 5778-84.
248. Soros, V.B., et al., *Inhibition of human immunodeficiency virus type 1 Rev function by a dominant-negative mutant of Sam68 through sequestration of unspliced RNA at perinuclear bundles.* J Virol, 2001. **75**(17): p. 8203-15.
249. Zhang, J., et al., *Requirement of an additional Sam68 domain for inhibition of human immunodeficiency virus type 1 replication by Sam68 dominant negative mutants lacking the nuclear localization signal.* Gene, 2005. **363**: p. 67-76.
250. Andreotti, A.H., et al., *Regulatory intramolecular association in a tyrosine kinase of the Tec family.* Nature, 1997. **385**(6611): p. 93-7.
251. Martin-Romero, C. and V. Sanchez-Margalet, *Human leptin activates PI3K and MAPK pathways in human peripheral blood mononuclear cells: possible role of Sam68.* Cell Immunol, 2001. **212**(2): p. 83-91.
252. Sanchez-Margalet, V. and S. Najib, *Sam68 is a docking protein linking GAP and PI3K in insulin receptor signaling.* Mol Cell Endocrinol, 2001. **183**(1-2): p. 113-21.
253. Fusaki, N., et al., *Interaction between Sam68 and Src family tyrosine kinases, Fyn and Lck, in T cell receptor signaling.* J Biol Chem, 1997. **272**(10): p. 6214-9.
254. Hawkins, J. and A. Marcy, *Characterization of Itk tyrosine kinase: contribution of noncatalytic domains to enzymatic activity.* Protein Expr Purif, 2001. **22**(2): p. 211-9.

255. Jauliac, S., et al., *Ligands of CD4 inhibit the association of phospholipase Cgamma1 with phosphoinositide 3 kinase in T cells: regulation of this association by the phosphoinositide 3 kinase activity.* Eur J Immunol, 1998. **28**(10): p. 3183-91.
256. Jabado, N., et al., *Sam68 association with p120GAP in CD4+ T cells is dependent on CD4 molecule expression.* J Immunol, 1998. **161**(6): p. 2798-803.
257. Douek, D., *HIV disease progression: immune activation, microbes, and a leaky gut.* Top HIV Med, 2007. **15**(4): p. 114-7.
258. Navarro, R.E. and T.K. Blackwell, *Requirement for P granules and meiosis for accumulation of the germline RNA helicase CGH-1.* Genesis, 2005. **42**(3): p. 172-80.
259. Schisa, J.A., J.N. Pitt, and J.R. Priess, *Analysis of RNA associated with P granules in germ cells of C. elegans adults.* Development, 2001. **128**(8): p. 1287-98.
260. Leatherman, J.L. and T.A. Jongens, *Transcriptional silencing and translational control: key features of early germline development.* Bioessays, 2003. **25**(4): p. 326-35.
261. Paronetto, M.P., et al., *Dynamic expression of the RNA-binding protein Sam68 during mouse pre-implantation development.* Gene Expr Patterns, 2008. **8**(5): p. 311-22.
262. Paronetto, M.P., et al., *The nuclear RNA-binding protein Sam68 translocates to the cytoplasm and associates with the polysomes in mouse spermatocytes.* Mol Biol Cell, 2006. **17**(1): p. 14-24.
263. Kosik, K.S. and A.M. Krichevsky, *The message and the messenger: delivering RNA in neurons.* Sci STKE, 2002. **2002**(126): p. PE16.
264. Ben Fredj, N., et al., *Depolarization-induced translocation of the RNA-binding protein Sam68 to the dendrites of hippocampal neurons.* J Cell Sci, 2004. **117**(Pt 7): p. 1079-90.
265. Grange, J., et al., *Somatodendritic localization and mRNA association of the splicing regulatory protein Sam68 in the hippocampus and cortex.* J Neurosci Res, 2004. **75**(5): p. 654-66.
266. Belly, A., et al., *Delocalization of the multifunctional RNA splicing factor TLS/FUS in hippocampal neurones: exclusion from the nucleus and accumulation in dendritic granules and spine heads.* Neurosci Lett, 2005. **379**(3): p. 152-7.
267. Marsh, K., V. Soros, and A. Cochrane, *Selective translational repression of HIV-1 RNA by Sam68DeltaC occurs by altering PABP1 binding to unspliced viral RNA.* Retrovirology, 2008. **5**: p. 97.
268. Hill, M.A., L. Schedlich, and P. Gunning, *Serum-induced signal transduction determines the peripheral location of beta-actin mRNA within the cell.* J Cell Biol, 1994. **126**(5): p. 1221-9.
269. Noble, S.L., et al., *Maternal mRNAs are regulated by diverse P body-related mRNP granules during early Caenorhabditis elegans development.* J Cell Biol, 2008. **182**(3): p. 559-72.

270. McBride, A.E., A. Schlegel, and K. Kirkegaard, *Human protein Sam68 relocalization and interaction with poliovirus RNA polymerase in infected cells.* Proc Natl Acad Sci U S A, 1996. **93**(6): p. 2296-301.
271. Daoud, R., et al., *Ischemia induces a translocation of the splicing factor tra2-beta 1 and changes alternative splicing patterns in the brain.* J Neurosci, 2002. **22**(14): p. 5889-99.
272. DeGracia, D.J., et al., *Convergence of stress granules and protein aggregates in hippocampal cornu ammonis 1 at later reperfusion following global brain ischemia.* Neuroscience, 2007. **146**(2): p. 562-72.
273. Gilbert, C., et al., *Evidence for a role for SAM68 in the responses of human neutrophils to ligation of CD32 and to monosodium urate crystals.* J Immunol, 2001. **166**(7): p. 4664-71.
274. Simarro, M., et al., *Fas-activated serine/threonine phosphoprotein (FAST) is a regulator of alternative splicing.* Proc Natl Acad Sci U S A, 2007. **104**(27): p. 11370-5.
275. Grossman, J.S., et al., *The use of antibodies to the polypyrimidine tract binding protein (PTB) to analyze the protein components that assemble on alternatively spliced pre-mRNAs that use distant branch points.* RNA, 1998. **4**(6): p. 613-25.
276. Ward, C.L., S. Omura, and R.R. Kopito, *Degradation of CFTR by the ubiquitin-proteasome pathway.* Cell, 1995. **83**(1): p. 121-7.
277. Imai, Y., et al., *An unfolded putative transmembrane polypeptide, which can lead to endoplasmic reticulum stress, is a substrate of Parkin.* Cell, 2001. **105**(7): p. 891-902.
278. Jacquenet, S., et al., *A second exon splicing silencer within human immunodeficiency virus type 1 tat exon 2 represses splicing of Tat mRNA and binds protein hnRNP H.* J Biol Chem, 2001. **276**(44): p. 40464-75.
279. Helseth, E., et al., *Rapid complementation assays measuring replicative potential of human immunodeficiency virus type 1 envelope glycoprotein mutants.* J Virol, 1990. **64**(5): p. 2416-20.
280. He, J., et al., *CCR3 and CCR5 are co-receptors for HIV-1 infection of microglia.* Nature, 1997. **385**(6617): p. 645-9.
281. He, J. and N.R. Landau, *Use of a novel human immunodeficiency virus type 1 reporter virus expressing human placental alkaline phosphatase to detect an alternative viral receptor.* J Virol, 1995. **69**(7): p. 4587-92.
282. Jan, E., et al., *The STAR protein, GLD-1, is a translational regulator of sexual identity in Caenorhabditis elegans.* EMBO J, 1999. **18**(1): p. 258-69.
283. Schumacher, B., et al., *Translational repression of C. elegans p53 by GLD-1 regulates DNA damage-induced apoptosis.* Cell, 2005. **120**(3): p. 357-68.
284. Larocque, D., et al., *Protection of p27(Kip1) mRNA by quaking RNA binding proteins promotes oligodendrocyte differentiation.* Nat Neurosci, 2005. **8**(1): p. 27-33.

285. Gherzi, R., et al., *A KH domain RNA binding protein, KSRP, promotes ARE-directed mRNA turnover by recruiting the degradation machinery.* Mol Cell, 2004. **14**(5): p. 571-83.
286. Bilodeau, P.S., J.K. Domsic, and C.M. Stoltzfus, *Splicing regulatory elements within tat exon 2 of human immunodeficiency virus type 1 (HIV-1) are characteristic of group M but not group O HIV-1 strains.* J Virol, 1999. **73**(12): p. 9764-72.
287. Madsen, J.M. and C.M. Stoltzfus, *A suboptimal 5' splice site downstream of HIV-1 splice site A1 is required for unspliced viral mRNA accumulation and efficient virus replication.* Retrovirology, 2006. **3**: p. 10.
288. Jacquenet, S., et al., *Conserved stem-loop structures in the HIV-1 RNA region containing the A3 3' splice site and its cis-regulatory element: possible involvement in RNA splicing.* Nucleic Acids Res, 2001. **29**(2): p. 464-78.
289. Kozak, M., *Structural features in eukaryotic mRNAs that modulate the initiation of translation.* J Biol Chem, 1991. **266**(30): p. 19867-70.
290. Tompa, P. and P. Csermely, *The role of structural disorder in the function of RNA and protein chaperones.* FASEB J, 2004. **18**(11): p. 1169-75.
291. Ivanyi-Nagy, R., et al., *Disordered RNA chaperone proteins: from functions to disease.* Cell Mol Life Sci, 2005. **62**(13): p. 1409-17.
292. Obradovic, Z., et al., *Predicting intrinsic disorder from amino acid sequence.* Proteins, 2003. **53 Suppl 6**: p. 566-72.
293. Rajkowitsch, L., et al., *Assays for the RNA chaperone activity of proteins.* Biochem Soc Trans, 2005. **33**(Pt 3): p. 450-6.
294. Fenger-Gron, M., et al., *Multiple processing body factors and the ARE binding protein TTP activate mRNA decapping.* Mol Cell, 2005. **20**(6): p. 905-15.
295. Tahtinen, M., et al., *DNA vaccination in mice using HIV-1 nef, rev and tat genes in self-replicating pBN-vector.* Vaccine, 2001. **19**(15-16): p. 2039-47.
296. Hofacker, I.L., *Vienna RNA secondary structure server.* Nucleic Acids Res, 2003. **31**(13): p. 3429-31.
297. SenGupta, D.J., et al., *A three-hybrid system to detect RNA-protein interactions in vivo.* Proc Natl Acad Sci U S A, 1996. **93**(16): p. 8496-501.
298. Kawai, T., et al., *Translational control of cytochrome c by RNA-binding proteins TIA-1 and HuR.* Mol Cell Biol, 2006. **26**(8): p. 3295-307.
299. Gilks, N., et al., *Stress granule assembly is mediated by prion-like aggregation of TIA-1.* Mol Biol Cell, 2004. **15**(12): p. 5383-98.
300. Afonina, E., R. Stauber, and G.N. Pavlakis, *The human poly(A)-binding protein 1 shuttles between the nucleus and the cytoplasm.* J Biol Chem, 1998. **273**(21): p. 13015-21.
301. Cande, C., et al., *Regulation of cytoplasmic stress granules by apoptosis-inducing factor.* J Cell Sci, 2004. **117**(Pt 19): p. 4461-8.
302. Lin, J.H., P. Walter, and T.S. Yen, *Endoplasmic reticulum stress in disease pathogenesis.* Annu Rev Pathol, 2008. **3**: p. 399-425.

303. McBride, A.E., et al., *KH domain integrity is required for wild-type localization of Sam68.* Exp Cell Res, 1998. **241**(1): p. 84-95.
304. Henao-Mejia, J., et al., *Suppression of HIV-1 Nef translation by Sam68 mutant-induced stress granules and nef mRNA sequestration.* Molecular Cell, 2009. **(in press)**((Jan. 16th issue, 2009)).
305. McDowall, M.D., M.S. Scott, and G.J. Barton, *PIPs: human protein-protein interaction prediction database.* Nucleic Acids Res, 2008.
306. Parker, F., et al., *A Ras-GTPase-activating protein SH3-domain-binding protein.* Mol Cell Biol, 1996. **16**(6): p. 2561-9.
307. Gallouzi, I.E., et al., *A novel phosphorylation-dependent RNase activity of GAP-SH3 binding protein: a potential link between signal transduction and RNA stability.* Mol Cell Biol, 1998. **18**(7): p. 3956-65.
308. Guitard, E., et al., *Sam68 is a Ras-GAP-associated protein in mitosis.* Biochem Biophys Res Commun, 1998. **245**(2): p. 562-6.
309. Tocque, B., et al., *Ras-GTPase activating protein (GAP): a putative effector for Ras.* Cell Signal, 1997. **9**(2): p. 153-8.
310. Dolzhanskaya, N., et al., *Methylation regulates the intracellular protein-protein and protein-RNA interactions of FMRP.* J Cell Sci, 2006. **119**(Pt 9): p. 1933-46.
311. Cockroft, D.L. and D.A. New, *Abnormalities induced in cultured rat embryos by hyperthermia.* Teratology, 1978. **17**(3): p. 277-83.
312. Mitchell, H.K. and L.S. Lipps, *Heat shock and phenocopy induction in Drosophila.* Cell, 1978. **15**(3): p. 907-18.
313. Gingras, A.C., B. Raught, and N. Sonenberg, *Regulation of translation initiation by FRAP/mTOR.* Genes Dev, 2001. **15**(7): p. 807-26.
314. Song, J., M. Takeda, and R.I. Morimoto, *Bag1-Hsp70 mediates a physiological stress signalling pathway that regulates Raf-1/ERK and cell growth.* Nat Cell Biol, 2001. **3**(3): p. 276-82.
315. Cowan, K.J. and K.B. Storey, *Mitogen-activated protein kinases: new signaling pathways functioning in cellular responses to environmental stress.* J Exp Biol, 2003. **206**(Pt 7): p. 1107-15.
316. Westermarck, J., et al., *p38 mitogen-activated protein kinase-dependent activation of protein phosphatases 1 and 2A inhibits MEK1 and MEK2 activity and collagenase 1 (MMP-1) gene expression.* Mol Cell Biol, 2001. **21**(7): p. 2373-83.
317. Liu, Q. and P.A. Hofmann, *Protein phosphatase 2A-mediated cross-talk between p38 MAPK and ERK in apoptosis of cardiac myocytes.* Am J Physiol Heart Circ Physiol, 2004. **286**(6): p. H2204-12.
318. Monick, M.M., et al., *Active ERK contributes to protein translation by preventing JNK-dependent inhibition of protein phosphatase 1.* J Immunol, 2006. **177**(3): p. 1636-45.
319. Thiaville, M.M., et al., *MEK signaling is required for phosphorylation of eIF2alpha following amino acid limitation of HepG2 human hepatoma cells.* J Biol Chem, 2008. **283**(16): p. 10848-57.
320. Mansour, S.J., et al., *Transformation of mammalian cells by constitutively active MAP kinase kinase.* Science, 1994. **265**(5174): p. 966-70.

321. Dreyfuss, G., V.N. Kim, and N. Kataoka, *Messenger-RNA-binding proteins and the messages they carry.* Nat Rev Mol Cell Biol, 2002. **3**(3): p. 195-205.
322. Kwon, S., E. Barbarese, and J.H. Carson, *The cis-acting RNA trafficking signal from myelin basic protein mRNA and its cognate trans-acting ligand hnRNP A2 enhance cap-dependent translation.* J Cell Biol, 1999. **147**(2): p. 247-56.
323. Cochrane, A.W., M.T. McNally, and A.J. Mouland, *The retrovirus RNA trafficking granule: from birth to maturity.* Retrovirology, 2006. **3**: p. 18.
324. Mouland, A.J., et al., *RNA trafficking signals in human immunodeficiency virus type 1.* Mol Cell Biol, 2001. **21**(6): p. 2133-43.
325. Levesque, K., et al., *Trafficking of HIV-1 RNA is mediated by heterogeneous nuclear ribonucleoprotein A2 expression and impacts on viral assembly.* Traffic, 2006. **7**(9): p. 1177-93.
326. Dugre-Brisson, S., et al., *Interaction of Staufen1 with the 5' end of mRNA facilitates translation of these RNAs.* Nucleic Acids Res, 2005. **33**(15): p. 4797-812.
327. Mazroui, R., et al., *Trapping of messenger RNA by Fragile X Mental Retardation protein into cytoplasmic granules induces translation repression.* Hum Mol Genet, 2002. **11**(24): p. 3007-17.
328. Mazan-Mamczarz, K., et al., *Translational repression by RNA-binding protein TIAR.* Mol Cell Biol, 2006. **26**(7): p. 2716-27.
329. Auweter, S.D., F.C. Oberstrass, and F.H. Allain, *Sequence-specific binding of single-stranded RNA: is there a code for recognition?* Nucleic Acids Res, 2006. **34**(17): p. 4943-59.
330. Berglund, J.A., M.L. Fleming, and M. Rosbash, *The KH domain of the branchpoint sequence binding protein determines specificity for the pre-mRNA branchpoint sequence.* RNA, 1998. **4**(8): p. 998-1006.
331. Robert-Guroff, M., et al., *Structure and expression of tat-, rev-, and nef-specific transcripts of human immunodeficiency virus type 1 in infected lymphocytes and macrophages.* J Virol, 1990. **64**(7): p. 3391-8.
332. Dowling, D., et al., *HIV-1 infection induces changes in expression of cellular splicing factors that regulate alternative viral splicing and virus production in macrophages.* Retrovirology, 2008. **5**: p. 18.
333. Najib, S., et al., *Sam68 is tyrosine phosphorylated and recruited to signalling in peripheral blood mononuclear cells from HIV infected patients.* Clin Exp Immunol, 2005. **141**(3): p. 518-25.
334. Gustin, K.E. and P. Sarnow, *Effects of poliovirus infection on nucleo-cytoplasmic trafficking and nuclear pore complex composition.* EMBO J, 2001. **20**(1-2): p. 240-9.
335. Lenart, P. and J. Ellenberg, *Monitoring the permeability of the nuclear envelope during the cell cycle.* Methods, 2006. **38**(1): p. 17-24.
336. Sanchez-Margalet, V., et al., *The expression of Sam68, a protein involved in insulin signal transduction, is enhanced by insulin stimulation.* Cell Mol Life Sci, 2003. **60**(4): p. 751-8.

337. Smida, M., et al., *A novel negative regulatory function of the phosphoprotein associated with glycosphingolipid-enriched microdomains: blocking Ras activation.* Blood, 2007. **110**(2): p. 596-615.
338. David, P.S., R. Tanveer, and J.D. Port, *FRET-detectable interactions between the ARE binding proteins, HuR and p37AUF1.* RNA, 2007. **13**(9): p. 1453-68.
339. Pilotte, J., D. Larocque, and S. Richard, *Nuclear translocation controlled by alternatively spliced isoforms inactivates the QUAKING apoptotic inducer.* Genes Dev, 2001. **15**(7): p. 845-58.
340. Lin, Q., S.J. Taylor, and D. Shalloway, *Specificity and determinants of Sam68 RNA binding. Implications for the biological function of K homology domains.* J Biol Chem, 1997. **272**(43): p. 27274-80.
341. Tremblay, G.A. and S. Richard, *mRNAs associated with the Sam68 RNA binding protein.* RNA Biol, 2006. **3**(2): p. 1-4.
342. Brush, M.H., D.C. Weiser, and S. Shenolikar, *Growth arrest and DNA damage-inducible protein GADD34 targets protein phosphatase 1 alpha to the endoplasmic reticulum and promotes dephosphorylation of the alpha subunit of eukaryotic translation initiation factor 2.* Mol Cell Biol, 2003. **23**(4): p. 1292-303.
343. Liu, Y., et al., *Uptake of HIV-1 tat protein mediated by low-density lipoprotein receptor-related protein disrupts the neuronal metabolic balance of the receptor ligands.* Nat Med, 2000. **6**(12): p. 1380-7.
344. Sanford, J.R., et al., *Identification of nuclear and cytoplasmic mRNA targets for the shuttling protein SF2/ASF.* PLoS ONE, 2008. **3**(10): p. e3369.
345. Sun, Z., et al., *Intrarectal transmission, systemic infection, and CD4+ T cell depletion in humanized mice infected with HIV-1.* J Exp Med, 2007. **204**(4): p. 705-14.
346. Pisareva, V.P., et al., *Translation initiation on mammalian mRNAs with structured 5'UTRs requires DExH-box protein DHX29.* Cell, 2008. **135**(7): p. 1237-50.
347. Lee, C.S., et al., *Human DDX3 functions in translation and interacts with the translation initiation factor eIF3.* Nucleic Acids Res, 2008. **36**(14): p. 4708-18.
348. Elmen, J., et al., *LNA-mediated microRNA silencing in non-human primates.* Nature, 2008. **452**(7189): p. 896-9.
349. Triboulet, R., et al., *Suppression of microRNA-silencing pathway by HIV-1 during virus replication.* Science, 2007. **315**(5818): p. 1579-82.
350. Huang, J., et al., *Cellular microRNAs contribute to HIV-1 latency in resting primary CD4+ T lymphocytes.* Nat Med, 2007. **13**(10): p. 1241-7.

CURRICULUM VITAE

Jorge Alejandro Henao-Mejia

Education

2005-2009 *Indiana University, Indianapolis, IN*
Degree: PhD in Microbiology and Immunology
Advisor: Professor Johnny He

1999-2005 *University of Antioquia School of Medicine, Medellin, Colombia*
Degree: MD

Honors, Awards, Fellowships

2009 Young Investigator Award
The 16th Conference on Retroviruses and Opportunistic Infections

2008 Graduate Travel Fellowship
Indiana University School of medicine

2003-2004 Young Scientist Fellowship
University of Antioquia

2002 Best project in basic science for an undergraduate student
IV meeting of basic research for undergraduate students
University of Antioquia

Research Experience

2001-2005 Young Scientist
Laboratory for Immunovirology
Center for Basic Research
University of Antioquia, Colombia

Nov 2002-
Feb 2003 Visiting Scientist
Professor Johnny He's Laboratory
Indiana University School of Medicine

Teaching Experience

2007 Teaching Assistant in Microbiology J210
Indiana University, School of Medicine

Publications

Peer Review Publications:

Henao-Mejia J, He JJ. Role of Sam68 on the nuclear exportation and translational initiation of HIV-1 RNAs. (*Manuscripts in preparation)*

Henao-Mejia J, He JJ. Sam68 Recruitment into Stress Granules in Response to Oxidative Stress through complexing with TIA-1. (Submitted)

Giraldo M, Archila ME, Cornejo W, **Henao J**, Jimenez M, Rugeles MT, Lahorgue Nunes M. Polysomnographic evaluation of babies born to HIV-1 positive mothers. (Submitted)

Henao-Mejia J, Liu Y, Park IW, Zhang J, Sanford J, He JJ (2009). Suppression of HIV-1 Nef Translation by Sam68 Mutant-Induced Stress Granules and *nef* mRNA Sequestration. Molecular Cell, 33(1):87-93.

Broxmeyer HE, **Mejia JA**, Hangoc G, Barese C, Dinauer M, Cooper S (2007). SDF-1/CXCL12 enhances In Vitro Replating capacity of murine and human multipotential and Macrophage Progenitor Cells. Stem Cells and Development, 16(4):589-596.

Henao J, Goez Y, Patiño PJ, Rugeles MT (2006). Diketo acids derivatives as integrase inhibitors: promising agents in the war to the acquired immunodeficiency syndrome. Recent Patents on Anti -Infective Drug Discovery, 1(2):255-265.

Zhang J, Liu Y, **Henao J**, Rugeles MT, Li J, Chen T, He JJ (2005). Requirement of an additional domain for inhibition of human immunodeficiency virus type 1 replication by Sam68 dominant negative mutants lacking the nuclear localization signal. Gene, 19(363):67-76.

Henao J, Vanegas N, Lopez JC, Cano OD, Rugeles MT (2005). The Human Immunodeficiency virus in the developing brain. Biomédica, 25(1):136-147.

Henao J, Rugeles MT. Pathogenesis of the Human Immunodeficiency Virus (2003). Annals of infectious diseases, 1:13-43.

Book Chapters:

Rugeles MT, **Henao J**, Bedoya VI. Immune response to Intracellular Pathogens: the Viral Model. Immunology: An active science - Vol II. 1st Edition. Medellín : Biogénesis, 2004.

Henao J, Rugeles MT. A Clinical Case. Immunology: An active science - Vol II. 1st Edition. Medellín : Biogénesis, 2004.

Abstracts:

Henao-Mejia J, Liu Y, Park IW, Zhang J, Sanford J, He JJ. Suppression of HIV-1 Nef Translation by Sam68 Mutant-Induced Stress Granules and nef mRNA Sequestration. The 16th Conference on Retroviruses and Opportunistic Infections, Montreal, 2/07-2/12, 2009.

Broxmeyer HE, Basu S, Clapp W, Cooper S, Hangoc G, **Henao J**, Pulliam A. Targeting Surface and intracellular molecules and the chemokine pathway for the mobilization and/or engraftment. Scientific committee on transfusion medicine. 2006.